School of Chemical and Petroleum Engineering

Experimental and Modelling Study of Advanced Aqueous Ammonia Based Post Combustion Capture Process

Kangkang Li

This thesis is presented for the degree of

Doctor of Philosophy

of

Curtin University

May 2016

Declaration

To the best of my knowledge and belief this thesis contains no material previously published by any other person except where due acknowledgment has been made.

This thesis contains no material which has been accepted for the award of any other degree or diploma in any university.

Signature : ……

Date : ……

Acknowledgements

This three-year Ph.D. study at CSIRO Energy and Curtin University has brought me many opportunities for personal growth and professional development. There are so many lovely people who offered their kind help throughout the whole period of Ph.D. study, and made me into the person who I am today. I would like to say my first thanks to Dr Hai Yu for all his guidance and support not only in my professional study but also in my personal life. He made my overseas life much easier than anticipated when I first moved to Australia from China. He always shared his knowledge and provided the best guidance he could to make my research smooth. He also did all he could to create every chance for students to attend conferences, seminars and workshops, which helped to build my network with other excellent research scientists.

I would also like to express my sincere thanks to my advisor Dr Paul Feron for his guidance and encouragement throughout the whole study at CSIRO. His insight and expertise in CO_2 capture technology made a deep impression on me. I always receive valuable feedback and comments from him to improve my research work. His creative and critical thinking regarding novel technology also impressed me a lot, and I hope I can learn the methodology from him to develop my own academic thinking.

I would also like to extend my thanks to my supervisor Prof. Moses Tadé for all his full support in making the Ph.D. study smooth. He always gave me positive and timely replies to deal with all the issues and difficulties I met during study. As I spent the whole time studying at CSIRO Newcastle site, his coordination and enthusiastic support made the remote study easy and efficient.

My sincere thanks also go to my colleagues at CSIRO and Curtin University, and the CSIRO visitors from Chinese Universities, Dr Wardhaugh Leigh, Dr Ashleigh Cousins, Dr Graeme Puxty, Dr Will Conway, Dr Tim Jones, Dr Shuiping Yan, Dr Zhen Wang, Lemlem Selomon, Dan Maher, Jingwen Yu, Nan Yang, Long Ji, Ruize Lu and Qinhui Ma, etc., for all their study guidance, technical support and suggestions, academic contributions and other help in making my job as a Ph.D. student much easier and making my life much happier.

I would also like to acknowledge the financial support of the International Postgraduate Research Scholarship (IPRS) and Australian Postgraduate Award (APA) from Curtin University and Australia government, and the CSIRO top-up scholarship. With this financial support and supervisors' encouragement, the domestic and international conferences, seminars, workshops were made possible, from which I definitely benefited a lot in terms of building my network and broadening my horizons. I have been very fortunate to have the opportunity to visit and study at the University of Texas at Austin, U.S.A. under the supervision of Dr. Gary Rochelle. I would like to specially thank him for his generosity, hospitality, kindness and particularly for the guidance he gave me during my stay in Austin.

Lastly and most importantly, I give special and sincere thanks to my beloved family, my wife Kaiqi Jiang, my father Xieming Li, my mother Zhenxian Jin, my father-in-law Ping Jiang and my mother-in-law Ping Yao, for their boundless love and unconditional support.

Abstract

Global warming, due to the massive carbon dioxide (CO_2) emissions into the atmosphere, has attracted great attention in recent decades, leading to a high level of interest in the technology development of CO_2 capture and storage (CCS). Ammonia (NH_3)-based post combustion capture (PCC) process is considered to be a promising technology for reducing the CO_2 emissions from the coal-fired power stations, because it provides many advantages over the benchmarking monoethanolamine (MEA) solvent, such as: high CO_2 absorption capacity, a low heat requirement for solvent regeneration, no solvent degradation and simultaneous capture of CO_2 and sulphur dioxide (SO_2). However, the obvious disadvantages of the NH_3 technology are the high NH_3 loss, high parasitic energy consumption and high economic burden, which restrict the industrial application of this technology. The proposed research therefore aims to (I) explore the advantages of the NH_3 process and make better use of them; and (II) develop innovative approaches to solving the attendant problems and make the aqueous NH_3 process technically and economically feasible. This research is based on the previous CSIRO pilot plant trials at Munmorah power station, NSW, Australia, and the process design is targeted at the typical Australian-based coal-fired power station where no flue gas desulphurisation (FGD) has been installed.

A rigorous, rate-based model using the commercial software Aspen Plus® is developed to evaluate the technical performance of the CO_2 capture and SO_2 removal by aqueous NH_3. The model is thermodynamically and kinetically validated against the experimental results, including those from open literature and CSIRO pilot plant trials, respectively. The developed model enables excellent predictions of the thermodynamic characteristics of the $NH_3/CO_2/SO_2/H_2O$ system, as well as the kinetic behaviours of the CO_2/SO_2 absorption by aqueous NH_3 in the packed column. This allows for a reasonable and reliable modelling and assessment of novel process configurations in the NH_3-based CO_2 capture process.

To solve the problems of NH_3 slip and flue gas cooling, an advanced and effective process of NH_3 abatement and recycling is proposed. This would entail installing an NH_3 absorber and utilizing the waste heat in flue gas from the power station. This advanced process design is proven to have excellent technical and environmental

advantages, such as: simplifying the NH_3 recycle system, over 99.5% NH_3 recycling efficiency and low NH_3 emission level and low energy requirement. Based on this effective NH_3 recycle process, the SO_2 removal process is incorporated into this system by using the scrubbed slipped NH_3. An SO_2 removal efficiency of over 99.9% is achieved. This advanced system incorporates NH_3 recycle and SO_2 removal into one process, which simplifies the FGD system and will significantly reduce the capital cost of the SO_2 removal facility.

A technical assessment of the NH_3-based CO_2 capture process integrated with 650 MW coal-fired power plants is conducted to gain insight into the technical and energy performance of the overall NH_3 process. The process parameters of the NH_3 process are optimised. The absorber modification of two-stage absorption is introduced to reduce the NH_3 slip, while stripper modifications of the rich-split and inter-heating processes are proposed to reduce the energy consumption. After process improvements, the regeneration duty of the advanced NH_3 process is reduced to 2.46 MJ/kg CO_2 leading to a net efficiency penalty of 8.0 %, which is lower than that in the MEA process (10.6%) and the modified chilled ammonia process (8.5%).

A techno-economic assessment is performed to understand the economic viability of the NH_3-based CO_2 capture process and its process improvements integrated with a 650 MW coal fired power station. A comprehensive economic model is proposed to determine the required capital investment and evaluate economic performance. The techno-economic model is validated with published cost results, which implies that the model is reliable and adequate for the assessment of the economic performance of the MEA-based and NH_3-based CO_2 capture processes. The NH_3-based CO_2 capture process is a capital intensive process with an estimated capital investment of US$ 832.8 million (2013 dollar) for the baseline process. The integration of the baseline PCC plant with the coal-fired power stations increases the levelised cost of electricity (LCOE) from $71.9/MWh to $118.0 /MWh, resulting in a CO_2 avoided cost of $67.3/tonne, which is much lower than the $86.4/ton CO_2 of the MEA process. The process modifications of the two-stage absorber, the rich-split and the inter-heating improve the technical performance and economic viability of the NH_3 process. It is demonstrated that the advanced process configurations significantly reduce the energy consumption by 31.7 MW (20.2% reduction) and the capital investment by US$ 55.4 million (6.7% reduction). This results in a decrease of LCOE from $118.0/MWh to

$109.0/MWh and a reduction of the CO_2 avoided cost from $67.3/tonne to $53.2/tonne CO_2. Lastly, a sensitivity analysis is performed to understand how economic assumptions and technical variables affect the economic performance, and also to provide technical research directions from the economic point of view. The results indicate that there is considerable room to further advance the techno-economic performance of the NH_3-based post combustion capture process.

Key words; NH_3, CO_2 capture, rate-based model, process design and modification, techno-economic assessment

Publications by Author

Published articles

1. Kangkang Li, Wardhaugh Leigh, Paul Feron, Hai Yu, Moses Tade. Systematic study of aqueous monoethanolamine-based CO_2 capture process: techno-economic assessment of the MEA process and its improvement. Applied Energy, 2015, accepted

2. Kangkang Li, Hai Yu, Paul Feron, Moses Tade, Leigh Wardhaugh. Technical and energy performance of an advanced, aqueous ammonia-based CO_2 capture technology for a 500-MW coal-fired power station. Environment Science & Technology, 2015, 49, 10243-10252. DOI: 10.1021/acs.est.5b02258

3. Kangkang Li, Hai Yu, Paul Feron, Moses Tade, Jingwen Yu, Shujuan Wang. Rate-based modelling of combined SO_2 removal and NH_3 recycling integrated with an aqueous NH_3-based CO_2 capture process. Applied Energy, 2015, 148, 66-77. DOI:10.1016/j.apenergy.2015.03.060

4. Kangkang Li, Ashleigh Cousin, Hai Yu, Paul Feron, Moses Tade, Weiliang Luo, Jian Chen. Systematic study of aqueous monoethanolamine-based CO_2 capture process (I): model development and process improvement. Energy Science & Engineering, 2015, 1-17. DOI: 10.1002/ese3.101

5. Kangkang Li, Hai Yu, Moses Tade, Paul Feron, Jingwen Yu, Shujuan Wang. Process modelling of an advanced NH_3 abatement and recycling system in ammonia based CO_2 capture process. Environment Science & Technology, 2014, 48 (12), 7179–7186. DOI: 10.1021/es501175x

6. Kangkang Li, Hai Yu, Moses Tade, Paul Feron. Theoretical and experimental study of NH_3 suppression by addition of Me(II) ions in an ammonia-based CO_2 capture process. International Journal of Greenhouse Gas Control, 2014, 24, 54-63. DOI:10.1016/j.ijggc.2014.02.019

7. Kangkang Li, Hai Yu, Paul Feron, Moses Tade. Modelling and experimental study of SO_2 removal and NH_3 recycling in an ammonia based CO_2 capture process. Energy Procedia, 2014, 63, 1162-1170. DOI:10.1016/j.egypro.2014.11.126

8. Kangkang Li, Hai Yu, Moses Tade, Paul Feron. Effect of Zinc(II) Additive on The ammonia loss and CO_2 absorption in ammonia-based CO_2 capture process. 2013 CHEMECA Conference in Brisbane, Australia.

To be submitted

9. Kangkang Li, Hai Yu, shuiping Yan, Paul Feron, Leigh Wardhaugh, Moses Tade. Techno-economic assessment of an advanced, aqueous ammonia-based post-combustion capture process integrated with a 650 MW coal-fired power station. *Applied Energy*, 2016, to be submitted.

10. Kangkang Li, Hai Yu, shuiping Yan, Leigh Wardhaugh, Paul Feron, Moses Tade. Techno-economic assessment of stripping modifications in an ammonia-based post combustion capture process. *Fuel Processing Technology*, 2016, to be submitted

Table of contents

List of Figures

List of Tables

Nomenclatures

AACE	Aspen Capital Cost Estimator
AACE	American Association of Cost Engineering
APC	Advanced Pulverized Coal
BEC	Bare Erected Cost
CAP	Chilled Ammonia Process
CCS	CO_2 Capture and Storage
CEPCI	Chemical Engineering Plant Cost Index
CO_2	Carbon Dioxide
CSIRO	Commonwealth Scientific and Industrial Research Organization
DOE	Department of Energy
EIA	Energy Information Administration
EPC	Engineering-Procurement-Construction (EPC)
FGD	Flue Gas Desulfurization
GHG	Greenhouse Gas
IEA	International Energy Agency
IPCC	Intergovernmental Panel on Climate Change
LCOE	Levelised Cost of Electricity
MEA	Monoethanolamine
NPV	Net Present Value
NIOSH	National Institute of Occupational Safety and Health
NSW	New South Wales
O&M	Operation and Maintenance
PCC	Post Combustion Capture
Ppmv	parts per million in volume
PVF	Production Validation Facility
SO_2	Sulphur Dioxide
TCI	Total capital investment
TDC	Total Direct Cost
TIC	Total Indirect cost
TPC	Total Plant Cost

Chapter 1 Introduction

1.1 Research background

In the light of climate change and global warming, due to increasing atmospheric concentration of CO_2, CO_2 capture and storage (CCS) has attracted great attention worldwide and is considered to be one of the most important technologies to mitigate CO_2 emissions from large-scale stationary point-source CO_2 emitters (Boot-Handford *et al.*, 2014; Markewitz *et al.*, 2012; Zhou *et al.*, 2010). According to the International Energy Agency (IEA), the combustion of fossil fuel supplies over 80% of the total world energy demand, while coal supplies only 29% of global energy but is responsible for 44% of global CO_2 emissions (IEA, 2014a). Therefore CO_2 emission reduction strategies aimed at coal-fired power plants are of extreme importance and are urgently needed to provide a path towards CO_2 emission reduction and to slow down the pace of global warming. A wide range of CCS technologies can be applied for CO_2 separation, i.e. pre-combustion, post-combustion and oxy-combustion (Boot-Handford *et al.*, 2014). Among them, post combustion capture (PCC) with chemical absorption is considered to be the most developed and feasible method for large-scale CO_2 removal from coal-fired power stations and energy-related industries. The amine scrubbing technology is considered to be the dominant technology for the large-scale application of post-combustion CO_2 capture from coal-fired power plants before 2030 (Rochelle, 2009).

Monoethanolamine (MEA), as a commercially available and benchmark amine solvent, is often regarded as the promising technology to be used in the early-stage implementation of CO_2 capture in coal-fired power stations because of its fast absorption rate, cheap cost and rich commercial experience in industrial application (Dinca *et al.*, 2013; Notz *et al.*, 2012). However, the major obstacle of this process being retrofitted into power stations is its high parasitic energy consumption, with the largest energy consumer (over 60%) being the solvent regeneration energy (stripper reboiler) (Aaron *et al.*, 2005; Herzog *et al.*, 2009). In coal-fired power plants this would lead to a 25-40% decrease in overall thermal efficiency and a 70-100% increase in the cost of electricity (Black, 2010; Haszeldine, 2009). In addition, the MEA solvents suffer degradation in the presence of SO_2 and O_2 and form thermally stable

and irreversible by-products. This reduces its absorption capacity and leads to additional costs for solvent make up and the treatment of by-products. Flue gas desulfurisation (FGD) is required in the MEA process to reduce the SO_2 concentration in the flue gas to below 10 ppmv before it enters the CO_2 capture plant, resulting in the significant increase of capital investment costs for the installation of a secondary FGD system (Markewitz *et al.*, 2012). Therefore, attention has shifted to alternative absorbents.

Aqueous ammonia (NH_3), as a promising and alternative solvent for CO_2 capture and, as one of the most widely produced chemicals in the world, provides many advantages over amine-based solvents. Specifically, these advantages include (Darde *et al.*, 2011a; Han *et al.*, 2013):

- A high CO_2 absorption capacity of a theoretical 1:1 ratio with CO_2 on a molar basis, which can potentially increase the CO_2 cyclic capacity of the NH_3 solvent and decrease the solvent circulation rate;
- No thermal and oxidative degradation, which allows for the NH_3 solvent to be regenerated at high temperature and high stripper pressure;
- Cheap chemical costs compared to amine solvents;
- Potentially lower regeneration energy of 0.93-2.9 MJ/kg CO_2 (Jilvero *et al.*, 2012) than the benchmark MEA solvent of 3.7-4.2 MJ/kg CO_2 (Abu-Zahra *et al.*, 2007; Tobiesen *et al.*, 2007);
- The simultaneous capture of multiple acid pollutants such as NO_x, SO_x, HCl and the production of value-added products such as ammonium sulphate and ammonium nitrate, which are widely used as fertilizers.

In the light of these advantages, intensive research has been carried out in the last decade to evaluate the technical feasibility of the NH_3-based CO_2 capture process. Experimentally, pilot-plant and demonstration trials have been conducted and operated by several industrial companies and research organisations, such as Alstom (Darde *et al.*, 2010a; Gal, 2006), Powerspan (McLarnon *et al.*, 2009) and the CSIRO (Commonwealth Scientific and Industrial Research Organization) (Yu *et al.*, 2011; Yu *et al.*, 2012), KIER (Korea Institute of Energy Research) (Han *et al.*, 2013; You *et al.*, 2007). The results of these pilot tests confirm the technical feasibility of NH_3-based technologies and demonstrate many of the expected benefits, such as high CO_2

removal efficiency, high-purity CO_2 production and low regeneration energies. Specifically, Alstom's Chilled Ammonia Process (CAP) can achieve a 90% CO_2 capture efficiency, >99.5% CO_2 product purity and a potential heat requirement for CO_2 regeneration of <2 MJ/kg CO_2 (Kozak *et al.*, 2009; Telikapalli *et al.*, 2011). Powerspan has developed the ECO-SO_2 process in which SO_2 present in the flue gas is used to recover and reutilise the vaporised NH_3 for the production of value added sulphur fertilizers. In collaboration with Delta Electricity, the CSIRO evaluated the NH_3 process in pilot-plant trials at Munmorah power station, New South Wales, Australia. An 80–90% CO_2 removal efficiency and >95% SO_2 removal efficiency were obtained with a CO_2 product purity of >99% (Yu *et al.*, 2011; Yu *et al.*, 2012).

Parallel to the field tests, modelling studies have been conducted to evaluate the energy penalty and economics of the NH_3-based capture processes, and these revealed that the NH_3-based technology consumes less regeneration energies than the MEA processes. Specifically, Darde et al. (2012) developed an Extended UNIQUAC model to thermodynamically simulate the CAP process, and the total heat requirement for CO_2 stripper and NH_3 stripper was estimated to be less than 2.7 MJ/kg CO_2. Niu et al. (2013) proposed a novel, aqueous NH_3-based PCC process and their thermodynamic analysis showed that energy consumption for CO_2 stripper was as low as 1.3 MJ/kg CO_2. Dave et al. (2009) claimed that by using 5% NH_3 solution the reboiler duty in the stripper was 2.9 MJ/kg CO_2 when the NH_3 process was integrated with a 500 MW coal-fired power plant. It is also estimated that the cost for CO_2 capture using aqueous NH_3 could be significantly lower than that for amines. A scoping study by the US Department of Energy suggested that the incremental cost of electricity using NH_3 could be less than half of that of traditional amines (Ciferno *et al.*, 2005). Therefore, the NH_3-based CO_2 capture technology has the potential to be technically and economically superior to the MEA solvent and also has the potential for promising application on a commercial scale.

1.2 Motivation for this thesis

Although the advantages of the aqueous NH_3-based CO_2 capture process were identified, the pilot-plant trials and modelling studies also revealed several technical and economic challenges of NH_3-based CO_2 capture technology, i.e. high NH_3 slip, a relatively high parasitic energy penalty involved in the capture process and high economic burdens in commercial implementation.

1.2.1 Issue of NH_3 loss

The most critical challenge is the high NH_3 slip due to its intrinsic high volatility. CSIRO conducted the CO_2 absorption process at relatively high temperatures (10-30 °C), resulting in a high NH_3 loss of over 10,000 parts per million in volume (ppmv), and high capital and running costs for the recovery of the vaporised NH_3. In addition, these trials by CSIRO also identified that the NH_3 vaporisation led to a practical issue of solid precipitation in the stripper condenser and reflux line, which caused the shutdown of a plant's operation (Yu *et al.*, 2012). To alleviate NH_3 emissions, the Alstom's CAP process has been designed to operate at low absorption temperatures (0-10 °C), but this occurs at the expense of a high chilling duty and problems in slurry handling. The drastic NH_3 loss requires both a high NH_3 makeup to keep the solvent NH_3 concentration constant in the capture process and more energy to recycle the slipped NH_3. Moreover, NH_3 itself is a hazardous gas that threatens the health of human beings and animals. Therefore, the NH_3 concentration should be controlled at < 25 ppmv in the workplace according to the United States National Institute of Occupational Safety and Health (NIOSH) (Busca *et al.*, 2003), and the NH_3 emission level is recommended to be controlled at less than 50 ppmv in industrial emissions according to the Korean government regulation of industrial exhaust gas (Han *et al.*, 2013).

Currently, the most common method of controlling NH_3 loss is by installing a separate NH_3 abatement system, which consists of an NH_3 absorber and NH_3 stripper, to capture and recycle vaporised NH_3 using a large amount of wash water. This method has been widely employed in many processes, such as the Alstom's CAP process and the KIER process. However, this conventional NH_3 recovery method places an extra energy consumption burden on the entire CO_2 capture system. Specifically, the thermodynamic analysis of Alstom's CAP process by Mathias et al. (2010) shows that the NH_3 abatement regenerator duty reached 2377 kJ/kg CO_2, while the CO_2 stripper duty was only 2291 kJ/kg CO_2 under the conditions of 26 wt% NH_3 and 10 °C absorption temperature. Niu et al. (2013) carried out a rigorous simulation of the CO_2 capture process by aqueous NH_3 at room temperature and normal pressure, in which the energy consumption for the NH_3 abatement system (1703 kJ/kg) was much higher than that for CO_2 regeneration (1285 kJ/kg CO_2). Both studies indicate that the energy penalty for recovering slipped NH_3 might be equivalent to or more than the energy

penalty for CO_2 capture alone. Although Darde et al. (2012) claimed that the heat requirement for the NH_3 stripper in the CAP process can be reduced to 167 kJ/ kg CO_2 after configuration improvement. It is worthwhile to mention that this result is based on the availability of low temperature cooling water, and the low temperature absorption process have to deal with the crystallization problem (Darde *et al.*, 2012). Therefore, the substantial energy consumption and the operation issues of the NH_3 recovery process makes the NH_3-based CO_2 capture technology less competitive.

To resolve the problem of NH_3 slip, the United States-based company Powerspan has developed an 'ECO_2' process which is integrated with the 'ECO' multi-pollutant control system and takes the advantage of NH_3 process's multi-capture of CO_2 and SO_2. It is claimed that this process can reuse the vaporised NH_3 to remove SO_2 and produce ammonium sulphate fertiliser (McLarnon *et al.*, 2009). However, no detailed reports on the performance of the process are available in the open literature. Even if the 'ECO_2' process is applied, it would face the challenge of the SO_2 concentration in the flue gas being variably dependent on the types of coal and boilers used, but generally being below 2000 ppmv. This concentration only requires up to 4000 ppmv NH_3 to stoichiometrically produce ammonium sulphite/sulphate. However, the NH_3 concentration in the flue gas leaving the absorber varies with the operating temperature and is generally >4000 ppmv. This will make it difficult to maintain the material balance between SO_2 and NH_3 in the combined process. To make the NH_3 process competitive over other solvents, it is both essential and imperative to develop effective approaches to solving the NH_3 slip problem and reducing the energy loads of the NH_3 recovery system.

1.2.2 Issue of high energy burden

Another major challenge faced by the aqueous NH_3-based CO_2 capture process is high parasitic energy consumption. Although the NH_3-based capture process uses less solvent regeneration duty than the MEA process, the energy consumption still renders the implementation of the NH_3 process unaffordable on a commercial scale. For instance, Linnenberg et al. (2012) investigated an integration of an aqueous NH_3 process with a hard-coal-fired power plant, and found that the capture process led to a 20-25% reduction of net power plant efficiency at 90% CO_2 capture efficiency. Versteeg et al. (2011) modelled an NH_3-based CO_2 capture process, and their results show that the NH_3 process reduced electricity output from the coal-fired power station

by 29%, with solvent regeneration energy being the largest contributor, accounting for over 50% of total energy consumption. Thus, reducing the energy requirement of solvent regeneration is imperative in order to improve the technical and economic feasibility of NH_3-based capture technology.

Process improvements can be regarded as a simple, quick but effective approach since they build on the existing technologies and require minimum modifications to be made to the well-established processes. For this reason, considerable efforts have been devoted to process improvements, including the parameter optimization (Abu-Zahra *et al.*, 2007; Salkuyeh *et al.*, 2013) and flow sheet modifications (Cousins *et al.*, 2011a; Moullec *et al.*, 2014), with the aim of significantly reducing the energy requirement involved in the CO_2 capture process. Cousins et al. screened fifteen different process flow sheet configurations and concluded that a considerable reduction of energy consumption can be achieved by process modifications (Cousins *et al.*, 2011a). Moullec et al. (2014) investigated twenty elementary process modifications and found that an energy reduction of up to 45% could be achieved dependent on the complexity and combinations of different process modifications. With respect to the application of process modification in the NH_3 process, Jilvero et al. (2014b) found that a staged absorption can significantly reduce NH_3 vaporisation and thus decrease the energy penalty of NH_3 recovery. The work by Yu et al. (2014a) showed that the rich-spit process can help reduce energy consumption and eliminate solid precipitation in the overhead condenser. These previous studies suggest that there is considerable room for energy reduction in solvent regeneration by process improvements.

1.2.3 Issue of high economic burden

In addition to the technical challenges for the aqueous NH_3 process, its high investment of capital cost is also an important barrier that constrains its commercial-scale implementation (Versteeg *et al.*, 2011). While most current work focuses on technical assessment and improvement of the NH_3-based capture process, less attention is paid to the economic performance of the NH_3 process being integrated with coal-fired power stations. The number of economic assessments of the NH_3 process is very limited in the open literature, resulting in a lack of knowledge regarding the economic performance of NH_3-based CO_2 capture processes. Moreover, as mentioned above, the process improvements can improve the technical performance of the CO_2 capture process, particularly in reducing the energy consumption. However, the overall

economic benefits from the process improvements are still uncertain, because most flow sheet modifications require additional equipment and piping, and will increase the total capital investment, which may offset the energy savings from process improvements. Therefore, a techno-economic analysis, which considers not only the energy performance, but also the extra equipment required and the additional cost involved, is essential to evaluate the integrated process improvements in the NH_3 process, and to determine whether or not they are both technically and economically feasible.

1.3 Contributions of the thesis

Corresponding to the identified issues, the proposed research program is dedicated to the process design, technical improvement and techno-economic evaluation of the aqueous NH_3-based PCC technology to attain a technical advancement for NH_3 technology and to achieve a cost reduction compared to MEA-based capture technology. The overall objectives of this thesis are to make use of the advantage of the NH_3 solvent and more importantly to develop new approaches to addressing the issues and advancing the NH_3-based capture process. The specific scope and objectives of this study are as follows:

1) Process design: development of an effective NH_3 abatement and recycling system to solve the issues of NH_3 loss, NH_3 make-up and flue gas cooling in the NH_3-based CO_2 capture process.
2) Simultaneous capture of CO_2 and SO_2: development of an effective combined SO_2 removal and NH_3 recycling system for the simultaneous capture of CO_2 and SO_2 for the cost reduction of controlling CO_2/SO_2 emissions from coal-fired power stations;
3) Energy reduction: development of an advanced aqueous NH_3-based capture process that integrates the NH_3 recycling system and SO_2 removal system and the process improvements (parameters optimizations, absorber modifications and stripper modifications) to significantly improve the energy performance of NH_3-based CO_2 capture process.
4) Techno-economic evaluation: detailed technical and economic assessment of advanced aqueous NH_3-based capture process integrated with a 650 MW coal-fired power station to evaluate its technical performance and economic viability compare to the MEA process.

In addition to the above work, the author has also conducted other relevant research work during the Ph.D. study, which is not presented in the main content of the thesis but is included in the appendices as supporting materials for this thesis. As the MEA is the benchmark solvent for CO_2 capture from coal-fired power stations, the NH_3-based CO_2 capture should be compared with the MEA process to demonstrate its benefits. A rate-based mode for MEA process is developed and validated, and then used in the comparison of technical and economic performance between the NH_3 process and MEA process. To reduce NH_3 vaporisation, transition metals ions (Ni(II), Cu(II) and Zn(II)) were introduced into the NH_3 solution to mitigate the NH_3 volatilisation via their complexation capability with an NH_3 ligand. Experiment work and theoretical analyses were conducted to examine the effectiveness of this approach. Specifically, these studies include:

1) Systematic study of aqueous MEA-based CO_2 capture process: rate-based model development and process improvement based on the PCC pilot plant, Tarong power station, Australia.
2) Systematic study of aqueous MEA-based CO_2 capture process: techno-economic assessment of the MEA process and its process improvements integrated with a 650 MW coal-fired power station.
3) Theoretical and experimental study of NH_3 suppression by addition of Me(II) ions (Ni, Cu and Zn) in an NH_3-based CO_2 capture process.

1.4 Structure of this thesis

To illustrate the research contribution, the roadmap of this thesis is depicted in Figure 1.1 and the descriptions of each chapter are explained as follows.

Chapter 1: This chapter briefly introduces the current research status of the aqueous NH_3-based CO_2 capture process and points out the critical challenges faced by the NH_3 technologies. The objectives and structure of this thesis are also summarised in this chapter.

Chapter 2: This chapter presents the literature review of the state-of-the-art CCS technologies, particularly with regards to the PCC technologies that include the amine scrubbing and NH_3-based CO_2 capture process. The pilot- and demonstration-scale

application and modelling work of NH_3-based CO_2 capture process is reviewed in detail.

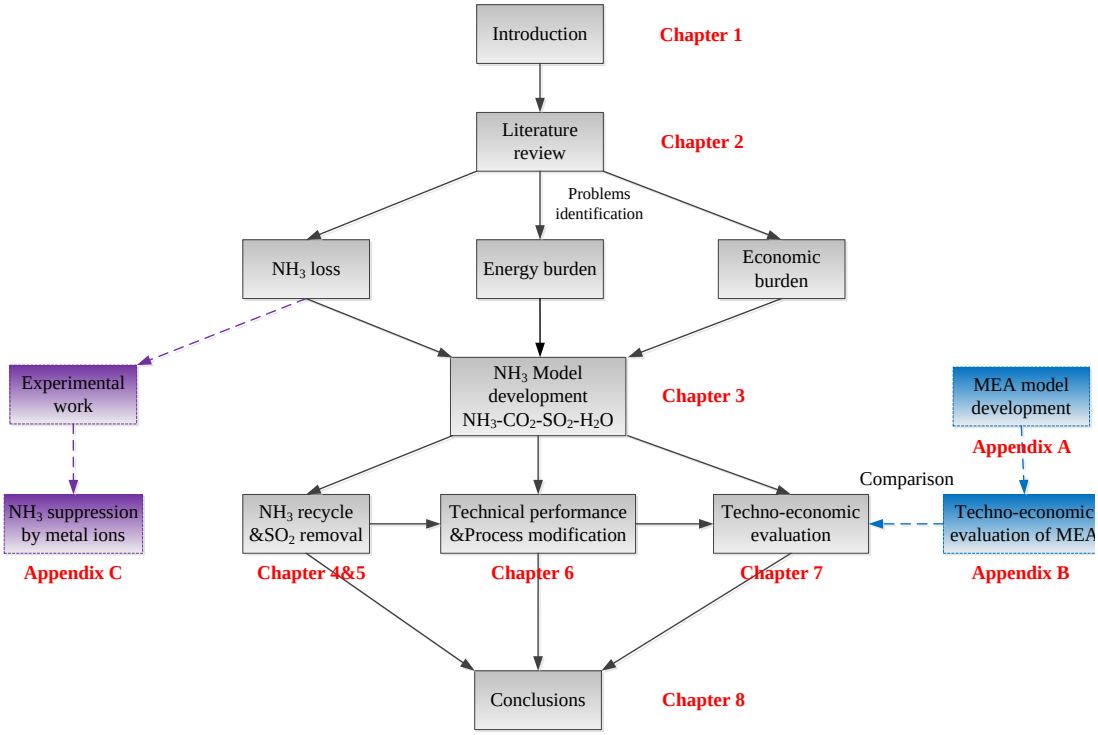

Figure 1-1 Roadmap of this thesis

Chapter 3: This chapter describes the model development and model validation. Using the commercial software Aspen Plus®, the rigorous rate-based model of NH_3-CO_2-SO_2-H_2O system is developed and validated by experimental data including those from open literature and CSIRO pilot trials at Munmorah Power Station, New South Wales, Australia. This model is used as a starting point and a guide for modelling more sophisticated NH_3-based CO_2 capture processes, such as process design development, debottlenecking, plant and equipment design, etc.

Chapter 4: This chapter proposes an advanced process design of an effective NH_3 abatement and recycling system that makes excellent use of the waste heat in flue gas to solve the problems of NH_3 slip, NH_3 make-up and flue gas cooling in the CO_2 capture process. The process parameters are optimised to improve the NH_3 abatement and recycling system and achieve a high NH_3 recycling efficiency with a low energy requirement. The mass balance and stream temperature profiles of this system are also discussed.

Chapter 5: This chapter proposes an advanced and effective process of combined SO_2 removal and NH_3 recycling which can be integrated with the aqueous NH_3-based CO_2 capture process to simultaneously achieve SO_2 and CO_2 removal, NH_3 recycling and flue gas cooling in one process. The behaviours of SO_2 removal and NH_3 recycling in the proposed process configuration are analysed. The feasibilities of the process under different scenarios, such as high SO_2 concentration in the flue gas, high NH_3 content from the CO_2 absorber and high-temperature flue gas, are also discussed.

Chapter 6: This chapter assesses the technical improvement and energy performance of an advanced, aqueous NH_3-based post combustion capture process integrated with a 650 MW coal-fired power station. The important process parameters are optimised to minimise the energy consumption involved in the CO_2 capture process. The absorber modification of two-stage absorption is introduced to mitigate the NH_3 loss. Stripper modifications of the rich-split process and inter-heating process are investigated to further reduce solvent regeneration energy. The mass balance and energy consumption of the CO_2 capture system are discussed in detail.

Chapter 7: This chapter examines the technical and economic evaluation of an advanced NH_3-based CO_2 capture process that is integrated with a 650 MW supercritical coal-fired power station. The techno-economic performances of the process improvements are explored to understand the trade-off between the increased capital cost and the reduced energy consumption. The comparison with the benchmarking MEA process is discussed. A sensitivity analysis is carried out to understand how the economic viability is affected by the economic variables and to identify the technical directions to advance the NH_3-based CO_2 capture process.

Chapter 8: This chapter draws the main conclusion of the thesis. The recommendations and identification of possible future research directions are made to further advance the aqueous NH_3-based CO_2 capture process.

Appendix A: This appendix provides the information of the model development of the MEA-based CO_2 capture process for the purpose of comparison with the NH_3 process. The rate-based model is validated by pilot plant data at Tarong Power Station, Queensland, Australia.

Appendix B: This appendix explores the techno-economic performance of the MEA-based CO_2 capture process**.** The technical performance of the entire MEA process is

presented using the rate-based model, while the cost performance of the MEA process is investigated using a comprehensive cost model. The same cost methodology as NH_3 process is applied to MEA process to make a consistent comparison between these two processes.

Appendix C: This appendix introduces a promising approach to mitigate the NH_3 slip during the capture process. It experimentally and theoretically investigates the potential of three transition metal ions – Ni(II), Cu(II) and Zn(II) – as additives to suppress NH_3 volatilisation by making use of their complexation capability with NH_3 ligand.

Some contributions of this study have been published as journal articles, and these materials are reused in the thesis with permission from the publishers (Appendix D).

Chapter 2 Literature Review

2.1 Global warming

Climate change, due to the emission of greenhouse gas (GHG) caused by human activities, is now well accepted, and has led to a great number of initiatives to reduce the pace of global warming. CO_2 is considered to be the primary greenhouse gas responsible for global warming and climate change. Driven by population growth and industrial civilisation, climate scientists have observed that the average atmospheric CO_2 level has increased significantly over the past centuries, from 280 ppmv in the pre-industrial period to the record high level of 396 ppmv in 2013. Accordingly, the average global surface temperature increased by 0.6°C -1 °C over the same period. The Fifth Assessment Report from the Intergovernmental Panel on Climate Change (IPCC Working Group III) states that, without considerable efforts to reduce GHG emissions, the atmospheric CO_2 concentration will continue to increase, exceeding 450 ppmv by 2030, and will reach between 750−1300 ppmv by 2100 (Pachauri *et al.*, 2014). This will result in a rise of the mean global surface temperature of about 3.7 °C−4.8 °C in 2100 compared to the pre-industrial temperature. To limit the temperature increase to below 2 °C, the atmospheric CO_2 level has to be restricted to less than 450 ppmv by substantial cuts in anthropogenic CO_2 emissions by 2050, through large-scale changes in energy systems and land use (IEA, 2014a; Li *et al.*, 2013).

Among a series of human activities that generate GHG, the energy system is the largest emission source, which accounts for 69% of the total GHG emissions. Within the energy sector, the combustion of fossil fuel produces more than 80% of the total energy supply worldwide, and thus is the major contributor for the increasing atmospheric CO_2 concentration. The combustion of coal, as a cheap fossil fuel and mature technology in commercial application, is one of the world's most important energy supplies. Given the growing population and economic growth of developing economies, coal will still continue to play an important role in powering the world's economy in the foreseeable future, particularly in those countries that are heavily dependent on coal for power generation (IEA, 2014b). For instance, in China more than 80% of their electricity is generated by coal combustion (Zhou *et al.*, 2010), while in Australia about 75% of power generation is coal based (Dave *et al.*, 2008). However, burning coal for power generation places a heavy burden on CO_2 emissions due to the

high carbon intensity per unit of energy generation. For instance, coal combustion supplies only 29% of global energy, but contributes to 44% of global CO_2 emissions (IEA, 2014a), as shown in Figure 2-1. It is therefore clear that CO_2 emission reduction strategies aimed at existing thermal power plants such as coal-fired stations are of extreme importance and are urgently needed to provide a path towards slowing down the pace of global warming

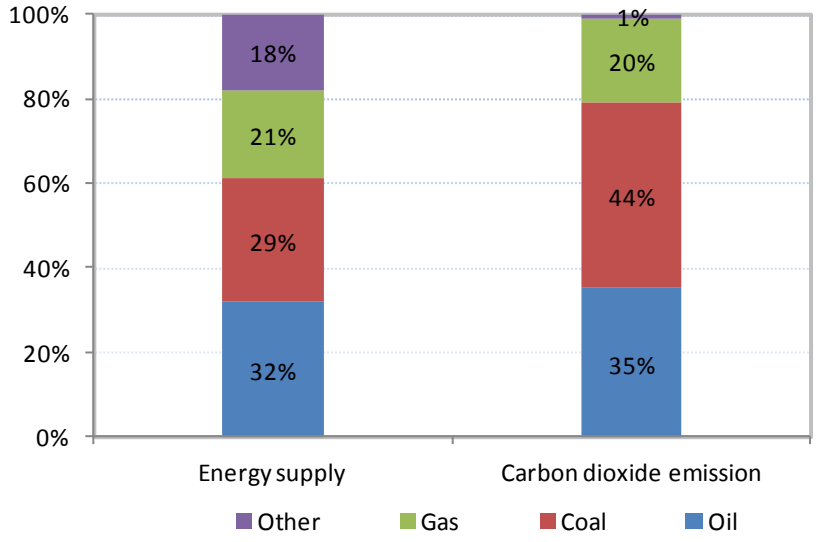

Figure 2-1 The worldwide energy supply and CO_2 emissions in 2012

To reduce the amount of CO_2 emissions from the energy system, there are several possible strategies which include: the improvement of energy conversion efficiency, an increase in the use of low carbon fuel, the deployment of renewable energy and CO_2 capture and storage. Among these approaches, capturing CO_2 and its geological sequestration is considered to be a promising route for achieving a significant mitigation of CO_2 emission in the near to medium term, and one which allows the continuous use of cheap coal until energy efficiency is significantly increased and new low-cost renewable energy systems are developed for commercial application (Li *et al.*, 2013). It is estimated that by 2050 CCS technology has the potential to reduce by 20% the CO_2 emissions that are produced from the energy system (Haszeldine, 2009). Furthermore, the captured CO_2 from CCS could be utilised as a carbon source for chemical processing and production, or for physical uses in the gas and petroleum industries such as: enhanced oil recovery, enhanced coal bed methane, etc. This gives CCS technology strong economic viability once the CO_2 utilization technology is developed for commercialization.

2.2 CO_2 capture technologies

Currently, there are three primary CO_2 capture systems that are generally accepted to be suitable for commercial application in the near or medium term: pre-combustion, oxy-fuel combustion and post-combustion. Figure 2-2 illustrates the schematics of the three CO_2 capture technologies and the brief descriptions are discussed below.

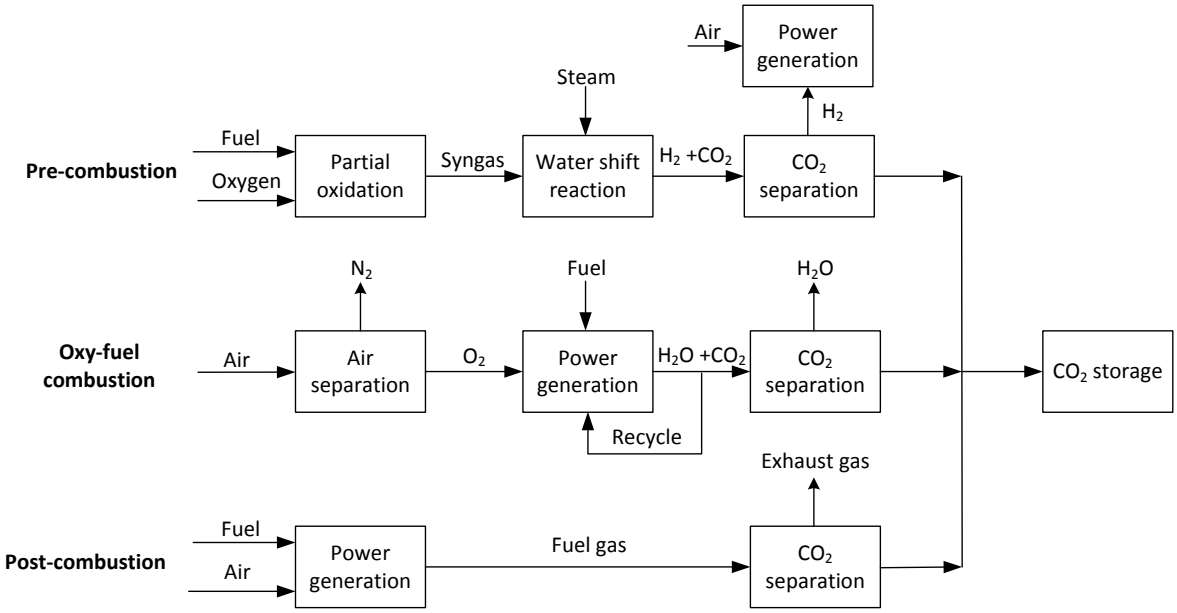

Figure 2-2 Schematic flow sheet of CO_2 capture technologies: pre-combustion, oxy-fuel combustion, post-combustion (Mondal *et al.*, 2012)

In the pre-combustion process, fuels such as coal and natural gas are pretreated with steam and oxygen or air to generate the synthesized gas consisting primarily of carbon monoxide (CO) and hydrogen (H_2). The synthesized gas undergoes further treatment via its reactions between CO and steam to produce more H_2 and CO_2. The resulting mixed gas contains a high CO_2 concentration of >20%, which facilitates CO_2 separation. The product H_2 is a carbon-free energy carrier and is ready to be combusted for heat/power generation. This capture process can be implemented in the integrated gasification combined cycle (IGCC) power station but at the expense of an energy efficiency penalty of 7-8% or more (Leung *et al.*, 2014).

In the oxygen-combustion process, the air is replaced by highly concentrated oxygen to combust the fossil fuel, thus reducing the nitrogen level and increasing the CO_2 concentration in the combusted flue gas. The particulates and SO_2 pollutants are first removed by conventional technologies, e.g. electrostatic precipitator and flue gas

desulphurisation. The resultant CO_2 concentration reaches 80-98%, which can be compressed directly for subsequent CO_2 transportation and sequestration. However the oxy-fuel process requires a great amount of pure oxygen from the energy-intensive air separation unit. The substantial energy use required for the oxygen separation results in an energy penalty of >7%. Moreover, the high SO_2 concentration in the flue gas would cause a serious corrosion issue.

In the post-combustion process, the CO_2 is first captured from flue gas after the fossil fuel combustion. After the CO_2 is separated from the capture agent, it is compressed for transportation and sequestration. The post-combustion technologies provide many advantages: (I) a high-purity CO_2 product of over 99%; (II) relatively easy deployment for retrofitting the existing fossil fuel power station; and (III) mature technology development for commercial application. However, this process is also confronted by some challenges, with the most critical one being the large parasitic energy consumption, leading to an energy penalty of overall thermal efficiency of over 7% (Black, 2010; Haszeldine, 2009). The world's first commercial CO_2 capture plant using post-combustion technology has been constructed, commissioned and operated at SaskPower Boundary Dam Power Station in Estevan, Saskatchewan, Canada (Stéphenne, 2013).

Among the three technologies, post-combustion CO_2 capture technology is often considered to be the most feasible option for the large-scale removal of CO_2 from flue gases emitted from power plants and other industries. There are several post-combustion technologies available for capturing CO_2 from fossil fuel based power stations, which involve chemical absorption, physical-chemical adsorption, membrane separation, etc. It is generally accepted that solvent-based chemical absorption is the most mature technology for commercial use. This chapter primarily focuses on the state-of-the-art amine technology and emerging NH_3-based technologies. Other capture technologies, such as ionic liquid, metal organic frameworks and enzyme based system, also hold promising prospects due to their unique properties of CO_2 capture. As these technologies are in the very early stage of commercial development, the details are not discussed in this dissertation.

2.3 Amine scrubbing technology

Fossil fuel based power stations usually use air as their oxygen source for fuel combustion, and emit low CO_2 concentration (< 15%) flue gases due to the large amount of Nitrogen present. Such a low CO_2 partial pressure leads to a limited thermodynamic driving force of CO_2 capture from flue gas, thereby posing some technical difficulties for the development and implementation of CO_2 capture technologies. Aqueous amine solvent can react with CO_2 and generate the water soluble compound amine-CO_2, which allows for the amine solvent to be capable of absorbing CO_2 at low partial pressure and a resultant high CO_2 removal efficiency. In conventional amine scrubbing, the CO_2 is absorbed at low temperatures (~40 °C), while being desorbed at high temperatures (120 °C ~ 150 °C). The CO_2 can be continuously captured from flue gas via an absorption/desorption process. This schematic flow sheet is described in Figure 2-3.

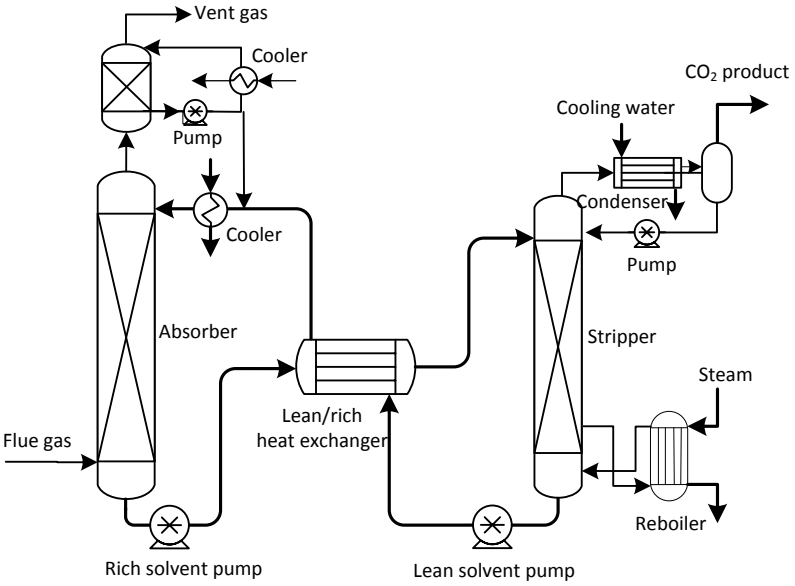

Figure 2-3 Schematic flow sheet of amine scrubbing process

The amine scrubbing technology for the removal of acid gas in the gas processing industry has been developed for decades, though not for CO_2 capture from power stations. The industrial practice of amine technology provides a wealth of knowledge, expertise and engineering experience for the application of CO_2 capture on a large scale. So the amine scrubbing technology is most likely to be the dominant technology for commercial-scale CO_2 capture from the coal-fired power station before 2030 (Rochelle, 2009).

Typical amine solvents used for CO_2 capture include three categories: primary amines such as MEA, secondary amines such as diethanolamine (DEA) and tertiary amines such as N-methyldiethanolamine (MDEA). Basically, their reaction rates with CO_2 are in contrast with their CO_2 absorption capacities. Specifically, the reaction constants with CO_2 at 25 °C are 7000 L/mol-sec for MEA, 1200 L/mol-sec for DEA and 3.5 L/mol-sec for MDEA (Bishnoi *et al.*, 2002; Hikita *et al.*, 1979; Sada *et al.*, 1976), while their theoretical CO_2 capacities are 0.5, 0.5, 1.0 mole CO_2/mole amine for MEA, DEA and MDEA, respectively. Their respective reactions with CO_2 are described below (Chowdhury *et al.*, 2013; Yu *et al.*, 2012a).

For the primary and secondary alkanolamines, the reaction mechanism involves three steps:

Zwitterion formation:

$$CO_2 + R^1R^2NH \leftrightarrow R^1R^2NH^+COO^- \quad (2\text{-}1)$$

Carbamate formation:

$$R^1R^2NH^+COO^- + R^1R^2NH \leftrightarrow R^1R^2NCOO^- + R^1R^2NH_2^+ \quad (2\text{-}2)$$

The overall reaction:

$$CO_2 + 2R^1R^2NH \leftrightarrow R^1R^2NCOO^- + R^1R^2NH_2^+ \quad (2\text{-}3)$$

Part of reaction product undergoes the conversion from carbamate to bicarbonate through the hydrolysis process.

Bicarbonate formation:

$$R^1R^2NCOO^- + H_2O \leftrightarrow R^1R^2NH + HCO_3^- \quad (2\text{-}4)$$

For the tertiary alkanolamine, the mechanism involved in the CO_2 absorption process is different with the primary/secondary amines. The tertiary amine does not react with CO_2 directly, but acts as a base to catalyse the hydration of CO_2 and generate the bicarbonate.

Bicarbonate formation:

$$R^1R^2R^3NH + H_2O + CO_2 \leftrightarrow R^1R^2R^3NH^+ + HCO_3^- \quad (2\text{-}5)$$

From reaction (2-1) to (2-5), it can be seen that the reactions between CO_2 and the primary/secondary amine are brought about to generate the carbamate via zwitterion formation, while the tertiary amine tends to form the bicarbonate instead of carbamate. Due to the formation of stable carbamate, the primary/secondary amines usually

require more heat duty for CO_2 stripping than the tertiary amine (Chowdhury *et al.*, 2013). One solvent alone seems not to be technically and economically applicable for CO_2 capture. The blends of amines are considered to be a promising and attractive approaches to taking advantage of the high CO_2 reaction rate from the primary/secondary amines, and high CO_2 capacity and low regeneration energy from the tertiary amine. Here are two examples.

The MEA solvent, as a simple primary amine, is often considered to be the benchmarking solvent to which alternative solvents must be compared. This is because of its commercial availability, relatively low cost, fast absorption rate and rich commercial experience in various industrial applications. However, its application for CO_2 capture is highly limited by drawbacks including: the low CO_2 absorption capacity, high energy requirement, solvent degradation by acid gas pollutants and oxygen, etc. The sterically hindered amine, 2-amino-2-methyl-1-propanol (AMP) is an attractive alternative solvent because it provides high absorption capacity with 1.0 mol CO_2/mol amine, low regeneration energy requirement and degradation resistance, while its CO_2 absorption rate is much lower than that of MEA. The solvent blend of MEA/AMP has the potential to utilise both advantages. Comparative studies have been conducted to reveal that MEA is superior to AMP in terms of CO_2 removal efficiency while AMP has advantages over MEA with respect to its CO_2 absorption capacity. The CO_2 removal rate increases with the increase in MEA concentration, while the CO_2 loading increases with the increase in AMP concentration (Dey *et al.*, 2009; Sakwattanapong *et al.*, 2009).

Piperazine (PZ) is a cyclic amine with two secondary amine nitrogens and has the advantages of a fast reaction rate with CO_2, high capacity and high resistance to oxidation and thermal degradation (Freeman *et al.*, 2010). It is widely recognized as an effective rate promoter in amine solutions to improve the kinetics and subsequently enhance the performance of CO_2 absorption (Bishnoi *et al.*, 2002; Bougie *et al.*, 2009). The research carried out at the University of Texas at Austin shows that the reaction rate between aqueous PZ and CO_2 is 2-3 times faster than that of MEA at equivalent CO_2 partial pressure, and 8 mol PZ has a CO_2 absorption capacity of 75% greater than that that of 7 mol MEA in various CO_2 loadings (Dugas *et al.*, 2009). The various investigations on the PZ blends, such as PZ/MDEA (Frailie, 2014) and PZ/MEA (Dugas, 2009), reveal that the CO_2 partial pressure in a certain CO_2 loading in the

blended solvent is lower than that in the individual solvent without PZ, indicating that the PZ promoted solvent has better CO_2 absorption performance.

However, amine scrubbing technology is confronted with several limitations, the most critical one being intensive energy consumption. Installing the current amine capture process in a coal-fired power plant would lead to a decrease of overall thermal efficiency by 25−40% and an increase of the cost of electricity by 70−100% (DOE, 2010; Haszeldine, 2009). The capital investment for the CO_2 capture plant is also a great challenge for commercial implementation. The large volume of flue gas and low CO_2 partial pressure require sizeable columns and a large amount of packing materials to achieve a high CO_2 removal efficiency. In addition, the amine technology requires clean flue gas with a low SO_X and NO_X concentration, which requires extra facilities and equipment for the SO_X/NO_X removal, resulting in additional capital investment. Thus, the CO_2 capture process is energy-intensive and capital-intensive, resulting in the total cost for capturing the CO_2 from coal fired power station being in the range of 52–77 US$/tonne CO_2 (Rochelle, 2009).

The amine degradation issue during the absorption and desorption process is another major challenge involved in amine scrubbing technology. For instance, the degradation causes MEA solvent loss rate at a rate of 0.35 and 2.0 kg per tonne of CO_2 captured, resulting in a great amount of MEA make-up and an increase in operating costs (Bailey *et al.*, 2005). Generally, the degradation can be classified into three categories: oxidative degradation in the presence of O_2; thermal degradation at a high temperature; carbamate polymerization (Goff *et al.*, 2006); and degradation by the acid gas pollutants, such as SO_X and NO_X which are present in the flue gas from power station. The amine degradation usually generates irreversible products, which not only require a large amount of amine make-up to maintain the solvent concentration, but also cause operational and environmental concerns. It is worth mentioning that the degradation process would be more complicated under industrial conditions, and the degradation mechanisms are still poorly understood when the amine solvents are simultaneously subject to CO_2, O_2, SO_2, NO_X, CO, fly ash and high temperatures in the flue gas.

2.4 NH_3-based CO_2 capture technology

NH_3, as an alternative solvent to amines, has received significant attention in the last decade, as it has several obvious advantages over amine solvents. Specifically:

- Aqueous NH_3 has a favourable CO_2 absorption capacity with stoichiometric 1.0 mol CO_2/mol NH_3, and a high capture efficiency of over 90% due to the low partial pressure of CO_2 at low temperatures (Yeh *et al.*, 1999). The NH_3 has a small molecule weight (MWt = 17), leading to a better CO_2 capacity (by weight) in comparison to the other amines, such as MEA (MWt = 61) under the same molar concentrations. It can be calculated that the NH_3's capacity for CO_2 loading is more than 7 times the aqueous MEA as per its weight ratio and stoichiometric absorption capacity/level. Specifically, 1 mol NH_3 (17 g) absorbs 1 mol CO_2 (44 g), while 1 mol MEA (61 g) absorbs 0.5 mol CO_2 (22 g), resulting in the NH_3's superiority of CO_2 capacity of 7.1 over MEA (44/17 vs 22/61).
- The solvent regeneration of the NH_3 process requires less energy than that of MEA solvents (Abu-Zahra *et al.*, 2007; Jilvero *et al.*, 2012; Shakerian *et al.*, 2015). One important reason for this is that the enthalpy of CO_2 absorption by NH_3 (60-80 kJ/mol (Que *et al.*, 2011) is lower than that of the MEA solvent (80-90 kJ/mol (McCann *et al.*, 2008)) in a 0-0.5 CO_2 loading. Another important reason for the lower heat requirement is that both the thermodynamic properties and high resistance to the thermal degradation allow for NH_3 to be regenerated at pressurised conditions, which reduces the heat of water vaporisation. The high pressure stripping is also very beneficial for the reduction of CO_2 compression duty.
- NH_3 has the simplest molecular structure among the amine derivatives, resulting in high tolerance to the thermal and oxidative degradation. The important reason for the high resistance of NH_3 to degradation might be the simplicity of the NH_3 structure and strong chemical bond between nitrogen and hydrogen. This strong bond makes it very unlikely that it will be broken by the high temperature and oxygen. Even if the bond is broken, the detached proton tends to re-combine with the electron-given nitrogen.
- NH_3 can simultaneously capture the multiple pollutants such as acid gas SO_X, NO_X, CO_2, etc, which exist in the flue gas from coal-fired power stations. Since

the SO_X and NO_X emissions in most countries must comply with the national air pollution control regulation, the NH_3-based CO_2 capture technology has great potential to integrate the various emission control technologies into one single process, thus reducing the system complexity and capital cost. The resultant products contain sulphur and nitrogen, which can be used as fertiliser in the agriculture industry.

2.4.1 Process chemistry

The dissolution and absorption of CO_2 into aqueous NH_3 involves a series of physical and chemical processes. Figure 2-4 illustrates the chemical species and vapour-liquid-solid phase equilibrium in the system of NH_3-CO_2-H_2O.

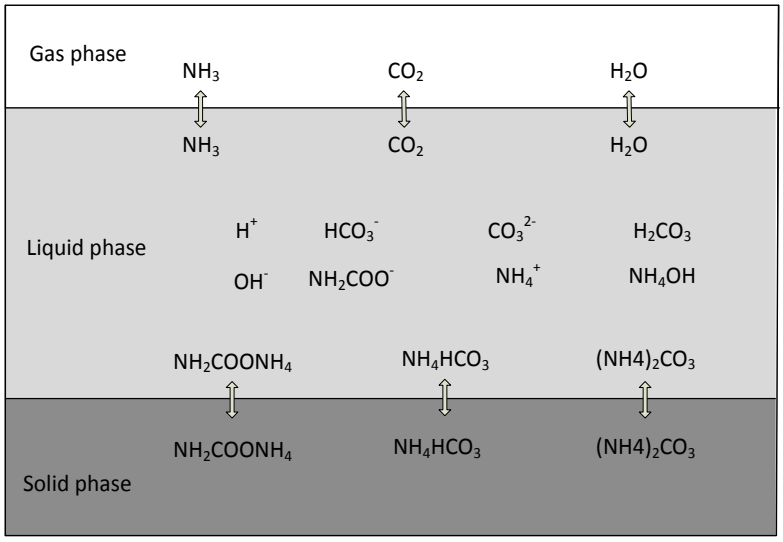

Figure 2-4 Chemical species and vapour-liquid-solid phase equilibrium in the NH_3–CO_2–H_2O system (Shakerian *et al.*, 2015; Zhao *et al.*, 2012)

In the aqueous medium, the CO_2 absorption by aqueous NH_3 involves the following steps.

Carbamate formation:

$$2NH_3 + CO_2 \leftrightarrow NH_2COONH_4 \quad (2\text{-}6)$$

Bicarbonate formation from carbamate hydrolysis:

$$NH_2COONH_4 + H_2O \leftrightarrow NH_4HCO_3 + NH_3 \quad (2\text{-}7)$$

Reaction of NH_3 and H_2O:

$$NH_3 + H_2O \leftrightarrow NH_4OH \quad (2\text{-}8)$$

Carbonate formation:

$$NH_4HCO_3 + NH_4OH \leftrightarrow (NH_4)_2CO_3 + H_2O \quad (2\text{-}9)$$

Bicarbonate formation through CO_2 absorption by $(NH_4)_2CO_3$:

$$(NH_4)_2CO_3 + H_2O + CO_2 \leftrightarrow 2NH_4HCO_3 \quad (2\text{-}10)$$

Solid formation:

$$NH_2COONH_4\ (aq) \leftrightarrow NH_2COONH_4\ (s) \quad (2\text{-}11)$$

$$NH_4HCO_3(aq) \leftrightarrow NH_4HCO_3(s) \quad (2\text{-}12)$$

$$(NH_4)_2CO_3(aq) \leftrightarrow (NH_4)_2CO_3\ (s) \quad (2\text{-}13)$$

The overall reaction of the aqueous NH_3 absorbing CO_2 can be expressed as:

$$NH_3 + CO_2 + H_2O \leftrightarrow NH_4HCO_3 + NH_2COONH_4 \quad (2\text{-}14)$$

In terms of the mechanism, the CO_2 absorption by aqueous NH_3 undergoes a similar pathway to the primary amine (Caplow, 1968; Derks *et al.*, 2009; Qin *et al.*, 2010a). The zwitterion reaction mechanism is well-developed, which accounts for kinetic behaviours in the CO_2 absorption process by aqueous NH_3. In the zwitterion system, the NH_3 first reacts with CO_2 to form the zwitterion molecule (NH_2COOH). The zwitterion is then deprotonated by a base (B). The base can be NH_3, OH^- and H_2O in the NH_3 system. Reactions (2-15) and (2-18) describe the zwitterion reaction mechanism.

$$NH_3 + CO_2 \overset{k_1}{\rightarrow} NH_3^+COO^- \quad (2\text{-}15)$$

$$NH_3^+COO^- \overset{k_{-1}}{\longrightarrow} NH_3 + CO_2 \quad (2\text{-}16)$$

$$NH_3^+COO^- + B \overset{k_2}{\rightarrow} NH_2COO^- + BH^+ \quad (2\text{-}17)$$

$$NH_2COO^- + BH^+ \overset{k_{-2}}{\longrightarrow} NH_3^+COO^- + B \quad (2\text{-}18)$$

The reaction rate between CO_2 and NH_3 can be expressed as:

$$r_{NH_3-CO_2} = \frac{[CO_2][NH_3]}{\left(\frac{1}{k_1}\right)+\left(\frac{k_{-1}}{k_1}\right)(1/\sum k_8[B])} \quad (2\text{-}19)$$

As aqueous NH_3 is a weak alkali solution, the hydroxyl ion (OH^-) also plays an important role in the absorption of CO_2. As suggested by Pinsent *et al.* (1956), the reaction (2-20) should be considered in the CO_2 absorption by aqueous NH_3.

$$CO_2 + OH^- \overset{k_3}{\rightarrow} HCO_3^- \quad (2\text{-}20)$$

The reaction rate between CO_2 and OH^- can be expressed as:

$$r_{OH^- - CO_2} = k_3[OH][CO_2] \quad (2\text{-}21)$$

The overall reaction rate in the CO_2 absorption by aqueous NH_3 is:

$$r_{overall} = r_{NH_3 - CO_2} + r_{OH^- - CO_2} \quad (2\text{-}22)$$

After CO_2 absorption, the regeneration process takes place in the CO_2 stripper, by which the NH_3 is regenerated by the heat for continuous capture, and the CO_2 is stripped out and concentrated for compression, transportation and storage. During the regeneration process, CO_2 will be desorbed by means of serval pathways, which can be summarised as follows (Jilvero *et al.*, 2012):

$$2NH_4^+ + 2HCO_3^- \leftrightarrow 2NH_4^+ + CO_3^{2-} + CO_2 + H_2O \quad \Delta H = 26.88 \text{ kJ/mol} \quad (2\text{-}23)$$

$$NH_4^+ + HCO_3^- \leftrightarrow NH_3 + CO_2 + H_2O \quad \Delta H = 64.26 \text{ kJ/mol} \quad (2\text{-}24)$$

$$NH_4^+ + NH_2COO^- \leftrightarrow 2NH_3 + CO_2 \quad \Delta H = 72.32 \text{ kJ/mol} \quad (2\text{-}25)$$

$$2NH_4^+ + CO_3^{2-} \leftrightarrow 2NH_3 + CO_2 + H_2O \quad \Delta H = 101.22 \text{ kJ/mol} \quad (2\text{-}26)$$

As the CO_2 stripping process is complex, one cannot single out that only one particular pathway dominates the solvent regeneration process. According to the abundant experiment measurements and modelling analyses (Que *et al.*, 2011), the enthalpy of CO_2 reaction with NH_3 is in the range of 60-80 kJ/mol. This suggests that the overall absorption/desorption pathway occurs primarily via the formation of ammonium bicarbonate (2-24) and ammonium carbamate (2-25), which agrees with the conclusion drawn by Jilvero *et al.* (2012).

2.4.2 Process development

Due to the unique properties of NH_3 solvent for CO_2 capture, several pilot and demonstration plants have been constructed and operated by industry and research organisations, such as U.S. based Alstom, Powerspan and the CSIRO, to evaluate the technical and economic feasibility of NH_3 based technology The results from intensive pilot trials imply that NH_3 technology holds the potential to be applied on a commercial-scale. The detailed process descriptions and technical characteristics of the various NH_3-based pilot processes are discussed in the following sections.

2.4.2.1 Alstom's chilled ammonia process

Alstom's chilled ammonia process is one of the leading technologies for CO_2 capture using aqueous NH_3. The CAP was first patented by Gal (2006). The typical feature for this process is the operation of the CO_2 absorption process at a low temperature of

below 10 °C to significantly mitigate NH_3 vaporisation allowing for the use of the high NH_3 concentration (typically 28%). The schematic flow sheet of the CAP process is illustrated in Figure 2-5.

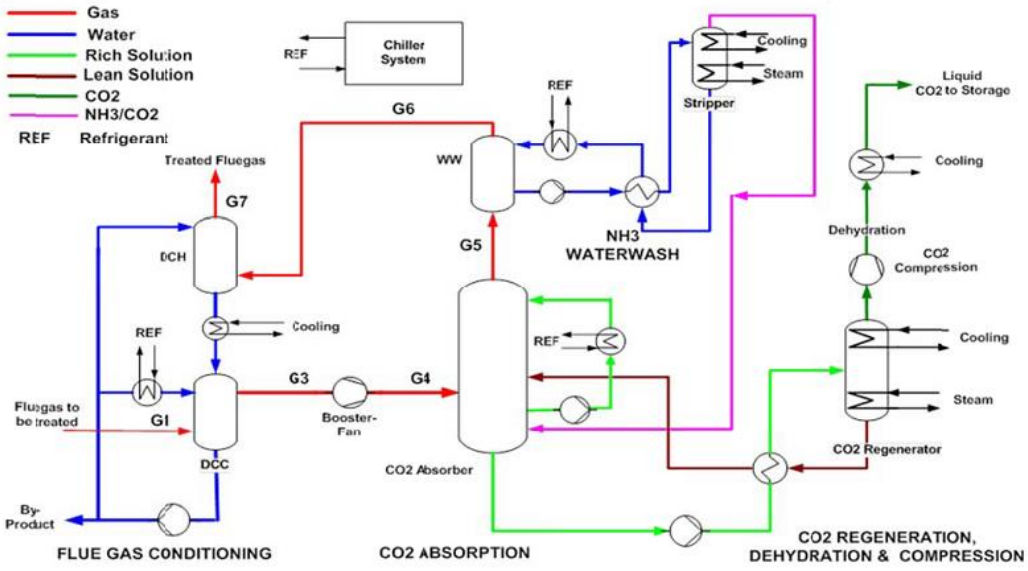

Figure 2-5 Schematic flow sheet of Alstom's CAP process (Lombardo *et al.*, 2014)

Basically, the CAP process is composed of the following operation units: (I) flue gas conditioning, where the feed gas is cooled down to a low temperature (<10 °C) by the direct contact cooler; (II) CO_2 absorber, in which the CO_2 is absorbed at a removal efficiency of 80-90% and the slurry (primarily ammonium bicarbonate) is produced during the absorption due to the low temperature and high NH_3 concentration; (III) water wash, to scrub the slipped NH_3 from CO_2 absorber; and (IV) CO_2 stripper, where the solvent is regenerated at high temperature and CO_2 is stripped out at high purity (>99%); (V) CO_2 compressor, to pressurise CO_2 product into liquid for subsequent transportation and storage.

The first of a kind of CO_2 capture pilot test of the CAP process was carried out in We Energies Field Pilot located at Pleasant Prairie, Wisconsin, U.S.A. The project commenced in June 2008 and operated through October 2009 with a designed CO_2 capture rate of over 15,000 tonnes/ year. In parallel with the pilot test at We Energies, a similar scale CAP field test was constructed and operated at the E.ON Karlshamm power plant in Sweden (Telikapalli *et al.*, 2011). Both of the field tests demonstrated the technical feasibility of the CAP process, production of a CO_2 product of a purity

over 99.5%, a CO_2 capture efficiency approaching 90%, low NH_3 emission of below 10 ppmv and low regeneration duty, etc.

Based on the operational experience and results from the two field tests, Alstom designed two upgraded and advanced demonstration projects of the Production Validation Facility (PVF), which were intended to demonstrate the full CO_2 capture and storage chain. The first PVF project was operated at the AEP Mountaineer Power Plant in New Haven, WVa, U.S.A., and was integrated with a coal-fired power station with a CO_2 capture capacity of 100,000 metric tonnes/year for underground CO_2 storage that were located beneath the plant filed. The second PVF was constructed and is now being operated in Test Centre Mongstad, Norway, with a CO_2 capture capacity of 80,000 metric tonnes/year from the flue gas that is produced by a Fluid Catalytic Cracking Unit and a gas turbine. The two demonstration projects further confirm the feasibility and advantages of CAP technology for CO_2 capture from coal-fired power stations and natural gas or other industries. In addition, the primary advancement of these two projects has been to successfully demonstrate the integration of CO_2 capture with compression and geological storage into an entire CCS chain. A recent publication indicates that Alstom has set up a road map of CCS development, which includes the commercialisation of the CAP process by 2020 (Lombardo *et al.*, 2014).

Although the chilled NH_3 technology seems to be technically mature, there are still some technical and economic issues associated with the CAP technology regarding commercialization. The first one is the high energy consumption for the cooling of the NH_3 solvent and flue gas. As pointed out by Versteeg et al. (2011), the viability of the CAP process is location dependent. A CO_2 capture plant requires direct access to low temperature cooling water, such as a deep water lake or cold ocean water, to reduce the parasitic energy demands for the process chilling duty. If there is no cheap low temperature cooling water (0-10 °C) available near the capture plant, this process is likely to be economically unfeasible. The second is the NH_3 loss issue, because of the high NH_3 concentration (~28 wt%) used to improve the absorption performance (Darde *et al.*, 2010a), even though the chilled temperature significantly suppresses the NH_3 vaporisation. The third issue is the solid precipitation and the slurry handling during the process owing to the low temperature and high NH_3 concentration used, which is a big barrier to engineering and commercialization. At this point in time, there is no appropriate technology to deal with the slurry in a packed column. The most

recent report about the CAP process does not show the slurry handling facility in the process flow sheet (Lombardo *et al.*, 2014). Therefore, it can be speculated that solid precipitation is most likely to be avoided in the CAP process.

2.4.2.2 Powerspan's ECO2 process

In collaboration with the U.S. DOE National Energy Technology Laboratory (NETL), the U.S. based company Powerspan developed a CO_2 capture process using aqueous NH_3, the so-called ECO2 process. The primary characteristic of this process is to use NH_3 to simultaneously capture CO_2 and SO_2. The schematic flow sheet of the ECO2 process is described in Figure 2-6. The process consists of two parts. One is the traditional CO_2 capture process by aqueous NH_3 via absorption and desorption. The distinguished part is the recovery of the vaporised NH_3 and reuse for SO_2 removal, before the flue gas enters the CO_2 capture system. This SO_2 product can be used as sulphur fertilizer for cost compensation.

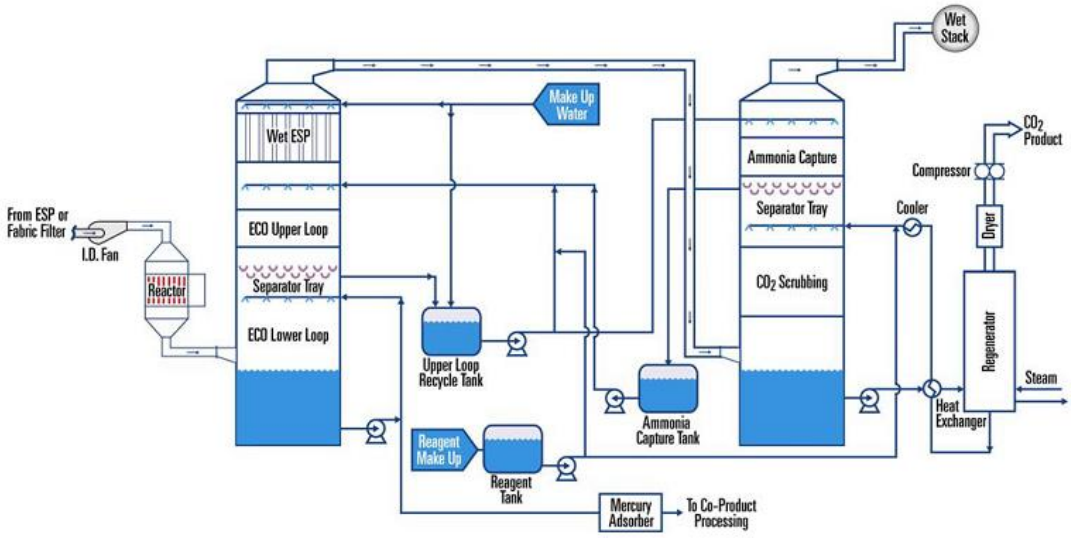

Figure 2-6 NH_3 based ECO2 scrubbing process (McLarnon *et al.*, 2009)

The pilot field test of the ECO2 process has been conducted at First Energy at the R.E. Burger Plant from 2008 (McLarnon *et al.*, 2009). The target is to deal with 1-MW slipstream from coal-fired power station, which is equivalent to the CO_2 capture of ~20 tonnes/day. Worley Parsons evaluated the ECO2 process and concluded that the capture cost (without storage) had the potential to be lower than $40/tonne of CO_2 captured for a project size of 220 MWe coal-fired power stations, based on a technical performance of 90% removal efficiency and low regeneration duty of 2.3 MJ/kg (Powerspan, 2010). It was planned that the ECO2 process would be scaled up to a 120

MW commercialisation process in 2012. However, the initial plan was cancelled. The updated report reveals that the Powerspan changed the solvent from NH_3 to an ammonium/alkali blend solution for CO_2 capture (Duncan *et al.*, 2010). However, a more recent report states that the solvent was replaced with aqueous blend amines (GCCSI, 2012).

Although there is no detailed information from technology owners accounting for the project termination, one can still speculate about some unsolved issues associated with the ECO2 process. As pointed out by Han et al. (2013), the ECO2 process requires a great amount of cooling duty to cool the flue gas. Another major issue is the materials imbalance of the SO_2 capturing process using the slipped NH_3. The amount of the NH_3 evaporated to flue gas in the absorber is not stoichiometrically consistent with the SO_2 concentration in flue gas. This leads to operational difficulties of material imbalance in the SO_2 removal process using the slipped NH_3.

2.4.2.3 CSIRO's NH_3 process

In collaboration with Delta Electricity, CSIRO carried out a pilot test of the NH_3-based CO_2 capture process at Munmorah power station, New South Wales, Australia (the pilot plant was recently relocated to Vales Point power station, NSW, Australia). The pilot plant was constructed in late 2008 and operated from February 2009 to August 2010. Figure 2-7 illustrates the schematic flow sheet of Munmorah pilot plant for CO_2 capture using aqueous NH_3 with two absorbers in parallel.

The design of the Munmorah pilot plant is based on a standard absorption/desorption process flow sheet. The pilot plant is composed of one pretreatment column, two absorber columns with a separate washing column at the top and one stripper. The pretreatment column works as a direct contact cooler for the flue gas and also serves as a scrubber for the removal of SO_2 in the flue gas. The two absorbers provide flexibility in operation with different arrangements (single column or two columns in series or parallel). The CSIRO pilot plant trials confirmed the technical feasibility of the NH_3 based capture process and some of the benefits expected. A CO_2 removal efficiency of 70- 85% was achieved, even with a low NH_3 content of up to 6 wt%. A high purity of CO_2 (between 99-100%) was obtained in the stripper under high pressure. The NH_3 solvent was proven to be effective for SO_2 removal with more than

95% removal efficiency in the pretreatment column, but has marginal removal efficiency for nitric oxide (NO) in the flue gas.

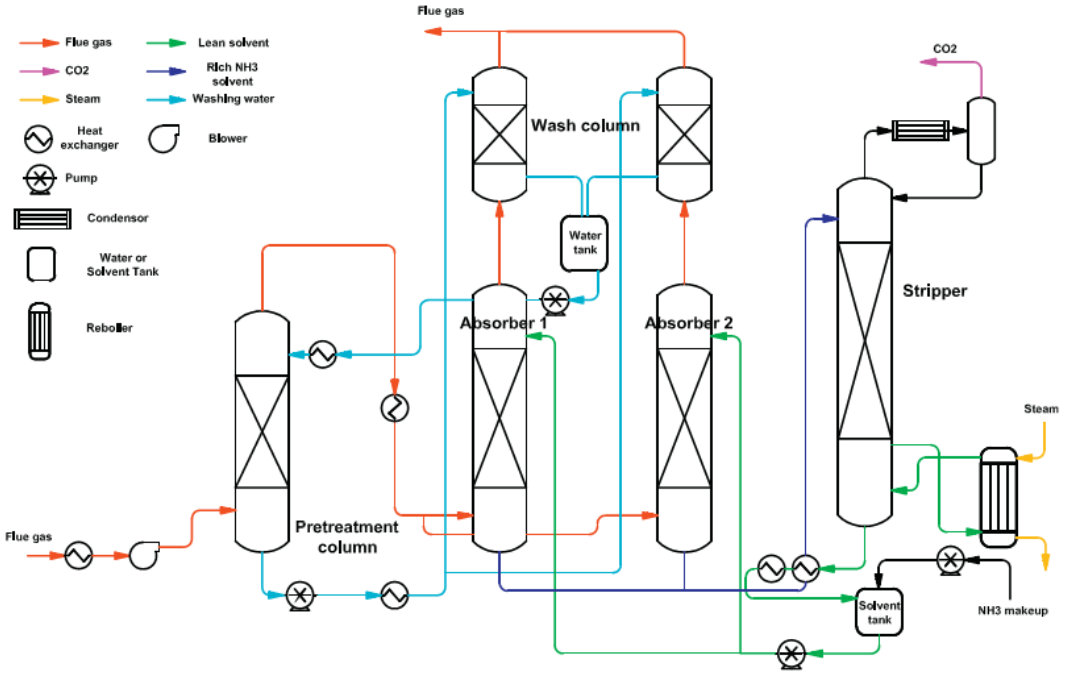

Figure 2-7 Schematic flow sheet of CSIRO process (Yu *et al.*, 2011)

However, the CSIRO process also encountered some critical problems (Yu *et al.*, 2011; Yu *et al.*, 2012). Due to the low NH_3 concentration used in the pilot trials, significant regeneration energy was used to heat the solvent, resulting in a high reboiler energy consumption of 4-7 MJ/kg CO_2, with the lowest duty being 4.0-4.2 MJ/kg CO_2 captured. This resulted in the NH_3 solvent losing its competitive edge of low regeneration energy. The low NH_3 concentration also resulted in a high solvent circulation rate to achieve the targeted CO_2 removal efficiency, and a subsequent increase of equipment sizes. Similar to the CAP and ECO2 process, the CSIRO process also encountered the issue of a heavy burden of cooling duty for solvent and gas cooling, as well as the issue of a high NH_3 loss of over 10,000 ppmv in the flue gas. In addition, this process suffered from the solid precipitation of ammonium bicarbonate in the condenser and reflux line, which forced the shut-down of pilot plant operation.

2.4.3 Process modelling

In parallel with the pilot plant evaluations, intensive research has also been focused on model development and process simulation to further gain insight into the NH_3-based CO_2 capture process. The process modelling can be divided into two categories: the thermodynamic model and the rate based model.

2.4.3.1 Thermodynamic model

Mathias et al. (2010) developed a rigorous thermodynamic model of NH_3 process and used it to evaluate the CAP process. Their work demonstrated that the combination of thermodynamic mode and process modelling provides a powerful tool to quantitatively evaluate the NH_3 process. The conditions of the CAP process were thermodynamically optimised at 26 wt% NH_3 concentration and 1.7 °C absorption temperature, which lead to the minimum overall energy requirement of 3.0 MJ/kg CO_2 including CO_2 regeneration duty and NH_3 regeneration duty. Darde et al. (2010b) also developed a thermodynamic model of the NH_3-CO_2-H_2O system using an extended UNIQUAC model. Based on the regression of more than 3700 experimental data, the model has been proven to accurately represent the vapour-liquid-solid equilibrium and the thermal properties of mixed solution of NH_3-CO_2-H_2O at the conditions investigated.

Using this model, Darde et al. (2012) evaluated the technical performance of a chilled ammonia process. Two different process configurations were proposed with either one single absorber or two absorbers connected in series, where the first absorber captured the majority of the CO_2 and the second limited the NH_3 slip. Their operation conditions were optimised to minimize the heat requirement involved in the capture process. The work has confirmed the advantages of the CAP process, with the total heat requirement being lower than 2700 kJ/kg CO_2 captured. Using the same UNIQUAC model and the same process configurations, Linnenberg et al. (2012) evaluated the influence of the CAP process on the thermal efficiency of a coal-fired power plant with different cooling temperatures. The results show that the two-absorber configuration has a better energy performance at a low cooling temperature, leading to a low net efficiency penalty of 8.5%, which is much lower than the 10.9% of MEA process.

In addition to evaluating the CAP process, a novel NH_3 process was proposed by Niu et al. (2013) who used the equilibrium based model, in which the CO_2 absorption process was conducted at room temperature to reduce the energy consumption for the flue gas and solvent cooling, while CO_2 desorption was operated at atmospheric pressure (85-95 °C) to increase the potential use of low-quality thermal energy resources, instead of steam, from the power station. The simulation result shows that the regeneration duty of the novel process is only 1285 kJ/kg CO_2, while the drawback of this process is the sizeable energy consumption for the NH_3 recovery at 1703 kJ/kg CO_2, due to the massive NH_3 slip at a high absorption temperature.

2.4.3.1 Rate-based model

In addition to the thermodynamic model, a few researchers have focused on the development of rate-based model for the CO_2 capture using aqueous NH_3 (Jilvero *et al.*, 2014b; Niu *et al.*, 2012; Strube *et al.*, 2011; Zhang *et al.*, 2013b, 2014). The rate model is considered to describe the characteristics and behaviours of the CO_2 capture processes in the tray or packed columns more accurately and realistically, and thus offers more reliable results for technical performance, such as column sizing and energy consumptions, et al. The rate-based model needs experimental data, preferably the pilot plant data, to confirm its validity. Strube et al. (2011) developed and validated a rate based model of the NH_3 process using experimental data and compared the difference between equilibrium based model and rate-based model. They revealed that the equilibrium method results in an overestimation of the CO_2 absorption performance, as it does not consider the mass transfer in the capture process.

Using experimental data from CSIRO Munmorah pilot results, some rate-based models for the aqueous NH_3-based CO_2 capture process were validated. The effectiveness of the rate-based approach was confirmed by Qi et al. (2013) who established a rigorous rate-based model for the CO_2 absorption process, and by Yu et al. (2014b) who developed a rate-based model for the CO_2 stripping process. Zhang et al. (2013a, 2014) also developed the rate-based model for both CO_2 absorption and regeneration process and used the model to estimate the reboiler duty (CO_2 regeneration energy) in an NH_3-based capture plant designed to capture 50% of the CO_2 emitted from a 500-MW coal-fired power station. The calculated regeneration energy was surprisingly high at 5750 kJ/kg CO_2. Hanak et al. (2015) used the experimental data from Munmorah pilot trials to validate a rate-based model and then turned to evaluating the large-scale chilled ammonia process dealing with the flue gas from a 580 MW supercritical coal-fired power plant. Under optimised conditions, the equivalent work requirement for the CAP process was found to be 15.7% less than for the reference MEA scrubbing process.

2.4.4 Techno-economic assessment

Based on either equilibrium or rate based model, the overall performance of the NH_3 process has been demonstrated to evaluate the techno-economic feasibility of the NH_3 technology, though there are very few techno-economic assessments of the NH_3

processes in the open literature. Table 2-1 lists the available cost performance studies of different NH_3-based CO_2 capture processes.

Table 2-1 Cost performance of NH_3-based CO_2 capture process integrated with coal-based power station

	Ciferno et al. (2005)	Versteeg et al. (2011)	Valenti et al. (2012)	Jilvero et al. (2014a)
Model type	Equilibrium	Equilibrium	Equilibrium	Equilibrium/rate
Reference power plant, MW	478	827.6	758	408.1
PCC power plant, MW	400	558.7	614	341.8
Capacity factor, %	80	75	85.6	90
Lean solvent temperature, °C	-	10	4	10
NH_3 concentration, %	-	14.4	20	14.3
Regeneration duty, GJ/ton CO_2	-	2.29	2.46	3.16
Year dollar and currency	2003 US$	2007 US$	2008 Euro€	2013 Euro€
LCOE without PCC, $ or €/MWh	46	53.5	59.5	-
LCOE with PCC, $ or €/MWh	64	105.4	82.3	-
CO_2 avoided cost with NH_3 PCC, $ or €/ton CO_2	27	73.2	38.6 [b]	35.0 [b]
CO_2 avoided cost with MEA PCC, $ or €/ton CO_2	47	72.2	51	-

Note: [a] rate based model for CO_2 absorption process, and thermodynamic model for other process; [b] the CO_2 avoided cost does not include the cost of CO_2 transportation and storage.

The first economic assessment of the NH_3 process is the scoping study conducted by Ciferno et al. (2005). The study indicates that the NH_3 process has significant advantages over traditional amine technologies in terms of cost performance. The cost of CO_2 avoided is only US$ 27/tonne, which is nearly half the cost of the MEA process. However, it should be noted that the scoping study was preliminary and was based on a limited knowledge and understanding of the NH_3 system. The conclusions from the scoping study did not seriously take into account the NH_3 vaporization and its cost for NH_3 recovery. The estimated cost performance for the NH_3 process is too optimistic. Valenti et al. (2012) developed the technical and cost models for the chilled ammonia process and performed a detailed techno-economic analysis guided by the European

Benchmark Task Force. The study showed that the chilled ammonia process is superior to the MEA process in terms of its energy performance and economic performance, e.g. 2.46 vs 4.0 MJ/kg CO_2 for reboiler duty, and € 38.6 vs € 51/tonne of CO_2 avoided cost.

Versteeg and Rubin (2011) also modelled a chilled NH_3-based post-combustion CO_2 capture process and assessed the technical and cost performance of the CAP process integrated with a supercritical coal-fired power plant. This chilled NH_3-based CO_2 capture process benefits from the low regeneration energy duty and reduced power consumption for CO_2 compression. However, the significant chilling loads and associated costs seem to offset these benefits. For a 90% CO_2 capture efficiency, the levelised cost of electricity for the CAP process integrated with the power plant was estimated at US$ 105/MWh, leading to the CO_2 avoided cost of US$ 73.2 tonne/CO_2. The cost is comparable to the levelised cost of electricity for the power station with an MEA-based capture system (US$ 72 tonne/CO_2). It is worthwhile mentioning that the validation of the technical model for the chilled ammonia process was not discussed, and the reliability of the model was unknown.

It should be pointed out that the above studies employed the equilibrium-based model to describe the CO_2 capture process, except for part of the work from Jilvero et al. (2014a) who applied the rate-based model for CO_2 absorber only. The results from equilibrium-based modelling are theoretically achieved, but would be different from the real process in which CO_2 absorption and desorption are affected by kinetic processes. Thus, the equilibrium-based results are likely to underestimate the energy consumption and column sizes, and consequently underestimate the capital cost and overall economics of PCC plant. A rate-based model is more rigorous and, therefore, is preferred in the assessment of the technical performance of aqueous NH_3-based capture process. From Table 2-1, it can also be seen that the CO_2 avoided cost varied greatly among the four different studies. This is because of: (1) the different NH_3 processes used, leading to different technical performances, and (2) the different cost model used, resulting in different estimations of capital costs. When comparing the performances between the NH_3 and MEA solvent, the technical-economic assessment should be conducted on the same basis and use the same cost model to have reasonable and consistent comparisons.

2.5 Summary

Global climate change caused by the increasing atmospheric concentration of greenhouse gases, such CO_2, has led to great interest in the technological development of CO_2 capture and storage. Coal combustion supplied 29% of global energy, but contributed to 44% of global CO_2 emissions in 2012. Thus, capturing CO_2 from coal-fired power station flue gas is extremely important. Three technological pathways can be applied to the capture of CO_2: pre-combustion, post-combustion and oxy-combustion. Of these, post-combustion CO_2 capture technology using chemical absorbents is often considered to be the most cost-effective and feasible option for the large-scale removal of CO_2 from flue gases emitted from power plants and other industry facilities. Amine scrubbing for CO_2 capture is state-of-the-art technology, which will most likely be the dominant technology for the commercial application in the near term. This technology, however, is being challenged by some critical issues, i.e. high parasitic energy consumption, solvent degradation, etc.

Aqueous NH_3 is a promising alternative candidate for CO_2 capture, due to the advantages of lower regeneration duty, no solvent degradation, lower solvent cost, lower CO_2 compression duty and the simultaneous capture of acid pollutant gases such as SO_X, NO_X and HCl. Intensive research has been conducted to evaluate the technical feasibility of the NH_3-based CO_2 capture process. Several industrial companies and research organisations, such as Alstom, Powerspan and the CSIRO, have carried out the pilot and demonstration trials and confirmed the technical feasibility of these technologies. In addition, they have demonstrated many of the benefits expected, such as high CO_2 removal efficiency (80–90%), high-purity CO_2 product (more than 99%), low regeneration energy requirement and simultaneous capture of SO_2 and CO_2. In parallel, the modelling work has also highlighted the technical advantages of the NH_3-based CO_2 capture process with respect to low regeneration duty and the incurrence of less of a net efficiency penalty to the power station. The results from the pilot plant and process simulation suggest that the NH_3-based CO_2 capture process is technically feasible to reduce CO_2 emission from coal-fired power stations.

However, the NH_3-based CO_2 capture processes are still confronted by some serious technical challenges identified in the pilot and demonstration trials. The most critical one is the high NH_3 loss during the CO_2 absorption process due to its intrinsic volatility. The recovery of NH_3 requires extra energy and facilities, adding a cost burden onto

the CO_2 capture process. Another critical issue is the significant chilling duty for cooling down the solvent and flue gas. As indicated by the CSIRO process, the NH_3 process also has the potential issue of high regeneration duty under some conditions. The techno-economic assessments show that the NH_3 technology has cost advantages over, or is at least comparable to, the traditional amine process. While most economic studies are based on equilibrium-based models, a rigorous rate based model is preferred and a detailed techno-economic investigation is required to achieve a reliable cost performance of the NH_3-based CO_2 capture process.

Chapter 3 Model Development of CO_2/SO_2 Absorption by Aqueous NH_3

Abstract: The present study is aimed at both exploring the advantages and resolving the problems of NH_3-based CO_2 capture process using a rigorous, validated rate-based model. A quaternary model of NH_3-CO_2-SO_2-H_2O is therefore developed to be capable of predicting the characteristics and behaviours of the processes of CO_2 absorption and SO_2 absorption by aqueous NH_3. This chapter elaborates upon the model development of quaternary system of NH_3-CO_2-SO_2-H_2O and includes two steps. The first step is to use the FLASH simulator embedded in Aspen Plus® V7.3 to build and validate a thermodynamic model of the NH_3-CO_2-SO_2-H_2O system. This quaternary model merges the two sub-models of CO_2 model of NH_3-CO_2-H_2O (CO_2 capture process) with the SO_2 model of NH_3-SO_2-H_2O (SO_2 capture process). The equilibrium model is required to accurately describe the thermodynamic properties of the NH_3-CO_2-SO_2-H_2O system, such as vapour-liquid equilibrium, chemical reactions equilibrium, speciation, etc. This model is the prerequisite and foundation for the development of the following rate-based model. The second step is to develop a rate-based model using the RateFrac simulator in Aspen Plus and validate it using the experiment results from the previous pilot plant trials operated at Munmorah Power Station, New South Wales, Australia. The rate-based model enables a better description and characterization of CO_2 capture and SO_2 absorption by aqueous NH_3, considering mass and heat transfer, materials and energy balance, and chemical kinetic, hydraulic and interface properties, etc. Therefore, it can more reliably describe the technical and economic performance of the aqueous NH_3-based CO_2 capture process.

3.1 Thermodynamic model

3.1.1 Model specification

In the thermodynamic model, the PITZER property method, which is based on the aqueous electrolyte activity coefficient model (embed in the Aspen Plus® Property Methods and Models), is applied to calculate the chemical and physical properties of the liquid phase, including the fugacity coefficient, entropy, enthalpy and Gibbs energy. The Redlich–Kwong–Soave equation of state is used to calculate the fugacity coefficient for the vapour phase.

The gaseous NH_3, CO_2, SO_2 and N_2 are defined as Henry components and their corresponding Henry's law constants are retrieved from the Electrolytes Expert System. The parameters in the PITZER model for the binary interactions in the NH_3-CO_2-SO_2-H_2O system are retrieved from the Aspen Plus databank, which have been regressed against the literature experimental data of vapour–liquid equilibrium, enthalpy, heat capacity and speciation (Aspen, 2010a, b).

The electrolyte solution characteristics and the vapour–liquid behaviours of the NH_3-CO_2-SO_2-H_2O system are modelled with an equilibrium chemistry package. Table 3-1 lists all the possible ionic reactions and their corresponding equilibrium constants.

Table 3-1 Chemical reactions and equilibrium constants of the NH_3-CO_2-SO_2-H_2O system

No.	Reaction	Equilibrium parameter			
		A	B	C	D
1	$2H_2O$ <--> $H_3O^+ + OH^-$	132.899	–13445.9	–22.5	0
2	$CO_2 + 2H_2O$ <--> $H_3O^+ + HCO_3^-$	231.465	–12092.1	–36.8	0
3	$HCO_3^- + H_2O$ <--> $CO_3^{2-} + H_3O^+$	216.049	–12431.7	–35.5	0
4	$NH_3 + H_2O$ <--> $NH_4^+ + OH^-$	–1.256	–3335.7	1.5	–0.037
5	$NH_3 + HCO_3^-$ <--> $NH_2COO^- + H_2O$	–4.583	2900	0	0
6	$2H_2O + SO_2$ <--> $H_3O^+ + HSO_3^-$	–5.978	637.4	0	–0.0151
7	$H_2O + HSO_3^-$ <--> $H_3O^+ + SO_3^{2-}$	–25.290	1333.4	0	0
8	HSO_3^- <-->$S_2O_5^{2-} + H_2O$	–10.226	2123.6	0	0
9	$NH_4HCO_{3(S)}$ <--> $NH_4^+ + HCO_3^-$	554.818	–22442.5	–89.0	0.0647
10	$(NH_4)_2SO_{3(S)}$ <--> $2\ NH_4^+ + SO_3^{2-}$	920.378	–44503.8	–139.3	0.0362
11	$(NH_4)_2SO_{3(S)}\cdot H_2O$ <--> $2\ NH_4^+ + SO_3^{2-} + H_2O$	–1297.041	33465.9	224.2	–0.351

The chemical equilibrium constants of these reactions are expressed as:

$$\ln K_{eq} = A + B/T + C\ln(T) + DT$$

where K_{eq} is the equilibrium constant of each reaction; T is the temperature, K; and constants A, B, C, D are adjustable parameters. The parameters for reactions 1–10 are available in the Aspen databank (Aspen, 2010b) and those for the reaction HSO_3^- <--> $S_2O_5^{2-} + H_2O$ are obtained from Ermatchkov et al. (2005)

3.1.2. Model validation

After the thermodynamic model settings are specified, the thermodynamic model of NH_3-CO_2-SO_2-H_2O is used to predict the chemical and physical properties in the ternary systems of NH_3-CO_2-H_2O (CO_2 capture process) and NH_3-SO_2-H_2O (SO_2 capture process), and the quaternary system of NH_3-SO_2-CO_2-H_2O (combined CO_2 and SO_2 capture). The modelling results are compared with the experimental data available in the literature. The present validation work is aimed to evaluate whether or not the quaternary system can be independently applied for the prediction of the two ternary systems in the absence of SO_2 or CO_2, and whether or not the quaternary system can accurately predict thermodynamic behaviours in the presence of CO_2 and SO_2.

3.1.2.1 Validation of NH_3-CO_2-H_2O system

The model for the NH_3-CO_2-SO_2-H_2O system in the absence of SO_2 is identical to that of the NH_3-CO_2-H_2O system. The thermodynamic model for the NH_3-CO_2-H_2O system is validated using the available experimental results, including the total vapour pressure, CO_2 partial pressure and liquid species distribution as a function of CO_2 molarity. The experimental data of the vapour-liquid equilibrium is from Göppert et al. (1988) and Kurz et al. (1995), and the experiment data of speciation is from Lichtfers (2000). As shown in Figures 3-1 and 3-2, the simulated total vapour pressures and CO_2 partial pressures agree very well with the experimental results at a wide NH_3 concentration range of 0.72−6.74 mol/kg and CO_2 loading of 0−1 mol/mol. These conditions cover all the conditions used in the pilot plant and simulation conditions used in this thesis. The results in Figure 3-3 also show that the model can satisfactorily predict the species concentration, including carbon- and nitrogen-containing species, in the liquid phase. The high level of agreement indicates that the quaternary model enables excellent prediction on the thermodynamic behaviours of the NH_3-CO_2-H_2O system.

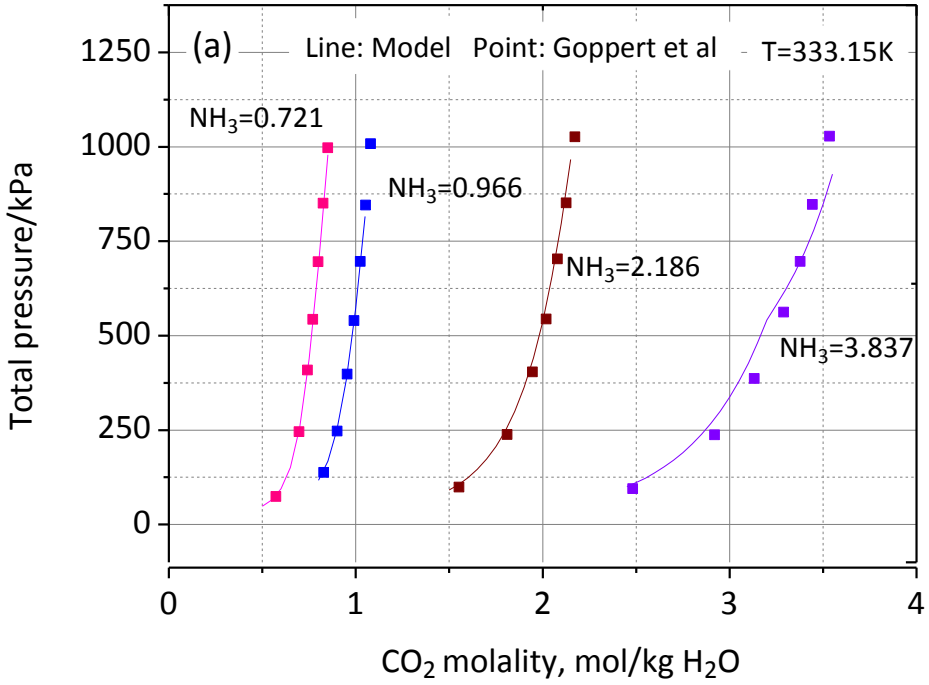
(a)
Line: Model
Point: Goppert et al
T=333.15K
NH3=0.721
NH3=0.966
NH3=2.186
NH3=3.837
Total pressure/kPa
CO2 molality, mol/kg H2O

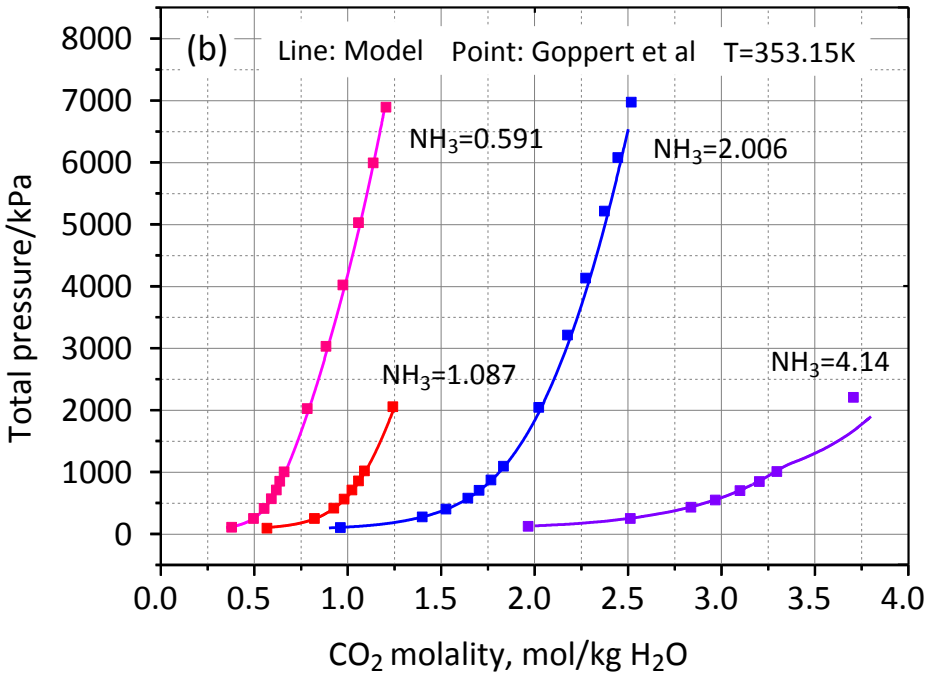
(b)
Line: Model
Point: Goppert et al
T=353.15K
NH3=0.591
NH3=2.006
NH3=1.087
NH3=4.14
Total pressure/kPa
CO2 molality, mol/kg H2O

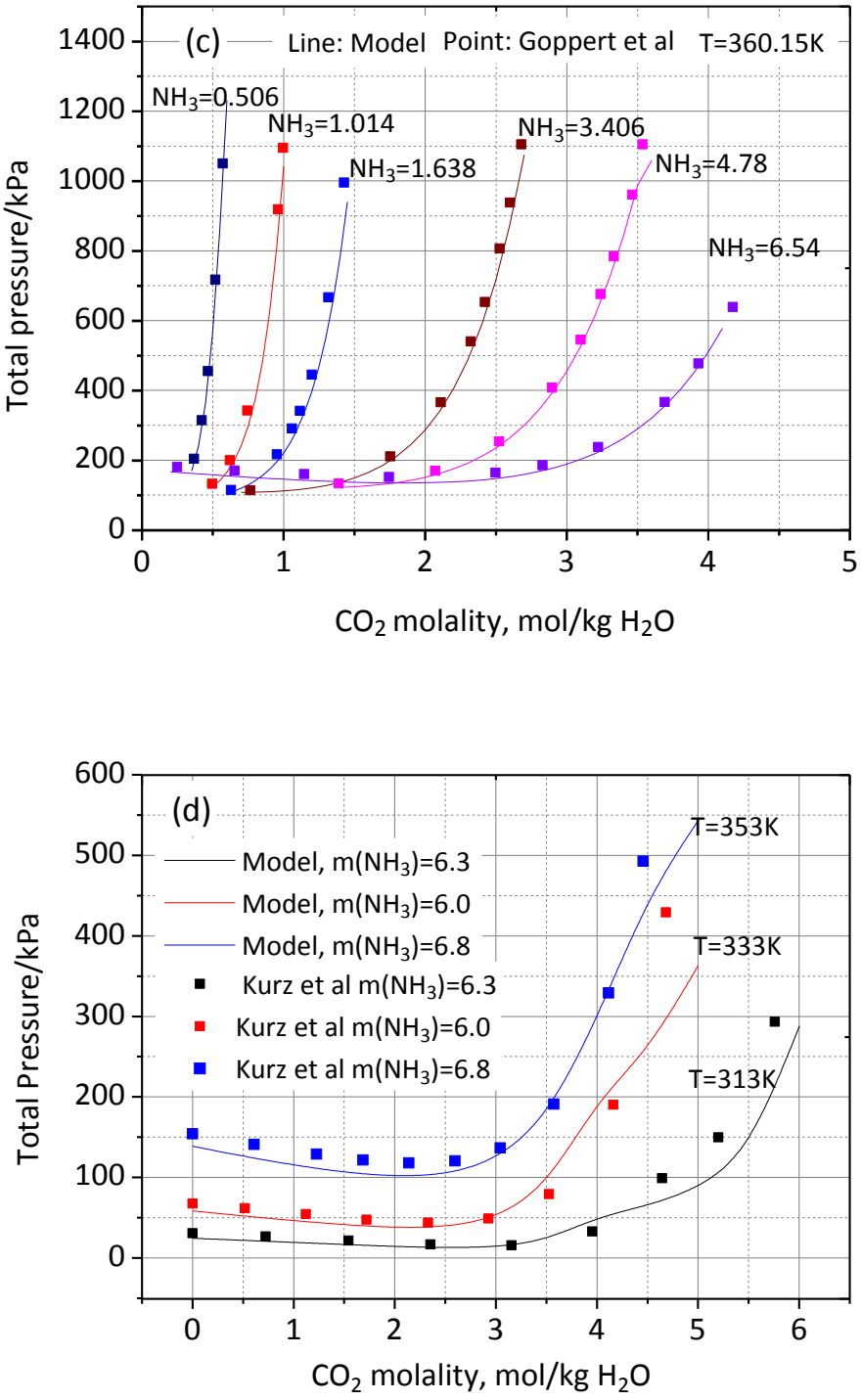

Figure 3-1 Total vapour pressure of NH_3-CO_2-H_2O mixture for various NH_3 and CO_2 molalities at different temperatures with model data (line).

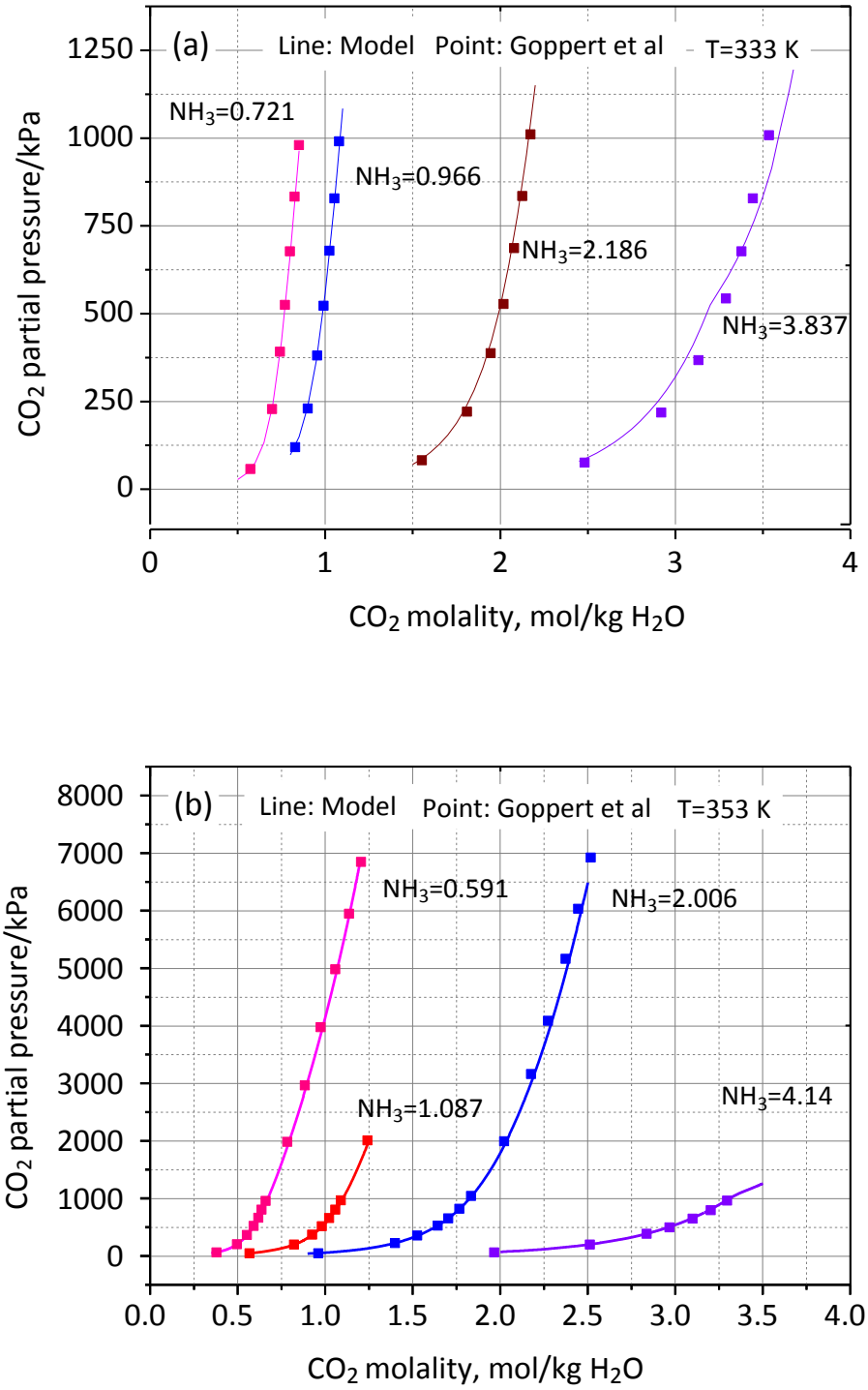

Figure 3-2 CO_2 partial pressure of NH_3-CO_2-H_2O mixture for various NH_3 and CO_2 molality at (a) T = 333 K and (b) T = 353 K with model data (line) and experimental data (point)

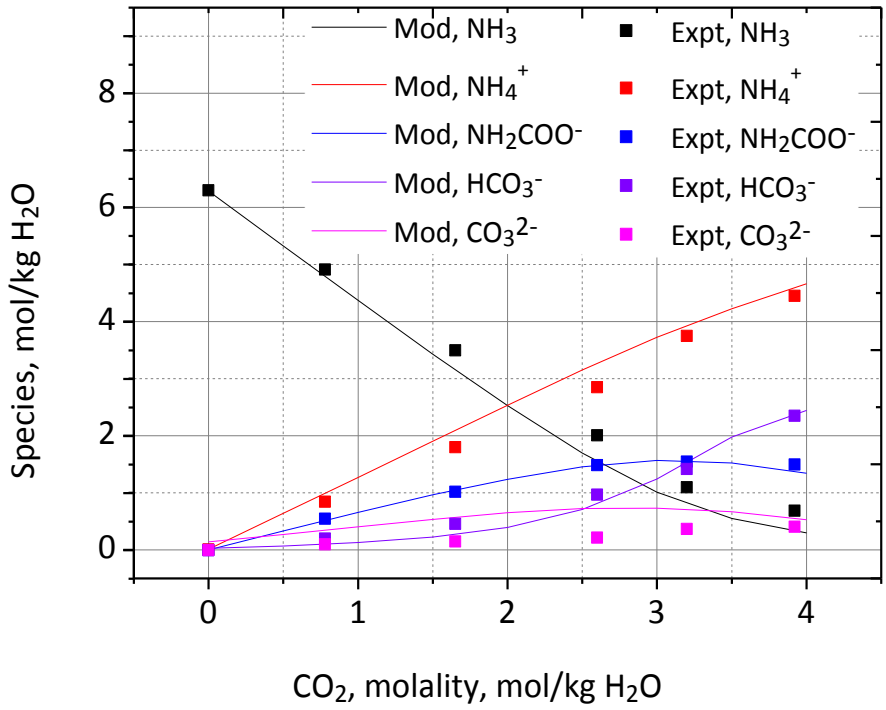

Figure 3-3 Experimental (point) and predicted (line) liquid species distribution in conditions of NH_3 concentration of 6.3 mol NH_3/kg H_2O and T = 313 K.

3.1.2.2 Validation of NH_3-SO_2-H_2O system

Figure 3-4 plots the simulated and experimental total pressures in the NH_3-SO_2-H_2O system as a function of SO_2 molality at two NH_3 concentrations. The experiment data is from Rumpf et al. (1993). The predicted total pressures agree reasonably well with the experimental measurements. Overestimations of the total pressure are observed at high SO_2 concentrations (>6 mol/kg H_2O). This is likely to be caused by the limitation of the PITZER model, in which the electrolyte concentration in the solution should be no more than 6 mol/L ionic strength (Aspen, 2010a). Another reason for the deviations might be the uncertainty of measurements at high temperatures and loadings. Considering that the process simulation of SO_2 removal systems in this thesis will be carried out at the electrolyte concentration range of 0–6 mol/L and at temperatures of below 353 K, this model is adequate for the prediction of the vapour–liquid equilibrium of the NH_3-SO_2-H_2O system.

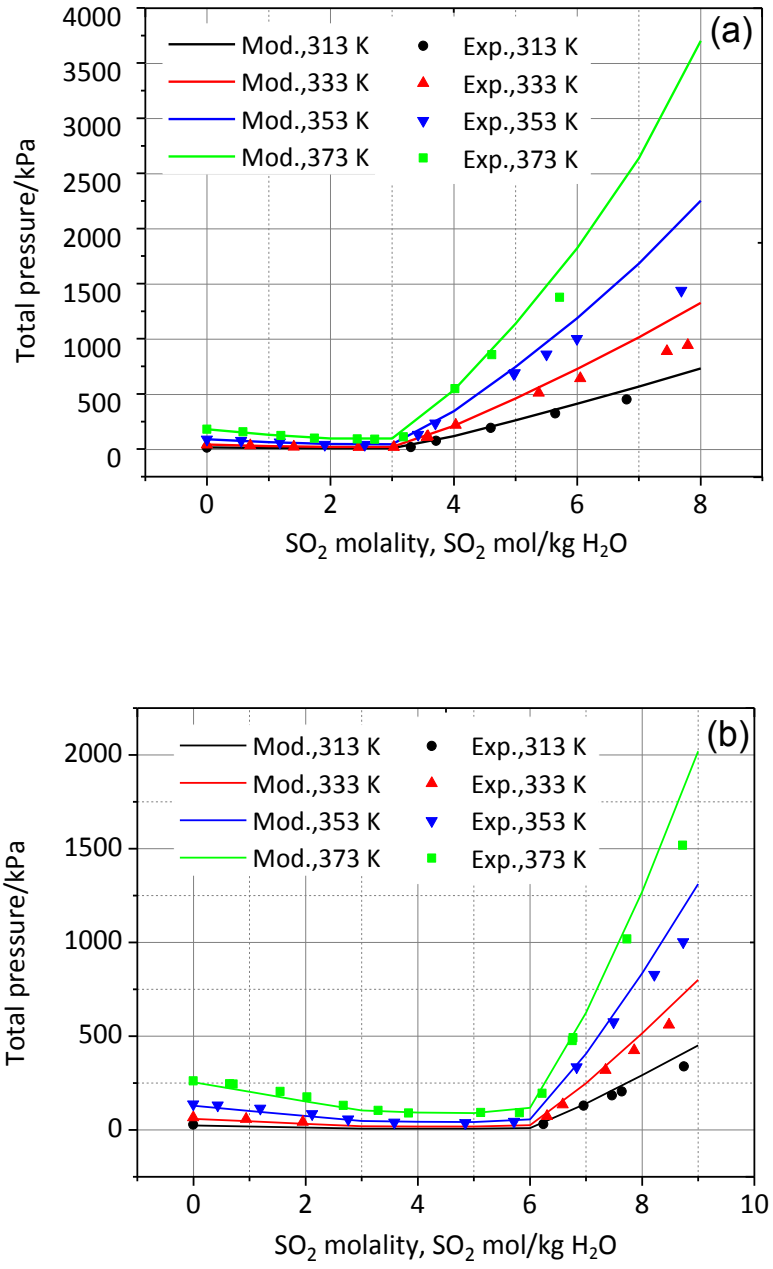

Figure 3-4 Total pressure of NH_3-SO_2-H_2O for different temperatures at (a) mNH_3 = 3.19 mol/kg H_2O, (b) mNH_3 = 6.08 mol/kg H_2O with model data (line) and experimental data (point)

In terms of liquid-phase validation, the solution pH reflects the species distribution, e.g. HSO_3^-, SO_3^{2-} and $S_2O_5^{2-}$. As shown in Figure 3-5 (experimental data obtained from Scott et al. (1967)), the simulated pH values are in excellent agreement with the experimental results at electrolyte concentrations ranging from 0.001 to 6 mol/L. This

implies that the developed model can accurately predict the solution pH and the ionic species concentration in the NH_3-SO_2-H_2O system.

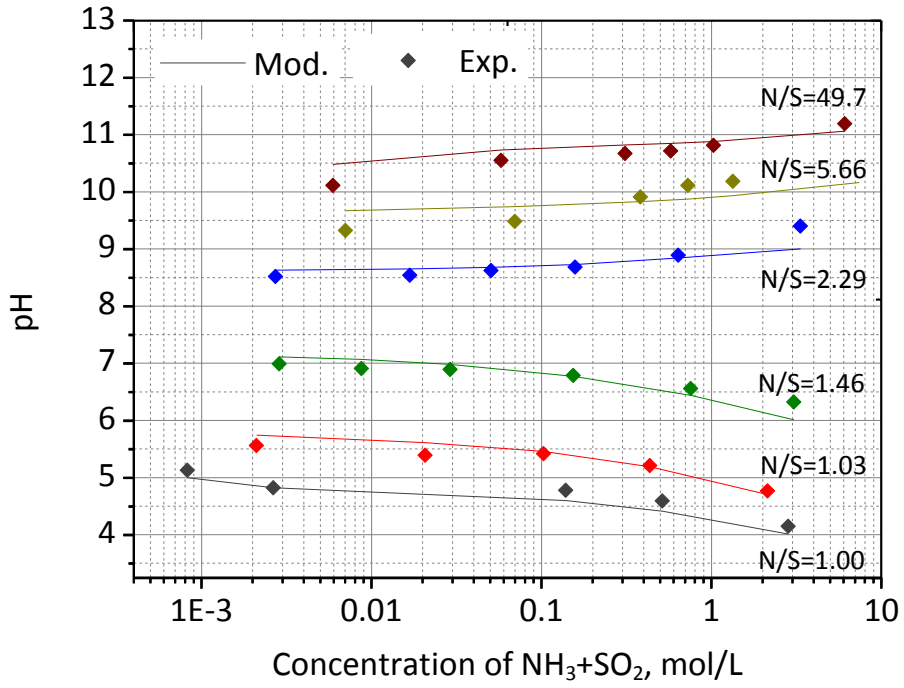

Figure 3-5 pH value of solutions as a function of $(NH_4)_2SO_3$ concentrations at different molar NH_3/SO_2 (N/S) ratios and at 293 K

3.1.2.3 Validation of NH_3-CO_2-SO_2-H_2O

Figure 3-6 compares the predicted and experimental CO_2 partial pressure in the SO_2 loading range of 0–0.3 ($molSO_2/molNH_3$) and temperature range of 20–60 °C. The experimental data is from Qi et al. (2015). The model's prediction agrees reasonably well with the experimental results, although a small deviation is observed at CO_2 molality >0.5 mol/kg H_2O. Considering that the SO_2 removal process will be conducted at low NH_3 concentration and low CO_2 concentrations (<0.5 mol/kg H_2O), the effect of the deviation can be ignored.

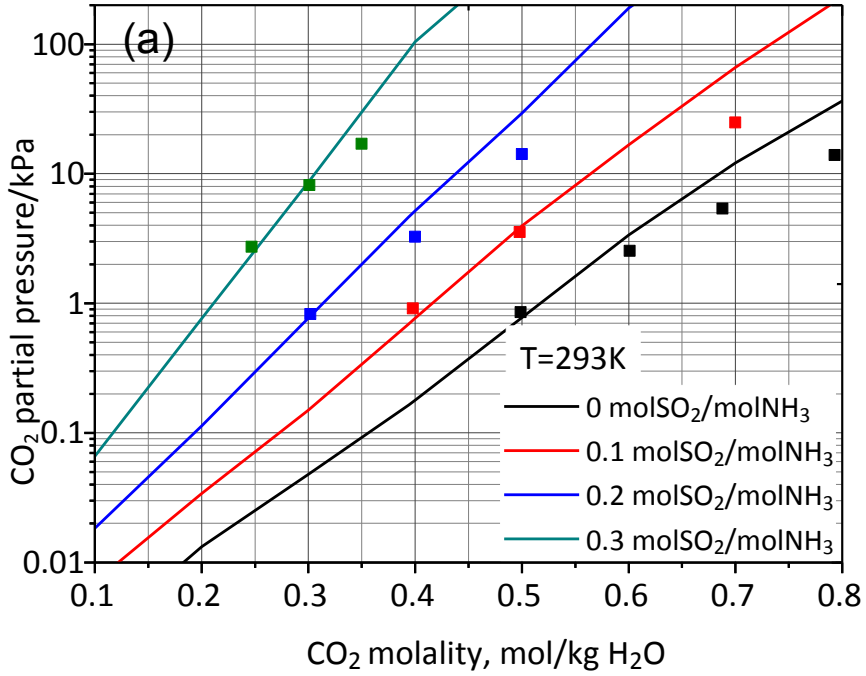
(a)
100
10
1
0.1
0.01
0.1
0.2
0.3
0.4
0.5
0.6
0.7
0.8
CO2 partial pressure/kPa
CO2 molality, mol/kg H2O
T=293K
0 molSO2/molNH3
0.1 molSO2/molNH3
0.2 molSO2/molNH3
0.3 molSO2/molNH3

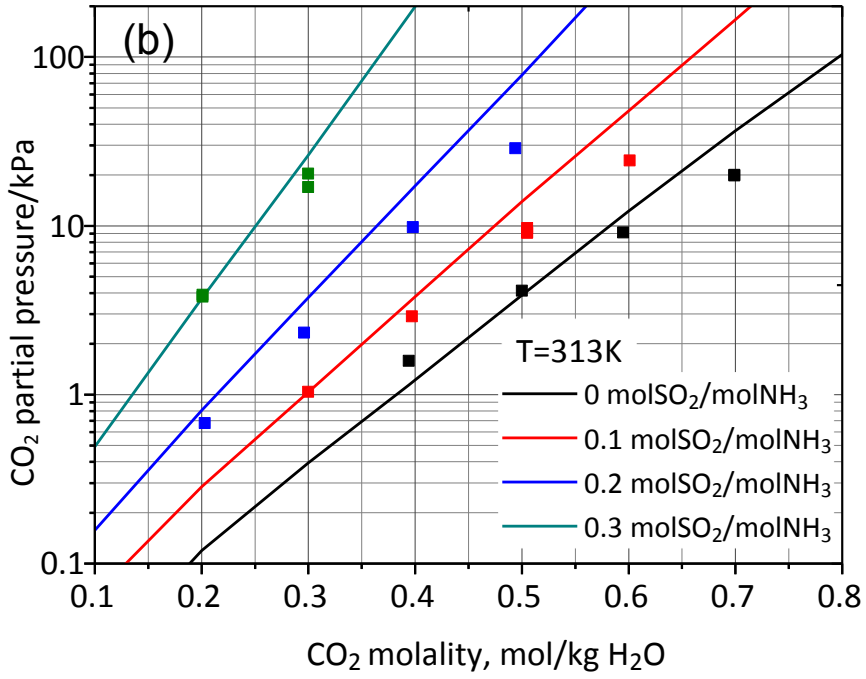
(b)
100
10
1
0.1
0.1
0.2
0.3
0.4
0.5
0.6
0.7
0.8
CO2 partial pressure/kPa
CO2 molality, mol/kg H2O
T=313K
0 molSO2/molNH3
0.1 molSO2/molNH3
0.2 molSO2/molNH3
0.3 molSO2/molNH3

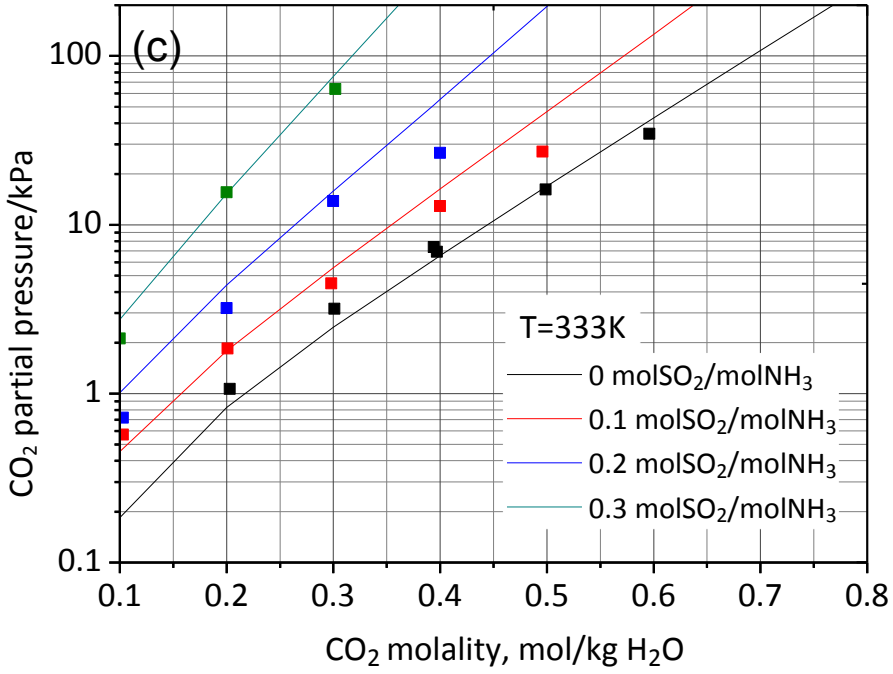

Figure 3-6 CO_2 partial pressure of NH_3-CO_2-SO_2-H_2O system as a function of CO_2 molality at various SO_2 loadings (molar ratio of SO_2 to NH_3) and the NH_3 concentration of 5 wt% (a) 293 K, (b) 313 K and (c) 333 K with model data (line) and experimental data (point)

In summary, the developed thermodynamic model can satisfactorily predict the vapour–liquid equilibrium and ion speciation for the ternary NH_3-CO_2-H_2O and NH_3-SO_2-H_2O systems, as well as the vapour–liquid equilibrium for the quaternary NH_3-CO_2-SO_2-H_2O system. This provides a solid foundation for the following rate-based modelling work.

3.2 Rate-based model

3.2.1 Model specification

Based on the validated thermodynamic model, the rate-based model has been developed using the RateFrac module in Aspen Plus®. In this model, it is assumed that the reactions involving SO_2 are thermodynamically controlled due to the following factors: (1) fast SO_2 absorption rate by the water (Miller *et al.*, 1972); and (2) the generated acid H_2SO_3 is quickly dissociated and neutralized by basic aqueous NH_3. Thus, the chemical reactions of the SO_2 absorption process by aqueous NH_3 in the rate-based model are consistent with those in the thermodynamic model. The reactions of

CO_2 with OH^- and NH_3 are assumed to be kinetically controlled. The power law expressions are used to express the kinetically controlled reactions:

$$r = kT^n e^{-\frac{E}{RT}} \prod_{i=1}^{n} C_i^{a_i}$$

where r is the rate of reaction; k is the pre-exponential factor; n is the temperature exponent, which has been chosen as zero for this simulation; E is the activation energy; R is the universal gas constant; T is the absolute temperature; c_i is the molarity concentration of component i; and a_i is the stoichiometric coefficient of component i in the reaction equation. The kinetic parameters k and E for kinetic reactions in Table 3-2 are derived from the work of Pinsent et al. (1956)

Table 3-2 The kinetic reactions and corresponding kinetic parameters in the NH_3-CO_2-SO_2-H_2O system

No.	Reaction	Parameters	
		K	E (cal/mol)
1	$CO_2 + OH^- \rightarrow HCO_3^-$	4.32e+13	13249
2	$HCO_3^- \rightarrow CO_2 + OH^-$	2.38e+17	29451
3	$NH_3 + CO_2 + H_2O \rightarrow NH_2COO^- + H_3O^+$	1.35e+11	11585
4	$NH_2COO^- + H_3O^+ \rightarrow NH_3 + CO_2 + H_2O$	4.75e+20	16529

The RateFrac module allows users to divide the column into stages and perform the mass and heat transfer, chemical reactions, and hydraulic and interface behaviours at each stage. The resistance of mass and heat transfer between the gas and liquid phase is also considered in the model. The two-film theory is used to describe the mass and heat transfer resistance (Whitman, 1923), and the Maxwell–Stefan theory is adopted to calculate multi-component mass and heat transfer between the liquid and vapour phases (Alopaeus *et al.*, 1999). Figure 3-7 illustrates the schematic view of the discretised two-film model in the rate-based model for CO_2/SO_2 absorption by aqueous NH_3. The film discretisation is chosen as geometric in which the ratio of film discretisation (the ratio of the thickness of each film region to the thickness of the next region closer to the interface) is set at a default of 2 and the discretisation point in the liquid film is set at 4.

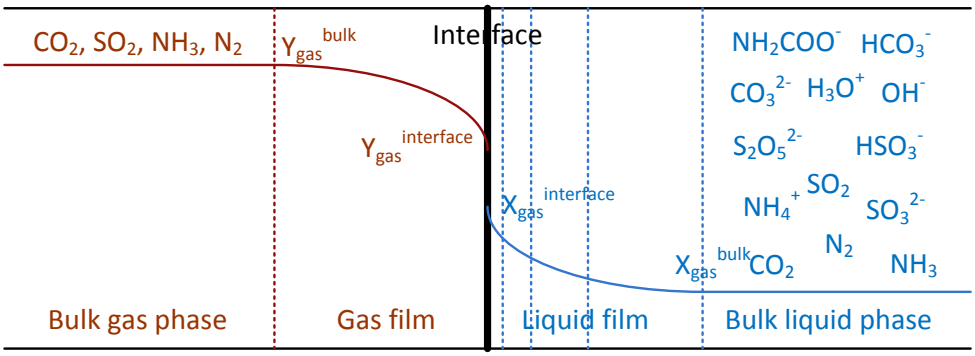

Figure 3-7 Schematic of the discretised two-film model of the rate-based model of CO_2/SO_2 absorption by aqueous NH_3

Table 3-3 lists the primary information of the column parameters and settings in the rate-based model.

Table 3-3 Summary of column settings in the rate-based model

No.	Parameters	patterns
1	Number of stage	25 for absorber and 15 for stripper
2	Packing material	The same as pilot plant or determined by process design
3	Total packed height	The same as pilot plant or determined by process design
4	Column diameter	The same as pilot plant or determined by process design
5	Flow model	Counter-current
6	Interfacial area factor	1.2
7	Heat transfer factor	1
8	Initial liquid holdup	0.03L
9	Mass transfer correlation method	Onda et al. (1968)
10	Heat transfer correlation method	Chilton-Colburn (1934)
11	Interfacial area factor method	Onda et al. (1968)
12	Liquid holdup correlation method	Stichlmair et al. (1989)

In the model verification, the packing material, packed height and column size are consistent with those of the pilot plant to ensure reliable and practical model validation

work. When the validated model is applied to process improvement or process scale-up, column size and packing material are adjusted to achieve technical advancement and an economic saving of the CO_2 capture process by aqueous NH_3. The interfacial area factor is set at 1.2, according to the experiment results from the CSIRO pilot plant (Yu *et al.*, 2011). The calculations of mass transfer and interfacial area are determined by the correlation method proposed by Onda et al. (1968). The correlations proposed by Chilton et al. (1934) and Stichlmair et al. (1989) are adopted for the calculation of heat transfer and liquid holdup, respectively. In addition, for transport properties the Jones–Dole electrolyte correction model, the Onsager–Samaras model and Riedel electrolyte correction model are used to calculate liquid viscosity, liquid surface tension and thermal conductivity, respectively (Aspen, 2010b).

3.2.2 Model validation of CO_2 absorption by aqueous NH_3

In this work, the rate-based model is validated against the CSIRO pilot-plant results. The validation work includes CO_2 absorption and SO_2 removal by aqueous NH_3 in packed columns.

3.2.2.1 Description of Munmorah PCC pilot plant

In 2009-2010, the CSIRO, in collaboration with Delta Electricity, trialled an NH_3-based CO_2 capture process under real flue gas conditions in a pilot plant located at the Munmorah power station, NSW, Australia (the pilot plant was relocated from Munmorah to Vales Point Power Station in NSW in 2014). Figure 3-8 shows the schematic flow sheet of the NH_3-based PCC pilot plant (Yu *et al.*, 2011), which consists of: (1) one pretreatment column working as a direct contact cooler for the flue gas cooling and also serving as a scrubber for the removal of SO_2 from the flue gas; (2) two absorber columns (in series or parallel) with each installing a separate washing column at the top to capture CO_2 from the flue gas after the pretreatment column; and (3) one stripper for the solvent regeneration, which reuses the solvent for CO_2 capture in the absorbers.

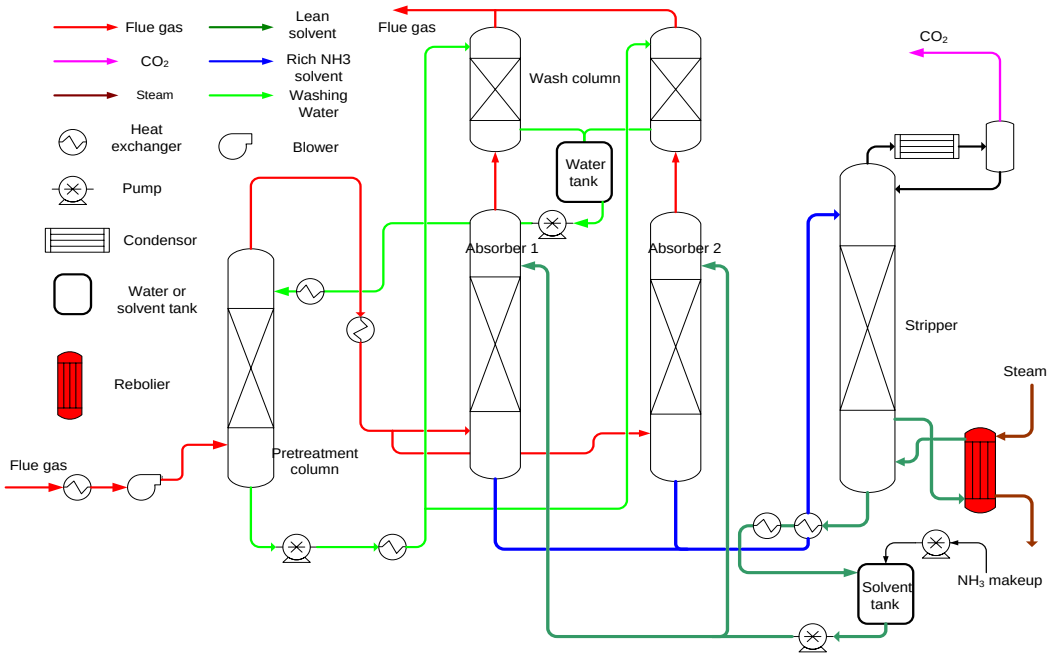

Figure 3-8 Schematic of Munmorah pilot plant of CO_2 capture process by aqueous NH_3

Table 3-4 lists the columns specifications in the Munmorah PCC pilot plant. The rate-based model uses the same column setting as the pilot plant to ensure reliable model validation.

Table 3-4 Columns' specifications in the Munmorah PCC pilot plant

Columns	Column diameter, m	Packing height, m	Packing materials
Pretreatment column	0.5	3	25 mm Pall ring
Absorber	0.6	2 × 3.9	25 mm Pall ring
Wash column	0.5	1.7	25 mm Pall ring
Stripper	0.4	3.5	16 mm Pall rings

3.2.2.2 Results comparison between pilot plant and model

The validity of the rate-based model is verified by comparing the results between the simulation and the CSIRO's pilot trials. Table 3-5 summarises the pilot plant conditions and results, together with the simulation results, based on the conditions of the pilot plant trials. It can be seen that the average relative error for overall CO_2

absorption rate in 30 tests is only ± 6.0%, and for the NH_3 loss rate in 24 tests ±11.1%, which shows that the predicted results from the established rate-based model agree reasonably well with the pilot plant results. It is also found that the relative error in the NH_3 loss rate is higher than that of the CO_2 absorption rate; in addition, some great deviations of the NH_3 loss rate between experiment and simulated results are found in some cases, e.g. test 45, 46, 47B, 50, 55. The reason for this might be that the detection range of Fourier Transform Infrared Spectroscopy (FTIR, Gasmet^{TM} Dx-4000) used in the pilot plant was up to 10000ppmv, and sometimes the NH_3 concentration from CO_2 absorber was outside of the suggested range. Another possible reason was the difficulties of maintaining the NH_3 measurement accurately and with the utmost stability at all times during the pilot plant trials due to the lack of regular NH_3 calibration. This is likely to result in the displayed data deviating from the real value. It is therefore advised here that a more accurate measurement of gaseous NH_3 concentration should be developed for process monitoring and control, and for providing more reliable results for model validation.

Table 3-5 Comparison between pilot plant test and rate based model simulation results under a variety of experimental conditions

Test ID	30	31	31R	31B	32	32A	32B	33	34	34R1	34R2	36	35B	35	39	38
Key test conditions																
Solvent flow-rate, L/min	134	134	134	134	134	134	134	100	67	67	67	134	134	134	134	134
Liquid inlet Temperature, ^{o}C	23.9	27	32.3	16.4	25.8	16.8	17.0	15.5	15.2	15.5	15.6	14.5	19.9	16.4	16.3	17.1
NH_3 wt%	4.91± 0.30	4.08± 0.10	4.21± 0.12	3.79± 0.24	3.56± 0.41	4.19± 0.30	3.98± 0.23	4.24± 0.43	4.37±0 .32	4.37±0 .25	4.00± 0.12	4.97± 0.20	5.82 n.a.	4.96± 0.12	4.49± 0.39	1.92± 0.14
Lean CO_2 loading [c]	0.24± 0.025	0.24± 0.014	0.23± 0.026	0.25± 0.012	0.24± 0.027	0.26± 0.014	0.22± 0.02	0.21± 0.04	0.22± 0.02	0.23± 0.06	0.22± 0.003	0.41± 0.002	0.36 n .a.	0.31± 0.001	0.28± 0.01	0.22± 0.002
Flue gas flow-rate, kg/h	646	646	632	750	780	760	821	817	906	915	916	799	799	799	898	912
Flue gas inlet CO_2, vol%	8.6	9.4	9.8	7.6	8.8	10.8	8.1	8.0	10.1	9.4	9.4	9.8	9.4	8.0	10.1	11.7
Comparison of test results and simulation results																
Test CO_2 absorption rate [g](Absorber1),kg/h	32.2	59.1	55.2	38.3	44.5	49.2	46.8	51.4	34.4	33.2	31.5	29.5	35.7	42.8	47.2	43.3
Simu. CO_2 absorption rate(Absorber1), kg/h	48.6	50.5	53.4	38.6	46.2	53.4	44.9	40.4	41.4	39	38.2	31.2	39.9	39	50.9	43.3
Relative error	--	14.5%	3.3%	0.8%	3.8%	8.5%	4.0%	21.4%	20.3%	17.4%	21.2%	5.7%	11.7%	8.8%	7.8%	0%
Test overall CO_2 absorption rate [g], kg/h	66.6± 5.0	79.6± 1.6	77.7± 3.6	68.2± 2.3	75.9± 5.0	87.8± 3.3	80.5± 4.3	85.9± 4.8	78.3± 4.3	74.4± 3.0	70.0± 2.4	60.4 ± 3.0	70.6± 1.0	81.2± 4.1	85.6± 1.7	74.9± 3.5
Simu. Overall CO_2 absorption rate, kg/h	70.1	74.8	77.3	61.7	75	87.2	71.9	67.1	75.8	72.4	72.9	57.6	68.3	64.3	87.1	83.8
Relative error	5.2%	6.0%	0.5%	9.5%	1.1%	0.7%	10.6%	19.5%	3.2%	2.7%	2.8%	4.6%	3.2%	20.8%	1.7%	11.8%
Test NH_3 loss rate [g](Absorber1),kg/h	7.10	6.10	10.08	3.93	5.68	4.46	5.58	5.39	3.88	5.31	4.08	2.48	3.74	3.77	4.99	1.91
Simu. NH_3 loss rate (Absorber1),kg/h	7.00	6.81	9.23	3.79	6.21	3.9	5.00	4.46	3.89	4.45	4.14	2.10	4.78	4.11	4.41	2.03
Relative error	1.4%	11.6%	8.4%	3.6%	9.3%	12.6%	10.4%	17.3%	0.3%	16.2%	1.0%	15.3%	--	9.0%	11.6%	6.3%

Continued

Test ID	44-1	44-2	45	46	47	47 B	48	50	51	52	53	54	55	56
Key test conditions														
Solvent flow-rate, L/min	67	67	67	67	67	67	67	50	50	100	50	67	67	67
Liquid inlet Temperature, ^{o}C	15.8	12.7	15.9	18.9	28.0	27.0	23.2	23.0	24.1	22.4	23.1	23.1	23.4	22.8
NH_3 wt%	3.30± 0.27	4.40± 0.26	4.04± 0.21	3.95± 0.10	4.53± 0.45	3.83± 0.66	4.56± 0.307	4.77± 0.256	4.22± 0.34	4.33± 0.54	4.08± 0.23	4.84± 0.30	4.62± 0.18	4.41± 0.27
Lean CO_2 loading [c]	0.22± 0.01	0.24± 0.013	0.21± 0.02	0.22± 0.02	0.23± 0.01	0.14± 0.02	0.22± 0.005	0.17± 0.01	0.18± 0.02	0.22± 0.05	0.18± 0.01	0.19± 0.01	0.18± 0.02	0.22± 0.025
Flue gas mass flow-rate, kg/h	795	774	641	638	667	665	1000	661	1003	1060	972	925	903	837
Gas temperature, ^{o}C	15-20	15-20	15-20	15-20	15-20	15-20	15-20	15-20	15-20	15-20	15-20	15-20	15-20	15-20
Inlet CO_2 flow-rate, kg/h	125.9	113.1	98.4	97.5	103.0	105.7	150.5	102.5	158.3	157	131.3	132.7	127	122
Inlet NH_3 flow-rate, kg/h	0.9	0.28	0.44	0.5	1.2	1.3	0.7	1.3	1.3	2.1	0.6	0.5	0.6	n.a
Inlet H_2O flow-rate, kg/h	6.8	5.3	4.6	4.4	6.0	6.7	7.2	6.8	8.8	6.6	6.5	6.6	n.a	n.a
Comparison of test results and simulation results														
Test CO_2 absorption rate [g], kg/h	69.6±4.5	69.1±1.7	67.3±3.6	65.9±2.8	71.2±2.2	79.9±6.0	86.2±4.2	72.1±1.1	83.9±2.1	99.6±6.8	65.3±3.9[l]	80.2±3.5[l]	89.7±4.17[l]	85
Simu. CO_2 absorption rate, kg/h	71.9	71.4	71.2	69.8	71.0	82.2	81.4	74.5	72.1	94.8	63.6	84.5	82.5	75.4
Relative error, %	3.3%	3.3%	5.8%	5.6%	0.3%	2.9%	5.7%	3.3%	14.1%	4.8%	2.6%	5.4%	8.0%	11.3%
Test NH_3 loss rate, kg/h	5.27±2.3	6.72±2.3	7.19±0.7	7.70±1.5	11.7±2.0	13.6±3.6	12.4±1.7	6.21±2.5	11.7±2.2	12.1±2.5	9.4±1.2	10.4±2.0	8.2±2.0	9.8±3.1
Simu. NH_3 loss rate, kg/h	4.1	5.2	4.3	4.8	9.5	9.5	11.5	8.9	12.6	11.0	11.3	12.3	12.1	9.1
Relative error, %	22.2%	22.6%	--	--	18.8%	--	7.2%	--	7.7%	9.1%	20.2%	18.2%	--	7.1%

Note: ‘c’: defined as the molar ratio of total C-containing species to the total N-containing species (C/N molar ratio). ‘--‘: great error between test and simulation; ‘g’: CO_2 absorption rate based on gas analysis; ‘l’: CO_2 absorption rate based on liquid analysis; ‘n.a’: not available

In order to make a clear comparison, Figure 3-9 plots the parity figures of the CO_2 absorption rate and NH_3 loss rate obtained from experiments and from the rate-based model.

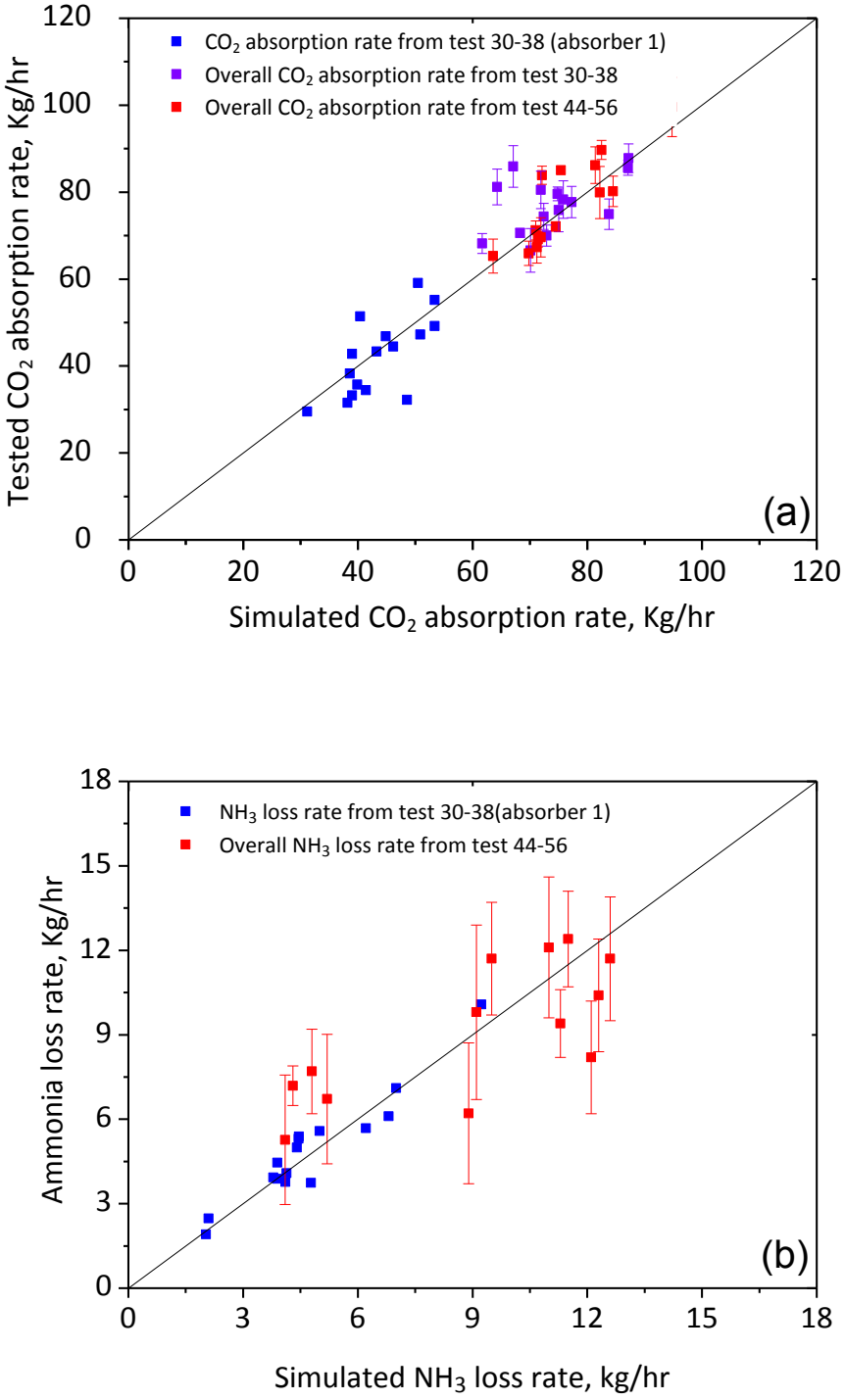

Figure 3-9 Comparison of (a) CO_2 absorption rate and (b) NH_3 loss rate between pilot plant tests and rate-based model under the conditions listed in Table 3-5

The pilot plant data together with the offset are just sitting around the parity plot. This excellent agreement implies that the rate-based model is capable of satisfactorily predicting CO_2 absorption and the NH_3 loss rate for the pilot plant tests. Therefore, the established model of CO_2 capture process by aqueous NH_3 is kinetically validated, which will reliably and practically to guide the process development and improvement of the NH_3-based CO_2 capture process.

3.2.3 Model validation of SO_2 removal by aqueous NH_3

3.2.3.1 Description of pilot SO_2 absorption process

In the pilot trials of the NH_3-based CO_2 capture process, the CSIRO also conducted the preliminary investigation of the process of SO_2 absorption by aqueous NH_3 under real flue gas conditions with the aim of better understanding the behaviours and characteristics of SO_2 removal by NH_3. The NH_3-dosing experiment was carried out in the pilot plant's pretreatment column. Figure 3-10 illustrates the schematic process of SO_2 absorption by NH_3-dosing.

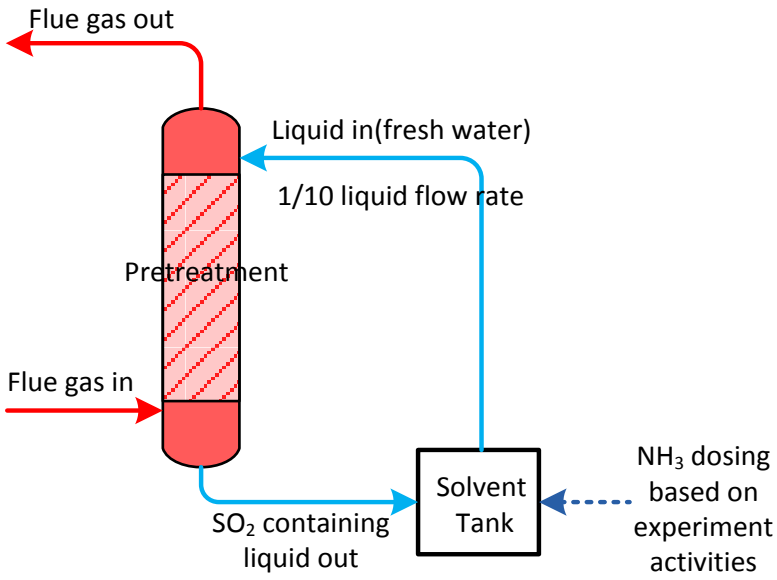

Figure 3-10 Schematic process of the SO_2 absorption by NH_3 dosing

The flue gas was introduced into the bottom of the column, initially without liquid circulation. After the introduction of flue gas, fresh water entered the column from the top and circulated between the column and the wash water tank. The NH_3 was dosed into the wash water in the storage solvent tank at different flow rates. A Gasmet^{TM} analyser (Fourier Transform Infrared Spectroscopy, CX-4000) equipped with a ZrO_2 oxygen analyser allowed online identification and the quantification of gas species,

including CO_2, SO_2, NH_3 and H_2O, in the flue gas at the inlet and outlet of the pretreatment column. The pH of the solution at the outlet of the pretreatment column was measured online using an industrial pH meter (Rosemount). The detailed experimental activities and observations during the NH_3-dosing experiment are listed in Table 3-6.

Table 3-6 Experimental activities and observations in the SO_2 removal experiment. Flue gas flow-rate = 936 kg/h, CO_2 flow-rate = 120 kg/h, SO_2 concentration = ca. 200 ppmv, liquid flow-rate = 39 L/min, gas inlet temperature = 35–38 °C, inlet wash water temperature = 25 °C

Stage	Time	Activities	pH	SO_2 removal	CO_2 removal	NH_3 outlet
1	09:04	Flue gas on	Not available	No	No	No
2	09:53	Water circulation	Drop to 2.5	Partial	No	No
3	11:40	Dosing NH_3 at 0.2 kg/h	Increase to 2.7	Partial	No	No
4	12:30	Dosing NH_3 at 0.5 kg/h	Increase to 7.2	Almost	No	No
5	13:33	Dosing NH_3 at 1 kg/h	Increase to 8.2	Complete	Possible	Some
6	14:20	Dosing NH_3 at 1.8 kg/h	Increase to 8.6	Complete	Possible	Sharp increase

3.2.3.2 Simulation approach

The results from the dosing experiments are used to validate the model for the SO_2 absorption process by aqueous NH_3. In the NH_3 dosing experiment, SO_2 removal by aqueous NH_3 is operated in a semi batch mode in which the gas is fed in constantly while the liquid is circuited in a cycle, and the SO_2 and NH_3 containing species build up in the solution. It is difficult to simulate the actual process using Aspen Plus, as this software only provides the steady state of simulation results; thus, a differential approach is proposed to realize the simulation of SO_2 removal by NH_3 dosing based on the experimental activities. In the simulation, one hour is divided into 10×6 minutes, and the simulation (SO_2 absorption) is run 10 times, at a time interval of 6 mins. For each run, on the gas side the flue gas components and the amount of flue gas are kept constant, whilst on the liquid side the amount of solvent is reduced to 1/10, i.e. 39

L/min ÷ 10 = 3.9 L/min. Considering that the liquid flow in the system is far away from the plug flow and the solvent leaving from the column will mix with part of liquid system, the built-up SO_2 products will be diluted by the rest of the bulk solvent in the storage tank after one batch simulation run. For example, in the first simulation run, the solvent starts with fresh water in which the amounts of SO_2 and NH_3 present are zero. In the second simulation, the solvent starts with the SO_2 diluted solvent for the next circulations, and so on. Figure 3-11 shows the schematic simulation procedures of the differential approach of SO_2 absorption by aqueous NH_3.

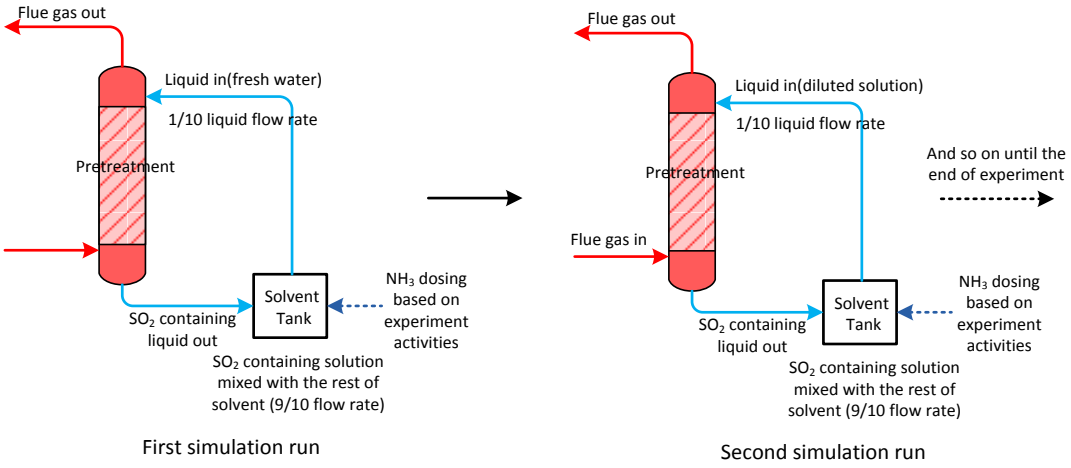

Figure 3-11 Schematic of differential simulation procedure of SO_2 absorption by NH_3 dosing

In the simulation, a dilution factor is employed and its value is affected by the solvent circulation rate, the solvent inventory and the extent of solvent mixing in the system. In this study, a dilution factor of 10 is determined by using the trial and error approach to achieve sound agreement between simulation and experimental results (detailed discussion in section 3.2.3.3), which suggests that the differential simulation method is reliable to describe the behaviours of SO_2 absorption by aqueous NH_3 in the packed column.

3.2.3.3 Results comparison between pilot plant and model

During SO_2 absorption, the oxidation process of S(IV) $\xrightarrow{O_2}$S(VI) inevitably occurs in the presence of oxygen. In our simulation, we assume that SO_2 in the gas phase and SO_3^{2-} in the aqueous solution are slightly oxidised by the oxygen during the capture process. This assumption is based on the following three considerations (Hegg *et al.*, 1978; McKay, 1971; Miller *et al.*, 1972). First, the oxidation of S(IV)→S(VI) primarily takes

place in the liquid phase after SO_2 is dissolved into the solution, generating SO_3^{2-} species. Thus, oxidation will have little influence on SO_2 transportation from the gas phase to the liquid phase. Second, the oxidation rate of SO_3^{2-} to SO_4^{2-} is kinetically controlled, which is generally expressed as $\frac{d[SO_4^{2-}]}{d_t} = K[SO_3^{2-}]$. This means that the rate of production of SO_4^{2-} is proportional to the concentration of SO_3^{2-}, while the SO_3^{2-} concentration is very low (<0.011 mol/L) in the pilot SO_2 removal process. The oxidation of S(IV)→S(VI) is supposed to be very slow. Third, the SO_2 removal process in the pilot plant was carried out in an oxygen-deficit environment, due to the relatively low oxygen concentration of <8.0% in the flue gas, which did not favour oxidation of S(IV). It is therefore anticipated that the SO_3^{2-} will be partly oxidised to SO_4^{2-}, but this minor sulphur oxidation will have little influence on the simulation of SO_2 removal by aqueous NH_3 in the pilot plant. This hypothesis is verified by the excellent agreement observed between the model predictions and experimental results in terms of the solution pH, NH_3, SO_2 and CO_2 concentration at the pretreatment column outlet (Figure 3-12). However, it is acknowledged that the sulphate will eventually dominate the sulphur species, as a result of the irreversible oxidation reaction after sulphite is exposed to oxygen. The study of sulphur oxidation is out of the scope of this thesis, but it is suggested that it should be conducted for better understanding of SO_2 removal by aqueous NH_3 in future.

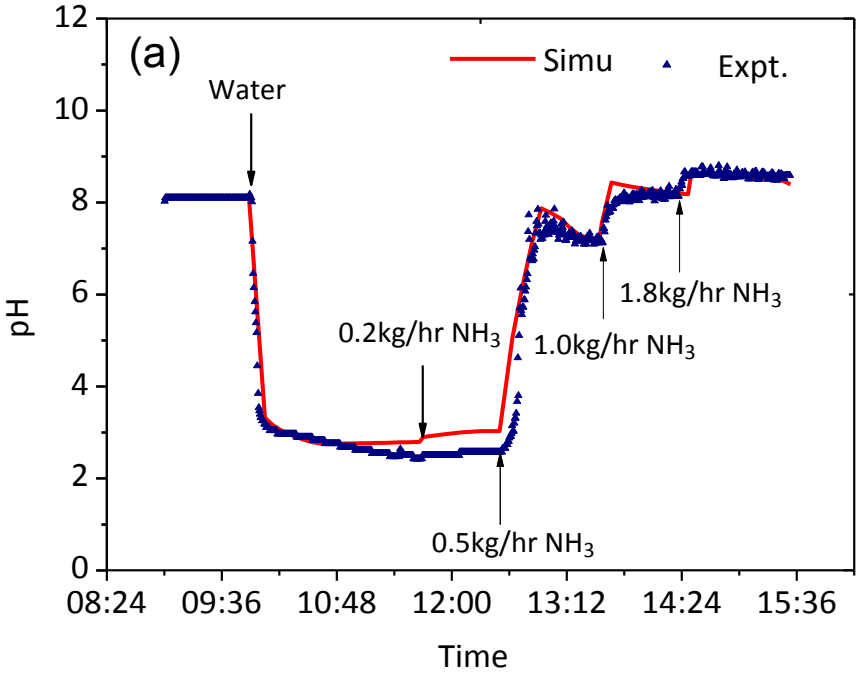
(a)
Simu
Expt.
Water
0.2kg/hr NH3
0.5kg/hr NH3
1.0kg/hr NH3
1.8kg/hr NH3
pH
Time
08:24
09:36
10:48
12:00
13:12
14:24
15:36

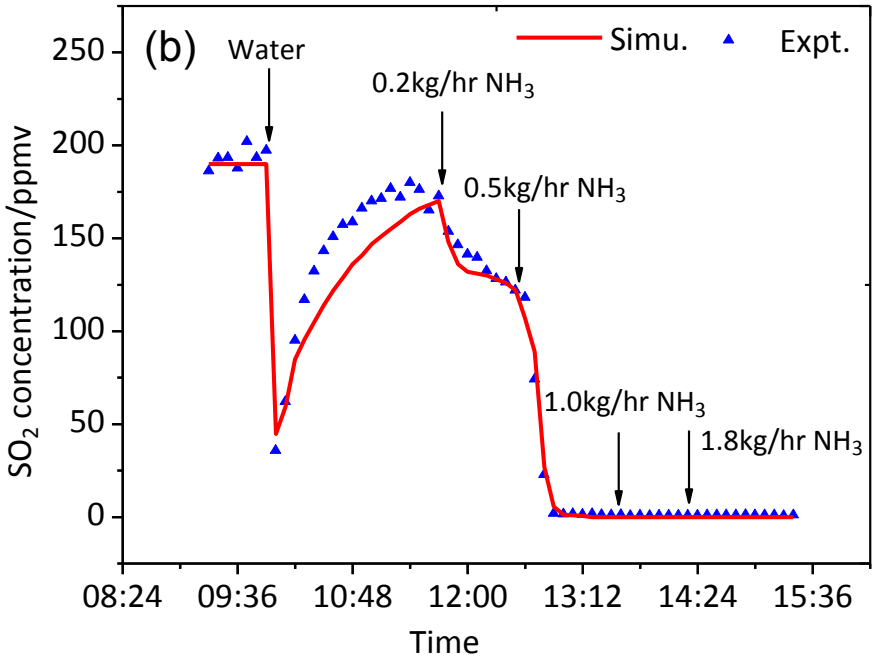
(b)
Simu.
Expt.
Water
0.2kg/hr NH3
0.5kg/hr NH3
1.0kg/hr NH3
1.8kg/hr NH3
SO2 concentration/ppmv
Time
08:24
09:36
10:48
12:00
13:12
14:24
15:36

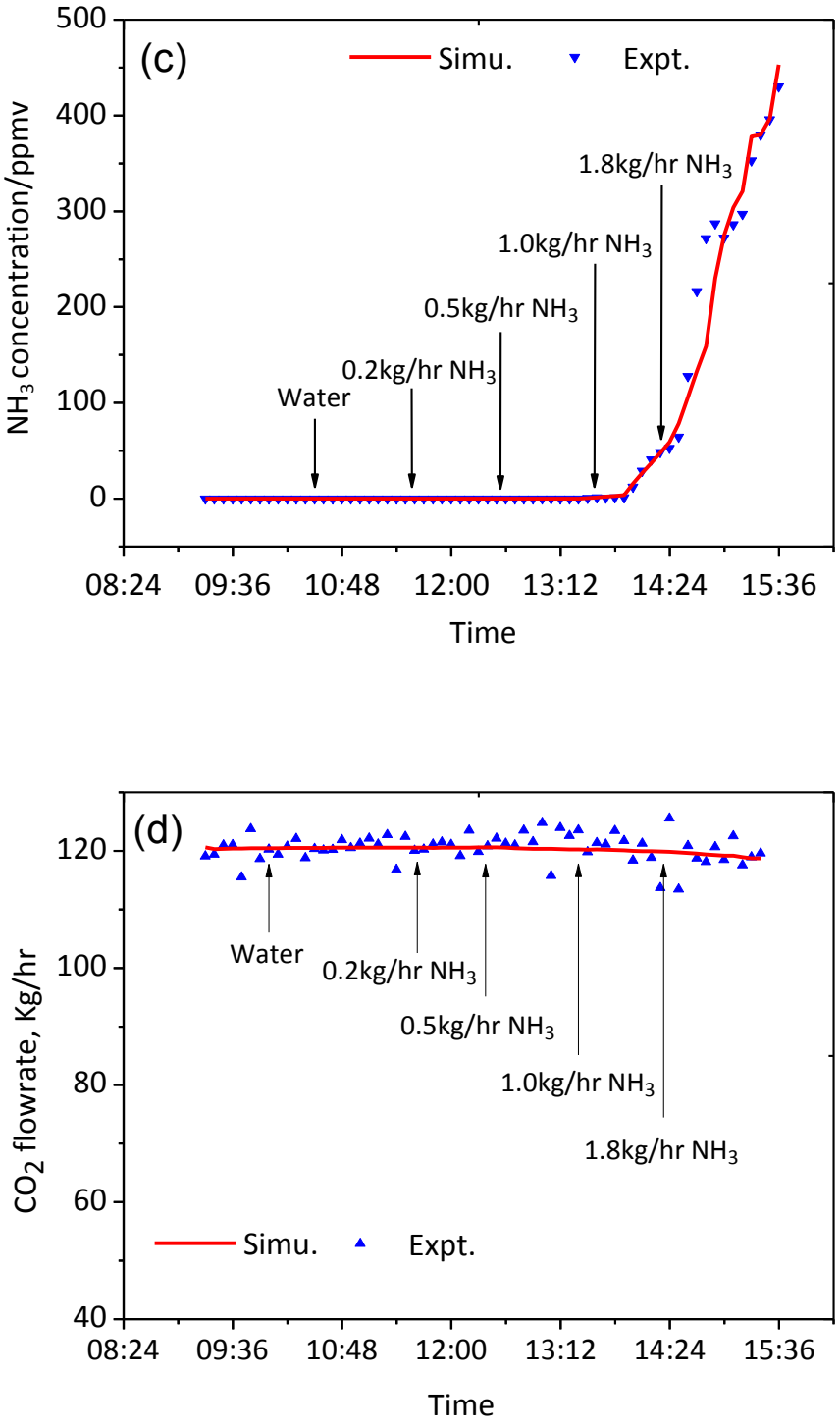

Figure 3-12 Comparison of pilot-plant data with simulation results: (a) outlet solution pH from column; (b) gas SO_2 concentration outlet from column; (c) gas NH_3 concentration outlet from column; and (d) gas CO_2 flow-rate outlet from column

Solution pH: The absorption of both of the acidic gas SO_2 and CO_2 into the aqueous solution leads to a decrease of solution pH. Owing to the great difference of the dissociation constants between H_2SO_3 (pKa=1.81) and H_2CO_3 (pKa=6.38), this pH decrease is primarily caused by the absorption of sulphur dioxide. As shown in Figure 3-12 (a), the solution pH dropped quickly with the SO_2 absorbed by the circulated water due to the increasing solution acidity. The pH value then increased step by step with the increasing NH_3 dosing rate. The experiment results satisfactorily follow the simulation curve, indicating the model can accurately predict the pH variation during the SO_2 removal process by aqueous NH_3. As the solution pH is a very important factor for indicating the distribution of sulphur-containing species, the validation of the solution pH to some extent indicates that the model enables the predication of the solution species in the system of NH_3-CO_2-SO_2-H_2O.

Gas outlet SO_2 concentration: The SO_2 level in the flue gas outlet directly reflects the SO_2 removal efficiency. As shown in Figure 3-12(b), upon water circulation, the outlet SO_2 concentration drops rapidly, but quickly increases to the level close to the inlet SO_2 concentration. This implies that fresh water has a relatively low SO_2 removal capacity. When the NH_3 dosing rate rises to >0.5 kg/hr, the SO_2 concentration drops to a very low level. The simulation results agree reasonably well with the experimental data at these NH_3 dosing stages.

Gas outlet NH_3 concentration: The NH_3 introduced into the water is used to neutralise the acidic SO_2 gas. If the dosed NH_3 is excessive for SO_2 absorption, some NH_3 will slip in to the flue gas, due to the high volatility of NH_3 and the high pH of the wash water. As shown in Figure 3-12(c), NH_3 starts to slip at a dosing rate of 1.0 kg/hr NH_3, above which NH_3 evaporation increases dramatically. The trend of outlet NH_3 concentration is consistent with the model results.

Gas outlet CO_2 flow-rate: When limited NH_3 is used to simultaneously remove SO_2 and CO_2, the SO_2 absorption will dominate the NH_3 competition in preference to CO_2, due to its faster reaction with aqueous NH_3. As shown in Figure 3-12(d), there is no appreciable CO_2 removal in the experiment. The results of CO_2 removal in Figure 3-12(d) and SO_2 removal in Figure 2-12(b) suggests that under the conditions studied SO_2 is absorbed into the solution in preference to CO_2. In other words, SO_2 can be selectively removed by wash water that contains a small amount of NH_3. The simulated

curve is just sitting at the experimental CO_2 flow rate, indicating that the rate-based model has satisfactory prediction on the CO_2 absorption.

In conclusion, the simulation results agree well with the experiment data in terms of solution pH, outlet SO_2 concentration, outlet NH_3 gas concentration and outlet CO_2 flow rate. This implies that the established model can accurately predict the SO_2/CO_2 absorption process by aqueous NH_3. These results, in turn, are sound evidence that the assumptions are reasonable at the studied conditions.

3.3 Summary

In this chapter, the rate-based model for simultaneous capture of CO_2 and SO_2 by aqueous NH_3 is developed using the commercial software Aspen Plus®. The rate-based model is thermodynamically and kinetically validated against the experimental results, including those from open literature and CSIRO pilot plant trials respectively. The results show that the established NH_3-CO_2-SO_2-H_2O model can accurately predict the CO_2/SO_2 absorption by aqueous NH_3 in terms of the thermodynamic characteristics (such as vapour-liquid equilibrium, liquid ion species, etc.) and kinetic behaviours along the packed column (such as chemical kinetic, mass transfer, etc.). This allows for the rate-based model to guide the process simulation of CO_2 absorption and SO_2 removal by aqueous NH_3. In the following chapters, this validated rate-based model is employed to investigate technical performance and improvement, and to generate detailed information for a techno-economic evaluation of the NH_3-based CO_2 capture process.

Chapter 4 Advanced NH_3 Abatement and Recycling Process

Abstract: NH_3 slip is one of the most critical technical and economic difficulties for the potential commercial application of NH_3-based CO_2 capture technology. The mitigation of NH_3 vaporisation usually requires significant energy input, i.e. a heavy duty of solvent cooling and large energy penalty of NH_3 regeneration. In this chapter, a simple but effective process for NH_3 abatement and recycling is proposed by way of the installation of an NH_3 absorber and the utilisation of a high level of waste heat in flue gas. The validated rate-based model is employed for process design, process optimization and an improvement of this NH_3 abatement and recycling system (without SO_2 absorption). After a thorough sensitivity analysis and process improvement, the NH_3 recycling efficiency reaches a high of 99.8% and NH_3 exhaust concentration is only 15.4 ppmv, which meets the NH_3 emission requirement of below 25 ppmv for the consideration of human respiratory safety (Busca *et al.*, 2003; Zhang *et al.*, 2013b). Most importantly, the energy consumption of the NH_3 abatement and recycling system is only 59.34 kJ/kg CO_2 of electricity. The evaluation of mass balance and temperature profile shows this NH_3 recovery process is technically effective and feasible. Therefore, this advanced process design has an excellent chance of being used in industrial application for NH_3 recovery.

4.1 Motivation of process design

The process design was initially a response to three major issues identified from CSIRO's CO_2 capture pilot trials at Delta Electricity's Munmorah Power Station. First, the vaporized NH_3 concentration after the CO_2 absorber reaches more than 10000 ppmv, while the NH_3 content in the CO_2 product stream is maintained to below 200 ppmv during high-pressure stripping (up to 850 kPa) (Yu *et al.*, 2012). Specifically, NH_3 slip predominately occurs during CO_2 absorption, so it is reasonable that significant attention be paid to the recovery of NH_3 from the CO_2 absorber. Second, the high-temperature flue gas (>120 °C) in Australian coal-fired power stations requires extra energy/cooling water to cool it before entering the CO_2 capture plant. The wasted heat from the hot flue gas could instead be used for NH_3 recovery through heat exchange between the flue gas and washing solution in the pretreatment stage, which would also save energy consumption for flue gas cooling. Third, the PCC plant

requires a large amount of make-up NH_3 to maintain an NH_3 balance during CO_2 capture. The new process can directly recycle almost all the slipped NH_3 to the CO_2 absorber, and thus significantly reduce the scale of NH_3 make-up process.

4.2 Process description and simulation

4.2.1 Description of NH_3 abatement and recycling process

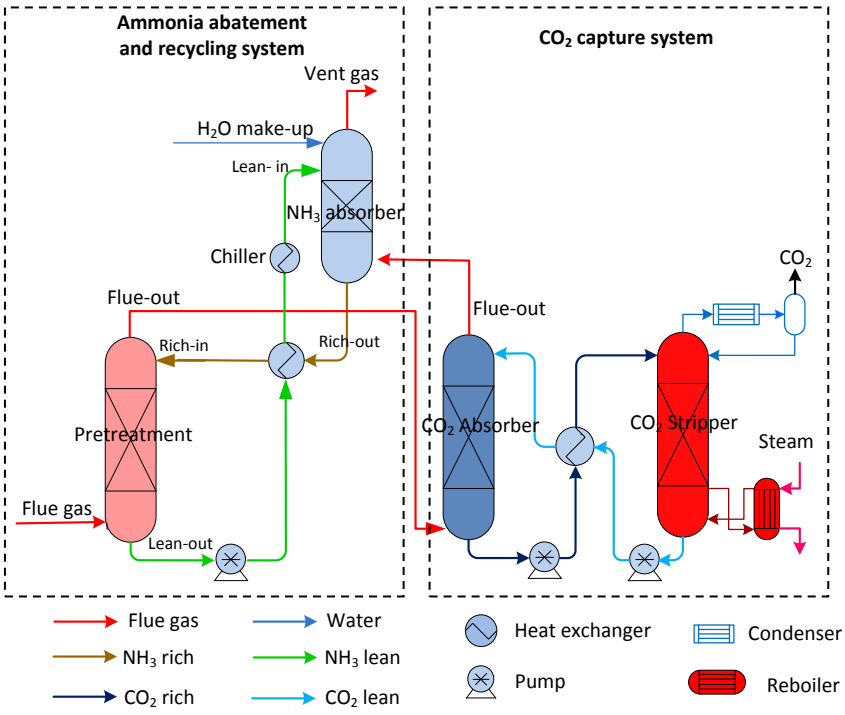

Figure 4- 1 Schematic flow-sheet of the NH_3-based CO_2 capture process

Figure 4-1 shows the schematic flow-sheet of the NH_3-based CO_2 capture process, which integrates the advanced NH_3 abatement and recycling system with a typical CO_2 capture system. The CO_2 capture system comprises a CO_2 absorber and a CO_2 stripper, while the NH_3 abatement and recycling system consists of an NH_3 absorber and a pretreatment column (NH_3 stripper). Initially, fresh water (Lean-in) is fed to the top of the NH_3 absorber to scrub the slipped NH_3. After NH_3 scrubbing, the vent gas meets the set NH_3 exhaust level (<25ppmv) and is discharged into the environment; the lean solvent (Lean-in) becomes rich solvent (Rich-out) and is pumped to the pretreatment column, where it directly contacts the high-temperature flue gas. At this stage, the pretreatment column acts as both a cooler and an NH_3 stripper: it cools down the high-temperature flue gas while also using the heat to release the captured NH_3. After NH_3 desorption, the rich NH_3 stream (Rich-in) returns to the lean NH_3 stream (Lean-out);

the released NH_3 is mixed with cooled flue gas and recycled to the CO_2 absorber as NH_3 make-up. This completes one cycle. The second cycle starts with the lean NH_3 stream (Lean-in) undergoing NH_3 scrubbing in the NH_3 absorber and NH_3 desorption in the pretreatment column. The determiner of the number of cycles is the cycle index, which counts the circulations of solution starting from the wash column, going through the pretreatment column and returning to the wash column. The circulation process continuously operates until the entire NH_3 abatement and recycling system reaches a steady state whereby the composition and temperature in each stream remain constant. During the process, the make-up H_2O is introduced into the NH_3 absorber column to maintain the water balance of the NH_3 recycle system. The NH_3 recycling efficiency is defined as follows.

$$\eta\% = \frac{\mathrm{NH_3\ to\ CO_2\ absorber}}{\mathrm{NH_3\ from\ CO_2\ absorber}} \times 100\%. \quad (4\text{-}1)$$

4.2.2 Description of process simulation

As the proposed NH_3 abatement and recycling process belongs to the chemical system of NH_3-H_2O-CO_2, the validated rate-based model is employed to guide the process development and optimization of this advanced NH_3 recycling process. The pretreatment column is divided into 20 stages and the total stage number of the NH_3 absorber is set to 25, in which the lean stream (Lean-in) is fed to the 5^{th} stage of the NH_3 absorber and the make-up water is fed to the 1^{st} stage for further NH_3 removal. The packing height and diameter are initially set at 2.5m and 0.6m for the washing column, and 3.0m and 0.6m for the pretreatment column, respectively. A 25mm pall ring with a 205 m^2/m^3 surface area is initially chosen as packing material for the washing and pretreatment columns. In the simulation process, the real flue gas from Munmorah Power Station and the typical pilot trial conditions of Test ID-32A of the CO_2 absorption process are applied to ensure reliable and practical simulation results. The properties of the composition of flue gas and vent gas after CO_2 absorber are shown in Table 4-1, and more details about Test ID-32A can be found in Table 3-5.

The real flue gas includes 200-300 ppmv SO_2, NO_x, CO and other trace impurities. However, the amounts of these impure gases are quite small, and the previous CSIRO pilot plant trials have confirmed that the presence of NO_X (mainly NO) and other trace gases have a minimal impact on the CO_2 capture process (Yu *et al.*, 2011). For simplicity, these gases are replaced by N_2 in this process simulation. For the liquid

stream, the fresh water is initially supplied to the NH_3 abatement and recycling process with a rate of 400kg/hr at 25 °C to scrub the vaporized NH_3.

Table 4-1 Typical gas composition from power station

Source	Flow-rate,	Temperature,	Composition, vol/%				
	Kg/hr	°C	CO_2	H_2O	O_2	N_2	NH_3
Flue gas	760	120	10.7	6.0	7.8	75.5	-
Gas after CO_2 absorber	656	16.9	3.23	1.83	9.0	84.2	1.15

The simulation process is divided into three steps. First, the base-case scenario without chiller and heat exchanger is set up to give a detailed description of the NH_3 abatement and recycling process. Second, a thorough sensitivity analysis of the main process parameters, such as liquid flow rate, column size and packing materials, is performed for process improvement and optimization. Third, the chilling process with a chiller and heat exchanger is applied to further improve NH_3 removal and recycling efficiency. The temperature approach between the hot inlet and cold outlet streams is set at 5°C for the heat exchanger. The chilling duty at different temperatures is converted into electricity consumption using a coefficient of performance (COP) of 5. The same values of temperature difference and COP have been used by Darde et al. (2012).

4.3 Base-case scenario

A base case simulation is carried out in order to perform the parameter sensitivity analysis and gain insight into the NH_3 abatement and recycling system.

4.3.1 NH_3 distribution

In the NH_3 abatement and recycling process, the slipped NH_3 from the CO_2 absorber (4.7 kg/hr) travels to three destinations. First, it is discharged into the atmosphere after the NH_3 absorber (gas phase); second, it is recycled to the CO_2 absorber after washing and the pretreatment column (gas phase); and third, it is reacted with CO_2 and H_2O and dissolved in the solution in the form of an aqueous N-containing species, such as the NH_3 molecule, NH_4^+ ions and NH_2COO- carbamate (liquid phase). Figure 4-2(a) shows the NH_3 distribution in different NH_3-containing streams in the gas and liquid phase. It can be seen that the NH_3 flow rates in all streams became stable after 12 cycles. The flow rate of NH_3 to the CO_2 absorber is consistently higher than those of the other NH_3-containing streams, and stabilizes at 4.4 kg/hr with a NH_3 recycling efficiency of 93.61%. The flow rate of the NH_3 absorbed by the liquid remains stable

at "zero", a steady state. This implies that the NH_3 absorption/desorption in the liquid phase reaches a dynamic equilibrium where the NH_3 absorbed by lean solvent is desorbed and recycled to the CO_2 absorber as gaseous NH_3.

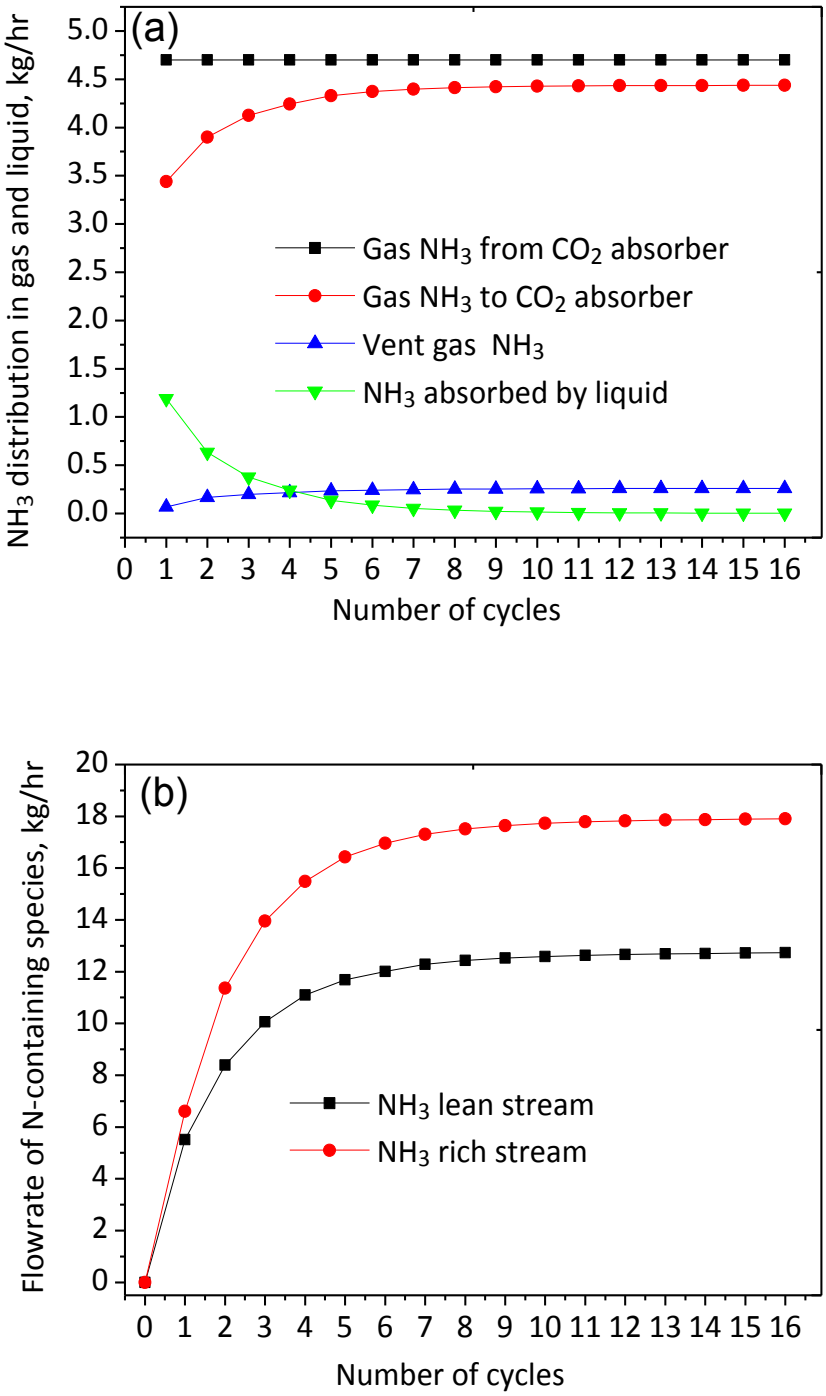

Figure 4-2 (a) NH_3 distribution in gas and liquid phases and (b) flow rate of N-containing species as a function of number of cycles

However, the 'zero' does not mean that there is no NH_3 in the solution. Figure 4-2 (b) shows the total flow rates of N-containing species in the lean stream and rich stream. Initially, the flow rates of NH_3 lean and NH_3 rich streams increase rapidly because the fresh water and low NH_3 concentration solution have a strong capability of NH_3 absorption. The flow rate gap between the lean stream and the rich stream indicates that the NH_3-rich solution is heated to release the scrubbed NH_3 and part of the CO_2. With the increasing time, the gap experiences a quick increase and stabilizes. Consistent with the trend in Figure 4-2(a), the flow rates of N-containing species in the lean and rich streams reach constant values after 12 cycles, these being 12.6 and 17.8 kg/hr respectively. It is interesting that the difference in flow rates between the two streams at a steady state is 5.2 kg/hr, which is higher than the total scrubbed NH_3 of 4.4 kg/hr. This is because, in addition to NH_3, part of the carbonate/carbamate/bicarbonate in the NH_3-rich solution is also decomposed in order to release part of the CO_2 in the pretreatment column.

4.3.2 CO_2 profile

Fig. 4-3 shows the effect of circulation cycles on the CO_2 flow rate in the gas streams.

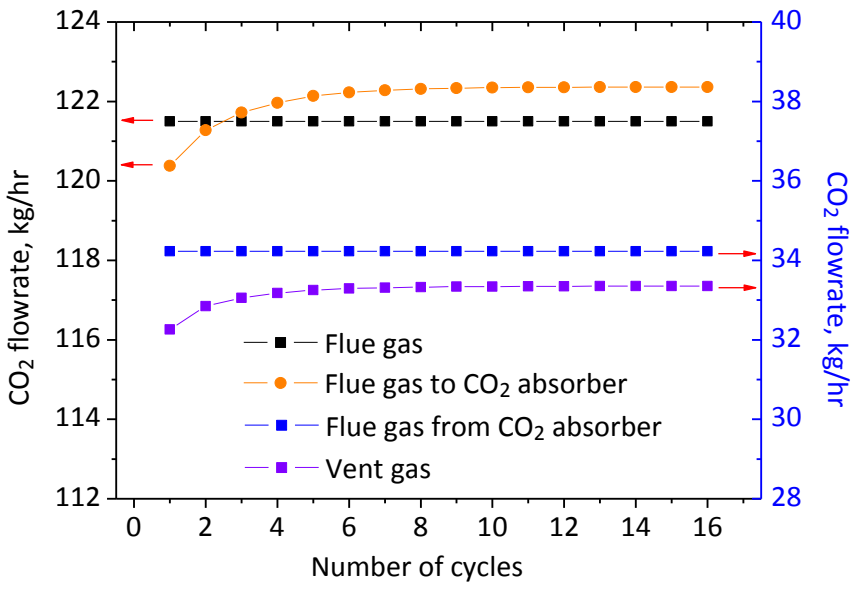

Figure 4-3 The CO_2 flow rate in different gas streams as a function of number of cycles

It can be found that there is a slight decrease of CO_2 flow rate from 34.25 kg/hr in the flue gas from the CO_2 absorber to 33.2 kg/hr in the vent gas after 12 cycles, implying

that the NH_3 washing column also plays a minor role in CO_2 absorption. Meanwhile, the CO_2 flow rate experiences a slight increase from 121.55 kg/hr to 122.4 kg/hr before and after the pretreatment column after 12 cycles, due to the composition of carbon containing species (primary NH_4HCO_3). The increased amount of CO_2 flow rate after the pretreatment column (0.85 kg/hr) is equal to the decreased CO_2 flow rate amount after the washing column (0.85 kg/hr). This indicates that the CO_2 absorption and desorption after 12 cycles has reached equilibrium in this NH_3 abatement and recycling system.

4.3.3 Temperature profile

Figure 4-4 illustrates the effect of circulation cycles on the temperature in the gas streams and liquid streams. It is obvious that all the stream temperatures can quickly reach a steady state. Specifically, the temperature of the lean stream from the pretreatment column increases sharply and stabilizes at 46.7 °C, while the temperature of the rich stream after NH_3 absorption is constant at 22.4 °C with a stable temperature difference of 24.3 °C(Figure 4-4(a)). The heat contained in the flue gas (120 °C) travels to two sections: one is for heating up the solvent; the other is for NH_3/H_2O vaporization and carbonate/bicarbonate decomposition. According to the gas stream temperature profile shown in Figure 4-4(b), the pretreatment column acts as a cooler to cool the flue gas temperature from 120 °C to 38.9 °C, which enables a substantial energy saving for the flue gas cooling. Although the temperature of 38.9 °C is higher than the 16.9 °C flue gas setting in the pilot plant, this increase has negligible effects on CO_2 absorption rate and NH_3 loss rate, which changes from 87.61 kg/hr to 87.58 kg/hr and from 4.700 kg/hr to 4.704 kg/hr, respectively. This is due to the low temperature flue gas containing a small amount of H_2O vapour, and the consequent small heat capacity of the flue gas.

According to the base case study, it can be concluded that this advanced process has the benefits of high NH_3 recovery efficiency and flue gas cooling without the exertion of any influence on the whole CO_2 capture system; and that the simulation has reached a stable state in terms of species concentrations and stream temperatures over 12 cycles. The following simulations are conducted in the same way as the base case. NH_3 flow rates, CO_2 flow rates and steady state temperatures are employed for parameters optimization and process improvement.

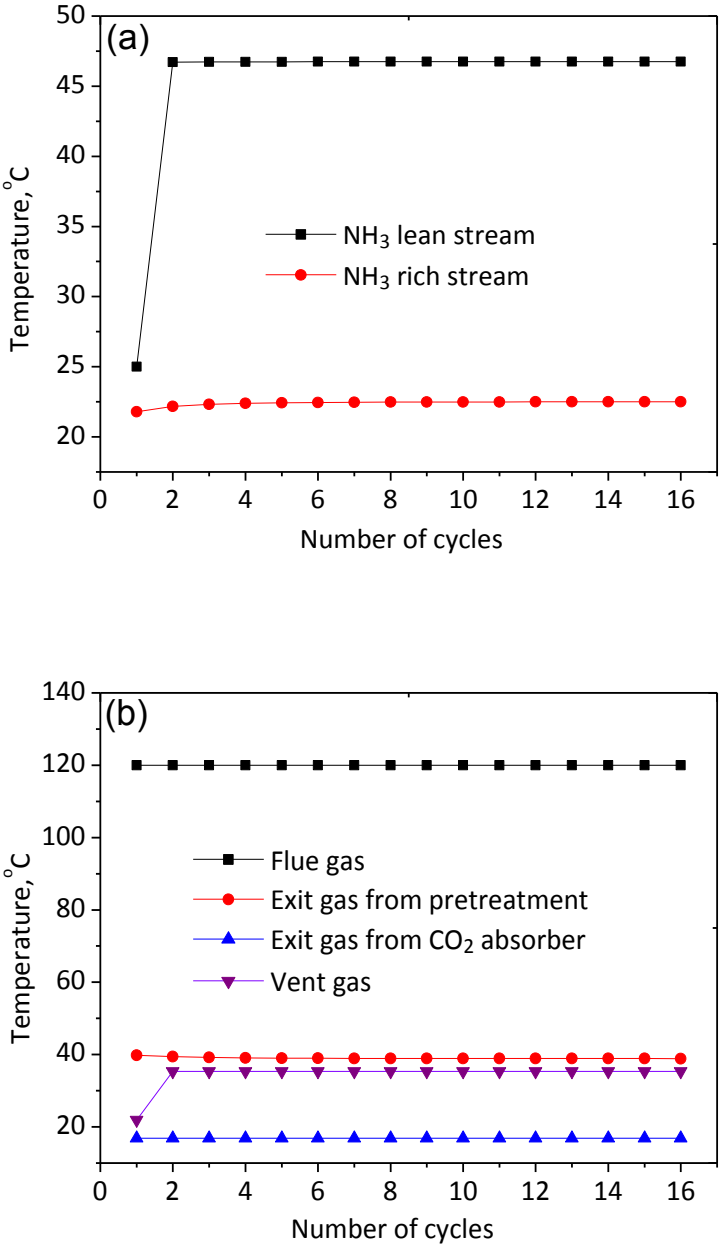

Figure 4-4 Temperature profile of (a) liquid streams and (b) gas streams as a function of number of cycles

4.4 Process optimization

4.4.1 Parameters optimization

A sensitivity study of washing solvent flow rate, column size and packing materials is conducted to understand how these parameters affect the NH_3 recycling efficiency and emission concentration.

4.4.1.1 Effect of solvent flow rate

The flow rate of washing solvent has a clear influence on the NH_3 recycling efficiency and emission concentration. A low liquid flow rate cannot provide sufficient water to absorb NH_3, resulting in the slippage of more NH_3 into the environment. While, at a high washing solvent flow rate, the heat in the flue gas is insufficient to heat the solution to the temperature required for desorbing most of the NH_3, leaving more to stay in solution and a resultant high NH_3 emission concentration. Therefore, the liquid flow rate should be determined for consideration of both a high NH_3 recycling efficiency and a low NH_3 emission rate. As shown in Figure 4-5, the NH_3 recycling efficiency first rises and then falls with the increasing liquid flow rate, reaching a maximum of 94.9% NH_3 recycle efficiency at a rate of 350 kg/hr. At this point, NH_3 emission concentration reaches a minimum value of 592 ppmv. The flow rate of 350 kg/hr in the NH_3 recycle system is very small compared to the 8040 kg/hr solvent circulation rate in the CO_2 capture system, which is able to significantly reduce the scale of NH_3 recovery and energy input created by solvent pumping.

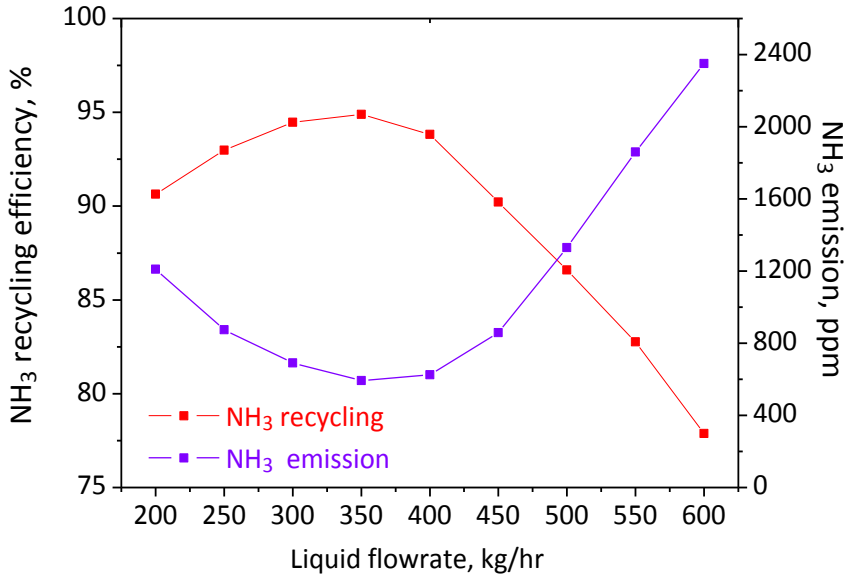

Figure 4-5 Effect of liquid flow rate on the NH_3 recycling efficiency and NH_3 emission concentration

4.4.1.2 Effect of column size

As the rate-based model is closely related to mass and heat transfer, chemical reaction kinetics and hydrodynamics, the size of the column has a significant influence on the

efficiency of NH_3 abatement and the recycling system. It is generally accepted that an increasing size especially the packing height can provide more residence time for the flue gas and the solvent inside the columns, which facilitates NH_3 capture and the recycling process. However, when designing a column for CO_2 capture it is also particularly important to keep low capital and operating costs. Thus, the column size should be determined by the balance of technical efficiency to capital investment. Figure 4-6 shows the effect of the size of a washing column and a pretreatment column on the NH_3 recycle efficiency and NH_3 emission concentration. As presented in Figure 4-6 (a), the NH_3 recycle efficiency increases sharply with an increase in the packing height of the washing column from 1.5 m to 3.0 m, due to the increasing contact time of the gas phase and liquid phase along the column. However, no obvious improvement in NH_3 recycling efficiency is found for column heights of between 3.0 m and 5.0 m. As for the NH_3 emission concentration, it drops quickly when the packed height is increased to 3.0 m, and shows a slight reduction from 3.0 m to 5.0 m. This indicates that the slipped NH_3 is primarily captured in the first 3 m of the washing column. A similar phenomenon is also found in the effect of the pretreatment column size, as shown in Figure 4-6(b). The NH_3 recycling efficiency increases and NH_3 emission concentration decreases greatly at first, then varies gently after the 3.0 m mark of the packed height of the pretreatment column.

In contrast, the inner diameters of the washing column and the pretreatment column have an insignificant impact on the NH_3 capture and recycle process (Figure 4-6 (b)). From the viewpoint of the gas dynamic, the flue gas can be well dispersed along a small diameter column, which facilitates gas-liquid chemical reactions and saves capital investment. However, the column with a small diameter cannot provide enough contact between the liquid and the gas phase. More importantly, the diameters of columns are limited by the flooding problem (80% of flood in this study). During the simulation, a warning of flooding appeared when using a 0.4m column diameter, where the gas encountered great resistance from the falling liquid. This will lead to a high pressure drop and make the operation difficult. Although increasing the column diameter to 0.5m and 0.6m eliminated the flooding risk, it increased the capital cost without much improvement in the NH_3 recycling efficiency in this study. The balanced diameter of 0.5 m was chosen for the washing and pretreatment columns based on the consideration of both technical efficiency and construction cost. Therefore, the packed

height and inner diameter are chosen as 3.0 m and 0.5 m for the washing column, and 3.0 m and 0.5 m for pretreatment column, respectively, at which the NH_3 recycle efficiency level reaches 96.46 % and the NH_3 emission concentration is 434 ppmv.

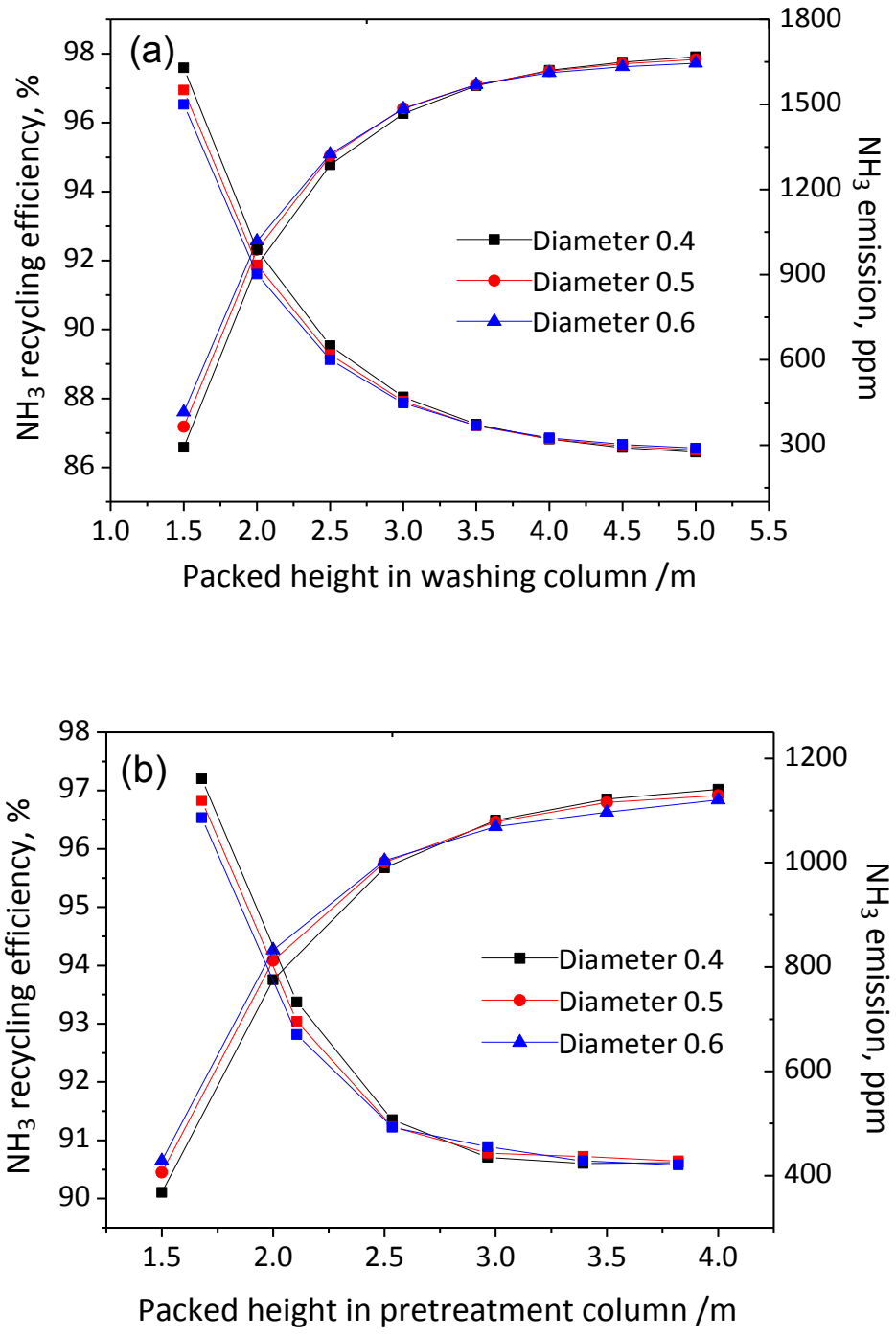

Figure 4-6 Effect of (a) washing column size and (b) pretreatment column size on the NH_3 recycling efficiency and emission concentration

4.4.1.3 Effect of packing material

Packing materials with different geometry also have a great effect on the mass/heat transfer coefficients, interfacial surface area and pressure drop, thereby influencing the NH_3 absorption and recycling process. Generally, a large geometric area and high level of void fraction is beneficial for a high mass transfer efficiency and low pressure drop, respectively. In this study, four different packing materials with effective areas ranging from 205 to 708 m^2/m^3 and void fractions (porosity) of over 93% are investigated. Table 4-2 shows the geometric characteristics of the packing materials which are automatically obtained from the Aspen Plus databank.

Table 4-2 The main parameters of different packing materials used in this study

No.	Pack type	Vendor	Surface area (m^2/m^3)	void fraction
1	Pall ring-25mm	GENERIC	205	0.94
2	Pall ring-16mm	GENERIC	341	0.93
3	Wire-pack -500Y	GENERIC	500	0.95
4	CY	SULZER	708	0.965

Figure 4-7 shows the NH_3 recycling efficiency and emission concentration as a function of four different packing materials.

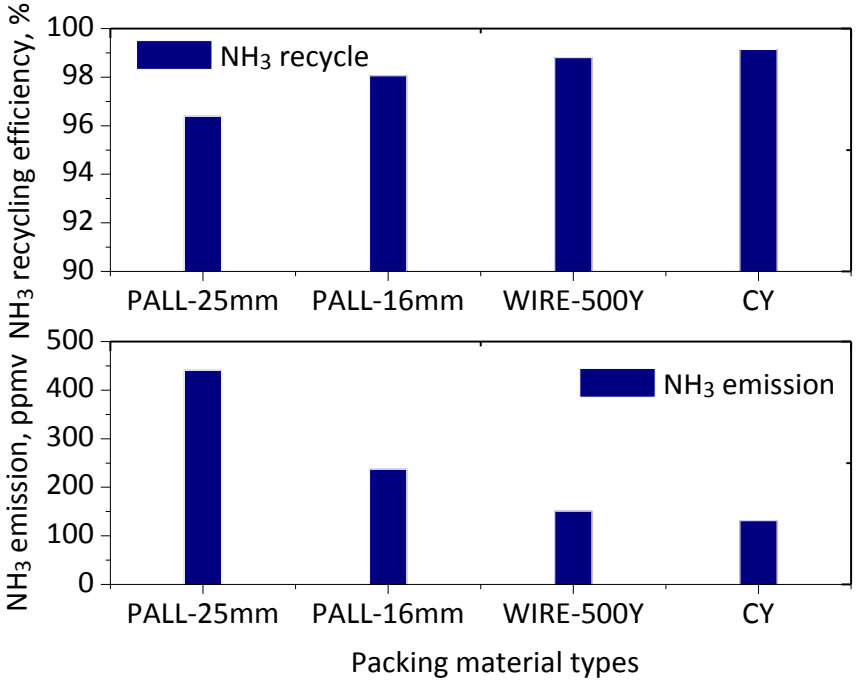

Figure 4-7 Effect of packing material types on the NH_3 recycling efficiency and NH_3 emission concentration

The results are based on the simulation conditions of a constant 80% flood and a 0.6 mbar/m pressure drop. It can be seen that the NH_3 emission concentration decreases significantly with the increasing surface area, suggesting that packing materials with a large effective area can provide more surface area at the same packing volume and facilitate NH_3 absorption. In terms of NH_3 recovery, the recycling efficiencies of Pall ring-16mm, Wire-pack-500Y and CY are quite satisfactory which exceed 98% recovery. When using CY packing material for washing and pretreatment columns, the NH_3 recycling efficiency can reach a high of 98.9 % and the NH_3 emission concentration is reduced to 131 ppmv.

4.4.2 Further improvement by chilling process

The above simulation results are based on utilizing the heat contained in the flue gas without adding energy to the system. Although there is a high NH_3 capture and recycling efficiency, the NH_3 emission concentration discharged into the environment is 131 ppmv, which far exceeds the targeted emission level of below 25 ppmv. To meet the NH_3 emission standard, chilling NH_3-lean solution is introduced to decrease NH_3 volatility, thereby ensuring a better NH_3 capture efficiency. Table 4-3 lists the NH_3 recycling efficiency, NH_3 concentration in vent gas and energy consumption at different cooling temperatures, and compares the results of NH_3 recovery in Darde's simulation.

Table 4-3 Results comparison between Darde's equilibrium simulation of two-stage NH_3 washing and this advanced process

	Darde's simulation*		Chilling Temperature/°C			
	Case A	Case B	22.5	15	10	5
NH_3 conc. gas out absorber(ppmv)	10105	1860	12000			
NH_3 emission conc.(ppmv)	14.6	8.7	131	36.6	15.2	3.8
NH_3 recycle efficiency (%)	99.85	99.53	98.9	99.69	99.87	99.96
Heat requirement (kJ/kg CO_2)	408	167	0	0	0	0
Electricity requirement (kJ/kg CO_2)	143	88	0	42.3	59.34	76.5

*10 °C chilling water is used for NH_3 recovery

It is evident that the NH_3 emission concentration drops significantly to below 25 ppmv when the washing solvent is chilled to below 10 °C. A lower chilling temperature of 5 °C even decreases the NH_3 content to below 10 ppmv, but this occurs at the expense of an increase in energy consumption for the solvent chilling. With the decrease of the chilling temperature, the NH_3 recycling efficiency experiences an increase to over 99.5%. In terms of energy consumption, this advanced NH_3 recovery system requires no heat duty input due to the use of the heat contained in the hot NH_3-lean stream from the pretreatment stream (46-47 °C) by means of a highly efficient heat exchanger. More importantly, due to the small amount of solvent needed in this system, this advanced process requires a very small chilling duty of 0.29 MJ/kg CO_2 (equivalent to electricity of 59.34 kJ/kg CO_2 captured) for NH_3 recovery, which is much lower than that of 2.37 MJ/kg CO_2 in the chilled ammonia process, as simulated by Mathias et al. (2010), and 1.7 MJ/kg CO_2 in the novel process simulated by Niu et al. (2013). The value is also extremely small compared to the heat requirement for the solvent regeneration in the CO_2 capture system (2000-3000 kJ/kg CO_2 captured) (Jilvero *et al.*, 2012).

Compared to Darde et al.'s work (2012), this advanced system has a better ability to recover high NH_3 concentration gas (12000 ppmv) and the advantages of a low energy penalty and simple facility requirement. Considering the technical and energy-saving targets, a chilling temperature of 10 °C has been chosen, at which NH_3 recycling efficiency is 99.87%, and vent gas NH_3 concentration is 15.2 ppmv and the total electricity consumption is only 59.34 kJ/kg CO_2 captured,

4.5 Material balance analysis of NH_3 recycling system

The temperature profile of each stream is necessary for understanding the heat flow and transport among gas and liquid streams. The streams temperature that is depicted as having a steady state in Figure 4-8 shows how the NH_3 recycle system make good use of the heat: (I) the waste heat contained in high-temperature flue gas is transferred to the NH_3-rich solvent by heating the solvent and recovering almost all of the captured NH_3; (II) the relatively high-temperature solvent from the pretreatment column transfers the heat for heating up the solvent from the NH_3 absorber through the heat exchanger for better NH_3 recycling efficiency. The flue gas is then cooled to 44.5 °C after the NH_3 recycle process; this is a suitable temperature for the CO_2 capture system. As aforementioned, the temperature of the flue gas in the inlet of the CO_2 absorber

ranges from 25 °C to 45 °C, which has a negligible effect on the CO_2 capture system. The CO_2 absorption rate ranges from 87.61 kg/hr to 87.58 kg/hr and the NH_3 loss rate ranges from 4.700 kg/hr to 4.704 kg/hr. This indicates that the flue gas cooling process could be removed with the assistance of this NH_3 abatement and recycling system.

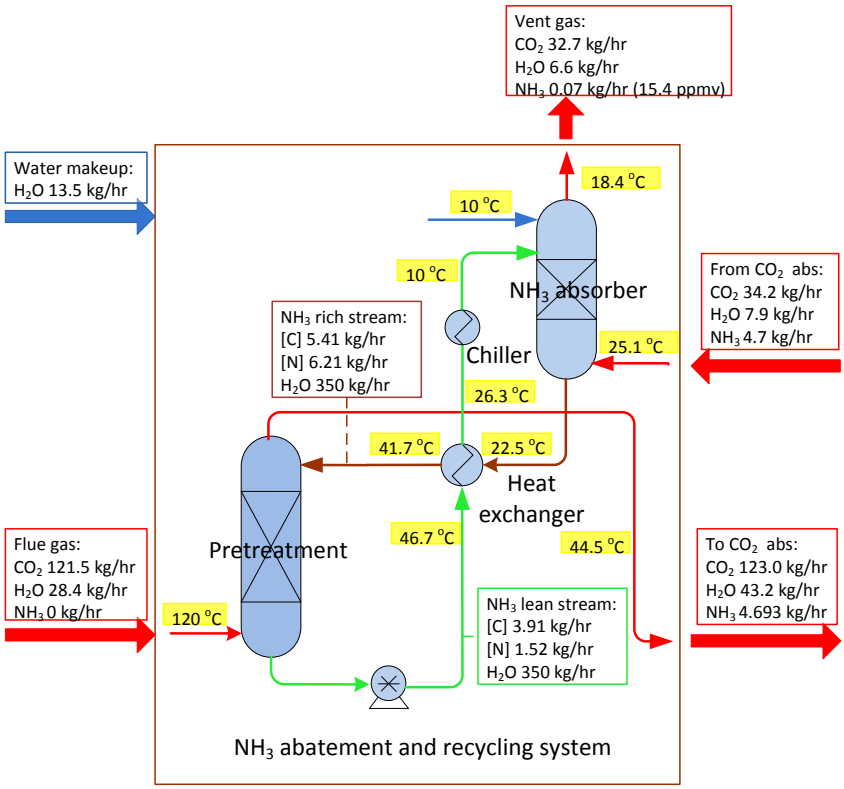

Figure 4-8 Mass balance of NH_3, CO_2, H_2O and streams temperature in the NH_3 abatement and recycling system. [C] and [N] represent the total C-containing and N-containing species in the liquid, respectively.

The mass balance is also particularly important to ensure the normal operation of NH_3 abatement and recycling process. Figure 4-8 shows how the system runs with the mass balance being in a steady state.

CO_2 balance: a small amount of CO_2 (1.5 kg/hr) is absorbed during the NH_3 capture process, while the same flow rate of CO_2 is regenerated by the high-temperature flue gas in the pretreatment column;

NH_3 balance: the majority of the NH_3 recycled to the CO_2 absorber, together with the exhaust NH_3 gas, is equal to the source NH_3 that is vaporized from the CO_2 absorber, indicating that almost all of the slipped NH_3 is recycled to the CO_2 absorber for the recapture of CO_2;

H_2O balance: H_2O make-up stream is used to maintain the water balance to achieve a steady state of operation, because more moisture is vaporized by the hot flue gas and flows into the CO_2 absorber. It has to be pointed out that the make-up water consumption is substantial when the process is applied to a full-scale CO_2 capture plant. Therefore, a water separation process consisting of a cooling tower and stripper is suggested for the separation of H_2O from the flue gas leaving the pretreatment column. A cooling tower with a condenser installed at the top is used for the condensation of the water vapour that accompanies the formation of the carbonate/carbomate species, while the stripper is used to strip off the CO_2 and NH_3 from the condensate to obtain relatively pure water (the details of this will be discussed in section 6.1.4). After water separation, the condensed water could be used as the H_2O makeup in the NH_3 recycle unit and CO_2 capture unit. This ensures that the water is balanced not only in the NH_3 abatement and recycling system, but also in the whole CO_2 capture system.

4.6 Summary

In this chapter, the process simulation has demonstrated that the proposed NH_3 abatement and recycling process can successfully solve the problems of NH_3 slip and flue gas cooling in the NH_3-based CO_2 capture process. Using the rate-based model, a base case scenario has been established to give a detailed description of the NH_3 capture and recycle process, and a sensitivity analysis of primary process parameters has been carried out to improve the performance of NH_3 recycling efficiency and NH_3 emission concentration. Further improvement through chilling process has been shown to significantly reduce the NH_3 level in the vent gas and enhance the NH_3 recycle performance. Under these optimised conditions, the proposed technology provides the following technical, environmental, and economic advantages: (i) a simplified NH_3 abatement system; (ii) over 99.5% of NH_3 recycling efficiency; (iii) 15.2 ppmv NH_3 content in the vent gas; (iv) 59.34 kJ/kg CO_2 electricity consumption by making effective use of flue gas waste heat; and (v) the maintenance of a system mass balance of NH_3, CO_2 and H_2O.

Chapter 5 Combined SO_2 Removal and NH_3 Recycling Process

Abstract: Burning coal for power generation causes emissions of acidic pollutants, such as NO_x, SO_2 and CO_2. Based on the process design of the NH_3 abatement and recycling system, an advanced and effective process of combined SO_2 removal and NH_3 recycling is proposed to simultaneously achieve SO_2 and CO_2 removal, NH_3 recycling and flue gas cooling in one process. The established rigorous rate-based model of the NH_3-CO_2-SO_2-H_2O system is employed to simulate this process. Using a base-case scenario based on a typical pilot-plant trial, the behaviours of SO_2 removal and NH_3 recycling in the proposed process configuration are analysed. The feasibility of the process according to different scenarios, such as high SO_2 concentration in the flue gas, high NH_3 content from the CO_2 absorber and high-temperature flue gas, is then discussed to evaluate the technical adaptability of this process. The purpose of this study is to further advance the NH_3 recycling process and to achieve high SO_2 removal efficiency. To our knowledge, this is the first time that a combined capture of SO_2 and CO_2, using aqueous NH_3 integrated with flue gas cooling and NH_3 recycling in CO_2 capture process, has been presented and analysed in detail.

5.1 Process description and simulation

Figure 5-1 shows the process flow-sheet diagram of the combined SO_2 removal and NH_3 recycling integrated with an aqueous NH_3-based CO_2 capture unit (stripper not shown). This process configuration is consistent with the NH_3 recycling system, consisting of a pretreatment column, an NH_3 wash column and a CO_2 absorber.

Initially, the stream (NH_3 lean) is fed to the top of the NH_3 absorber to scrub the slipped NH_3 from the CO_2 absorber. After NH_3 absorption, the vent gas meets the set NH_3 exhaust level (<25ppmv) and is discharged into the environment; the lean solvent (NH_3 lean) becomes rich solvent (NH_3 rich) and is pumped to the pretreatment column, where it makes direct contact with the high-temperature flue gas. At this stage, the pretreatment column acts as not only a flue gas cooler, but also an NH_3 stripper and a SO_2 scrubber: it cools the high-temperature flue gas, uses the heat in the flue gas to release the captured NH_3, and absorbs the SO_2 by using the NH_3-rich solution. After being in the pretreatment column, the rich NH_3 stream (NH_3 rich) becomes a lean NH_3 stream (NH_3 lean); the released NH_3 is mixed with cooled flue gas and recycled to the

CO_2 absorber as NH_3 make-up; the absorbed SO_2 is formed as sulphite and remains in the solution. This completes one cycle.

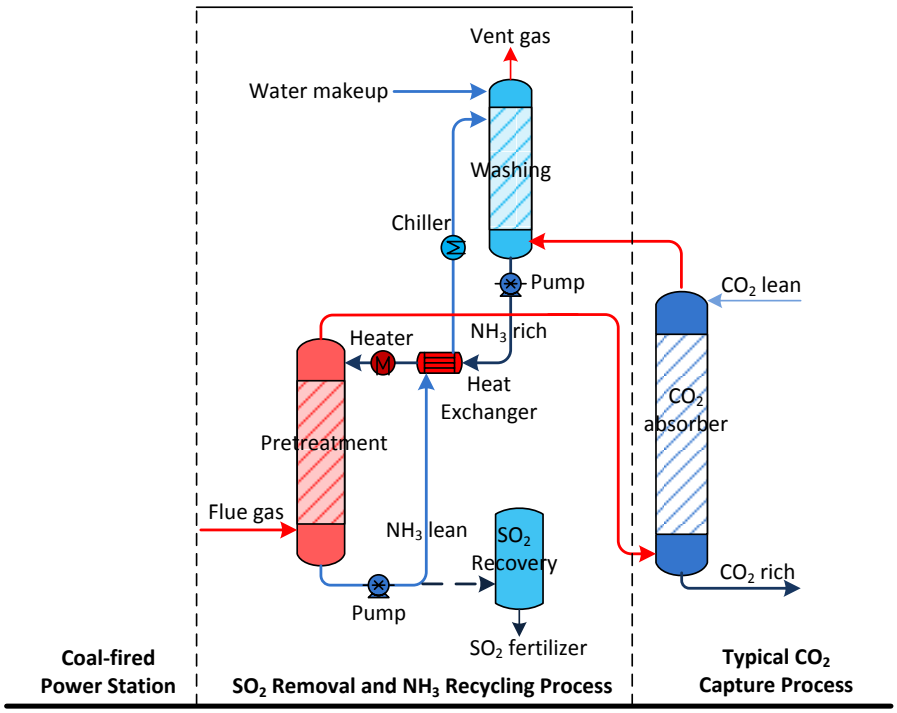

Figure 5- 1 Combined SO_2 removal and NH_3 recycling process for CO_2 capture by aqueous NH_3

The second cycle starts with the lean NH_3 stream (NH_3 Lean) undergoing NH_3 scrubbing in the NH_3 absorber and NH_3 desorption and SO_2 absorption in the pretreatment column. The solution is continuously circulated between the pretreatment column and the wash column, while absorbed SO_2 is accumulated in the circulated solution. After a number of circulations, the entire system reaches a semi-steady state in which the temperatures of each stream remain constant. The solution looping halts after the sulphur-containing electrolyte concentration reaches the saturation point (35 wt% $(NH_4)_2SO_3$ at 10 °C), and the saturated solution can be used for the ammonium sulphate production for further treatment (not included in this thesis). The H_2O makeup is introduced into the wash column to maintain the water balance in the NH_3 recycle and SO_2 recovery system. A chiller is used to cool the NH_3-lean solvent to achieve a high NH_3 capture efficiency, while a heater heats the NH_3-lean solvent to enhance the performance of NH_3 desorption and recycling.

The optimised process conditions determined in the NH_3 recycling system (chapter 4) are used, i.e. a 350 kg/hr wash water circulation rate, a 10 °C wash water inlet

temperature, a wash column size $\emptyset 0.5\ m \times h3.0\ m$, a pretreatment column size of $\emptyset 0.5\ m \times h3.0\ m$, and a 5 °C temperature approach of the heat exchanger between the hot inlet stream and the cold outlet stream (hot side). The flue gas conditions are kept the same as the NH_3 recycling process (Table 4-1), except that the flue gas contains SO_2 and an average concentration of the 200 ppmv is used.

The process simulation is divided into two steps. The first is to propose a base case to figure out the NH_3 profile, SO_2 profile and column profiles of the combined SO_2 removal and NH_3 recycling process. The second is to investigate the effect of SO_2 content in flue gas, the NH_3 content from the CO_2 absorber and the flue gas temperature of the SO_2 removal efficiency and NH_3 reuse efficiency, and to evaluate the technical adaptability and feasibility of the SO_2 removal and NH_3 recycle process.

5.2 Base-case scenario

The combined SO_2 removal and NH_3 recycling process involves the continuous circulation of wash water between the pretreatment column and wash column. During the continuous circulation, SO_2 is absorbed and accumulated in the solvent, while NH_3 is absorbed in the wash column and desorbed in the pretreatment column. The amounts of SO_2 and NH_3 present in the wash water and gas phase depend on the operation conditions and number of cycles (time of operation). Using the rate-based model, the base-case scenario is simulated to investigate NH_3 recycling, SO_2 removal and column profiles as a function of the number of cycles, and determine the effectiveness of SO_2 removal and NH_3 recycling..

5.2.1 NH_3 profiles

In the combined SO_2 removal and NH_3 recycling system, the NH_3 that has slipped from the CO_2 absorber is either reused (recycled back to the CO_2 absorber or retained in the wash water for SO_2 removal) or emitted to the environment. Figure 5-2 shows the NH_3 reuse efficiency and vent gas NH_3 emission concentration as a function of the number of cycles. The NH_3 reuse efficiency is defined as the ratio of NH_3 used for recycling and SO_2 capture to the total NH_3 that slipped from the CO_2 absorber. At a steady state, 96.62% of NH_3 is recycled to the CO_2 absorber, while 3.36% of NH_3 is used for SO_2 capture. The total NH_3 reuse efficiency reaches as high as 99.98%. The rest of the NH_3 is discharged into the environment. As aforementioned, NH_3 vapour is a hazardous pollutant and its emission level must meet the NH_3 emission standard to

below 25 ppmv (Busca *et al.*, 2003). In the simulation, the emitted NH_3 concentration is consistently below 15 ppmv during the circulation times that are studied. This indicates that the clean vent gas can be directly discharged into the atmosphere without exceeding emission levels.

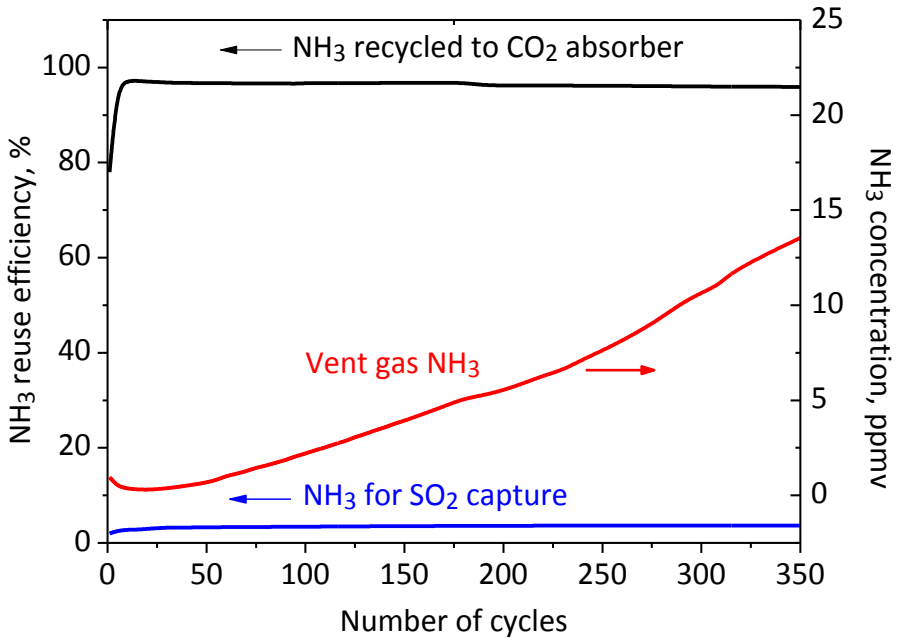

Figure 5-2 NH_3 reuse efficiency and vent gas NH_3 emission concentration as a function of the number of cycles

5.2.2 SO_2 profiles

As shown in Figure 5-3(a), the proposed process achieves a high SO_2 capture efficiency, which is constantly >99.98%. Trace levels of SO_2 emissions vary from 10 to 30 ppbv. This high-efficiency removal is primarily attributed to the fast reaction between SO_2 and H_2O, and because the generated HSO_3^- is quickly neutralised by basic aqueous NH_3. Figure 5-3(b) shows the concentration profiles of sulphur-containing species in the wash water at the outlet of the pretreatment column as a function of number of cycles. SO_2 is accumulated in the solution in the forms of $(NH_4)_2SO_3$, NH_4HSO_3 and $(NH_4)_2S_2O_5$ as the cycle number increases. $(NH_4)_2SO_3$ is persistently the dominant species in the wash water. Its concentration increases gradually to 35% (saturated concentration of $(NH_4)_2SO_3$ at 10 °C), while the NH_4HSO_3 and $(NH_4)_2S_2O_5$ stay at relatively low levels. This is because the SO_2 absorption process by aqueous NH_3 is conducted at a pH >7 and the alkaline environment facilitates the generation of

the SO_3^{2-} species. The concentrated SO_2 solution is expected to undergo a further treatment, e.g. producing ammonium sulphite/sulphate fertilisers for cost compensation.

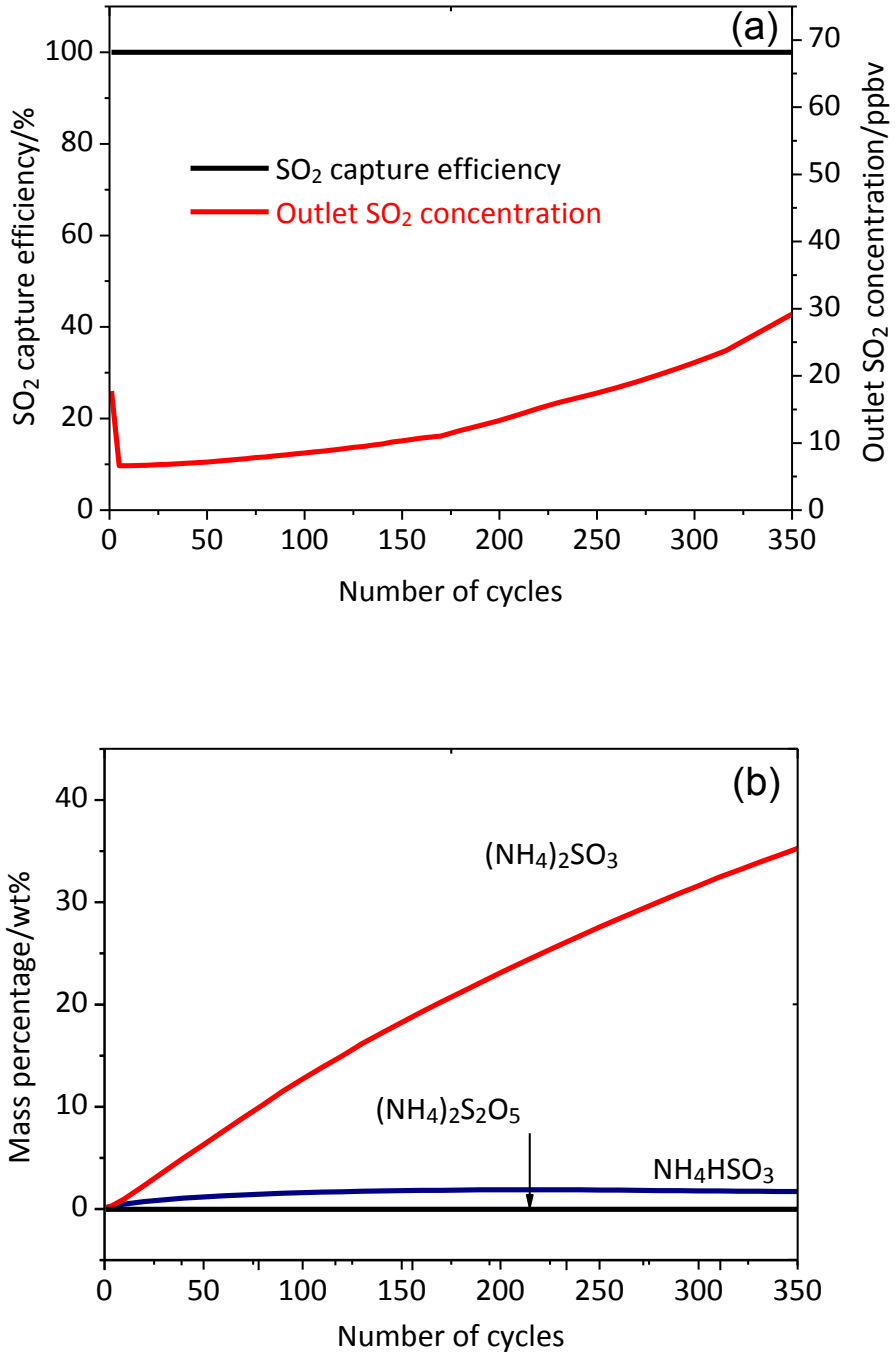

Figure 5-3 (a) SO_2 capture efficiency and SO_2 emission level from the pretreatment column and (b) concentration profiles of sulphur-containing species in SO_2-rich solution as a function of the number of cycles

5.2.3 Column profiles

To gain insight into how NH_3 is scrubbed and recycled, and how SO_2 is removed, the NH_3 and CO_2 profiles along the wash column and the NH_3 and SO_2 profiles along the pretreatment column are investigated. As shown in Figure 5-4(a), the absorption of NH_3 primarily takes place in the bottom half of the wash column, where the NH_3 absorption has a powerful driving force because of the high NH_3 concentration in the flue gas. The vent gas after the wash column contains a low concentration of NH_3 and can be discharged into the atmosphere without further treatment. As gaseous NH_3 is dissolved in the washing solution, a small amount of CO_2 is absorbed into the solution in the wash column. This is due to the presence of free NH_3 in the wash water, and the high pH of the solution.

The NH_3-loaded solvent in the pretreatment column is heated by the hot flue gas to release the scrubbed NH_3. As indicated in Figure 5-4(b), the NH_3 is vaporised rigorously, particularly in the bottom stages. During NH_3 vaporization, the SO_2 in the flue gas is quickly removed by the NH_3-loaded solution, and the SO_2 absorption mainly occurs in the first 1 metre from the bottom of the column. Accompanying the NH_3 evaporation and SO_2 absorption, the CO_2 absorbed in the wash column is desorbed in the pretreatment column. Overall, virtually no CO_2 absorption occurs in the combined capture process, which has been discussed in section 4.3.2.

Figure 5-4 (c) shows that the flue gas temperature decreases significantly (from 120 to 42 °C) along the pretreatment column after contact with the circulating solvent. This is of particular importance for saving the energy used to cool the flue gas. In summary, the pretreatment column in the proposed configuration plays three significant roles: (1) as a chiller, to cool down the hot flue gas; (2) as a heater, to strip and recycle almost all of the slipped NH_3; and (3) as an efficient desulphurisation facility to remove SO_2.

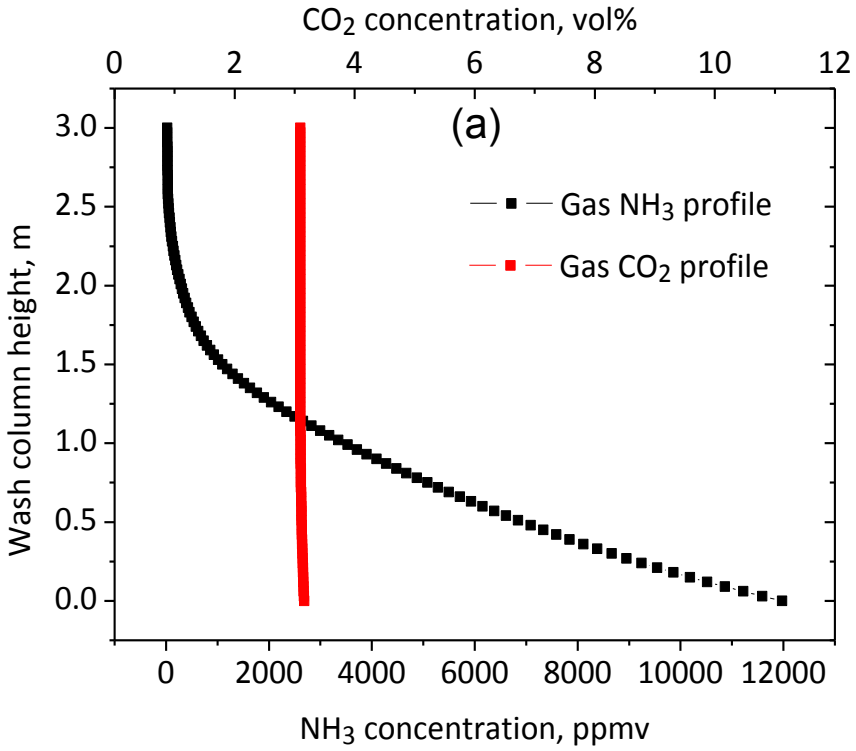
CO2 concentration, vol%
0
2
4
6
8
10
12
(a)
Gas NH3 profile
Gas CO2 profile
Wash column height, m
3.0
2.5
2.0
1.5
1.0
0.5
0.0
0
2000
4000
6000
8000
10000
12000
NH3 concentration, ppmv

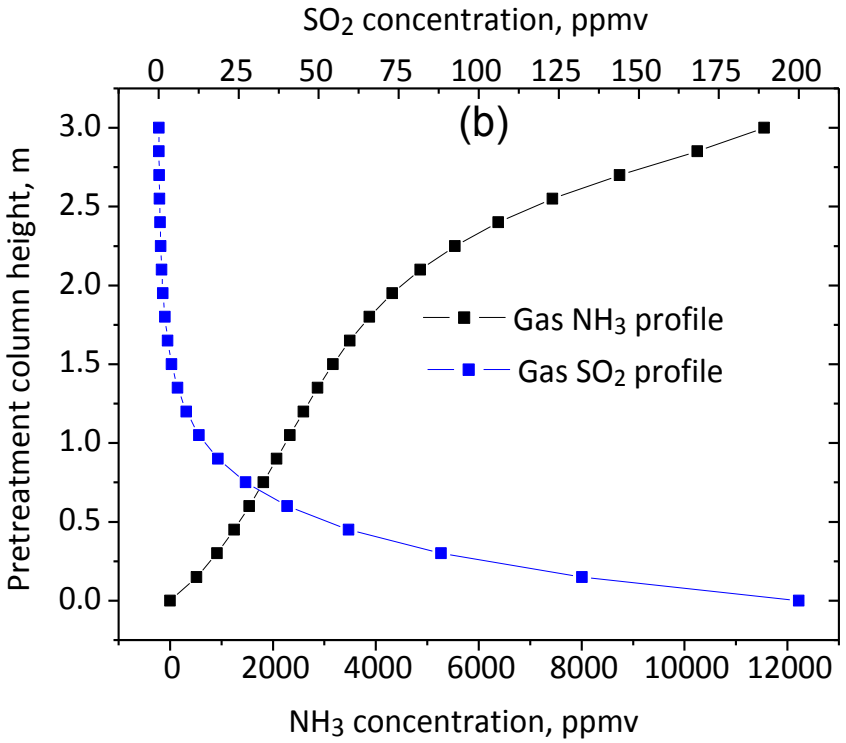
SO2 concentration, ppmv
0
25
50
75
100
125
150
175
200
(b)
Gas NH3 profile
Gas SO2 profile
Pretreatment column height, m
3.0
2.5
2.0
1.5
1.0
0.5
0.0
0
2000
4000
6000
8000
10000
12000
NH3 concentration, ppmv

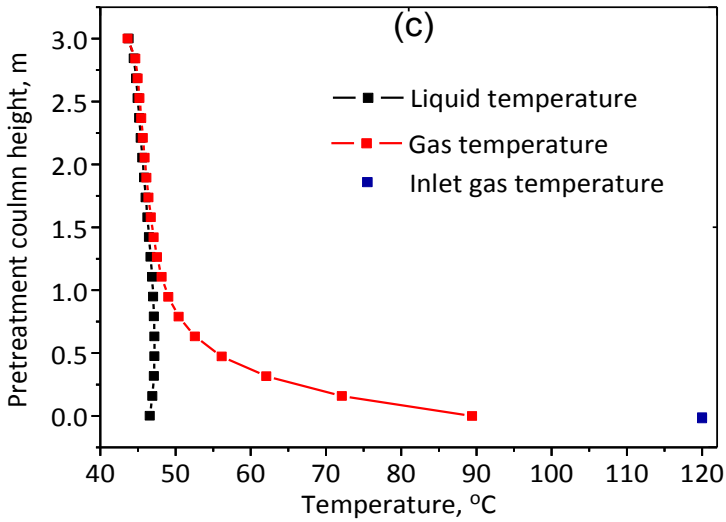

Figure 5-4 (a) NH_3 and CO_2 profiles along the wash column height; (b) NH_3 and SO_2 profiles along the pretreatment column height; and (c) temperature profiles along the pretreatment column during 175 cycles (20 wt% $(NH_4)_2SO_3$)

5.3 Process adaptability

Table 5-1 shows the effect of primary parameters on the effectiveness and efficiency of this combined SO_2 removal and NH_3 recycling process. These parameters include SO_2 concentrations in the flue gas up to 2000 ppmv, NH_3 levels from the CO_2 absorber up to 34,500 ppmv and a flue gas temperature of up to 180 °C.

Table 5-1 Adaptability of the combined SO_2 removal and NH_3 recycling process to different SO_2 concentrations in the flue gas, NH_3 levels from the CO_2 absorber and flue gas temperature

	Base case [a]	SO_2 concentration in flue gas, ppmv		NH_3 level from CO_2 absorber, ppmv		Flue gas temp,°C
		0	2000	23,000	34,500	180
Water circulation rate, kg/h	350	350	350	700	1200	350
Heater temperature, °C	–	–	–	80	90	–
Chiller temperature, °C	10	10	10	5	5	10
SO_2 removal efficiency, %	>99.9	0	>99.9	>99.9	>99.9	>99.9
NH_3 reuse for recycle, %	~96.4	~99.8	~71.3	~97.9	~98.5	~96.4
NH_3 reuse for SO_2 capture, %	~3.5	0	~28.6	~2.0	~1.3	~3.5
Total NH_3 reuse efficiency, %	>99.9	>99.8	>99.9	>99.9	>99.6	>99.9
NH_3 emission, ppmv	<20	<16	<5	<80	<150	<25
SO_2 emission, ppbv	<30	0	<2.5 ppmv	<25	<5	<100
Electricity of heater, kJ/kg CO_2 [b]	0	0	0	293.7	658.0	0
Electricity of chiller, kJ/kg CO_2 [b]	68.7	60.9	69.6	169.8	220.8	68.8

Note: [a] the conditions of base case were 200 ppmv SO_2, 12,000 ppmv NH_3, 120 °C flue gas

[b] the electricity usage of the heater and chiller is calculated on the basis of CO_2 capture rate of 87.2 kg/hr, coefficient of performance of 5.0 and 350 cycles.

5.3.1 Adaptability to SO_2 concentration in flue gas

The SO_2 concentrations are heavily dependent on the type and quality of the coal combusted in the power station. If poor quality coal is fired, the SO_2 concentration will exceed 2000 ppmv in the flue gas. As shown in Table 5-1, both the NH_3 reuse efficiency and SO_2 removal efficiency are maintained at >99.9%, with the flue gas SO_2 level ranging from 0–2000 ppmv. This suggests that the advanced process adapts well to different SO_2 concentrations. The high SO_2 level is beneficial for reducing NH_3 emissions, because the acid gas SO_2 is dissolved into the solution, decreasing the pH value and facilitating the absorption of alkaline NH_3 gas. However, the rising SO_2 level increases effluent SO_2 concentrations to the CO_2 absorber to close to 2.5 ppmv. The SO_2 removal efficiency is still as high as 99.85%. This SO_2 concentration is considered acceptable for entry into the CO_2 absorber, because the SO_2 content tolerance in the conventional MEA-based CO_2 capture process is <10 ppmv. Moreover, this increasing SO_2 concentration places no extra burden on the energy requirements of chilling duty, and the value is small compared to the reboiler duty for CO_2 regeneration: in the range of 2000–3000 kJ/kg CO_2 captured (Jilvero *et al.*, 2012).

5.3.2 Adaptability to NH_3 concentration from CO_2 absorber

As shown in Table 5-1, the proposed process performs well at high NH_3 concentrations up to 34,500 ppmv, achieving >99.6% NH_3 reuse efficiency and 99.9% SO_2 removal efficiency. This high adaptability allows the use of an NH_3 solvent with a higher NH_3 concentration and a lower CO_2 loading for CO_2 absorption, and thus potentially reduces the size of the CO_2 absorber. However, this strong adaptability to higher NH_3 concentrations comes at the expense of greater energy consumption. Specifically, a higher water circulation rate and a lower chilling temperature are required to ensure a higher NH_3 capture efficiency, and a heater is required to raise the temperature of the NH_3-rich solution for efficient NH_3 recycling. This leads to an increase of the energy penalty for chilling duty and heat duty, respectively. Compared with the large energy penalty of CO_2 capture, the energy duties for heating and cooling are considered acceptable for the recovery of such high levels of NH_3. Moreover, if low temperature steam (80–100 °C) is available in the power station, the energy consumption of the heater can be significantly reduced.

5.3.3 Adaptability to flue gas temperature

The temperature of flue gas from coal-fired power stations is typically dependent on the type of coal combusted: ca.120 °C for black coal and ca.180 °C for brown coal in Australian power plants. The high-temperature flue gas provides more latent heat for NH_3 desorption and recycling in the pretreatment column, which enables a greater saving of heat duty – especially in the case of a high NH_3 content from the CO_2 absorber. Compared to the base case in Table 5-1, there is little difference between 120 °C and 180 °C flue gas in terms of energy consumption, SO_2 removal and NH_3 recycling efficiency, which implies that the proposed process is widely adaptable to a range of flue gas temperatures.

Therefore, the proposed combined process of SO_2 removal and NH_3 recycling has proved strongly adaptable to extreme conditions, such as high SO_2 content in flue gas, high NH_3 content from the CO_2 absorber and high flue gas temperature. The principle behind the strong adaptabilities is the adjustment of the chilling temperature for high NH_3 scrubbing efficiency and the heating temperature for high NH_3 recycling efficiency. This can be used to guide other extreme scenarios, such as different gas compositions or flue gas temperatures.

5.4. Summary

In this chapter, a novel, effective NH_3-based capture process is developed that simultaneously removes SO_2 and CO_2, recycles slipped NH_3 and cools the flue gas. The validated rate-based model is used to analyse the combined SO_2 removal and NH_3 recycling process. The results of a base-case scenario show that >99.9% of SO_2 is captured and >99.9% of slipped NH_3 is reused for NH_3 recycling and SO_2 capture, with a low energy requirement. SO_2 is continuously accumulated in the circulating solution until the saturation of $(NH_4)_2SO_3$ there. The resulting sulphur-containing chemicals can be used to produce sulphur-containing fertilisers. The proposed process can deal with a wide range of SO_2 concentrations in the flue gas, NH_3 contents from the CO_2 absorber and flue gas temperatures. This indicates that the process is strongly adaptable to the variable scenarios in real industrial applications. As the process simplifies flue gas desulphurisation and resolves the problems of NH_3 loss and SO_2 removal, it could significantly reduce the cost of CO_2 and SO_2 capture by aqueous NH_3.

Chapter 6 Technical and Energy Performance of an Advanced, Aqueous NH_3-based CO_2 Capture Technology for a 650-MW Coal-fired Power Station

Abstract: Previously a novel and effective system was designed in which flue gas cooling, NH_3 recycling and SO_2 removal were achieved simultaneously with a very low energy requirement by way of utilizing latent heat in high-temperature flue gas. In this chapter, this advanced process and the NH_3-based CO_2 capture process are scaled up to deal with large-scale flue gas from a 650 MW coal-fired power station. In addition to this configuration, the proposed process also incorporates several effective approaches, including high temperature absorption, two-stage CO_2 absorption, a rich-split process and stripper inter-heating to improve its technical feasibility. The technical and energy performances are assessed for the aqueous NH_3-based post combustion capture process. As the SO_2 removal process has marginal influence on the energy performance of the entire CO_2 capture process, the present study mainly focuses on CO_2 capture. The rate-based model is employed to evaluate the potential benefits of these new configurations, as well as the thermal and electric energy consumption involved in the CO_2 capture process. A sensitivity study of important parameters, such as NH_3 concentration, lean CO_2 loading and stripper pressure, is performed to minimise the energy consumption. Process modifications, including rich-split and stripper inter-heating, are investigated as to whether they can further reduce solvent regeneration energy. The integrated capture system is then evaluated with respect to the mass balance and energy consumption in each unit.

6.1 Methodology

6.1.1 Description of CO_2 capture plant

Figure 6-1 shows the entire NH_3-based post-combustion capture process, which integrates the power station, NH_3 recycle system and CO_2 compression section with a typical CO_2 capture unit.

6.1.1.1 Power plant

The advanced CO_2 capture system is assumed to be integrated with a new advanced pulverized coal (APC) power station, which is based on a supercritical Rankine power cycle with a designed electricity output of 650 MWe and a net efficiency of 38.9%.

The detailed technical design of this APC power station was described in the 2013 report by US Energy Information Administration (EIA) (EIA, 2013).

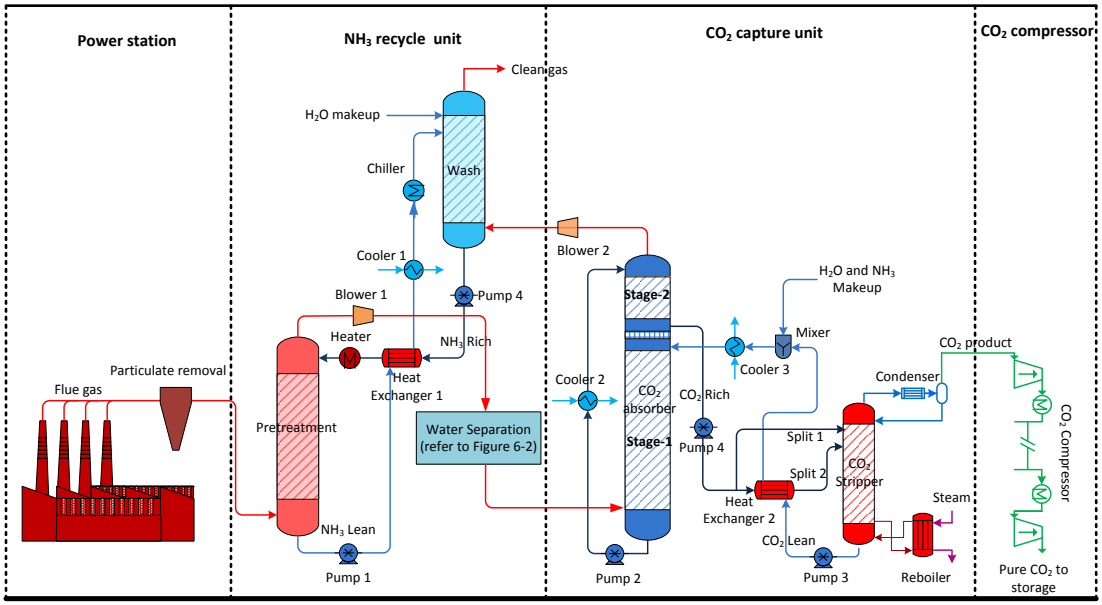

Figure 6-1 Flow sheet diagram of aqueous NH_3-based post-combustion capture process integrated with a coal-fired power station

The intermediate/low pressure steam from the power station is expected to be extracted for solvent regeneration at the expense of a net efficiency penalty to the power station. The power plant island is assumed to be either equipped with a natural draft cooling tower, which, in normal conditions, can supply plenty of cooling water between 16 and 20 °C dependent on ambient air temperature and humidity (Drbal *et al.*, 1995), or be near a cold location such as a lake or sea where low temperature water is available for cooling the NH_3 solvent to room temperature, that is, 25 °C. The flue gas properties and composition in the APC power station are shown in Table 6-1, in which the flue gas composition are kept the same as in the earlier study mentioned above.

Table 6-1 Flue gas properties from the APC power station

Temperature	Pressure	Mass flow-rate	CO_2 flow-rate	Composition, vol/%			
°C	bar	ton/h	tonne/h	CO_2	H_2O	O_2	N_2
120	1.01325	3179.2	560	10.7	6.0	7.8	75.5

6.1.1.2 CO_2 capture unit

The CO_2 capture process is designed with a CO_2 capture efficiency of 85%. The rate-based model is employed to simulate the CO_2 absorption/desorption process in the packed column. The CO_2 absorption process is modelled assuming a 25 °C and 4-10 wt% lean aqueous NH_3 solution entering the absorber. The high temperature of 25 °C for the NH_3 solution is intended to avoid the substantial energy input for solvent chilling and to avoid solid precipitation problems. However, at this temperature the NH_3 loss would significantly increase due to the high volatility of NH_3. So a two-stage CO_2 absorption process with intermediate cooling is applied to reduce the NH_3 slip. In this process configuration (CO_2 absorber in Figure 6-1), the CO_2 lean solution goes through the stage-1 absorber for the scrubbing of the majority of CO_2 and becomes a high CO_2 loading solution. The solvent is then fed to the top of stage-2 absorber to capture the vaporised NH_3 that leaves the stage-1 absorber. An intermediate cooling to 25°C between the two stages is used to enhance the CO_2/NH_3 absorption performance in stage-2 and also mitigate the NH_3 vaporization from the absorption process. This configuration has been proven to be effective in significantly reducing the vaporised NH_3 level (Darde *et al.*, 2012; Jilvero *et al.*, 2014b).

The CO_2 desorption process is modelled in the stripper column to be at pressurized conditions. After going through the pressurised pump and heat exchanger, the CO_2-rich stream is fed to the top of stripper and the CO_2 is stripped off by means of the heat supplied from reboiler (steam extraction from the power station). A sensitivity study of three of the most important process parameters, solution NH_3 concentration, lean CO_2 loading and stripper pressure, are carried out to minimise the energy consumption. Process modifications of the rich-split process and stripper inter-heating process are implemented to reduce the reboiler duty, and the combined process of rich split and inter-heating is applied to further reduce the energy requirement (details in section 6.3).

6.1.1.3 NH_3 recycle unit

The NH_3 recycle unit was discussed in detail in chapter 4 and 5. Basically, it includes a wash column where the vaporised NH_3 is scrubbed by wash water and a pretreatment column where the heat contained in the high temperature flue gas is utilised to regenerate NH_3 in the wash water and recycle it back to the CO_2 absorber. In the previous chapters, this advanced process was proven to be able to achieve the reuse of

over 99 % slipped NH_3, and over 99% SO_2 removal efficiency with a low energy penalty.

6.1.1.4 Water separation unit

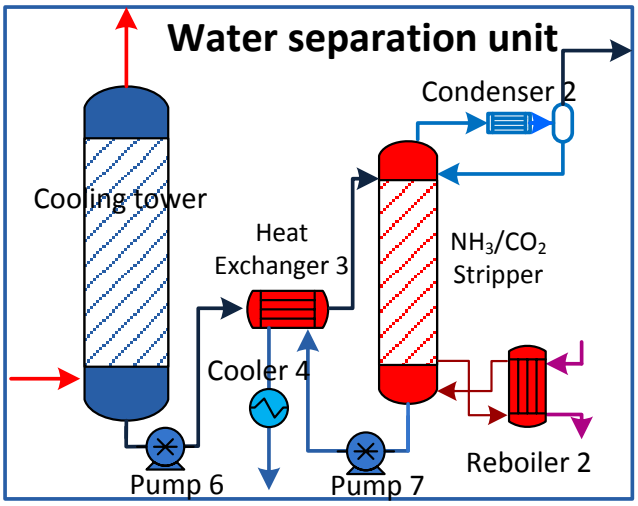

Figure 6-2 Process flow diagram of water separation unit

A water separation unit (Figure 6-2) is included in the process to separate H_2O from flue gas, which leaves the NH_3 recycle unit to help maintain the H_2O balance in the entire system. The separation unit, which consists of a cooling tower and a stripper column, is simulated using the rate- based model. The purpose of the cooling tower is to cool down the flue gas and to condense part of water in the flue gas. The available 25 $^{\circ}C$ water is used as the cooling source for the gas condensing. Accompanying the water condensation, a small amount of NH_3 and CO_2 is absorbed in the condensate, leading to the formation of some species such as ammonium carbonate and carbamate. The stripper is used to strip off the CO_2 and NH_3 from the condensate at atmospheric pressure. The stripped vapour is sent to the CO_2 capture unit as NH_3 makeup. Relatively pure water is obtained after the use of the stripper and this water is then used for the H_2O makeup in the NH_3 recycle unit and as excessive water for other usage or storage.

6.1.1.5 CO_2 compression

The captured CO_2 is compressed for subsequent geological sequestration. The compression process is modelled to include six stages and fixed discharge conditions (150 bar, 40 ^{o}C) using a pressure changer modular-MCompr simulator embedded in Aspen Plus. Three intercoolers in stages 1, 3, 5 are used in the CO_2 compressor to

remove the gaseous NH_3 and moisture from the pressurized CO_2 product. Following the energy requirement of the reboiler, the CO_2 compressor would have the second largest energy penalty in the overall CO_2 capture process and also require a large cooling duty during the gas compression.

6.1.1.6 Auxiliary equipment

Heat exchangers (HEATX simulator) are used to achieve the heat transfer between the hot and cold streams and save energy consumption. The temperature approach at the hot end of the heat exchanger is set at a reasonable 10 K. Blowers (COMPR simulator) are employed to compensate the pressure drop of the pretreatment column and CO_2 absorber. The pipelines (PIPE simulator) are used to calculate the pressure drop of solvent circulation when elevating the solution to a high location in columns/towers. Pumps (PUMP simulator) are used to transport the circulation solution or pressurize the solvent before it enters the stripper. The isentropic efficiency and mechanical efficiency of both pumps and blowers are set to be 80% and 95%, respectively.

6.1.2 Column size estimation

Since CO_2 capture by aqueous NH_3 is a slow process compared to the MEA solvent, column size must be considered to ensure that the columns are technically and economically feasible for construction. In this study, the column diameters of the absorber and stripper are determined to be at 60% flooding points for a flexible operation, while the pretreatment and wash column diameters are determined to be at 80% flooding points. The packing heights are determined by achieving the targeted CO_2 removal efficiency of 85%. An increment of a 25% packing height is added to the total column height to allow for the necessary space at the bottom and top of column, and 0.75 m is added to each 10 m of packing height for liquid collection, liquid distribution and the supporting grid (Linnenberg *et al.*, 2012). Compared to an equilibrium-based model, the rate-based model provides a more practical estimation of column size, particularly for the absorber column, NH_3 wash column and pretreatment column.

6.1.3 Evaluation of energy performance

6.1.3.1 Heat distribution of reboiler duty

Generally, the heat requirement of solvent regeneration consists of three components: heat of desorption, sensible heat and heat of vaporisation. The analysis of these three

heat contributions to the total regeneration duty can provide the fundamental information for the technical improvement of a stripper system. Analysing the individual heat requirement is based on the following equations.

(I)$Q_{des,CO_2} = \sum n_i\, H_i + n_{CO_2} H_{CO_2}$, where n_i is the mole for all the species, mol; H_i is the molar enthalpies for all the species and kJ/mol; H_{CO_2} is the enthalpy per mole CO_2 desorbed from the solution; the calculation is taken from Que et al. (2011), kJ/mol. The heat of CO_2 desorption is required to break the chemical bond between NH_3 and CO_2. Basically, this heat requirement is an inherent property of solvent and is dependent on the NH_3 concentration and rich CO_2 loading. The heat of desorption can be determined by using the Flash Module in the Aspen Plus by way of the differential method in which the energy difference is obtained by a differential CO_2 input at a certain CO_2 loading.

(II) $Q_{sens} = \bar{m}_{solv} \bar{C}_P (T_{in} - T_{out})$, where m_{solv} is the mass flow rate of solvent flowing through the stripper, kg/h; C_P is specific heat capacity of the solvent, kJ/kg·K; $(T_{in} - T_{out})$ solvent temperature difference in and out of the stripper, K. Narrowing the temperature difference and lowering the solvent mass flow rate are the primary approaches to reducing the sensible heat.

(III) $Q_{vap,H_2O} = n_{vap,H_2O} H_{vap,H_2O} + n_{vap,NH_3} H_{vap,NH_3}$, where n_{vap,H_2O} is the moles of excess steam leaving the stripping column, mol; H_{vap,H_2O} is the latent heat of steam generation; n_{vap,NH_3} is the moles of NH_3 vapour leaving the stripping column, mol; and H_{vap,NH_3} is the latent heat of NH_3 vaporisation.

6.1.3.2 Energy conversion to electricity

To complete the assessment of this advanced NH_3-based PCC system that is integrated with a power station, we have performed an overall energy evaluation. The cooling/chilling duty is converted into electricity using a coefficient of a performance of 5. The electrical duties of the CO_2 compressor, pumps and blowers are directly derived from the Aspen simulation results based on the rate-based model. The most important energy duty for solvent regeneration is provided by intermediate/low-pressure steam extraction from the water-steam-cycle of the power station. This leads to a subsequent net efficiency penalty to the power plant. To quantify the power loss, an adequate correlation based on the Carnot cycle is introduced, where the heat duty

from steam extraction is transformed into an equivalent electric power loss. The following equations have been proven to accurately calculate the power loss for extraction temperatures from 131 to 155 °C (Oexmann *et al.*, 2008):

$$\Delta P_{loss} = \theta_{eff} \times \theta_{Carnot} \times M_{CO_2} \times H_{reg} \quad (6\text{-}1)$$

where ΔP_{loss} is the electric power loss; MWe; M_{CO_2} is the CO_2 capture rate, kg/hr; and H_{reg} is the mass specific heat duty of regeneration, MJ/kg CO_2. The additional power loss in the power cycle due to stream extraction, θ_{eff}, is calculated by:

$$\theta_{eff} = 0.6102 + 0.00165(T_{sat,stream} - 273.15) \quad (6\text{-}2)$$

For the Carnot efficiency θ_{Carnot}:

$$\theta_{Carnot} = 1 - \frac{T_{cond}}{T_{sat,stream}} \quad (6\text{-}3)$$

where T_{cond} is the condenser temperature in the water steam cycle, which is assumed to be 313 K in this study; and $T_{sat,stream}$ is the saturation temperature of the extracted steam at the extraction pressure, which is assumed to be 10 K higher than that of the reboiler temperature, K.

6.2 Column size determination

Owing to the massive flue gas and low CO_2 partial pressure in flue gas from a power station, large columns are required to achieve a high CO_2 capture rate and avoid high pressure drop and flooding problems. It is estimated that a very large absorber column with a 24 m inner diameter would be required to treat the full flue gas flow rate of 560 t/h CO_2 from a 650 MWe power station (~4 million ton CO_2/year). In reality, such a large column might not be practical in standard chemical engineering, because it would be heavily limited by its transportation and construction, although a concrete column can be built as a rectangle to increase the diameter. As suggested by Chapel et al. (1999), the maximum absorber diameter should be no more than 12.8 m. Thus, multiple process trains are employed in parallel for the CO_2 capture system, with each capture train containing a CO_2 capture unit, an NH_3 recycling unit, a water separation unit and a CO_2 compressor. Such a system configuration has been proposed by Singh et al. (2003) and Kuramochi et al. (2010). This process design has the following advantages: (1) smaller columns can be shop-fabricated instead of fabricated on-site; (2) smaller equipment, such as blowers, pumps and exchangers, are commercially

available without requiring customer design; and (3) greater flexibility of operation due to the independent capture systems.

The number of process trains for the CO_2 capture system is primarily determined by the number of absorbers. The scale of a single absorber is largely limited by the diameter of the absorber column. In this study, four parallel process trains of CO_2 capture are proposed to treat large-scale flue gas from a 650-MWe power station. Accordingly, each process train is designed to deal with a flow rate of 140 t/h CO_2 (one-fourth of the total flue gas, ~1 million ton CO_2/year) in an absorber column of 12 m inner diameter, which is fractionally smaller than the recommended maximum size of 12.8 m (Chapel *et al.*, 1999). The scale of one process train is consistent with the world's first commercial CCS plant at Boundary Dam Power Station in Estevan, Canada, which has the CO_2 capture capacity of 1 million ton/year (Stéphenne, 2013).

Table 6-2 shows the column sizes and corresponding packed materials for each column in one individual process train.

Table 6-2 The primary parameters of each column in one process train

		Main design parameters		
Columns		Packing material	Packing height	Column size*
CO_2 absorber	Stage 1	Mellapak-250Y	15m	Ø12m×H26.5m
	Stage 2	Mellapak-250Y	5m	
CO_2 stripper		Mellapak-250Y	8m	Ø6.8m×H10.75m
NH_3 wash column		Mellapak-350Y	10m	Ø10m×H13.25m
Pretreatment column		Mellapak-250Y	8m	Ø10m×H10.75m

Note: * the column diameters are the inner diameters and the column heights column heights include the additional height for the necessary space, collectors and distributors.

The determination of column size is based on the principles of minimising column size and ensuring normal operation without flooding problems. Sulzer Mellapak packing materials with a high surface area and a high void fraction are used in the

process modelling. Due to the slow reaction rate between NH_3 and CO_2 and the two-stage absorption, the NH_3 process requires a tall absorber column of 26.5 m to achieve the 85% CO_2 capture efficiency. The capture system also requires a tall wash column of 13.25 m, because of the high NH_3 loss of 12,000 ppmv from the CO_2 absorber, and requires a tall pretreatment column to achieve a high NH_3 recycling and SO_2 removal efficiency. Moreover, the wash column requires packing material with a larger surface area to scrub over 99.9% slipped NH_3 and to reduce the NH_3 level in the vent gas to below 25 ppmv.

6.3 Sensitivity study of the process parameters

Three of the most important process parameters – NH_3 concentration, lean CO_2 loading and stripper pressure – are investigated with respect to their influence on the energy requirement of the CO_2 capture process. As the stripper reboiler duty accounts for the largest energy consumption in the overall capture system, the heat requirement of solvent regeneration is selected as the most significant indicator when optimising these parameters.

6.3.1 Effect of NH_3 concentration

Since NH_3 concentration and lean CO_2 loading are closely relevant to the NH_3 loss and the associated energy consumption of the NH_3 recycle process, the determination of these two parameters is based on the minimisation of the total energies in the CO_2 capture unit and NH_3 recycle unit. As shown in Figure 6-3, NH_3 concentration has conflicting influences on the energy requirement of the CO_2 capture unit and NH_3 recycle unit. On the one hand, increasing the NH_3 concentration is beneficial for the decrease of heat requirement for solvent regeneration. This is mainly because high NH_3 concentration allows an increase of CO_2 absorption rate and CO_2 absorption capacity per kilogram solvent. When the NH_3 concentration increases from 4% to 10 % at the studied conditions, the solution circulation rate decreases from 1656 kg/s to 927 kg/s, which results in a decrease in sensible heat and, consequently, a reduction in regeneration duty from 4.18 MJ/kg CO_2 to 3.82 MJ/kg CO_2. Moreover, increasing the NH_3 concentration from 4% to 10% enables a decrease in the regeneration temperature from 132.7 to 126.2 $^{\circ}$C. This entails a lower quality of steam required from the power station, which is likely to result in a decrease in steam consumption for solvent regeneration.

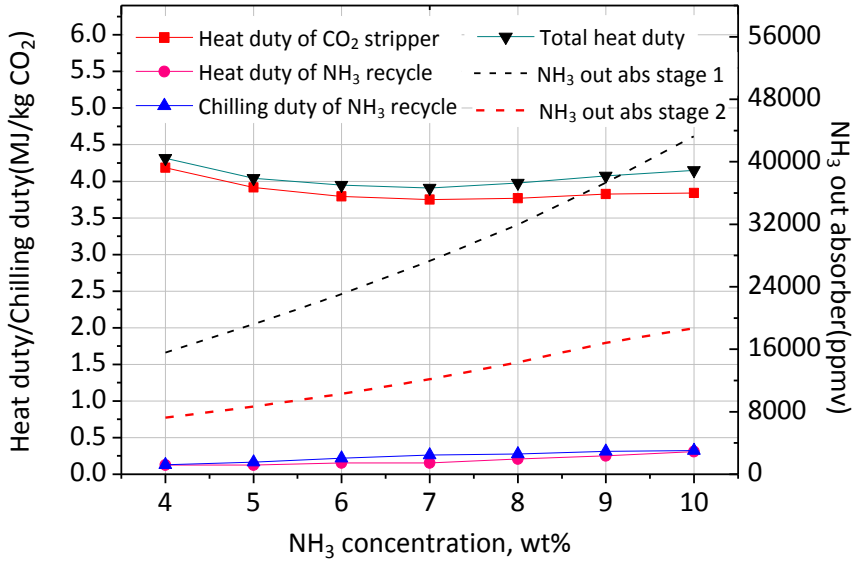

Figure 6-3 Effect of NH_3 concentration on the energy requirement for CO_2 capture unit and for NH_3 recycling units, at conditions of 298 K inlet NH_3 solution temperature, 0.25 lean CO_2 loading, 6 bar stripper pressure, 85% CO_2 capture efficiency and 10 K temperature

From Figure 6-3, it can also be seen that the two-stage absorption is effective in alleviatingNH_3 mitigation over 50% from the CO_2 absorber. This is because the solvent fed to the top stage (stage 2) has a high CO_2 loading and low NH_3 pressure, leading to a relatively high capacity for NH_3 absorption. However, the NH_3 slip is still very challenging. The increased level of NH_3 concentration from 4% to 10 % results in a significant increase in NH_3 slip from 7240 to 17721 ppmv, even if the staged absorption process is applied. This causes an increase of energy burden for the NH_3 recycle unit including an increase in heat duty from 0.126 to 0.309 MJ/kg CO_2 and an increase in chilling duty from 0.128 to 0.323 MJ/kg, respectively. It is worth mentioning that the energy duties in the NH_3 recycle unit are significantly lower than that for solvent regeneration. This is mainly attributed to the fact that the advanced NH_3 recycle process proposed in this study utilises waste heat in flue gas and that the staged absorption configuration significantly reduces the NH_3 slip by over 50%. After a sensitivity study of solution NH_3 concentration, the minimum heat requirement of both the CO_2 capture process and NH_3 recycle process is observed to be at 6.8 wt% NH_3 concentration, at which the reboiler duty is 3.91 MJ/kg CO_2 and chilling duty is 0.26 MJ/kg CO_2.

6.3.2 Effect of lean CO_2 loading

Figure 6-4 shows the effect of lean CO_2 loading on the energy requirement of CO_2 capture and NH_3 recycle process.

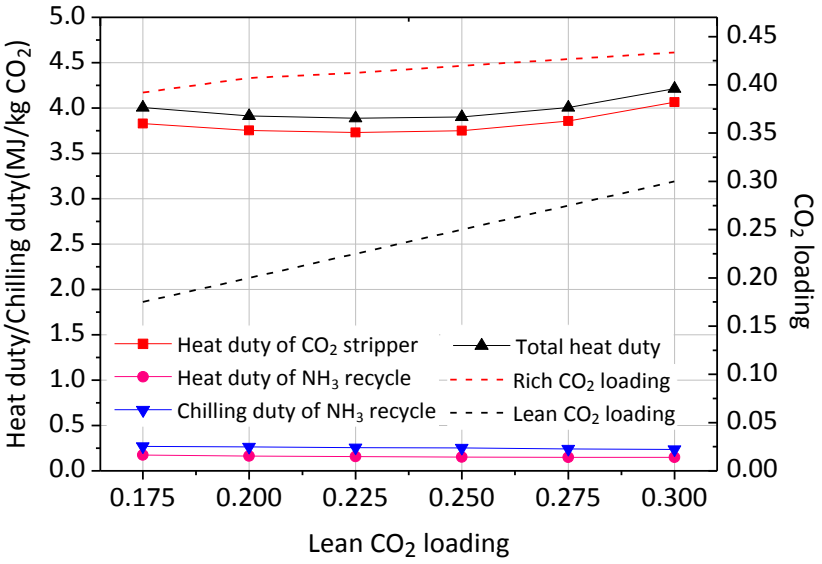

Figure 6-4 Effect of lean CO_2 loading on the energy requirement for the CO_2 capture unit and NH_3 recycling units, at conditions of 298 K inlet NH_3 solution temperature, NH_3 concentration of 6.8 wt%, 6 bar stripper pressure, 85%CO_2 capture efficiency and 10 K temperature

It can be seen that there exists an optimal lean CO_2 loading for the minimal energy consumption. This is because a low lean loading causes a high NH_3 loss and an increase in reboiler temperature, while a high lean loading leads to a decrease in CO_2 absorption capability and a high solvent circulation rate, both of which results in the increase of the total heat requirement. In this study, a balanced lean CO_2 loading of 0.225 is observed at which the total heat duty reached a weak minimum of 3.86 MJ/kg CO_2 accompanied by a 0.257 MJ/kg CO_2 of chilling duty. It can also be noticed that although the lean loading has a large increment, from 0.175 to 0.30, the CO_2 loading of the rich solvent experiences a slight increase from 0.40 to 0.43 (at a fixed CO_2 capture rate). In our simulation, it is found that the rich CO_2 loading is particularly limited in the range of 0.4-0.5 at the studied conditions and configuration, which is consistent with the modelling results from Jilvero et al. (2014b), namely that the CO_2 rich loading will not exceed 0.5. At the beginning of absorption, the lean solvent can quickly absorb CO_2 due to the relatively fast carbamate formation rate. With CO_2

loading increasing to close to or over 0.5, the slow reaction of bicarbonate formation dominates the CO_2 absorption, which is too slow to be applicable. It is therefore suggested that the targeted rich loading using aqueous NH_3 should not exceed 0.5 to ensure a relatively fast absorption rate and, subsequently, a smaller absorber.

6.3.3 Effect of stripper pressure

The CO_2 product after the stripper process is directly transported to a CO_2 compressor for further treatment to meet the requirements for CO_2 storage. So stripper pressure influences not only the heat duty of CO_2 stripper, but also the energy duty of CO_2 compression and pump energy for solvent pressurizing. It is generally accepted that the heat requirement of solvent regeneration consists of sensible heat, heat of water/NH_3 vaporization and heat of desorption, shown in Figure 6-5. As shown in Figure 6-5(a), the heat of desorption changes very little with an increase in stripper pressure. This is understandable, because the heat of desorption, as an inherent property of the solvent, is predominately dependent on the NH_3 and CO_2 concentration in the solvent (the composition of rich solvent entering the stripper and the CO_2 desorption rate are the same at different pressures). The sensible heat also changes very little due to the same temperature approach (10 °C) of solvent in and out stripper and the same solvent flow rate used at different pressures. The reduction of regeneration duty by elevating the stripper pressure is primarily attributed to suppressing the H_2O/NH_3 vaporization, which reduces the reboiler duty from 4.12 MJ/kg CO_2 at 4 bar to 2.87 MJ/kg CO_2 at 20 bar. Moreover, a rise of stripper pressure significantly reduces the energy penalty of CO_2 compression due to the elevating inlet pressure to the CO_2 compressor. The power duty and chilling duty of CO_2 compression decreases from 289 to 131 kJ/kg CO_2 and 454 to 271 kJ/kg CO_2, respectively (Figure 6-5(b)).

However, high stripper pressure also has some drawbacks. As indicated in equation (6-1)-(6-3) in section 6.2.2, a rise in reboiler temperature will increase the steam extraction (power loss), and a subsequent increase in the net efficiency penalty to the power station. Moreover, high stripper pressure will involve more energy consumption of the solvent pump. In order to precisely determine the optimal stripper pressure, the energy consumptions of the three parts – stripper reboiler, CO_2 compressor and pump– are converted into electricity and corresponding power loss.

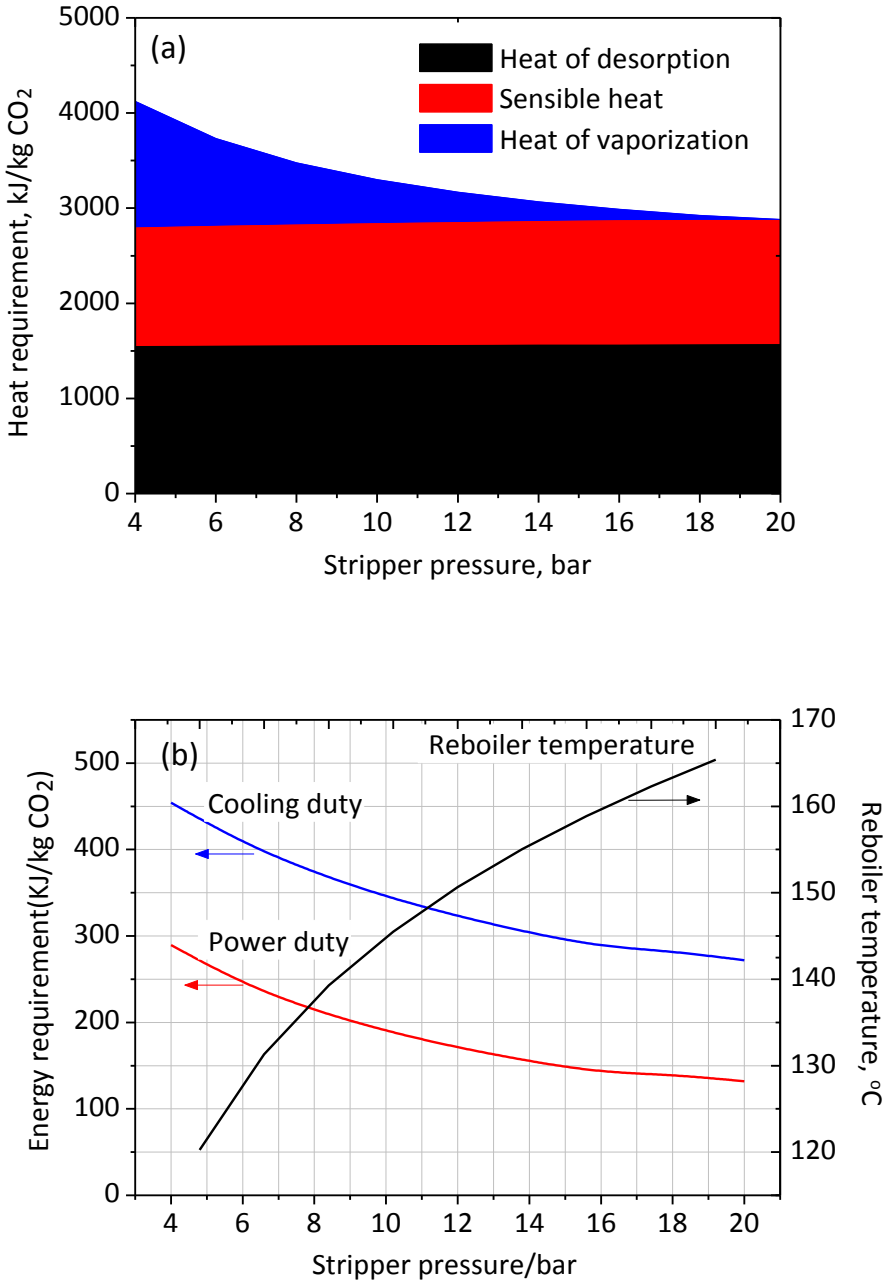

Figure 6-5 (a) Heat requirement and (b) power duty and cooling duty of CO_2 compressor and reboiler temperature as a function of stripper pressure at 6.8% wt NH_3 concentration and 0.225 CO_2 loading

As shown in Figure 6-6, it is clear that the energy consumption of the stripper reboiler is the largest contributor to the power loss at the studied pressure range. The net efficiency penalty of three parts reaches the minimum stage at the stripper pressure range of 10-16 bar. Apart from energy consumption, the determination of stripper pressure should also take into account the construction cost of a high pressure stripper,

which generally increases with pressure. Considering that there is very little penalty difference between 10 bar and 16 bar, the relatively low pressure of 10 bar has been selected. At this pressure, the regeneration energy is 3.27 MJ/kg CO_2 with a reboiler temperature 145.5 $^{\circ}$C, and a condenser duty is 1.45 MJ/kg CO_2.

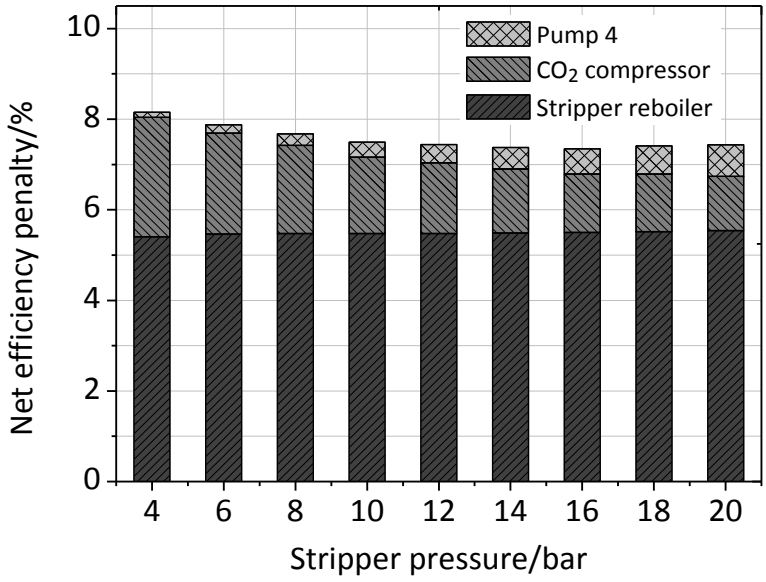

Figure 6-6 Effect of stripper pressure on the net efficiency penalty of stripper reboiler, CO_2 compressor and pump on the power station

6.4 Advanced stripper configurations

Process modifications of rich-split and stripper inter-heating are proposed to further reduce the energy consumption of solvent regeneration. Simplified flow sheets are shown in Figure 6-7.

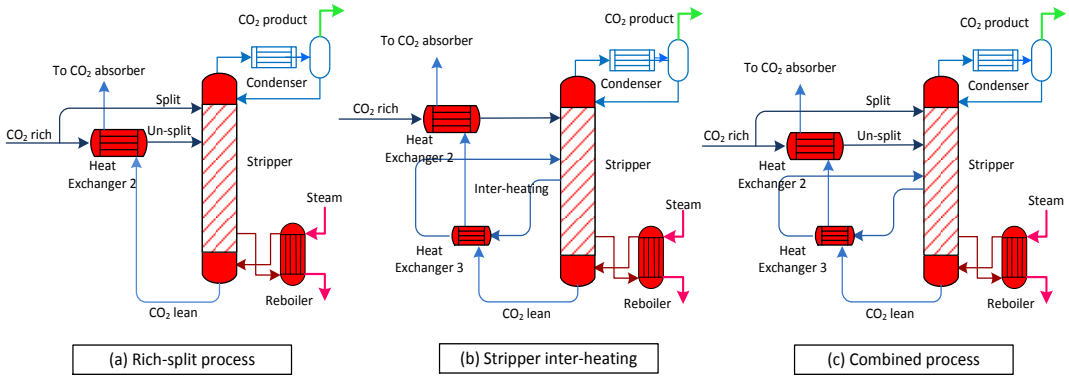

Figure 6-7 Stripping process modifications of (a) rich-split process; (b) stripper inter-heating process; and (c) combined process

During the process simulation, the rich-split process feeds the split stream to stage 2 and un-split stream to stage 5; the stripper inter-heating process is used to extract the solvent from stage 5 and feed back to stage 5 after inter-heating; the combined process is used to feed the split stream to stage 2, the un-split stream to stage 5 and inter-heating at Stage 8. The total stage number of strippers is 15 with the condenser at stage 1 and reboiler at stage 15; the temperature approach between rich solvent entering the stripper and the lean solvent leaving the stripper is kept at 10 K. Table 6-3 summarises the simulation conditions and results of the different process modifications. The details of each process modification are discussed below.

Table 6-3 Summary of simulation conditions and results of rich-split, stripper inter-heating and combined process in one process train

Simulation conditions	Reference	Rich-split	Inter-heating	Combined process
Flow rate of flue gas, tonne/h	781.6	781.6	781.6	781.6
CO_2 flow rate of flue gas, tonne/h	139.5	139.5	139.5	139.5
CO_2 loading of lean solvent, mol/mol	0.225	0.225	0.225	0.225
CO_2 loading of rich solvent, mol/mol	0.41	0.41	0.41	0.41
Solvent flow rate, ton/h	3,744	3,744	3,744	3,744
Solvent rate, tonne/tonne CO_2	31.7	31.7	31.7	31.7
L/G, mass ratio	4.8	4.8	4.8	4.8
Split fraction, ton/ton	-	0.05	-	0.05
Inter-heating flow rate, ton/h	-	-	2,000	2,000
Simulation results				
CO_2 capture rate, ton/h	118.1	118.1	118.1	118.1
CO_2 mass purity, %	99	99	99	99
Condenser temperature, ^oC	64	64	64	64
Condensate rate, kg/kg CO_2	0.70	0.16	0.55	0.15
Condenser duty, MJ/kg CO_2	1.45	0.39	1.16	0.24
Reboiler temperature, ^oC	145.5	145.5	145.5	145.5
Heat of vaporisation, MJ/kg CO_2	0.46	0.21	0.41	0.19
Sensible heat, MJ/kg CO_2	1.27	1.15	1.05	0.73
Heat of desorption, MJ/kg CO_2	1.54	1.54	1.54	1.54
Total reboiler duty , MJ/kg CO_2	3.27	2.89	3.00	2.46

6.4.1 Rich-split process

The process rich-split modification (Figure 6-7(a)) is adopted to reduce the energy consumption for solvent regeneration. In this process modification, a small portion of the rich solvent bypasses the rich/lean heat exchanger and enters the top of stripper directly; the major portion passes through the heat exchanger and is introduced to the middle of the stripper. The cold rich stream is split to recover the energy contained in the upcoming high temperature water vapour, while the rich solvent is heated to release part of the CO_2. This process configuration has been proven to be effective in the reduction of solvent regeneration duty in the simulation and the pilot plant trials of an MEA-based CO_2 capture process at Tarong Power Station, Queensland, Australia (Cousins *et al.*, 2012; Cousins *et al.*, 2011b). A recent study also shows that the rich-split process can reduce reboiler duty in the NH_3-based capture process (Yu *et al.*, 2014a).

To discern how the energy is saved by the rich-split process, the distribution of the three heat requirements is determined as shown in Figure 6-8(a). It can be seen that the rich-split process significantly decreases the heat of vaporization with an increasing split fraction, which is favourable for lowering the condenser duty and the subsequent regeneration duty. However, at higher split fractions, the cold split stream starts to cool the stripper and more sensible heat is required to heat the split solvent to the required temperature, which increases the reboiler duty. The heat of vaporization and sensible heat compete with each other, resulting in an appropriate split fraction that maximizes the saving of energy duty. As shown in Figure 6-8 (b), when a 0.05 split fraction is applied, the total energy duty reaches a minimum of 3.28 MJ/kg CO_2 with a reboiler duty of 2.89 MJ/kg CO_2 and condenser duty of 0.39 MJ/kg CO_2.

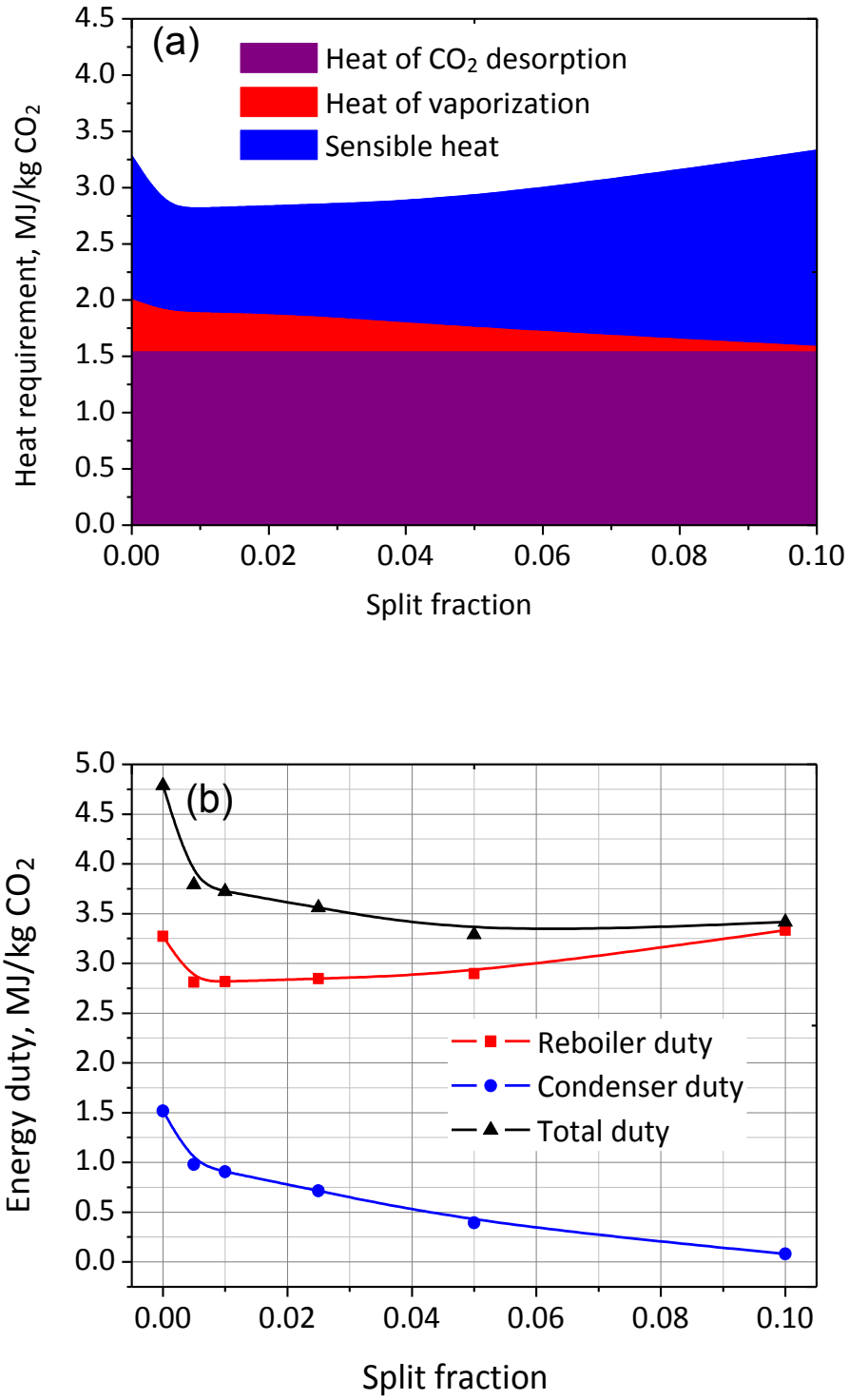

Figure 6-8 Effect of rich-split ratio (mass ratio of split solvent to the total rich solvent) on the (a) energy consumption and (b) distribution of three heat components: heat of CO_2 desorption, heat of vaporization and sensible heat.

6.4.2 Inter-heating process

The process modification of an inter-heated stripper is also applied to reduce the reboiler duty. This process was initially patented by Sarkisian et al. (2003). The investigation in the process modelling shows that the heat requirement of solvent regeneration can be reduced by using the heat in the lean solvent as it leaves the stripper (Frailie *et al.*, 2013; Karimi *et al.*, 2012). As shown in Figure 6-7(b), the inter-heating process is used to exchange the heat between the hot lean stream as it leaves the bottom stripper and the rich solution that has been extracted from the middle stripper, before the hot lean stream moves to the main cross-exchanger, thus making better utilization of the heat in hot lean stream. This process design is aimed at reducing the reboiler duty and condenser duty by means of (1) recycling the high quality and high temperature heat in the hot lean stream, which elevates the overall temperature along the stripper column; and (2) reducing the energy loss associated with steam generation by lowering the temperature of the rich solvent as it enters the top of stripper column.

In the simulation, the temperature difference of the heat exchanger 2 on the cold side for both reference stripper and inter-heated stripper is kept the same to ensure the same amount of energy is taken from the CO_2 lean solvent for both configurations. As shown in Figure 6-9 (a), the inter-heated stripper reallocates the distribution of temperature profiles along the stripper column, which increases the temperatures at the bottom section whilst it decreases the temperatures in the top section of the stripper. This, accordingly, reduces the energy consumption for sensible heat and the heat of the water vaporization (Figure 6-9 (b)). Consequently, the reboiler duty is reduced to 3.00 MJ/kg CO_2 with the application of the inter-heating process.

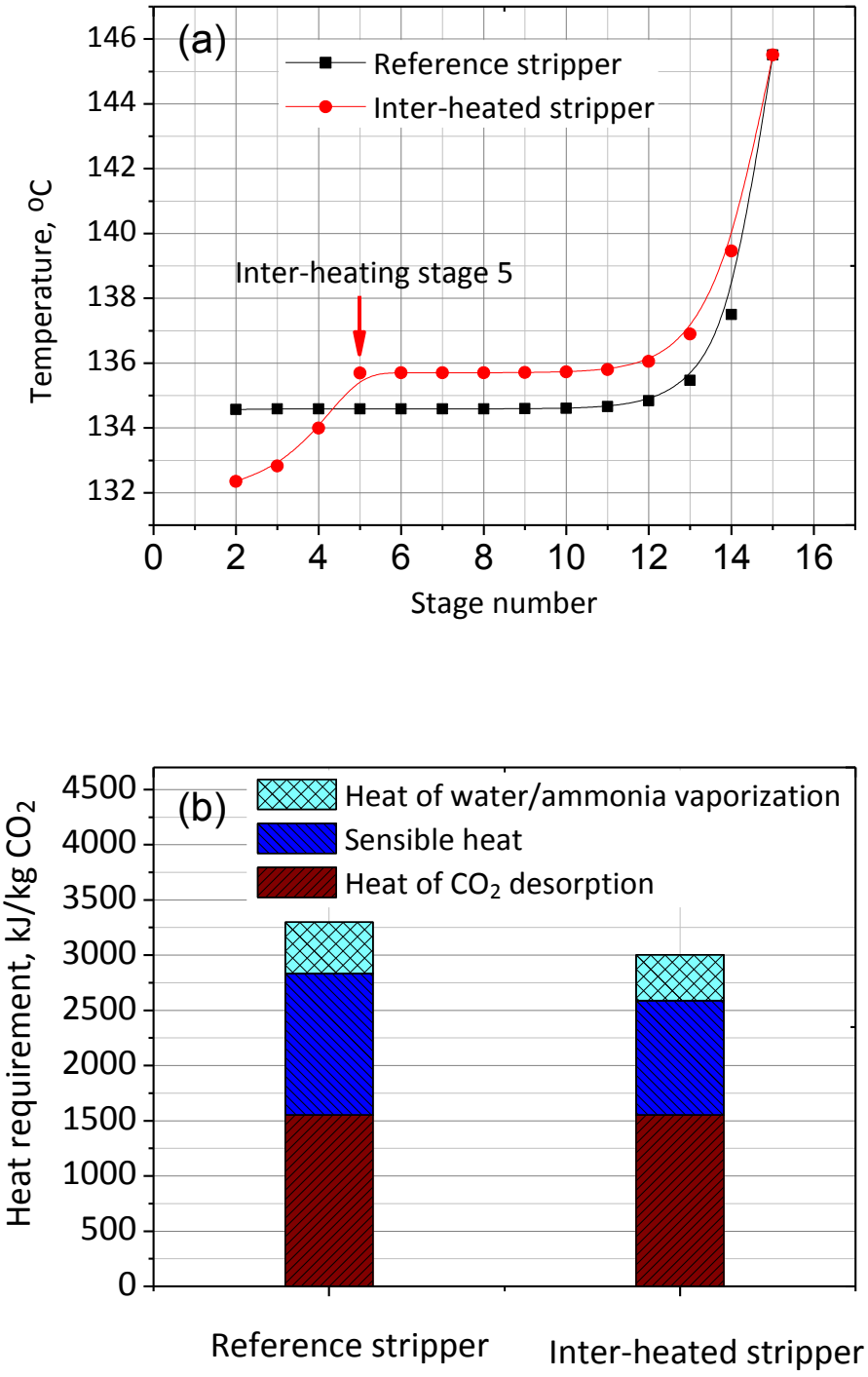

Figure 6-9 (a) temperature profiles and (b) distribution of heat requirement of reference stripper and inter-heated stripper with inter-heated solvent in and out at stage 5 (Condenser is at stage 1 and reboiler at stage 15)

6.4.3 Combined rich split and inter-heating process

As discussed before, the role of the rich spilt process is primarily to reduce the heat of water vaporisation while the inter-heating process is used to reduce the sensible heat during the regeneration. The combined process (Figure 6-7(c)) is supposed to enable a better use of their advantages and a further reduction of the energy consumption. As shown in Table 6-3, when the rich-split process with a 0.05 split fraction and inter-heating process are applied, and the temperature difference between the split 2 stream and CO_2 lean stream is controlled at 10 $^{\circ}$C, the regeneration duty is reduced to 2.46 MJ/kg CO_2, while the cooling duty of condenser remains at only 0.24 MJ/kg CO_2. This is a reduction of 24.8% of the reboiler duty and 83.4% of the condenser duty compared to the reference case without the rich-split and inter-heating process.

6.5 Process assessment

6.5.1 Mass balance analysis

The analysis of the system material balance is necessary to calculate the material consumption, H_2O/NH_3 makeup, intermediate and final product yield of each section and the entire process. The N_2, O_2 and trace inert gas in the flue gas are not considered in the analysis as they do not react with the absorbents. Figure 6-10 shows the mass flow rates of the three most important components, CO_2, NH_3 and H_2O, at various locations in the CO_2 capture system at a CO_2 capture rate of 118.1 tonne (t) /hr and a capture efficiency of 84.7%. Specifically,

- **NH_3 recycle unit:** more than 99% of the slipped NH_3 that leaves the CO_2 absorber is recycled. The NH_3 emission concentration in the clean flue gas is 19 ppmv, which is acceptable according to the regulation of the United States National Institute of Occupational Safety and Health (<25 ppmv) (Busca *et al.*, 2003) and the Korean government regulations relating to industrial exhaust gas (<50 ppmv) (Han *et al.*, 2013); the amount of CO_2 scrubbed in the washing column equals the amount of CO_2 that is desorbed in the pretreatment column (1.2 t/hr); the H_2O mass balance is maintained by water makeup in the wash column.

  CO_2 capture unit: a 116.6 t/hr CO_2 is captured by two stage absorption and an extra 1.5 t/h CO_2 is supplied from the H_2O separation unit. Both are desorbed in the stripper at a flow rate of 118.1 t/h CO_2; since the advanced NH_3

recycle process and water separation process enable a recycle of almost all the vaporised NH_3, only a small amount of makeup, NH_3 33.4 kg/hr, is needed to compensate the NH_3 loss in the vent gas (7.5 kg/hr), in the CO_2 product (4.5 kg/hr) and in the water reservoir (21.4 kg/hr). The NH_3 makeup rate is about 0.28 kg of NH_3 per tonne of CO_2 captured and is much lower than the amine make up rate in the amine-based CO_2 capture process, which is between 0.35 and 2.0 kg/tonne CO_2 captured, according to Bailey & Feron (2005).

- **Water separation unit:** the main role of this unit is to avoid the H_2O that is redundant in the CO_2 capture unit and to maintain the H_2O balance of the entire system. A 38.8 t/hr H_2O vapour in the flue gas from the pretreatment column is condensed in the cooling tower. The condensed water becomes two parts after the stripper process: one is transferred to CO_2 capture unit (2.3 t/hr), together with CO_2 and NH_3 vapour; the other becomes relatively pure water (36.5 t/hr) which can be used for the water supply for the NH_3 recycle unit (15.1 t/hr), and water storage (21.4 t/hr).
- **CO_2 compression unit:** the material balance in this unit is easily maintained, because no additional stream is introduced to the CO_2 compressor. Due to the increasing pressure of the CO_2 stream and the inter-cooling process, a decant flow is generated, which removes almost all the moisture and NH_3 vapour, resulting in a CO_2 product that has high purity and high pressure.

In summary, the CO_2 capture plant does not require water makeup from the external system; instead it produces the excessive water. The material balances of CO_2, NH_3, and H_2O in each unit of the entire CO_2 capture system are maintained through making up the NH_3 and using a water separation unit.

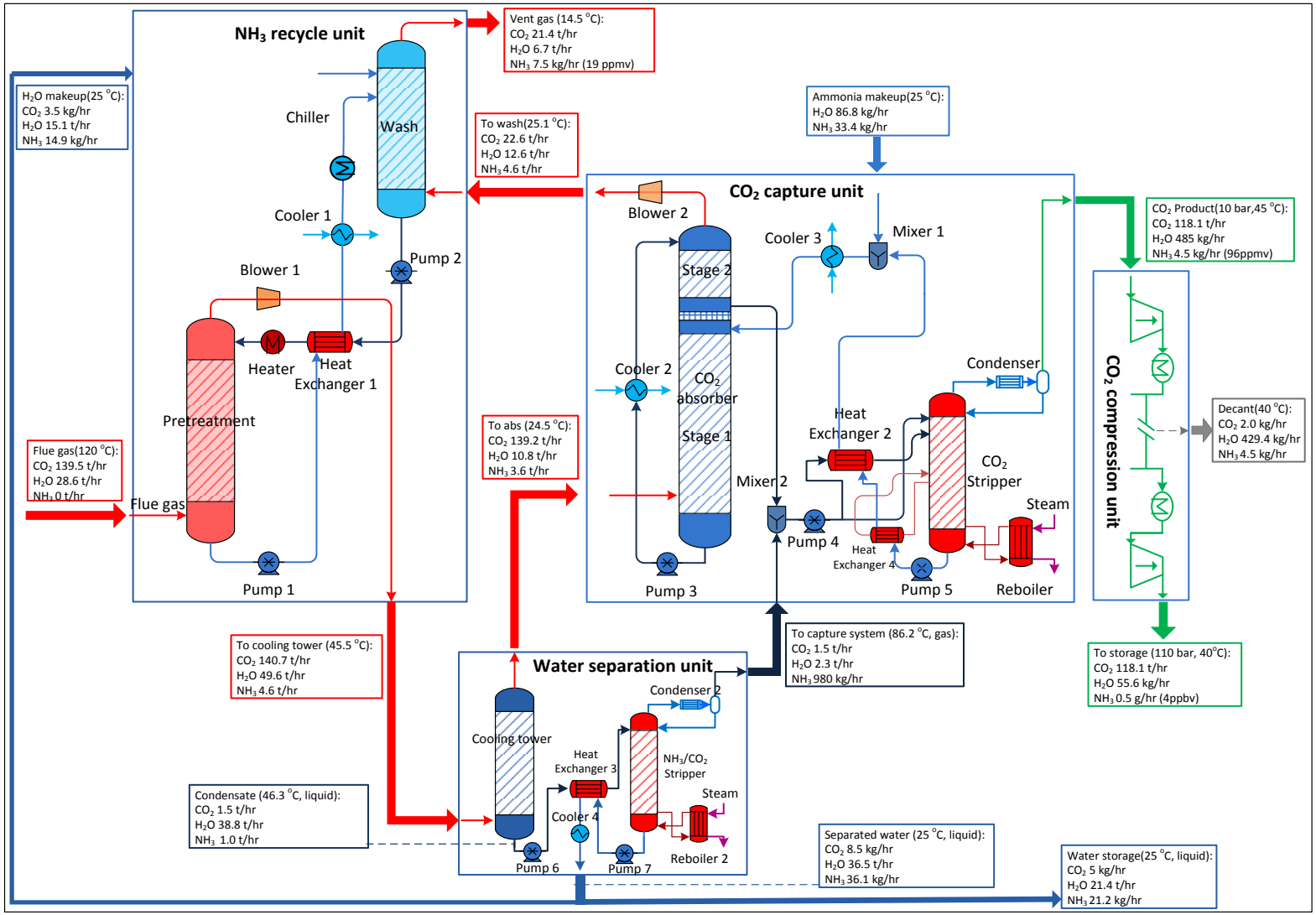

Figure 6-10 Material balance of a single process train for the NH_3-based CO_2 capture process

6.5.2 Energy penalty

Table 6-4 lists the energy duties and the corresponding net efficiency penalties involved in each unit of the proposed NH_3-based CO_2 capture process. It is clear that the CO_2 capture system is an energy-intensive process with a large net efficiency penalty, which leads to a decrease of 38.9% to 30.9% in the net output efficiency of a power station. It should be mentioned that the overall net efficiency penalty of 8.0% includes the electricity for pumping the cooling water, but does not incorporate the cooling duty for producing cooling water. This is primarily attributed to the proposed advanced process that elevates the inlet CO_2 lean solvent at 25 °C, thus avoiding the heavy reliance on chilled water (<10 °C) and saving substantial chilling duty. In this study, 16-20°C cooled water is assumed to be available in the power plant and is used to cool the lean solvent to 25 °C. This would consume 660 m^3/min – 1200 m^3/min cool water (depending on the temperature of cooling water) to cool the lean solvent to 25 °C. If cooling water is not available in the power plant and the cooling duty is supplied by electricity, an extra 24,336 kW electricity would be consumed for cooling water and a subsequent 1.2% net efficiency penalty would be placed on the power system. Therefore, the PCC plant would receive a significant energy saving from the available cooling water.

Table 6-4 also reveals that the CO_2 stripper and the CO_2 compressor are the two largest power consumers, accounting for 56.2% and 16.0% of the total energy consumption, respectively. Great attention should therefore be focused on these two components, particularly on the reboiler duty, in order to reduce energy consumption. As demonstrated in sections 6.3 and 6.4, parameter optimizations and process modifications play important roles in the reduction of solvent regeneration duty. The reboiler duty could be further reduced by decreasing the sensible heat (accounting for 30%-50% of total regeneration duty) by applying the other advanced process modifications or by using the advanced cross heat exchanger. Specifically, as the sensible heat is closely related to the temperature difference between the solvent in and out of the stripper, and assuming the temperature difference can be reduced from 10 ^oC to 8 ^oC, the specific heat requirement of solvent regeneration can potentially decrease from 2467 to 2175 kJ/kg CO_2, which will decrease the overall net efficiency penalty by 0.54%.

Table 6-4 Energy consumption and net efficiency penalty of the advanced NH_3-based CO_2 capture process

	Energy type	Energy duty, kJ/kg CO_2	Power output penalty, kW	Design specification [a]
Coal-fired power station				
Power plant island	Electricity	–	+650,000	38.9% net efficiency [b]
NH_3 recycling unit				
Chiller	Electricity	260	–6,568	5 °C, 4×5.9 m^3/min
Heater	Heat	172	–4,528	50 °C, 4× 6.4 m^3/min
Pump 1	Electricity	0.48	–61	4× 6.4 m^3/min
Pump 2	Electricity	0.70	–91	4× 5.9 m^3/min
Blower 1	Electricity	39.6	–5,196	3.05 kPa increase
Cooler 1	Cool water	148	0	25 °C, 4× 5.9 m^3/min
CO_2 capture unit				
CO_2 stripper	steam	2467	–75,600	10 bar, 145.5 °C
Pump 3	Electricity	11.0	–144	4×70.2 m^3/min
Pump 4	Electricity	49.6	–6,499	10 bar, 4×69.1 m^3/min
Pump 5	Electricity	8.2	–1073	4×76.2 m^3/min
Blower 2	Electricity	32.6	–4,290	3.05 kPa increase
Cooler 2	Cool water	2022	0	25 °C , 4×70.2 m^3/min
Cooler 3	Cool water	1451	0	25 °C , 4×76.2 m^3/min
Water separation unit				
NH_3/CO_2 stripper	Heat (steam)	130	–2,304	95 °C,4×0.68 m^3/min
Pump 6	Electricity	0.02	–2	4×0.68 m^3/min
Pump 7	Electricity	0.02	–2	4×0.68 m^3/min
Cooler 4	Cool water	14.0	0	25 °C , 4×0.68 m^3/min
CO_2 compression unit				
Compressor	Electricity	164	–21,520	150 bar
Intercooler	Cool water	251	0	40 °C
Auxiliary				
Pumps for cooling water	Electricity	8.3	–1096	4×165 m^3/min
Others	Electricity	42.5	–5,616	
Total power penalty	Electricity		–134,590	
Overall net efficiency penalty				8.0 %
Net plant efficiency with PCC plant				+30.9%

[a] The flow rates represent the solvent flowing through the corresponding equipment

[b] Gross thermal input to the power station is 1670 MW

Moreover, heat integration in a power plant can play an important role in reducing the energy requirement of this NH_3-based PCC process. For instance, the energy consumption of the heater (4,528 kW) in the NH_3 recycling unit can be reduced, because the solvent is only heated to 50 °C. Due to the relative low regeneration temperature of 95 °C used in the NH_3/CO_2 stripper of a water separation unit, the heat consumption (2,304 kW) can also be reduced if low-quality heat is supplied from the power station. Therefore, through process improvement and heat integration, the overall net efficiency penalty has the potential to be decreased to approximately 7.0%

6.5.3 Comparison with MEA and modified CAP process

To allow for a clear assessment of the proposed NH_3-based CO_2 capture process, the benchmarking MEA process simulated by the author (Appendix A) and the modified CAP simulated by Linnenberg et al. (2012) and Darde et al. (2012) based on the UNIQUAC thermodynamic model, are used for comparisons. Different from previous work, the rate-based model is employed in this study, which enables a more realistic calculation of energy consumption in each unit of the NH_3-based capture process. As shown in Table 6-5, the proposed process takes the obvious energy advantages over the MEA process with an efficiency saving of 2.6%. This is primarily attributed to the lower solvent regeneration duty and the decrease of CO_2 compression duty in the high stripper pressure in the NH_3 process.

Compared to the modified CAP, this process also has the competitive advantage of an energy penalty with a 0.5% efficiency saving. Two reasons can account for this low energy consumption. The first is that the parameters optimization and process modification greatly reduce the energy consumption of solvent regeneration and CO_2 compression. The second is the advanced NH_3 recycle process used in this study, which makes good use of the latent heat in the high temperature flue gas and reduces the energy penalty for the NH_3 recovery. In addition to an energy-saving advantage, the proposed process offers better operational feasibility than the CAP process, because the inlet CO_2 lean solvent is elevated to 25 $^{\circ}$C. This avoids solid precipitation and the heavy energy penalty of solvent chilling, which makes the process more flexible and feasible for application in an inland or coastal power station.

Table 6-5 Comparison of the advanced NH_3 process with MEA process and modified chilled ammonia process

	MEA	Modified chilled ammonia process	This study
Conditions			
Solvent concentration, wt%	30	8.5	6.8
Absolute stripper pressure, bar	2.0	4	10
Available cooling water, ˚C	-	10	20
CO_2 capture efficiency,%	85	~90	84.7
Net efficiency of power station, %	38.9	36.2	38.9
Results			
Reboiler temperature, ˚C	123.7	~120	145.5
Regeneration duty, MJ/kg CO_2	4.0	~2.50	2.47
Net efficiency penalty of regeneration, %	6.1	4.6	4.5
Net efficiency penalty of CO_2 compressor, %	3.1	2.2	1.3
Overall net efficiency penalty, %	10.6	8.5	8.0

6.5 Summary

In this study, a comprehensive investigation of an advanced NH_3-based CO_2 capture process integrated into a 650 MW coal-fired power plant is performed to evaluate the technical feasibility and energy performance of the overall CO_2 capture process. Four parallel process trains are proposed for dealing with the massive amounts flue gas that come from power stations, with each installing a CO_2 capture unit, an NH_3 recycling unit, a water separation unit and a CO_2 compressor. The process parameters of 6.8 wt% NH_3, 0.225 CO_2 lean loading and 10 bar stripper pressure are optimised through a sensitivity study. The process modifications of a rich-split and inter-heating process are used to further reduce the energy duties of solvent regeneration to 2.46 MJ/kg CO_2 and condenser duty to 0.24 MJ/kg CO_2. This is a reduction of 24.8% of the reboiler duty and 83.4% of the condenser duty compared to the reference case without the rich-split and inter-heating process.

After process optimization and modification, the advanced NH_3 process is evaluated through mass balance analysis, energy penalty analysis and comparison with modified CAP and MEA processes. It is shown that the material balance of CO_2, NH_3 and H_2O can be technically maintained by applying water separation and NH_3 make-up; the advanced NH_3-based process has a net efficiency penalty of 8.0 %, which is 2.6% lower than that in the MEA process and 0.6% lower than the modified chilled ammonia process. Thus, the advanced NH_3-based CO_2 capture process can be technically and economically competitive in terms of energy consumption and operational feasibility and thus has great potential for commercial application.

Chapter 7 Techno-economic Assessment of the Advanced NH_3-based Post combustion Capture Process Integrated with a 650 MW Coal-fired Power Station

Part A: Techno-economic assessment of baseline NH_3-based CO_2 capture process

Abstract: While most research work focuses on the technical assessment and improvement of the NH_3-based capture process, less attention is paid to the economic performance of the NH_3 process integrated with a coal-fired power station. The study of economic assessments of NH_3 processes is very limited in the open literature, resulting in a knowledge gap regarding the economic performance of NH_3-based CO_2 capture processes. In this study, the technical and economic performance is investigated for the baseline NH_3-based CO_2 capture process that is integrated with a 650-MW coal-fired power station. The validated rate-based model is employed to evaluate the technical performance and guide the column and equipment sizing, while a comprehensive cost model using the Aspen Capital Cost Estimator (ACCE) is proposed for the calculation of the capital cost of the NH_3-based capture process. A detailed analysis of the techno-economic performance is conducted to gain insight into the baseline NH_3 process. The reliability of the economic model, including the capital costing and CO_2 avoided cost, is discussed.

7.1. Methodology

7.1.1 Framework of techno-economic assessment

Figure 7-1 shows the framework for the technical and economic assessment of the PCC process integrated coal-fired power station. The framework is based on the structure recommended by Rubin (2012). The keys to achieving an adequate techno-economic estimation of a PCC integrated power station include: (1) development of an accurate technical model whereby rigorous, rate-based models validated against pilot plant data are considered to realistically and accurately represent the NH_3-based CO_2 capture process and guide process optimisation and scale-up; and (2) the establishment of an adequate economic model which is able to generate costing data close to the commercial practice.

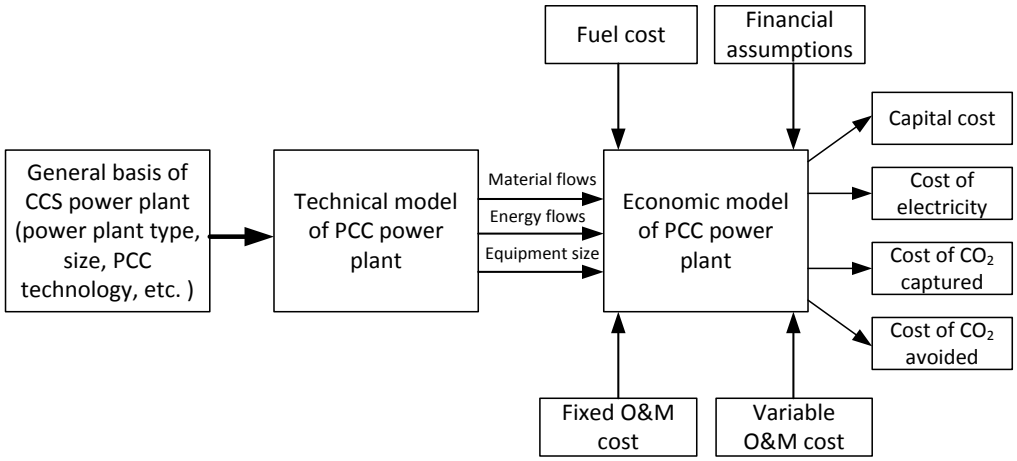

Figure 7-1 Analytical framework of a technical and economic estimation of a PCC plant integrated coal-fired power station

In the public domain, the economic studies of MEA process is much more than those for NH_3 process. To determine the reliability of the proposed economic model, the cost comparisons between published results and the results in this study, are first conducted, which is guarantee for the NH_3 process as they share the same economic model. In addition, the world's first commercial-scale post-combustion coal-fired CCS project, constructed and operated at the SaskPower Boundary Dam Power Station in Estevan, Canada (Stéphenne, 2013), is use to guide the process design and economic model. Although the Boundary Dam project employs amine solvent for CO_2 scrubbing and the costing information is limited in details, the published capital cost data from the Boundary Dam CCS project still provides an important economic guideline for the plant design and capital costing in this study.

7.1.2 Process description

Figure 7-2 illustrates the schematic of the NH_3-based PCC process that is integrated with a 650 MW coal-fired power station. It consists of a power station, NH_3 recycle unit, CO_2 capture unit and CO_2 compressor. CO_2 transportation and storage are not included in this study.

7.1.2.1 Power station

The present study assumes the technical design and capital cost estimation of an advanced pulverised-coal power station, as described by the United States Energy Information Administration (EIA, 2013). The study is based on a supercritical Rankine

power cycle with a designed electricity output of 650 MWe and a net efficiency of 38.9%.

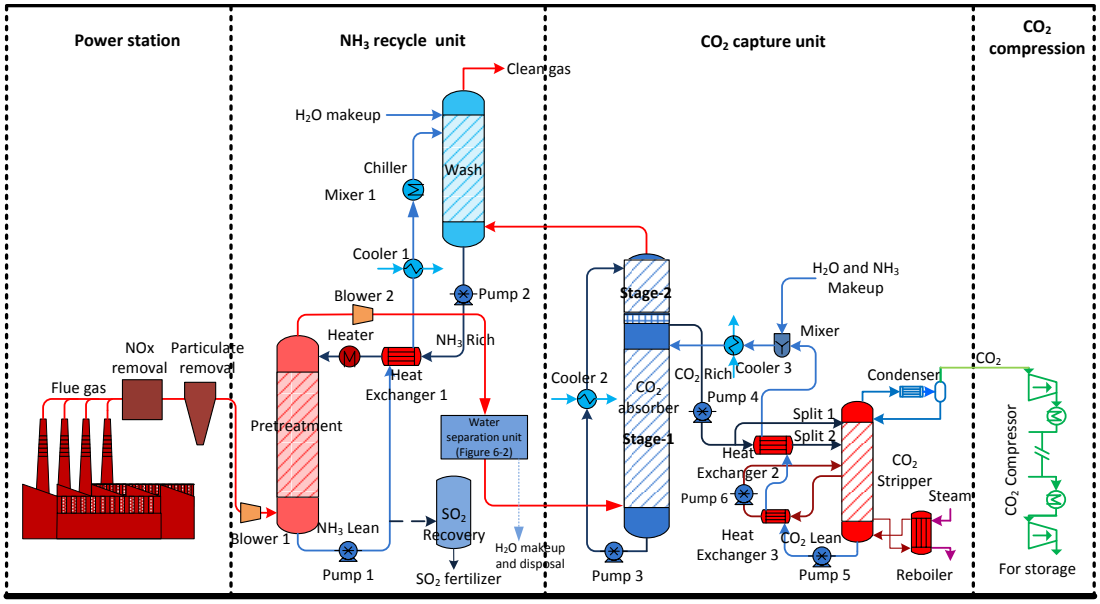

Figure 7-2 Schematic of advanced aqueous NH_3-based PCC plant integrated with a 650 MW coal-fired power station. Note: the baseline process is without two-stage absorption, rich-split and inter-heating.

Table 7-1 summarises the technical and costing information of the APC power station.

Table 7-1 Technical and cost information of an advanced pulverised-coal power station (in 2013 US dollar).

Parameter	Unit	Value
Net electricity output	MW	650
Net efficiency	%	38.9
Total flue gas flow rate	ton/h	3,180
CO_2 flow rate	ton/h	560
SO_2 content	ppmv	~30
Fixed operation and maintenance (O&M) cost	$/kW-year	37.8
Variable operation and maintenance cost	$/MWh	4.5
Total capital investment with FGD	million US$	2,110
Fixed operation & maintenance cost without FGD	$/kW-year	32.9
Variable operation and maintenance cost without FGD	$/MWh	3.9
Total capital investment without FGD	million US$	1,834

The total capital cost includes the selective catalyst reactor equipment for NO_X reduction and wet FGD equipment for SO_2 removal. As discussed in chapter 5, the advanced NH_3 process has high SO_2 removal efficiency and strong adaptability to the SO_2 concentration in the combined SO_2 recovery and NH_3 recycle process. It is believed that the wet FGD can be removed and replaced by the NH_3 recycle system when the advanced NH_3 process is integrated with the APC power station. This can reduce the capital cost of wet FGD system. As indicated by a report by Cichanowicz (2010), the capital investment of a wet FGD system for a 650 MW unit increased from US$ 320/kW in 2004-2006 to US$ 376/kW in the 2008-2010 timeframe (in 2008 dollars). This is an increase of $56/kW over a mean time period of four years – an escalation of approximately $16/kW per year. It can thus be calculated that the capital cost of the FGD system in 2012-2014 is US$ 433/kW in 2008 dollars. In this study, the Chemical Engineering Plant Cost Index (CEPCI, 2014) is used to convert the cost to 2013 dollars. Therefore, the capital investment of the FGD system is estimated at US$ 425/kW, which means the NH_3 process can reduce the total capital cost of a 650 MW power station by approximately US$ 276 million. By integrating the advanced NH_3 process into the power station, the removal of an FGD system can lead to a reduction of the capital cost of a power station from US$ 2,110 million to US$ 1,834 million. Accordingly, the fixed and variable O&M costs can also be reduced at the same ratio as the total capital investment of a power station.

7.1.2.2 NH_3-based CO_2 capture process

The detailed NH_3-based CO_2 capture process has been discussed earlier (refer to section 6.1.1). Simply speaking, the NH_3-based PCC process is designed at 85% CO_2 removal efficiency as it relates to the 560 ton/h (~ 4 million ton) CO_2 from a 650 MW APC coal-fired power station. Four parallel process trains are proposed to deal with the massive flue gas, with each including a CO_2 capture unit, an NH_3 recycling unit, a water separation unit and a CO_2 compressor. After CO_2 stripping, the captured CO_2 is compressed to 150 bar for geological sequestration.

A baseline NH_3 process without process modifications is used as a base case for the purpose of techno-economic comparison. The baseline process does not have two-stage absorption, rich-split and inter-heating, but has the advanced process of NH_3 recycling. The process conditions for the baseline process are 25 $^{\circ}$C lean solvent, 6.8% NH_3 concentration, 0.225 mol/mol lean CO_2 loading and 10 bar stripper pressure. The

rigorous, validated rate-based model is used to simulate the NH_3-based CO_2 capture, determine the column and equipment sizing, and calculate the energy consumption of the entire CO_2 capture process.

Due to the large amount of flue gas flow rate, the CO_2 capture process requires a large sized column to achieve a high CO_2 capture efficiency, which will lead to a high capital cost in column construction. This is confirmed by the costing results from Valenti et al. (2012) and Manzolini et al. (2015), in which the expenditure for packed columns plays a significant role in the total capital cost of the CO_2 capture plant. Thus, column sizing is of particular importance in the accuracy of the total capital cost of a PCC project. Table 7-2 shows the column sizes and corresponding packing information for the primary columns in the baseline NH_3 process. Since the baseline process does not apply two-stage absorption, the absorber column can be reduced to 21.5 m (instead of 26.5 m) to achieve the 85% CO_2 capture efficiency, but it does require a taller washing column of 20.25 m (instead of 13.25 m) and taller pretreatment column of 13.25 m (instead of 10.75 m), because of the increasing NH_3 loss from 12,000 ppmv to 26,500 ppmv emitted from the CO_2 absorber.

Table 7-2 The primary parameters of each column in the baseline NH_3-based CO_2 capture system

Columns	Column number	Packing material [a]	Surface area, m^2/m^3	Void fraction	Packing height, m	Column size, m×m [b]
Absorber	4	SS	256	0.987	16	Ø12×H21.5
Stripper	4	SS	256	0.987	8	Ø6.8×H10.75
NH_3 wash	4	SS	353	0.982	15	Ø10×H20.25
Pretreatment	4	SS	256	0.982	10	Ø10×H13.25

Note: [a] SS refers to stainless steel; [b] the column diameters are the inner diameters.

7.1.3 Economic model

7.1.3.1 Capital costing of the PCC plant

An academically preferred bottom-up approach based on the detailed process flow, insight in equipment parameters, material and energy balance is used to undertake the

economic assessment of NH_3-based PCC plant. Figure 7-3 shows the capital costing methodology of a PCC plant proposed by DOE/NETL (DOE, 2010).

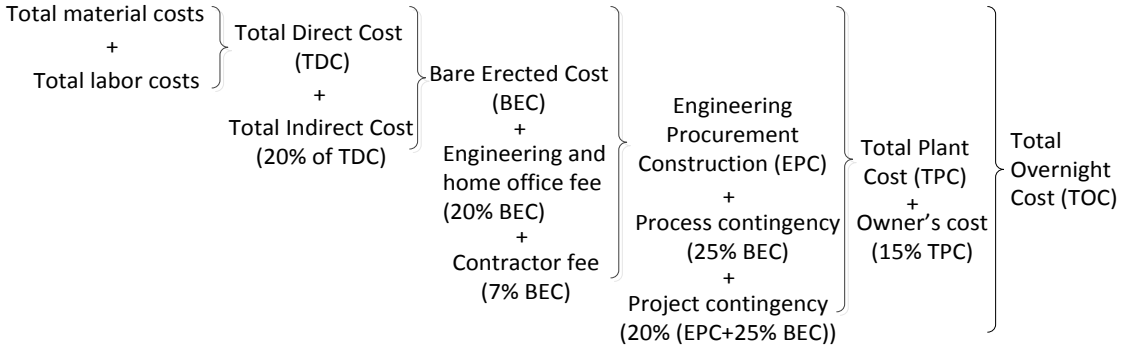

Figure 7-3 Capital costing methodology of the NH_3-based PCC plant

The Aspen Capital Cost Estimator® (ACCE) V8.6 is employed, on the basis of the 2013 US dollar, to calculate the equipment cost of the NH_3-based CO_2 capture process. ACCE uses the equipment models contained in the Icarus Evaluation Engine to generate preliminary equipment designs and simulate vendor-costing procedures to develop detailed Engineering-Procurement-Construction (EPC) estimates (Aspen, 2014). The total material costs of the PCC plant are the sum of all the equipment costs and the associated material costs of piping, civil, structural steel, instrumentation, electrical, insulation and paint. The manpower hours used in the construction and installation of the equipment comprise the total labour costs. The total material and labour costs are calculated by applying the specific equipment cost module through mapping, sizing and evaluating in the ACCE. The total indirect costs include the yard improvement, service facilities, engineering/consultancy cost, building and miscellaneous.

The process contingency and project contingency are also included in cost estimates, to compensate for the process uncertainties and the unknown costs due to a lack of complete project definition and engineering. Due to the start-up stage of the PCC technology in commercial application, the techno-economic study of the advanced NH_3-based CO_2 capture technology is classified as a "feasibility study". Accordingly, the American Association of Cost Engineering (AACE) Class IV is applied to attain the cost estimates, and the percentages used in the costing are guided by the AACE International Recommended Practice (AACE, 2011) and the DOE/NETL economic study (DOE, 2011), with an expected accuracy of total capital cost being ± 30%.

7.1.3.2 Economic assumptions

Table 7-3 lists the main assumptions relating to the economic assessment of the PCC process integrated with a coal-fired power plant, which follows the criteria set out by the International Energy Agency Greenhouse Gas (IEAGHG) for the technical and economic assessment of a power plant with low CO_2 emission (IEA, 2009).

Table 7-3 Primary economic assumptions of an NH_3-based PCC process integrated APC power plant

Parameters	Value
Present value	1st quarter of 2013 US dollar
Plant life	30 years
Capital cost	calculated
Discounted cash flow rate	8%
Construction year	3 years
Budget allocated in construction year 1	40%
Budget allocated in construction year 2	30%
Budget allocated in construction year 3	30%
Plant capacity factor	85%
Plant capacity factor of first year operation	50%

The operation and maintenance (O&M) cost is composed of fixed O&M costs and variable O&M costs. The fixed O&M cost is assumed to be 3.5% of the total capital investment of the PCC plant, including the total maintenance and labour costs for maintenance, operation and administration and support labour (Rao *et al.*, 2002). The variable O&M cost is obtained based on the assumptions listed in Table 7-4. The consumption rates of cooling water and demineralised water are determined from the Aspen process simulation based on the heat and mass balance of the entire CO_2 capture process. The waste treatment is the excessive water discharged from the water separation unit. The consumption is calculated from the water material balance (Figure 6-9). It is worth mentioning that the electricity and steam consumed in the PCC process is assumed to be supplied from the power station at the expense of a net power penalty. This penalty is reflected in the overall economic performance of the cost of electricity and the CO_2 avoided cost.

Table 7-4 The assumptions of operating &maintenance (O&M) costs relating to the economic assessment of a PCC integrated power plant

Parameters	Value	Consumption
Fixed O&M cost	3.5% of total overnight cost	
Variable O&M cost	calculated	
Fuel cost	\$2/GJ	
Cooling water	\$0.35/m^3	1.75 m^3/ton CO_2
Demineralised water	\$2.0/m^3	0.73 kg /ton CO_2
NH_3 solvent *	\$600/ton	1.56 kg/ton CO_2
Wastewater treatment	\$100/m^3	1.8 L/ton CO_2

Note: *the price is quoted from Alibaba http://www.alibaba.com/

7.1.3.3 Cost measurements

Based on the above assumptions, the economic calculation is carried out based on the method of net present value (NPV) on a basis of 2013 dollars, in which the income received from selling electricity and the expenditure for the capital cost and O&M cost are balanced over the entire economic life. The NPV of zero leads a breakeven electricity price termed the levelised cost of electricity (LCOE) (\$/MWh), which is the minimum price sold to the grid system so that the power plant owner can receive the revenue to cover all capital costs and O&M costs during the plant life. As aforementioned, the NH_3 process can produce ammonium-sulphate fertilizers. The production of sulphur-fertilizer by NH_3 is a mature technology. Although the SO_2 recovery system requires some additional equipment and capital cost, it is believed that the income derived from selling sulphur-fertilizer can compensate for the extra capital expense. For the purpose of simplification, it is assumed that the income and the capital investment meet the balance.

The LCOE calculation method is shown in equation (7-1):

$$LCOE = \frac{\sum_t [\frac{(Capital\ Expenditure)_t}{(1+r)^t} + \frac{Fixed\ O\&M_t}{(1+r)^t} + \frac{Variable\ O\&M_t}{(1+r)^t}]}{\sum_t \frac{(Electricity\ Sold)_t}{(1+r)^t}} \quad (7\text{-}1)$$

where $(\text{capital expenditure})_t$ is the capital cost invested in the construction of power plant with and without PCC in year t, \$; fixed $O\&M_t$ is the fixed operating and maintenance cost in year t, \$; variable $O\&M_t$ is the variable operating and maintenance

cost in year t, $; (electricity sold)$_t$ is the produced and sold electricity in year t, MW; and *r* is the discount rate.

The CO_2 avoided cost ($/ton CO_2) is calculated to quantify the economic performance of the NH_3-based PCC process. The avoided cost is an important economic indicator for PCC technology, because it considers the increased LCOE and decreased CO_2 emission rates from the power station, and accounts for the energy consumption of the capture process. Note that the avoided cost excludes the costs of CO_2 transportation and storage, because they vary greatly from case to case, such as location, geological formations, topography and socioeconomic aspects. The calculation method is shown in equation (7-2):

$$Cost\ of\ CO_2\ avoided = \frac{(LCOE)_{PCC} - (LCOE)_{Ref}}{(CO_2\ emission)_{Ref} - (CO_2\ emission)_{PCC}} \qquad (7\text{-}2)$$

where $(LCOE)_{PCC}$ and $(LCOE)_{Ref}$ are the levelised cost of electricity exported from the power plant with and without PCC, respectively, $/MWh; and $(CO_2\ emission)_{PCC}$ and $(CO_2\ emission)_{Ref}$ are the mass of CO_2 emitted from a power plant with and without PCC, respectively, ton CO_2/MWh.

7.2 Technical performance of baseline NH_3 process

Table 7-5 shows the energy performance of the baseline NH_3-based PCC process integrated with a 650 MW coal-fired power station. The detailed energy calculation method is referred to in section 6.1.3. It is can be seen that the NH_3 process is energy-intensive, which places the energy burden of 157 MWe on and decreases the net efficiency from 38.9% to 29.4% for the 650 MWe coal-fired power station. The heat requirement in the CO_2 stripper is the largest power consumer, accounting for 64% of the total energy consumption. The second largest contributor to the energy penalty is the CO_2 compressor, but this only accounts for 14%. This is primarily attributed to the high pressure of 10 bar used in the stripping process to significantly reduce the compression energy.

To make a fair comparison, the baseline MEA process is simulated based on the same technical conditions and economic assumptions. The technical performance of the MEA process is obtained from a rigorous rate-based model, which has been validated by the pilot plant results located at Tarong power station, Queensland, Australia, for

both the CO_2 absorption process and the CO_2 stripping process (for details refer to Appendix A).

Table 7-5 Energy performance of baseline NH_3 process and baseline MEA process with a CO_2 capture capacity of ~4 million ton CO_2/year (Four process train)

	Baseline NH_3 [a]	Baseline MEA [b]
Power island (Reference)		
Net electricity output without PCC, MW	+650	+650
Net efficiency, %	+38.9	+38.9
PCC island		
Stream extraction, MW	-100.1	-101.7
Compressor, MW	-21.5	-52.6
Blowers, MW	-9.5	-14.3
Pumps, MW	-7.8	-2.4
Chiller, MW	-13.5	-
Auxiliary, MW	-4.6	-6.0
Total energy penalty of PCC, MW	-157	-177
Power output with PCC, MW	+493	+473
Power output reduction, %	-24.2	-27.2
Net efficiency penalty, %	-9.5	-10.6
Net efficiency with PCC, %	+29.4	+28.3

Note: [a] the reboiler duty is based on 3.27 MJ/kg CO_2; [b] detailed energy calculation and performance refer to appendix B and the reboiler duty is based on 4.0 MJ/kg CO_2.

It can be seen from Table 7-5 that the steam consumption of the NH_3 process is similar to that of the MEA process, although the regeneration duty of 3.27 MJ/kg CO_2 in the NH_3 process is lower than 4.0 MJ/kg CO_2 in the MEA process. This is because the NH_3 process operates the CO_2 stripping process at a high pressure of 10 bar, resulting in the high-temperature and high-quality steam used for the stripping process. This subsequently causes a high net efficiency loss for the power station on the basis of the same amount of heat duty. From the viewpoint of steam consumption, it seems the NH_3 process has marginal advantages to the MEA process. However, the high stripper pressure brings a significant reduction of CO_2 compression duty due to the decreasing compression ratio. For the two base cases in the studied conditions, the NH_3 process has the energy advantage over the MEA process—a 1.1% saving in the net efficiency

penalty. The energy advantage of NH_3 over MEA is primarily owing to the high stripper pressure and lower CO_2 compression duty.

7.3 Economic performance of baseline NH_3 process

7.3.1 Capital costing of CO_2 capture plant

Table 7-6 shows the details of the breakdown of equipment costs and total capital investment of the baseline NH_3-based CO_2 capture plant for one process train. The costs include all the necessary equipment involved in the NH_3 recycling unit, CO_2 capture unit and CO_2 compression unit. It is worthwhile mentioning that the pretreatment column, washing column, CO_2 absorber and stripper are assumed to be clad with SS304 stainless steel to prevent the corrosion problems. The packing materials in each column are also assumed to be made of SS304 stainless steel. The other equipment is made of carbon steel. A TEMA shell and a tube heat exchanger with a thermal conductivity coefficient of 2000 W/m^2 K are used for all of the heat exchangers in the NH_3 process. The total capital investment of for a CO_2 capture plant with one process train (~1 million ton/year) is estimated to be US$ 208.2 million, including the equipment costs, indirect costs, process and project contingencies, and owner's costs.

While the absolute capital cost from different studies cannot be easily compared due to the different cost model used, the percentages of equipment costs within the total equipment cost can somehow reflect the costing characteristics of different CO_2 capture processes. Specifically, in the proposed NH_3 process, the CO_2 compressor is the largest contributor, accounting for 18% of the total direct cost, which is much lower than 46% of the MEA process estimated by DOE (Ramezan *et al.*, 2007). This is because of the high pressure of 10 bar used in the NH_3 process, enabling the reduction in compression stages and, as a result, a decrease in the CO_2 compressor size. The CO_2 absorber accounts for 18% of the total equipment cost, which is smaller than the 28% of chilled ammonia processes proposed by Versteeg et al. (2011).This is due to the high absorption temperatures of >25 $^{\circ}C$ used in this study to increase the CO_2 absorption rate and, thus, reduce the size of the absorber column; the chilled ammonia process is conducted at a low absorption process below 10 ^{o}C and requires a 15% total equipment cost for the chilling water system, according to Versteeg et al. (2011).

Table 7-6 Total capital investment cost of baseline aqueous NH_3-based PCC plant for one process train (~1 million ton/year), in 2013 US$

Equipment	Material	Manpower	Direct cost	Specification*
NH_3 recycle unit				
Blower	730,930	81,303	812,233	200 m^3/s
Pretreatment column	3,481,402	1,283,870	4,765,300	Ø10m× H13.25m
Pretreatment packing	3,641,900	89,075	3,641,900	Ø10m× H10m
Washing column	3,824,621	1,322,576	5,147,200	Ø10m× H20m
Washing packing	7,272,900	141,803	7,414,700	Ø10m× H15m
Heat exchanger	197,483	38,593	236,076	TEMA ,510 m^2
Cooler	190,633	38,398	229,031	TEMA ,460 m^2
Chiller	510,840	64,386	575,226	TEMA ,2000 m^2
Pumps	74,846	23,643	98,489	5.9 m^3/min
Solvent tank	160,954	48,192	209,146	66 m^3
CO_2 capture unit				
Blower	730,930	81,303	812,233	200 m^3/s
Absorber	6,220,677	2,294,001	8,514,700	Ø12m× H21.5m
Absorber packing	6,309,520	92,638	6,402,158	Ø12m× H16m
Stripper	2,312,507	242,937	2,555,400	Ø6.8m× H10.75m
Stripper packing	1,166,003	259,791	1,418,094	Ø6.8m× H8m
Stripper reboiler	2,044,219	165,744	2,209,963	TEMA, 9,987m^2
Stripper condenser	371,059	51,959	423,018	TEMA, 1,329m^2
Main heat exchanger	9,070,237	4,465,863	13,536,100	TEMA, 46,300 m^2
Lean solvent cooler	401,144	56,568	460,700	TEMA, 1,970 m^2
Pumps	2,149,592	249,156	2,398,748	76.2 m^3/min
Solvent tank	491,708	63,962	555,670	702 m^3
CO_2 compression				
CO_2 compressor	12,700,000	2,279,500	14,979,500	6 stages, 150 bar
Auxiliary				
Water separation unit	3,914,379	906895	4,821,274	
Others	358,857	91,643	450,500	
Total Direct Cost (TDC)			82,714,409	
Total Indirect cost (TIC)			16,542,882	0.2 TDC
Bare Erected Cost (BEC)			99,257,291	TDC + TIC
Engineering, Procurement, construction (EPC)			126,056,759	1.27 BEC
Total Plant Cost (TPC)			181,045,298	1.2 EPC + 0.3 BEC
Total capital investment (TCI)			208,202,093	1.15 TPC

The cost for the lean/rich heat exchanger also contributes 18% to the total equipment cost. As aforementioned (in section 6.3), the lean solvent from the CO_2 stripper is 145.5 °C, while the rich solvent from the CO_2 absorber is about 30 °C. This significant temperature difference leads to a large heat transfer area and a subsequently large cross heat exchanger to achieve the targeted temperature approach. The wash column and pretreatment column are the significant cost contributors, accounting for 15% and 10%, respectively. This is mainly because of the massive NH_3 loss, which requires the large columns to have a high NH_3 removal and recycling efficiency as well as a high SO_2 scrubbing efficiency.

The cost distributions of the equipment, in a sense, provide the technical research directions on reducing the capital cost, i.e. the improvement of the CO_2 absorption rate would reduce the absorber column height and, subsequently, the packing materials; the enhancement of the CO_2 capacity by a solvent would decrease the solvent flow rate per CO_2 captured and lead to a subsequent size reduction of heat exchangers; the decrease of NH_3 vaporisation enables the reduction of the wash and pretreatment columns. Thus, it is suggested in this thesis that more attention should be focused on these large cost items to reduce the total capital cost. In addition to technical improvements, cheap construction materials can also play important roles in the reduction of capital costs. For instance, the column can be constructed with concrete material instead of carbon steel. This has been applied in the Boundary Dam CCS plant to reduce the capital cost of column construction (MIT, 2015b). As the temperatures along the absorber and washing columns are in the range of 10-40 ˚C, the stainless steel packing materials could be replaced by plastic materials. As estimated by Jilvero et al. (2014), using plastic packing instead of stainless steel can reduce the material cost by 90%.

7.3.2 Economic performance of PCC integrated power station

Table 7-7 illustrates the cost performance of the APC power station integrated with the NH_3-based PCC plant. It is obvious that the NH_3-based PCC process is capital-intensive, which places a heavy economic burden on the power station. With the integration of the PCC plant, the LCOE of power station increases from $71.9/MWh to $118.0/MWh, that is, by about 64%, resulting in the CO_2 avoided cost of $67.3/ton CO_2.

Table 7-7 Summary of economic performance of the power station integrated with a baseline NH_3-based and baseline MEA-based PCC process, costs in 2013 US$

Item	Unit	NH_3	MEA*
Capital cost and O&M cost			
Capital investment of power station	$/kW	2820	3,246
Capital cost of PCC plant	$/kW	1675	1,357
Fixed O&M cost of power station	million dollars/year	21.3	24.6
Variable O&M cost of power	million dollars/year	18.8	2.16
Coal cost	million dollars/year	89.4	89.4
Fixed O&M cost of PCC plant	million dollars/year	29.1	22.6
Variable O&M cost of PCC plant	million dollars/year	5.5	23.2
Economic performance of MEA process			
LCOE of power station	$/MWh	71.9	71.9
LCOE of power station and PCC plant	$/MWh	118.0	130.8
CO_2 avoided cost	$/ton CO_2	67.3	86.4

Note: *the capital cost for the baseline MEA process is US$ 643 million

The benchmark MEA process is again used to make a fair comparison of economic performances between the two solvents. Compared with the MEA process, the NH_3 process includes cost advantages ($67.3/ton vs $86.4/ton) -a saving of $19.1/ton CO_2. Three reasons can be given for the cost advantage of the NH_3 process. The most important reason is that less energy is required for the NH_3 process (refer to Table 7-6). The second reason is the removal of the FGD system due to the advanced design of the combined NH_3 recycle and SO_2 removal that achieves a high SO_2 removal efficiency of over 99%. This reduces the capital cost of a power station by approximately US$ 276 million. The third is the cheap cost of the NH_3 solvent and the lack of degradation in the capture process. This subsequently leads to a low variable O&M cost. However, the drawback of the NH_3 process is the high capital cost, because the slow reaction rate leads to a large CO_2 absorber, and a high NH_3 loss results in a large NH_3 wash column. Thus, process improvements are necessary in order to decrease capital investment and reduce energy consumption, thus making the NH_3 process more technically and economically competitive.

7.3.3 Cost breakdown of the baseline NH_3 process

Figure 7-4 illustrates the breakdown of the energy consumption, capital cost and CO_2 avoided cost for the baseline NH_3-based CO_2 capture process. The energy and cost distributions provide the guideline for the technical improvements necessary to increase the economic viability of the NH_3-based CO_2 capture process. Note that the energy cost is based on energy consumption and the LCOE after the PCC plant is integrated with the power station

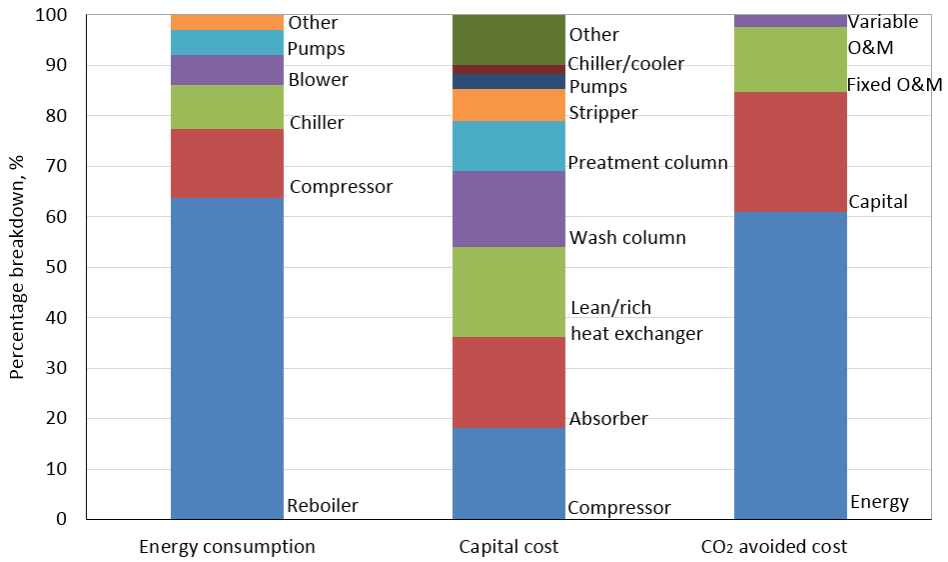

Figure 7-4 The breakdown of energy consumption, capital cost and CO_2 avoided cost in the baseline NH_3-based CO_2 capture process.

It can be seen that energy consumption is the major burden for the commercial application of the NH_3 process that is integrated with the power station; the process accounts for 60% of the CO_2 avoided cost. As the reboiler duty is the major contributor to the total energy consumption, the reduction of regeneration duty is the top priority in decreasing the cost of CO_2 avoided. The capital investment is the second contributor, representing 24% of the CO_2 avoided cost. The relatively low percentage of capital cost is ascribed to the removal of the FGD system from the power station where the simultaneous capture of CO_2 and SO_2 is realised in the NH_3 process. This results in the capital reduction of the power station and, in a sense, reduces the capital investment of the NH_3-based PCC plant. Technically, the practical approaches to reducing the capital cost include the reduction of NH_3 vaporisation to decrease the sizes of the pretreatment column and wash column, and the improvement of the CO_2 absorption rate to reduce the column size. The variable O&M cost contributes only 2.4% of the

CO_2 avoided cost. This is primarily because of the cheap NH_3 solvent, no degradation, low NH_3 emission into the environment and low NH_3 make-up.

7.3.4 Reliability of economic model

Currently, there is no commercial-scale NH_3-based PCC plant available in the world; therefore, it is impossible to use real plant data to validate the economic model, leaving the reliability of the economic model unclear. However, the economic studies from different research organisations and institutions have provided valuable information on the economic performance of the CO_2 capture processes. Their published results can be used to compare and determine the reliability of the proposed economic model. Very few economic studies pay attention to the NH_3 process and most of economic publications focus on the MEA process. The present study is the first to employ the economic model to evaluate the MEA process and use the resultant economic performance to compare with the published data. As the NH_3 process utilises the same economic model as the MEA process, the reliability of the MEA model is a guarantee for the NH_3 economic model. An economic assessment of the MEA process has been conducted to support this thesis and the details can be found in Appendix B.

7.3.4.1 Comparison of capital costing

Since the equipment cost is the essential element of the capital cost, the cost accuracy is of particular importance in ensuring reliable economic results. To determine the cost accuracy of the equipment, the most detailed cost analysis of an MEA-based CO_2 capture plant from the US DOE report (Ramezan *et al.*, 2007) is used and compared with the equipment cost generated from this study. All equipment parameters are set to be the same as the DOE equipment and the cost is converted to 2013 US$ using the Chemical Engineering Plant Cost Index (CEPCI, 2014). As shown in Table 7-8, the relative discrepancy of equipment costs between the two cost sources are in the range of ±17% and the discrepancy of the total equipment cost is only 5.2%, indicating the reasonable equipment cost estimation that arises from this study.

Table 7-8 Direct cost comparison of important equipment between United States Department of Energy (DOE) analysis and Aspen Capital Cost Estimator®(ACCE), in 2013 US$

Item	DOE, 1000 US$	ACCE, 1000 US$	Relative error,%
Exchangers and aircoolers	22,199	18,414	–17.0
Vessel and filters	5,848	6,502	+11.2
Towers and internals	26,303	25,711	–2.2
Pumps	3,904	4,560	+16.8
Total cost	58,253	55,999	–5.2

The total capital investment of the MEA based PCC plant is estimated to be around US$ 152 million (in 2013), based on the capital methodology as illustrated in Figure 7-3. The detailed capital costing refers to Appendix B. The commercial Boundary Dam CCS plant, which has a similar CO_2 capture capacity as the present study (~1 million ton/year), is used as the reference for the capital cost. Although the Boundary Dam CCS project is based on amine scrubbing technology (rather than MEA) and the columns are made of concrete material, the cost values are still meaningful, or at least can be a reference and guideline for the proposed CO_2 capture plant. The total project cost is claimed to be approximately 1.4 billion Canadian dollars and includes ~$500 million for power plant retrofits and ~$800 million for the CCS process (MIT, 2015a). Based on the SaskPower Boundary Dam project, the IPCC estimates that the cost of retrofitting a CCS plant to a coal-fired plant would be one-third of what SaskPower spent at Boundary Dam with its upgrade of CCS technology and scale of economies. It is about US$ 200 million if a currency exchange rate of 1.4 US/Canadian dollar (in 2013) is used. In addition, Saskpower also states that the project cost has the potential to be reduced to 200 million dollars or less for a similar CCS project when using the lessons learnt from the Boundary Dam project (MIT, 2015b). Considering that the Boundary Dam CCS project includes CO_2 transportation and storage, the cost estimation of $152 million is close to or at least in the appropriate order of magnitude for the future capital cost if the CCS plant is at a commercially mature stage, as estimated by IPCC and Saskpower.

7.3.4.2 Comparison of capital investment and CO_2 avoided cost.

To further determine the reliability of the estimated costs, the capital cost of the PCC plant and CO_2 avoided cost as found in the published studies are compared with this study, as illustrated in Figure 7-5. The capital cost and CO_2 avoided cost can be found in the published studies of Manzolini *et al.* (2015), Raksajati et al. (2013), Oexmann et al. (2009), DOE (Rederstorff, 2007) and Singh et al. (2003). To provide consistent comparison, the capital costs in the published studies have been converted to 2013 US$ using the Chemical Engineering Plant Cost Index (CEPCI, 2014) and the Euro/United States currency exchange in the cost year (XE, 2015). The CO_2 avoided costs from published studies have also been recalculated using the equation (7-2) and converted to 2013 US$ for consistent and reasonable comparison.

As shown in Figure 7-5, the specific capital costs of the PCC plant range from US$890 to1550/kW, while the CO_2 avoided cost ranges from US$62.0 to 95.2/ton CO_2. The wide cost range is due to the different capital cost models, process boundaries and economic assumptions used in the studies. In the present study, the specific capital cost and the CO_2 avoided cost is estimated to be US$1357/kWh and US$86.4/ton CO_2, respectively, which are within the range of the published costs. This indicates that the proposed economic model is valid and adequate for estimation of the economic evaluation of the MEA-based as well as the NH_3-based CO_2 capture process, which can be used to guide the following techno-economic performance of the process improvements in the NH_3-based CO_2 capture process.

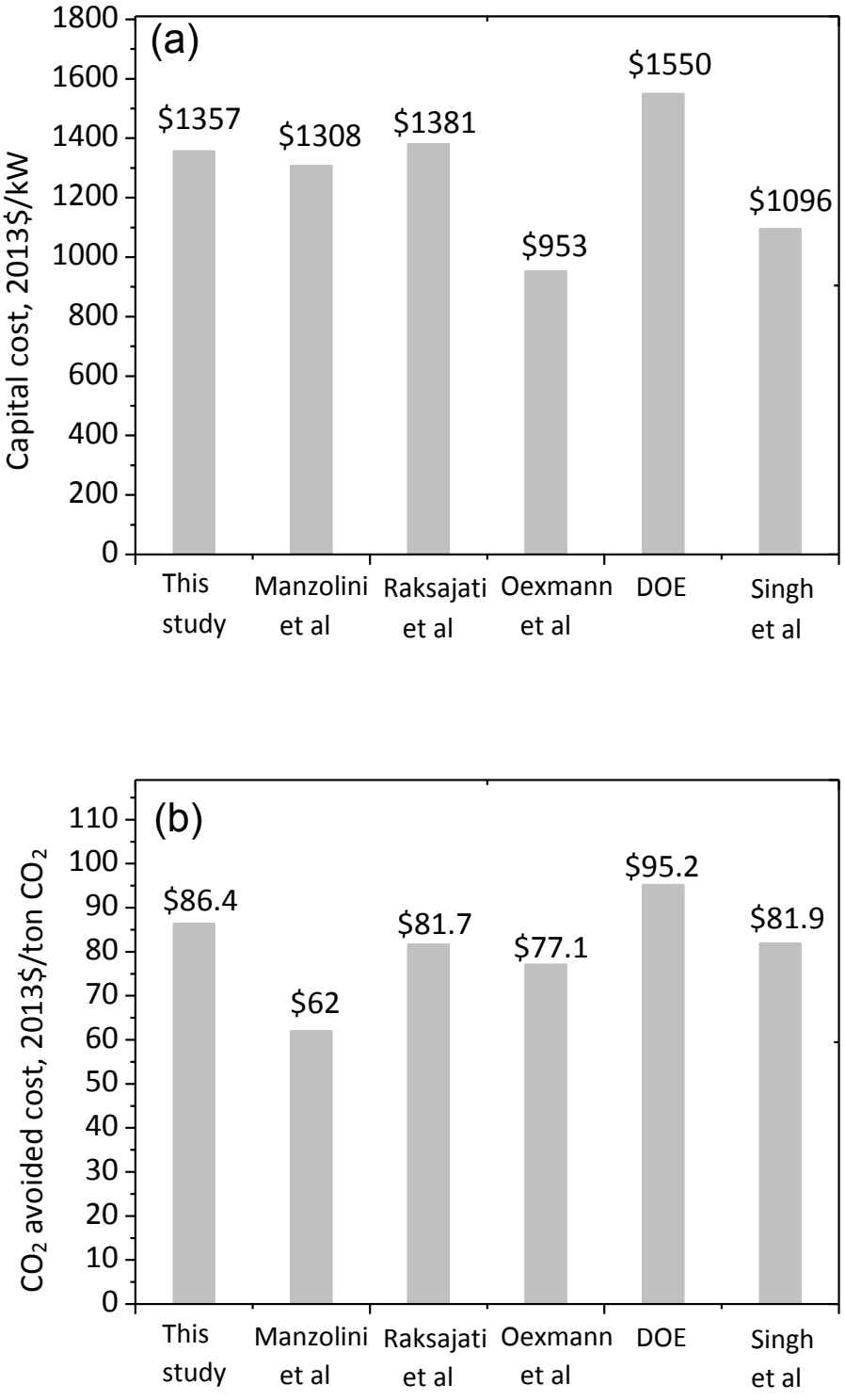

Figure 7-5 Comparison of (a) specific capital cost with ±30% cost accuracy and (b) CO_2 avoided cost between the present study and published studies

Part B Techno-economic assessment of process improvements in the NH_3-based CO2 capture process

Abstract: The previous study has demonstrated that the process improvements are technically feasible to significantly reduce the energy consumption involved in the NH_3-based CO_2 capture process. However, the overall economic benefits from the process improvements are still uncertain, because the process modifications require additional equipment and piping, and will increase the total capital investment, which may offset the benefits obtained through energy savings. Therefore, part B examines the techno-economic evaluation of the advanced NH_3-based CO_2 capture process integrated with a 650 MW coal-fired power station. Process modifications of two-stage absorption, the rich-split process and stripper inter-heating are introduced into the NH_3 process to improve its technical and economic performance. The technical prospects leading to the improvement of the NH_3-based capture process are proposed to provide technical research directions from an economic point of view. The results imply that there is considerable room to further advance the techno-economic performance of NH_3 process via the reduction of regeneration energy consumption, mitigation of NH_3 slip and improvement of the CO_2 absorption rate.

7.4 Process improvements

Previous study has shown that process modifications enable a great improvement in technical performance. This section explores the economic performance of the process modifications. The process improvements include two parts: the first is the advanced absorber configuration with two-stage absorption; the second is the advanced stripper configuration of a rich-split process and stripper inter-heating to significantly reduce the heat requirement of solvent regeneration. The process configurations are depicted in Figure 6-1 and Figure 6-6.

7.4.1 Advanced absorber configuration

A two-stage absorption configuration with intermediate cooling is introduced to mitigate the NH_3 slip during the CO_2 absorption process, and thus reduce the size of the column and decrease the chilling duty that results from the decreasing flow rate of the solvent when undertaking NH_3 washing. In this process, the bottom stage is responsible for scrubbing the majority of the CO_2, while the top stage captures the

vaporised NH_3 that leaves from the bottom absorber. Table 7-9 summarises the main changes to the technical and cost performance after two-stage absorption is introduced.

Table 7-9 Comparison of the technical and economic performance between two-stage absorber and base case, in 2013 US$.

	Base	Two-stage absorption
Main changes of technical performance		
NH_3 emission after absorber, ppmv	26,500	12,000
NH_3 emission after wash column, ppmv	~50	~15
Heat transfer area of Inter-cooler, m^2	-	4500
Chilling temperature, °C	5	0
Chilling duty, MWe	-13.5	-5.5
Regeneration duty, GJ/ton CO_2	3.27	3.27
Reboiler duty, MWe	-100.1	-100.1
Total energy penalty, MW	-157	-150
Main changes of capital cost performance (one process train), US$		
Wash column packing height, m	15	10
Pretreatment column packing height, m	10	8
Absorber column packing height, m	15	20
Wash column and packing, $	12,561,900	8,378,600
Pretreatment column and packing, $	8,496,275	6,797,020
Absorber column and packing, $	14,916,858	17,160,551
Absorber inter-cooler and pump, $	0	1,135,391
Others such as cooler, chiller etc. , $	1,138,822	379,607
Saving of capital cost, US$	0	3,262,686
Economic performance		
Capital cost, million US$	832.8	800.0
LCOE, $/MWh	118.0	115.2
CO_2 avoided cost, $/ton CO_2	67.3	62.9

Technically, the two-stage absorber configuration enables the reduction of the NH_3 emission level from 26,500 ppmv to 12,000 ppmv. The significant reduction of NH_3

emission brings many benefits. It reduces the flow rate and chilling temperature of the NH_3 wash solvent, thus decreasing the chilling duty from 13.5 MW to 5.5 MW. From the viewpoint of capital cost, this advanced configuration also greatly facilitates the column size reduction of NH_3 recycling system in which the packing height of the NH_3 washing column is reduced from 15 m to 10 m, while the pretreatment column is decreased from 10 m to 8 m, due to the reduced NH_3 emission from the CO_2 absorber. Although the two-stage absorption process increases the absorber packing height from 16 m to 20 m and includes an extra inter-cooler for solvent cooling, the benefits from energy saving and capital cost saving can offset the additional cost. As a result, the two-stage absorption reduces the US$ 32.8 million of capital cost and results in a subsequent saving of $2.8/MWh in LCOE and a saving of $4.4/ton in CO_2 avoided cost. Therefore, the two-stage absorption brings not only the technical benefits of NH_3 emission reduction, which will greatly facilitate NH_3 control and make the NH_3 process more technically feasible, but also the economic benefits of capital cost saving and CO_2 avoided cost saving.

7.4.2 Advanced stripper configuration

Table 7-10 summarises the technical changes and economic improvement of process modifications: a rich-split, inter-heating process. The stripper modifications are based on the conditions and results of two-stage absorption. It is evident that the proposed stripper modifications can reduce energy consumption and save the cost of CO_2 avoided.

7.4.2.1 Rich-split process

The rich-split process splits the cold solvent to recover the steam heat in the CO_2 stripping process. This process configuration has been proven to be effective in the reduction of regeneration duty from 3.27 to 2.89 MJ/kg CO_2 and reduction of condenser duty from 1.45 to 0.39 MJ/kg CO_2. The rich-split configuration is considered to be optimal, because it requires minimal additional equipment and brings many benefits relating to cost and energy savings. Firstly, it reduces the capital cost of stripper reboiler and stripper condenser due to the decreased reboiler duty and condenser duty. Secondly, this modification reduces the heat surface area and the capital cost of a lean/rich heat exchanger owing to the decreasing rich solvent that flows through the heat exchanger; this leads to a total capital saving of US$ 66.4 million for the four process trains.

Table 7-10 Primary technical changes and economic improvement of stripper modifications: rich-split, inter-heating process and combined process.

	Reference [a]	Rich- split	Inter-heating	Combined process
Technical performance				
Heat transfer area of main HeatX, m^2	46,300	25,300	46,300	37,500
Heat transfer area of inter-heater, m^2	-	-	3,100	1,900
Condenser duty, GJ/ton CO_2	1.45	0.36	1.16	0.24
Reboiler temperature, °C	145.7	145.7	145.7	145.5
Reboiler duty, GJ/ton CO_2	3.27	2.88	3.00	2.46
Reboiler duty, MW	-100.1	-87.4	-91.6	-75.3
Total energy penalty, MW	-150	-137.3	-141.6	-125.3
Capital cost performance (one process train)				
Stripper reboiler	2,209,963	1,533,686	1,586,940	1,310,024
Stripper condenser	423,018	106,000	338,950	106,000
Rich/lean heat exchanger [b]	13,536,100	7,727,700	17,481,600	11,664,300
Lean solvent cooler	460,712	669,700	475,100	537,800
Inter-heating heat exchanger	-	-	889,400	546,000
Inter-heating pump	-	-	225,800	225,800
Changes of capital cost	0	-6,592,707	4,367,997	-2,239,869
Economic performance				
Capital cost, million $	800.0	733.6	843.9	777.4
LCOE, $/MWh	115.2	110.0	114.8	109.0
CO_2 avoided cost, $/ton CO_2	62.9	55.2	62.2	53.2

Note: [a] the reference case is based on two-stage absorption; [b] the temperature difference between solvent in and out of stripper is 10 K.

Most importantly, this advanced configuration significantly reduces the reboiler duty and the subsequent energy consumption by 12.7 MW. In addition, the rich-split process is easy to operate in a practical process as it does not increase plant complexity. As a result, the application of the rich-split process is shown to enable a saving of $4.2/MWh of LCOE and a saving of $7.7/ton of CO_2 avoided cost.

7.4.2.2 Inter-heating process

The stripper inter-heating process makes better use of high-quality, high-temperature heat in the hot lean stream. This particular process can reduce the reboiler duty from

3.27 to 3.0 MJ/kg CO_2 and the condenser duty from 1.45 to 1.16 MJ/kg CO_2. This accordingly reduces the sizes and the capital costs of the stripper reboiler and condenser. However, to realise and maximise the energy saving of the inter-heating process, extra equipment, such as an inter-heating exchanger and pump and an advanced rich/lean cross heat exchanger with a larger heat transfer area, is required. This will result in a capital investment increase of US$ 43.9 million compared to the reference case. However, the inter-heating process reduces the reboiler duty by 8.3% and enables a 8.4 MW reduction in electricity consumption. The benefit from this energy saving outweighs the disadvantages of the capital cost increase and leads to saving LCOE by $0.4/MWh and CO_2 avoided cost by $0.7/ton CO_2.

7.4.3 Combination of three process improvement

As aforementioned, all of the three process modifications have positive influences on the technical and economic performance of the NH_3-based CO_2 capture process. The two-stage absorption reduces the chilling duty and capital cost of the NH_3 recycle system due to the decrease in the NH_3 emission; the rich-split process significantly decreases the regeneration duty via the recovery of steam heat and reduces the capital cost of the cross heat exchanger, stripper reboiler and condenser; the stripper inter-heating process reduces the reboiler duty by utilising the heat in the hot lean solvent and brings some cost benefits. The combined process is proposed with a view to integrating these advantages.

As shown in Table 7-10, the application of the three process modifications brings significant improvements to both the technical and economic performances. Technically, the modified NH_3 process enables a 31.7 MW electricity saving due to the significant reduction in the reboiler duty and chilling duty, which is a 20.2 % reduction of total energy consumption involved in the capture process. Economically, this combined process leads to a decrease in the capital investment of PCC plant from 832.8 million to 810.7 million USD, reducing the LCOE from $118.0/MWh to $109.0/MWh. Consequently, the CO_2 avoided cost is reduced from $67.3/ton to $53.2/ton. This is a saving of $14.1/ton CO_2 in the CO_2 avoided cost compared to the baseline NH_3 process. It is worth mentioning that the complexity of a PCC plant is increased by the application of these advanced process configurations, which appends an inter-cooling heat exchanger to the absorber and an inter-heating heat exchanger to

the stripper. However, the increased plant complexity is considered to be affordable because of the significant savings in energy consumption and the CO_2 avoided cost.

7.5 Techno-economic prospects of the NH_3 process

The sensitivity analysis is undertaken to understand how the LCOE and CO_2 avoided cost would be apportioned to the parameters involved in the cost calculation. The sensitivity studies are divided into two parts: economic assumptions and technical-driven parameters. The economic variables include the capacity factor of a power station, the discounted rate and the capital investment of PCC plant and coal cost, while the technical-driven parameters include the regeneration duty, energy compression duty and solvent cost, which, if improved by technology breakthroughs, could decrease the cost of the CO_2 avoided.

7.5.1 Sensitivity analysis of economic assumptions

As the LCOE and CO_2 avoided cost are heavily reliant on economic assumptions, a sensitivity analysis is undertaken to characterize the effect of some key economic parameters on the economic performances of the modified NH_3-based CO_2 capture process. Figure 7-6 shows the sensitivity of the LCOE and CO_2 avoided cost as a function of the economic parameters: the capacity factor of a power station (50%-100%), the discount rate (4%-12%), the capital cost of a PCC plant (-50% - +50%) and the coal price (-50% - +50%). The conditions at the starting point are an 85% capacity factor of a power station, an 8% discount rate, US$ 777.4 million of capital investment and US$2/GJ in coal costs. The LCOE and CO_2 avoided costs at the starting point are $109.0/MWh and $53.2/ton CO_2, respectively.

As shown in Figure 7-6, the capacity factor of a power plant has the largest impact on the LCOE and CO_2 avoided costs. When the capacity factor decreases to 50%, the LCOE increases to $161.2/MWh and a subsequent more-than-double cost of $128.2/ton CO_2 avoided. The decline in the capacity factor means a decrease in the electricity generated by the power station, which forces the electricity to be sold at a high price in order to compensate for the capital investment and the energy consumption of the PCC plant. This indicates that a power station is better operated at high capacity so as to ensure relatively low LCOE and CO_2 avoided costs.

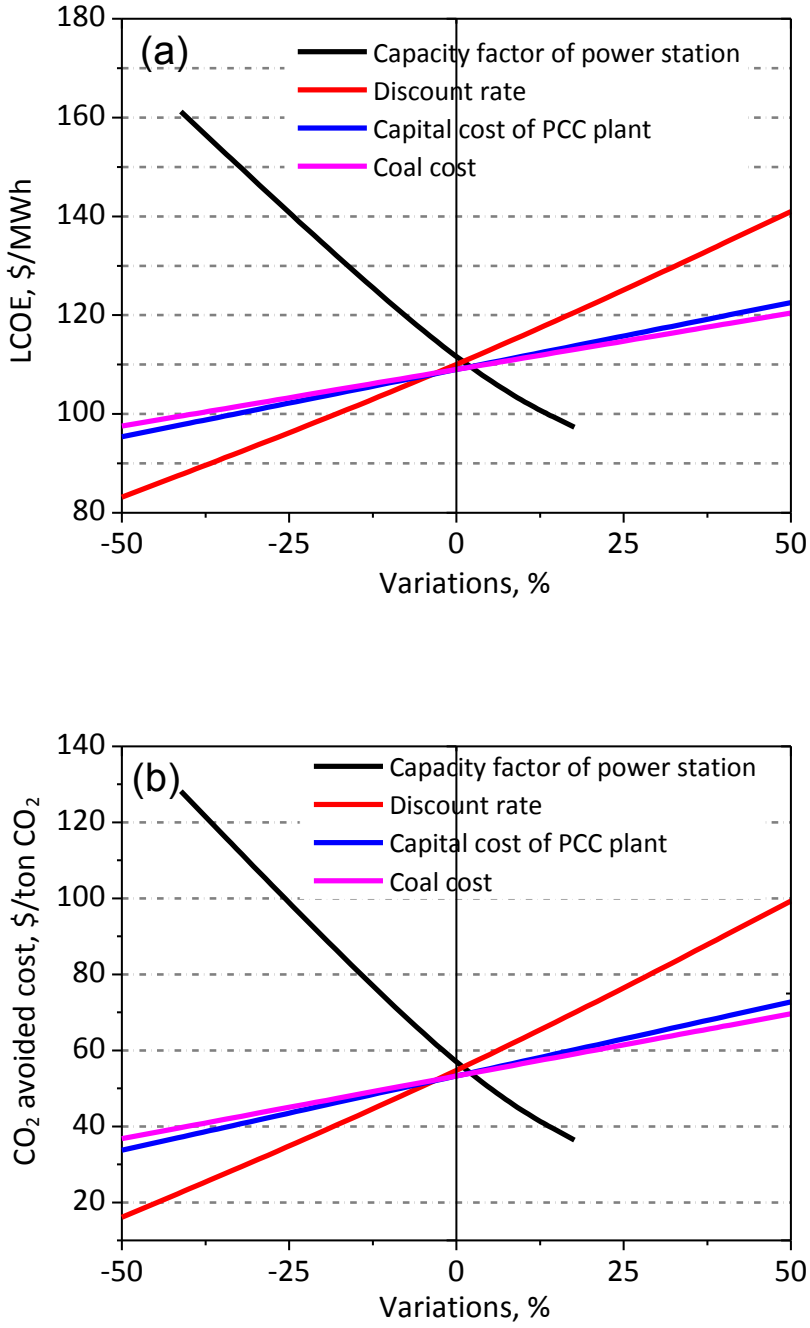

Figure 7-6 Sensitivity of (a) LCOE and (b) CO_2 avoided cost as functions of the economic parameters

The second sensitive factor is the discounted rate. If the rate increases from 4% to 12%, the CO_2 avoided cost increases greatly from \$16.1 to \$99.3/ton CO_2 (-70% to +86%). Thus the PCC project is most important in securing a favourable discounted cash flow rate to ensure a low carbon capture price, for example through government support and guarantees. The capital investment of PCC plant and coal prices have a moderate

influence on the overall economics of LCOE and CO_2 avoided cost. If the capital cost and the coal price varied by ± 50%, the CO_2 avoided cost would change to a range of US$33.7–72.7/ton CO_2 (± 37%) and US36.8–69.7/ton CO_2 (± 31%), respectively.

7.5.2 Sensitivity analysis of technical parameters

Figure 7-7 shows the technical outlook on the reduction of LCOE and CO_2 avoided cost as functions of technology improvements in the NH_3-based CO_2 capture process.

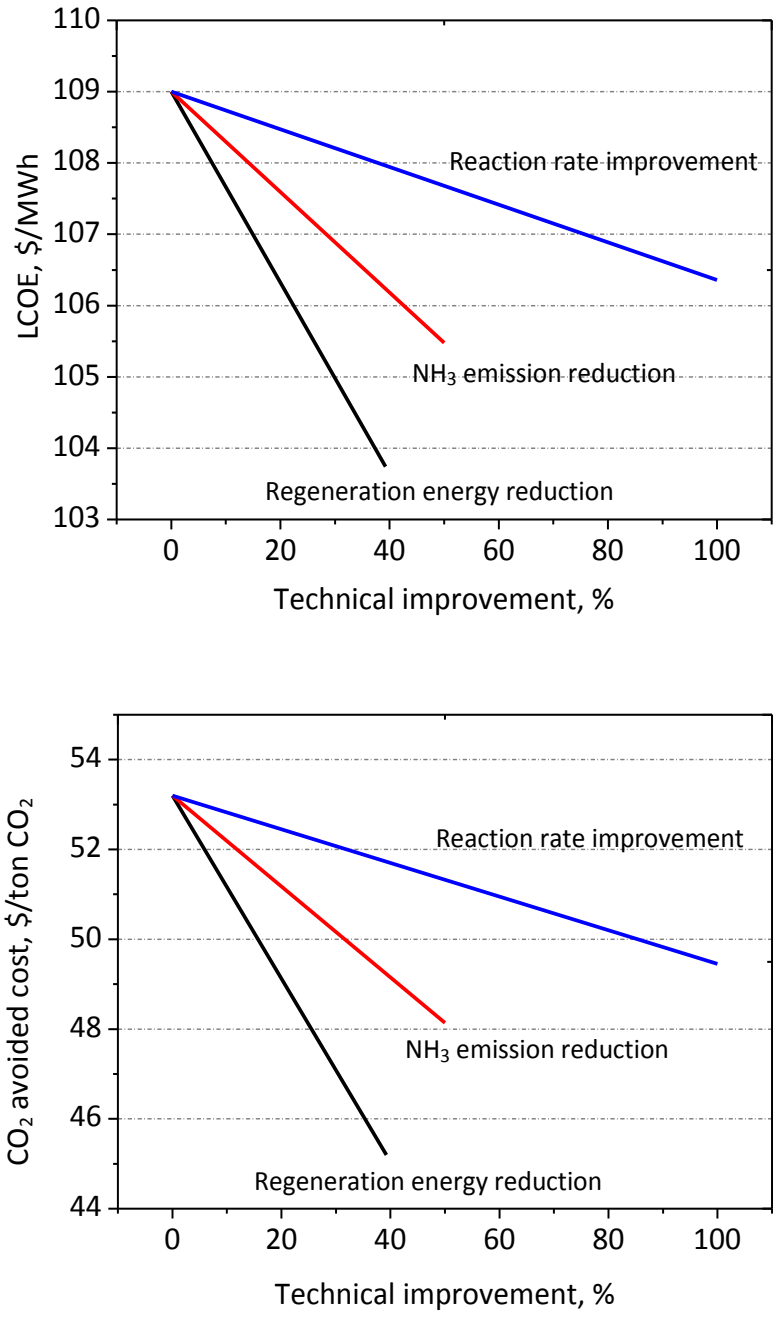

Figure 7-7 Sensitivity of LCOE and CO_2 avoided cost as functions of technical improvements.

As pointed out by Versteeg et al. (2011), the NH_3-based CO_2 capture process is a less mature technology than the amine-based capture process. Issues that are associated with NH_3 based CO_2 capture process include the low reaction rate, high NH_3 slip and relatively high regeneration duty. Most work is dedicated to improving the performances of these shortages from technical a viewpoint; little research has ever linked the technical advancement with the economic performance in the NH_3-based CO_2 capture process. This section discusses the potential benefits if technical performance is improved. It is worth mentioning that the percentage of technical improvements in Figure 7-7 means that the regeneration duty decreases from 2.47 MJ/kg CO_2 to 1.60 MJ/kg CO_2 (35.2% of technical improvement); the NH_3 emission level decreases from 12,000 ppmv to 6,000 ppmv (50% of technical improvement); the CO_2 absorption rate increases by double and reduces half of the absorber packing materials (100% of technical improvement). The LCOE and CO_2 avoided cost of the starting point are \$109.0/MWh and \$53.2/ton CO_2, respectively.

7.5.2.1 Reduction of regeneration duty

It can be seen that the solvent regeneration duty is the most sensitive factor that should be a top priority for reduction in order to advance the NH_3 process. As pointed out by Goto et al. (2013), an approximate 2% improvement in power station net efficiency can be achieved by decreasing 1 MJ/kg CO_2 of the regeneration duty. Although the modified NH_3 process in this study has provided an already low reboiler duty of 2.47 MJ/kg CO_2, more advanced process improvements are likely to further reduce the energy consumption of solvent regeneration. Theoretically, the heat of the CO_2 desorption in the NH_3 regeneration process ranges from 0.65 MJ/kg CO_2 to 1.6 MJ/kg CO_2 (Jilvero *et al.*, 2012; McLarnon *et al.*, 2009) when dependent on the solvent compositions such as NH_3 concentration and CO_2 loading. There is considerable room to decrease the energy penalty of the regeneration process through the improvements of the NH_3 process that are undertaken to reduce the sensible heat and vaporisation heat. If the regeneration duty is decreased to 1.6 MJ/kg CO_2, the LCOE and CO_2 avoided cost would be reduced to \$103.7/MWh and \$45.2 /ton CO_2, respectively. It is worth mentioning that the reduction in energy consumption is not isolated from the process itself, and is likely to occur at the expense of increased capital cost, expensive solvent and greater O&M costs. The cost reduction of CO_2 avoided will not be as significant as the result from the sensitivity analysis in the present study. However,

due to the large cost sensitivity of energy consumption, reducing the energy penalty should be the top priority in the development of NH_3 technology.

7.5.2.2 Mitigation of NH_3 emission

Due to its intrinsic property of volatility, NH_3 emission is another important factor that influences the cost performance. It is suggested that NH_3 inhibitors be introduced into the NH_3 solution. The author introduces the transition metal ions (Ni^{2+}, Cu^{2+}, Zn^{2+}) into the NH_3 solution and reduces NH_3 vaporisation by 20-40% through the complexation of metal ions and NH_3 ligand (for details refer to Appendix C). Yu et al. (2013) added the NH_3 suppressant of propylene carbonate to mitigate NH_3 vaporisation by 38% through the interaction of physical-chemical hydrogen bonding. If the NH_3 emission level is mitigated from 12,000 ppmv to 6,000 ppmv by adding NH_3 suppressants, without deteriorating the CO_2 absorption performance, the CO_2 avoided cost would be reduced to \$48.1/ton CO_2 due to the significant reduction in the capital cost and a decrease in the chilling duty in the NH_3 recycling unit.

7.5.2.3 Improvement of CO_2 absorption rate

The enhancement of the CO_2 absorption rate has the slowest response to the LCOE and CO_2 avoided cost. However, this does not mean that less attention should be paid to the CO_2 absorption rate. In contrast, it is suggested that major effort should be dedicated to the improvement of the CO_2 reaction rate. Experimental work has suggested that the CO_2 reaction rate of the NH_3-based CO_2 capture process is 2-10 times slower than that of the MEA-based CO_2 capture process (Darde *et al.*, 2011b; Qin *et al.*, 2010b). Some research has been conducted into improving the CO_2 absorption rate by way of adding some rate promoters. Fang et al. (2014) experimentally screened six different additives for the promotion of the CO_2 reaction rate and revealed that MEA and piperazine are able to significantly increase the mass transfer coefficient of CO_2 into aqueous NH_3 3-4 times. Yang et al. (2014) investigated the potassium sarcosinate promoted aqueous NH_3 solution and found that the sarcosine has the potential to quadruple the CO_2 absorption rate. If the CO_2 absorption rate can be doubled by rate promoters without impacting the regeneration duty, the CO_2 avoided cost would be reduced to \$49.4/ton CO_2 due to the reduction of the capital cost in the CO_2 absorber.

If the ideal scenario is achieved, that is, the regeneration duty is reduced to 1.6 MJ/kg CO_2; the NH_3 emission level is decreased to 6,000 ppmv; the CO_2 absorption rate is improved to compete with MEA; and the LCOE has the potential to be reduced to \$98.1/MWh, resulting in a \$37.1/ton of CO_2 avoided. This is an approximate 45 % cost reduction compared to the baseline NH_3 process, which implies that the NH_3-based PCC process has considerable room to be further advanced and improved in its commercial attractiveness.

7.6 Summary

The part A study has evaluated the technical and economic performances of the baseline NH_3-based CO_2 capture process when integrated with a 650 MW coal fired power station. A rigorous technical model and a comprehensive cost model are proposed to conduct the techno-economic studies of the baseline NH_3-based PCC process. The techno-economic performance of a baseline MEA-based CO_2 capture process is also carried out and used as a reference to the NH_3 process. The results of the equipment costs, total capital costs and the CO_2 avoided cost are compared with the proposed model, the commercial Boundary Dam project and published results, and the satisfactory agreements indicate that the proposed economic model is valid and adequate for an estimation of the economic performance of the MEA-based as well as the NH_3-based CO_2 capture process. For the baseline NH_3 process, the capital investment of the PCC plant is 832.8 million 2013 US dollar. The integration of a PCC plant with a coal-fired power station increases the LCOE from \$71.9/MWh to \$118.0 /MWh, resulting in a CO_2 avoided cost of \$67.3/ton. The cost is economically advantageous over the conventional MEA process of \$86.4/ton of CO_2 avoided.

In part B, the advanced process configurations of two-stage absorption, a rich-split process and stripper inter-heating are introduced to improve the technical and economic viability of the NH_3-based capture process. The results suggest that all three process modifications are technically and economically feasible for reducing the CO_2 avoided cost. The two-stage absorption reduces the US\$ 32.8 million of capital cost due to the decrease of NH_3 emission, resulting in a saving of \$4.4/ton of CO_2 avoided. The rich-split process enables an energy saving of 12.7 MW and a capital saving of US\$ 64.4 million, leading to a saving of \$7.7/ton of the CO_2 avoided cost. Although an inter-heating application increases the capital investment of US\$ 43.9 million, the energy saving of 8.4 MW outweighs the disadvantages of capital cost increase, leading

to a saving \$0.7/ton of CO_2 avoided. The combined process integrates the advantages of the three process modifications, which reduces the energy consumption by 20.2% and decreases the LCOE from \$118.0/MWh to \$109.0/MWh. Consequently, the CO_2 avoided cost is reduced from \$67.3/ton to \$53.2/ton CO_2 avoided. This is a saving of \$14.1/ton CO_2 of the CO_2 avoided cost compared to the baseline NH_3 process.

A sensitivity analysis is performed to understand how the CO_2 avoided cost would be apportioned to the economic and technical parameters. The sensitivity study on economic parameters suggests that the plant capacity factor and discount rate are the most two important factors. A high capacity factor of a power station and a guaranteed low discount rate are very significant in ensuring a relatively low cost of CO_2 avoided. Technical prospects regarding the improvements of NH_3-based PCC process are proposed to provide the technical research directions. The results suggest that there is considerable room to further advance the NH_3 process via the reduction of regeneration energy consumption, the mitigation of NH_3 slip and the improvement in the CO_2 absorption rate. Overall, the economic factors are more sensitive to the technical factors, and it is suggested that more attention be paid to the overall evaluation of the NH_3 process, both technically and economically. The resulting cost performance can be widely observed, such as in technologies assessments, CCS legislation and regulations, policy analysis and government decision-making.

Chapter 8 Conclusions and Recommendations

8.1 Conclusions

This thesis focuses on the development and advancement of an NH_3-based CO_2 capture process that will significantly reduce CO_2 emissions from coal-fired power stations. The previous pilot plant trials carried out by the CSIRO revealed some issues relating to the NH_3-based process, such as high NH_3 loss, intensive energy consumption, etc. The objectives of this study are to tackle these identified drawbacks in order to make the NH_3 process technically feasible and economically viable. A rigorous rate-based model is developed and validated to simulate the behaviours and characteristics of CO_2/SO_2 absorption along a packed column, and advance the technical and energy performance of the NH_3-based CO_2 capture process. The comprehensive modelling study has demonstrated the significant technical improvements of the NH_3 process by way of the effective process design and advanced absorber/stripper configurations. A comprehensive economic model is proposed in order to simulate the economic performance of the NH_3-based CO_2 capture process. The economic analysis indicates that the NH_3 process has better economic viability than the benchmarking MEA solvent and that the economic performance can be greatly enhanced by the process improvements. This chapter draws the primary conclusions obtained from this work and presents some recommendations on the further technical and economic advancement of the NH_3-based CO_2 capture process.

8.1.1 Model development

A rigorous, rate-based model is developed for the simultaneous capture of CO_2 and SO_2 by aqueous NH_3 using the commercial software Aspen Plus®. The model is thermodynamically and kinetically validated against the experimental results, including those from open literature and CSIRO pilot plant trials, respectively. It is demonstrated that the developed model can accurately predict the thermodynamic characteristics of the NH_3/CO_2/SO_2/H_2O system and the kinetic behaviours of the CO_2/SO_2 absorption by aqueous NH_3 along the packed column, which allows for the established rate-based model to reliably and practically guide the process simulation of CO_2 capture and SO_2 removal in the NH_3-based capture process.

8.1.2 Advanced NH_3 abatement and recycling process

A simple but effective process for NH_3 abatement and recycling is proposed by way of the installation of an NH_3 absorber and by maximally utilising the waste heat in flue gas. Using the rate-based model, it is demonstrated that the advanced process design can successfully solve the problems of NH_3 slip and flue gas cooling in the NH_3-based CO_2 capture process, as it provides the following technical and environmental advantages: (i) a simplified NH_3 abatement system; (ii) over 99.5% of NH_3 recycling efficiency; (iii) low NH_3 emissions of 15.2 ppmv; and (iv) low energy consumption of 59.34 kJ/kg CO_2 electricity by making use of flue gas waste heat.

8.1.3 Combined SO_2 removal and NH_3 recycling process

Based on the NH_3 recycling system, an advanced process that simultaneously removes SO_2 and CO_2 and recycles slipped NH_3 is developed. The modelling results highlight many benefits that arise from the combined SO_2 removal and NH_3 recycling process; i.e. >99.9% SO_2 scrubbing efficiency, >99.9% NH_3 reuse efficiency and a low energy requirement. The proposed process can deal with a wide range of SO_2 concentrations in the flue gas, NH_3 content from the CO_2 absorber and flue gas temperature, indicating its adaptability and viability for the variable scenarios in real industrial applications. Moreover, this advanced process simplifies FGD, which will significantly reduce the capital cost of a SO_2 removal facility.

8.1.4 Technical and energy assessment of the NH_3-based CO_2 capture process

An advanced NH_3-based CO_2 capture process integrated with a 650 MW coal-fired power plant is investigated to evaluate the technical feasibility and energy performance of the overall capture process. The process parameters of the NH_3 process are optimised through a sensitivity study and include 25 °C lean solvent, 6.8 wt% NH_3, 0.25 CO_2 lean loading and 10 bar stripper pressure. The process modifications of a rich-split and inter-heating process are introduced to reduce the energy consumption. The material balance of NH_3, CO_2 and H_2O in the entire capture process is maintained. After process optimization and modification, the regeneration duty of the advanced NH_3 process is reduced to 2.46 MJ/kg CO_2, leading to a net efficiency penalty of 8.0 %, which is lower than that in MEA process and modified CAP. This indicates that the advanced NH_3-based CO_2 capture process is technically competitive in terms of energy consumption and operational feasibility.

8.1.5 Economic assessment of the NH_3-based CO_2 capture process

Based on technical performance, the NH_3-based CO_2 capture processes with and without process improvements that are integrated with a 650 MW coal fired power station are investigated to evaluate their economic performances. A comprehensive cost model based on the Aspen Capital Cost Estimator is used to calculate the capital cost and evaluate the economic performance of the NH_3 processes. The economic model is proven to be valid and adequate for the estimation of economic performance by comparing published results such as equipment cost, total capital investment and CO_2 avoided cost. For the baseline NH_3 process, the capital investment of the PCC plant is estimated to be $832.8 million in 2013 US dollar. The integration of a PCC plant with a coal-fired power station increases the LCOE from $71.9/MWh to $118.0 /MWh, resulting in a CO_2 avoided cost of $67.3/ton, which is competitive with the traditional MEA process of $86.4/ton. Compared with the baseline NH_3-based CO_2 capture process, the process improvements of a two-stage absorber, rich-split and inter-heating can significantly reduce the energy consumption by 31.7 MW (20.2% reduction) and the capital investment by US$ 55.4 million (6.7% reduction). The LCOE decreases from $118.0/MWh to $109.0/MWh and the CO_2 avoided cost is reduced from $67.3/ton to $53.2/ton CO_2 avoided, which is a saving of $14.1/ton CO_2 in the CO_2 avoided cost compared to the baseline NH_3 process. This indicates that the advanced process configurations not only improve the technical and energy performance, but also increase the economic viability of the NH_3-based CO_2 capture process.

8.2 Recommendations

Sensitivity study has indicated the economic and technical directions that need to be taken towards the further development and advancement of the NH_3-based post combustion capture process. While the economic parameters are the complicated controlling factors which are heavily dependent on the CO_2 market, CO_2 emission regulation, government support and guarantee, etc., the technical improvement of the NH_3-based CO_2 capture process seems to be a practical perspective from the viewpoint of academic research and engineering. The following research work is recommended so as to gain a more comprehensive understanding and further advancement of the NH_3-based post combustion capture process.

1. Pilot plant trials should be carried out to demonstrate the technical and economic advantages of the combined SO_2 removal and NH_3 recycling process, and advanced process configurations such as two-stage absorption, rich-split and inter-heating. In return, pilot plant data can be used to re-validate the rate-based model enabling more accurate and reliable process simulations.
2. Pilot plant trials of the SO_2 removal process is required to better understand oxidation behaviours and produce the sulphur-containing fertilizers.
3. Reduction of regeneration energy via a more advanced stripper configuration is required to reduce the irreversible energy loss during the CO_2 stripping process, such as sensible heat and steam heat and/or the catalyst to reduce the heat of desorption.
4. Reduction of NH_3 loss is necessary by introducing advanced absorber configuration, such as multi-stage absorption and/or adjusting the absorption temperature dependent on the cooling source, and/or introducing NH_3 inhibitor into the solvent
5. Improvement of the CO_2 absorption rate may be considered via the addition of rate promoters, which can significantly enhance the absorption performance, but not adversely affect NH_3 vaporisation and energy consumption.

Appendix A: Rate-based Model Development for the MEA-based CO_2 Capture Process

This appendix introduces the information that relates to the rate based model for the MEA-based capture process used to support this thesis. More detailed descriptions of the model development and MEA process improvement can be found in the following published paper:

Kangkang Li, Ashleigh Cousin, Hai Yu, Paul Feron, Moses Tade, Weiliang Luo, Jian Chen. Systematic study of aqueous monoethanolamine-based CO_2 capture process: model development and process improvement. Energy Science & Engineering, 2015, 1-17. DOI: 10.1002/ese3.101

Model description

Table A-1 lists the electrolyte solution chemistry of the MEA-CO_2-H_2O system, taking into account the equilibrium and kinetic reactions.

Table A-1 Chemical reactions in the MEA-CO_2-H_2O system

No.	Type	Reactions
1	Equilibrium	$2H_2O$ <--> $H_3O^+ + OH^-$
2	Equilibrium	$CO_2 + 2H_2O$ <--> $H_3O^+ + HCO_3^-$
3	Equilibrium	$HCO_3^- + H_2O$ <--> $CO_3^{2-} + H_3O^+$
4	Equilibrium	$MEAH^+ + H_2O$ <--> $MEA + H_3O^+$
5	Kinetic	CO_2 + OH- --> HCO_3^-
6	Kinetic	HCO_3^- --> $CO_2 + OH^-$
7	Kinetic	$MEA + CO_2 + H_2O$ --> $MEACOO^- + H_3O^+$
8	Kinetic	$MEACOO^- + H_3O^+$ --> $NH_3 + CO_2 + H_2O$

The commercially available Aspen Plus® software is used to simulate the MEA-based CO_2 capture process. The electrolyte NRTL (Non-Random Two-Liquid) method and RK (Redlich–Kwong) equation of state are used to compute liquid properties (activity coefficient, Gibbs energy, enthalpy and entropy) and vapour properties (fugacity coefficients) of the model MEA-CO_2-H_2O system, respectively. This electrolyte

NRTL model has been validated to accurately predict the vapour-liquid equilibrium, aqueous speciation, heat capacity, CO_2 absorption enthalpy of the MEA–H_2O–CO_2 system with a wide application range: MEA concentration up to 40 wt%, CO_2 loading up to 1.33, temperature up to 443 K and pressure up to 20 MPa. These conditions cover all the conditions used in the pilot plant and simulations studied. The gases CO_2, N_2 and O_2 are selected as Henry-components to which Henry's law is applied. The Henry's constants, transport and thermal properties of the MEA-CO_2-H_2O system are retrieved from the Aspen Plus databanks, which have been proven to accurately describe the physical and transport characteristics based on experimental data.

Rate-based modelling

The rate-based model validation of the CO_2 capture process using aqueous MEA is carried out based on the Tarong pilot plant configuration as shown in Figure A-1.

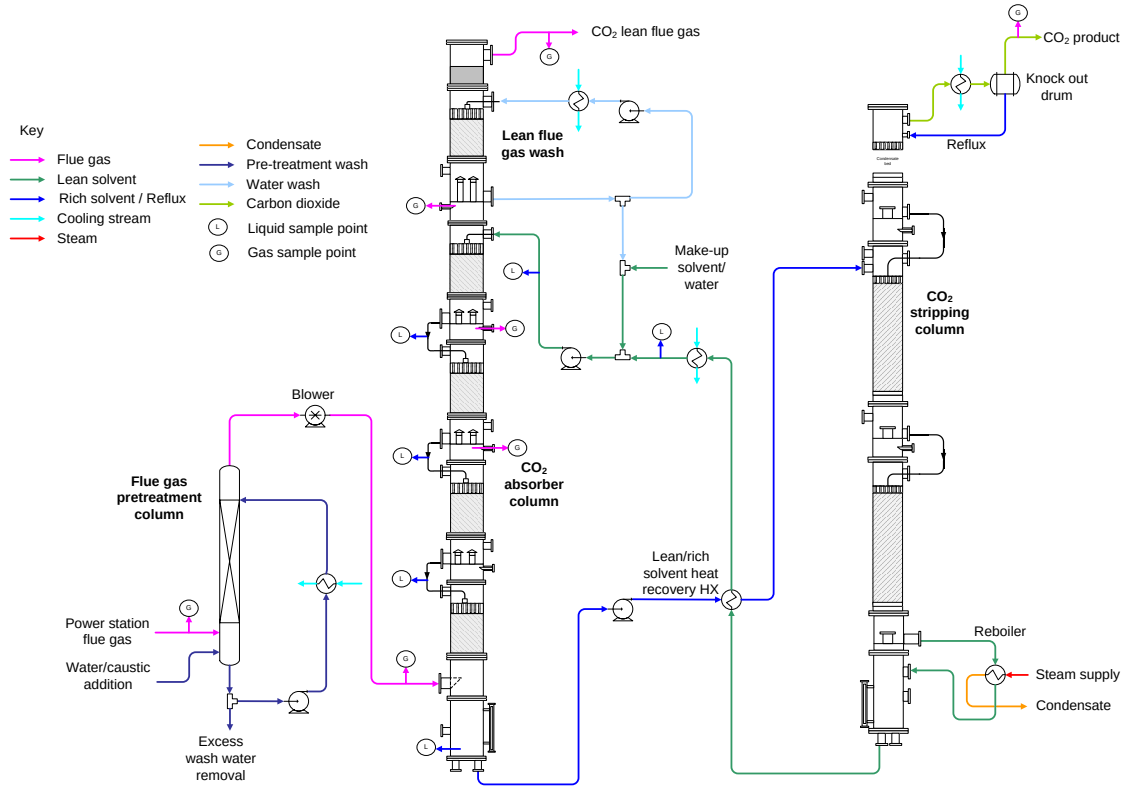

Figure A-1 Process flow-sheet of Tarong CO_2 capture pilot plant

The RateSep simulator embedded in Aspen Plus is used to simulate the aqueous MEA-based CO_2 capture process. In order to reflect the actual pilot MEA process, the rate-based model uses the same column parameters as the pilot plant, such as packing material, column diameters and packed heights. Table A-2 lists the column parameters

of both the CO_2 absorber and CO_2 stripper, together with the primary correlations and settings of the rate-based absorber/stripper model. The interfacial area factor is adjusted from 1.0 to 2.0 to provide a good agreement between experimental and simulation results. The value 1.8 is chosen due to the excellent agreement between the experimental and simulation results. This is shown by average relative error deviations between experimental and simulation results of 2.7% for CO_2 rich loading, 5.8% for CO_2 absorption rate, 1.3% for reboiler temperature, 0.3% for CO_2 purity and 4.0% for regeneration energy. Given the 10% uncertainty associated with the comparison between predicted and pilot results, the proposed rate-based model enables a reasonable prediction of the CO_2 absorption and desorption process. Details are discussed further in the next section.

Table A-2 Summary of model parameters and column settings

model and column properties	Absorber	Desorber
Number of stages	20	20
Packing material	Mellapak M250X	Mellapak M350X
Total packed height	7.136 m (4 × 1.784m)	7.168 m (2 × 3.584m)
Column diameter	350mm	250mm
Flow model	Mixed model	Mixed model
Interfacial area factor	1.8	1.8
Initial liquid holdup	0.03L	0.03L
Mass transfer correlation method	Bravo et al. (1985)	Bravo et al. (1985)
Heat transfer correlation method	Chilton-Colburn	Chilton-Colburn
Interfacial area method	Bravo et al. (1985)	Bravo et al. (1985
Liquid holdup correlation	Bravo et al. (1992)	Bravo et al. (1992)

Model validation against Tarong pilot plant results

The CO_2 capture process using aqueous MEA in the Tarong PCC pilot plant consists of two major parts: absorption process and desorption process. Accordingly, the rate-based modelling for the MEA process is carried out through the validation of the packed absorber column and stripper column, respectively. Table A-3 summarises the operating conditions and pilot results of both the CO_2 absorber and CO_2 stripper, together with the simulation results based on the conditions of the 22 pilot plant trials.

Table A-3 Comparison between pilot plant trials and rate-based model simulation results under a variety of experimental conditions

Test Date (2011)	01 Feb	03 Feb	07 Feb	11 Feb	22 Mar	24 Mar	25 Mar	30 Mar	04 Apr	05 Apr	13 Apr
Test conditions of CO_2 absorption											
Lean temp. ˚C	31.7	31.4	31.3	35.5	33.9	34.8	35.3	33.5	32.4	37.5	35.6
Lean flow rate, l/min	31.7	32.0	27.0	31.3	26.9	33.0	35.8	32.0	24.0	24.4	32.0
Lean MEA conc., wt%	25.1	24	27.9	25.5	31.6	29.6	29.2	30.3	33.5	34.0	29.3
Lean CO_2 loading, mol/mol	0.279	0.294	0.284	0.280	0.314	0.333	0.347	0.316	0.254	0.278	0.414
Inlet flue gas temp. ˚C	51.7	50.5	48.1	51.3	53.6	54.2	55.8	65.5	66.1	63.9	49.8
Inlet gas pressure, kPa-a	106.1	105.6	106.3	106.6	107.5	107.3	107.3	107.3	108.7	108.3	107.2
Inlet flue gas flow rate, kg/hr	489.6	491.1	488.6	489.4	482.8	483.9	484.8	483.2	646.1	644.4	487.5
Inlet flue gas CO_2 vol%	11.9	11.8	11.8	12.1	13.4	13.5	13.5	12.8	12.9	13.2	12.7
Inlet flue gas H_2O vol%	4.2	5.0	3.8	3.9	4.3	4.0	3.9	3.6	4.3	4.1	3.8
Test conditions of CO_2 desorption											
Condenser Temp. ˚C	30.2	29	26.2	29.6	32.0	29.9	29.4	25.4	26.9	24.8	28.8
Stripper top pressure, kPa-a	181.9	180.4	177.5	189.9	189.2	195.0	195.5	191.5	223.3	222.1	151.8
Temp. difference [a], K	16.7	16.9	18.5	17.4	21.0	20.0	19.8	19.0	23.8	25.6	17.6
CO_2 desorption rate, kg/hr	71.6	71.0	70.6	73.6	72.6	76.8	76.7	76.0	93.9	94.2	49.3
Results comparison of pilot plant and simulation											
Expt. rich CO_2 loading, mol/mol	0.466 ±0.007	0.480 ±0.005	0.469 ±0.004	0.471 ±0.001	0.481 ±0.001	0.486 ±0.004	0.488 ±0.002	0.494 ±0.007	0.494 ±0.001	0.489 ±0.003	0.525 ±0.003
Simu. rich CO_2 loading, mol/mol	0.491	0.497	0.493	0.493	0.509	0.499	0.496	0.490	0.504	0.505	0.502
Expt. CO_2 abs rate, kg/hr [b]	73.5±1.4	74.2±1.6	72.3±1.6	74.4±1.6	74.2±1.7	77.8±1.8	77.4±1.4	75.5±1.5	96.9±1.8	94.1±1.4	49.2±1.9
Simu. CO_2 abs rate, kg/hr	80.6	75.3	80.2	81.0	68.8	80.8	80.4	83.5	96.3	91.1	45.2
Expt. reboiler temp., ˚C	116.9±0.3	116.4±0.2	117.0±0.2	117.6±0.2	117.2±0.4	117.1±0.2	115.9±0.2	117.5±0.2	125.3±0.3	125.8±0.4	104.7±0.6
Simu. reboiler temp., ˚C	118.6	117.9	118.4	119.1	119.2	119.6	119.3	119.5	126.7	126.5	110.0
Expt. regen. energy, MJ/kg CO_2	4.48	4.45	4.35	4.50	4.33	4.51	4.60	4.49	4.01	4.04	4.55
Simu. regen. energy, MJ/kg CO_2	4.60	4.56	4.57	4.65	4.66	4.68	4.83	4.66	4.01	4.11	5.20
Expt. CO_2 product purity, vol%	97.7	97.7	97.8	97.7	97.6	97.8	97.8	98.0	98.9	99.0	98.1
Simu. CO_2 product purity, vol%	97.6	97.7	98.0	97.7	97.4	97.8	97.8	98.2	98.3	98.5	97.3

Continued

Test Date	19 Apr	20 Apr	11 May	12 May	13 May	18 May	20 May	24 May	25 May	26 May	27 May
Test conditions of CO_2 absorption											
Lean temp. ^oC	38.7	38.7	39.4	39.3	39.2	39.7	40.5	39.6	39.4	39.6	39.5
Lean flow rate, l/min	21.1	21.1	27.1	27.0	27.0	32.1	27.0	27.0	26.9	27.2	27.0
Lean MEA conc., wt%	32.3	32.8	29.2	29.2	28.9	26.2	27.4	28.1	28.3	28.5	28.5
Lean CO_2 loading, mol/mol	0.285	0.291	0.285	0.285	0.280	0.314	0.288	0.295	0.297	0.283	0.283
Inlet flue gas temp. ^oC	48.3	48.8	58.3	59.4	56.7	61.8	60.7	60.0	56.1	58.2	57.9
Inlet gas pressure, kPa-a	106.7	106.6	108.9	108.7	108.8	108.3	108.5	109.0	108.8	108.9	109.0
Inlet flue gas flow rate, kg/hr	485.5	487.5	598.7	598.4	597.2	598.0	597.2	596.8	596.0	598.5	597.8
Inlet flue gas CO_2, vol%	12.2	12.2	11.1	11.2	11.2	11.1	11.0	11.6	11.6	11.6	11.1
Inlet flue gas H_2O, vol%	3.9	3.9	5.2	5.3	5.0	5.5	5.4	5.5	5.1	5.2	5.2
Test conditions of CO_2 desorption											
Condenser Temp. $^\circ C$	24.7	23.9	19.2	20.4	18.2	20.7	19.8	19.4	17.6	18.6	17.0
Stripper top pressure, kPa-a	186.9	182.0	202.7	200.0	202.2	200.5	202.2	203.1	202.0	203.3	202.2
Temp. difference [a], K	18.6	18.5	18.3	18.8	18.8	17.4	19.6	18.9	19.4	19.2	18.7
CO_2 desorption rate, kg/hr	73.3	71.1	84.3	83.6	84.0	82.4	84.2	84.6	84.1	84.7	84.2
Results comparison of pilot plant and simulation											
Expt. rich CO_2 loading, mol/mol	0.486 ±0.001	0.500 ±0.001	0.488 ±0.001	0.488 ±0.001	0.491 ±0.002	0.499 ±0.005	0.503 ±0.001	0.511 ±0.006	0.512 ±0.001	0.492 ±0.001	0.492 ±0.006
Simu. rich CO_2 loading, mol/mol	0.506	0.506	0.500	0.500	0.501	0.499	0.501	0.503	0.504	0.502	0.503
Expt. CO_2 abs rate, kg/hr [b]	76.0±2.1	72.0±1.7	85.3±1.5	83.3±1.6	83.4±2.0	82.8±1.7	84.3±1.6	83.9±2.0	83.8±1.8	85.7±1.5	85.0±1.4
Simu. CO_2 abs rate, kg/hr	72.9	72.3	81.8	81.7	82.5	75.6	75.6	76.0	75.8	81.4	80.9
Expt. reboiler temp., $^\circ C$	119.9±0.3	118.7±0.3	121.5±0.2	121.1±0.4	121.2±0.3	119.9±0.1	121.7±0.3	121.3±0.3	121.1±0.2	121.4±0.3	121.6±0.2
Simu. reboiler temp., $^\circ C$	120.6	119.7	122.4	122.0	122.3	121.0	122.3	122.4	122.2	121.8	122.3
Expt. regeneration, MJ/kg CO_2	3.86	3.88	4.10	4.12	4.15	4.28	4.18	4.10	4.11	4.12	4.11
Simu. regeneration, MJ/kg CO_2	4.01	4.02	4.21	4.23	4.23	4.46	4.29	4.23	4.24	4.19	4.22
Expt. CO_2 product purity, vol%	98.5	98.8	99.4	98.7	99.4	99.2	99.4	99.0	99.1	99.3	99.5
Simu. CO_2 product purity, vol%	98.3	98.3	98.8	98.7	98.9	98.7	98.8	98.8	99.0	98.9	99.0

Note: [a] temperature difference of solvent in and out of stripper; [b] the difference of CO_2 mass flow rate across the CO_2 absorber

Validation of CO_2 absorption process: The CO_2 absorption rate is considered to be one of the most significant indicators for developing a reliable rate-based model, as it closely represents the reaction properties such as equilibrium and kinetic constants. Figure A-2 (a) shows the excellent match between model results and pilot plant data for a wide range of CO_2 absorption rates 40-100 kg/hr. The average relative error deviation for the 22 tests was 5.6%

Figure A-2 (b) shows the parity plot of CO_2 loading (mole ratios of CO_2/MEA) in the rich solvent after absorption between experimental and pilot results. It can be seen that the model gave a 2.7% overestimation on the rich CO_2 loading compared to the experimental data. This overestimation is likely caused by the samples being analysed offline. A small portion of the absorbed CO_2 is most likely lost during sample collection and measurement due to the high CO_2 partial pressure of the rich solvent samples. Overall, the predictions of CO_2 loading are considered satisfactory.

Figures A-2 (c) and A-2 (d) suggest that the experimental temperature has a good agreement with the simulation results, implying that the rate-based model is able to predict the temperature profile along the absorber column. However, it should be noted that the experimental temperatures along the column in Figure 2 (d) are always lower than the model data and the deviation is even greater at the high temperature sections at a packed height of 4-6m. This is most likely due to heat loss along the column wall during the CO_2 absorption process. Another possibility is that the solvent lost heat through the uninsulated pipe, whilst the solvent was removed from the column between the packed sections.

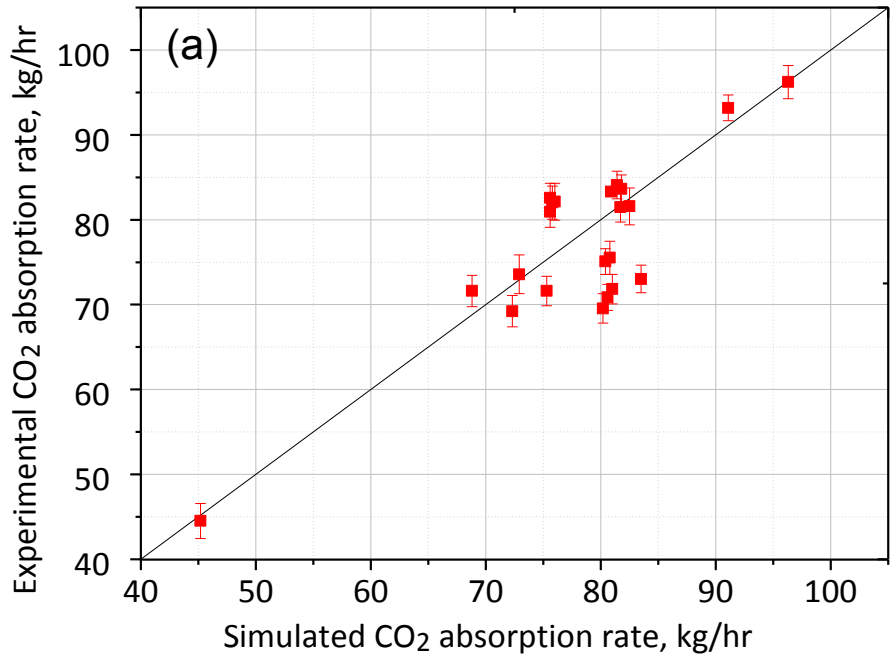
(a)
Experimental CO_2 absorption rate, kg/hr
Simulated CO_2 absorption rate, kg/hr
40
50
60
70
80
90
100

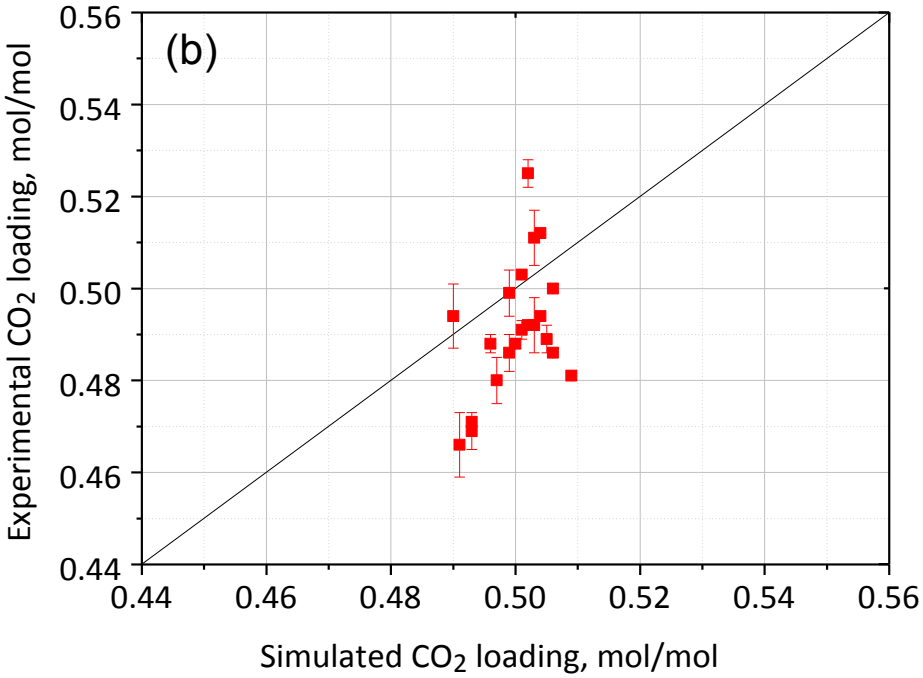
(b)
Experimental CO_2 loading, mol/mol
Simulated CO_2 loading, mol/mol
0.44
0.46
0.48
0.50
0.52
0.54
0.56

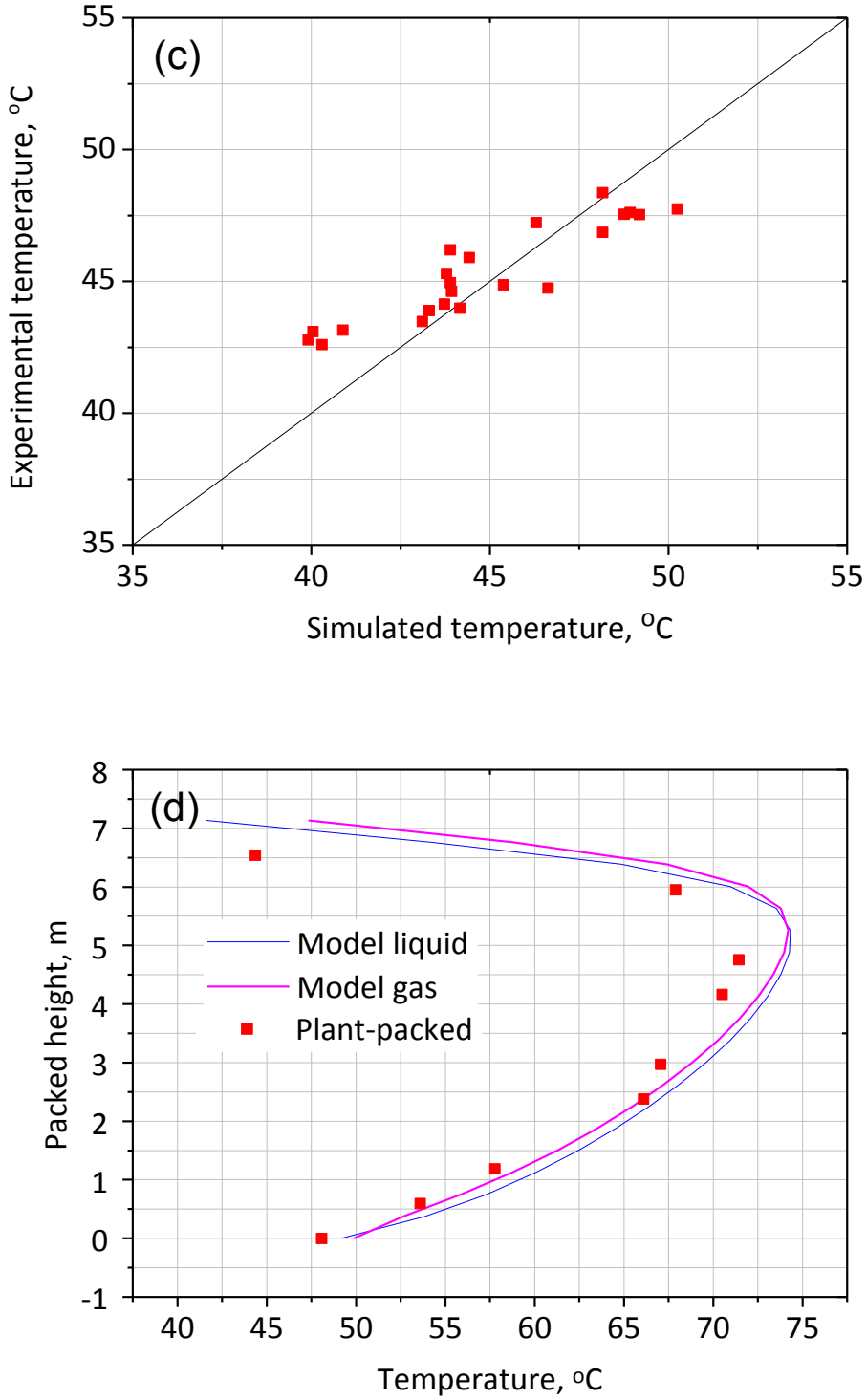

Figure A-2 Results of comparison between simulation and Tarong pilot plant measurements: (a) CO_2 absorption rate in absorber; (b) CO_2 loading of rich solvent leaving absorber; (c) temperature of rich solvent leaving absorber; and (d) temperature profiles along absorber column (01 Feb)

Validation of CO_2 stripping process: Figure A-3 (a) shows the parity plot of the stripper reboiler temperature between the simulation results and pilot plant data. It is found that the experimental values were consistently lower than those of the simulation because of the drastic heat loss in the high temperature stripper (90 ^oC-130 ^oC). This is demonstrated by the temperature profiles indicated in Figure 3(b). Heat loss is always occurring along the stripper column, which is reflected by the temperature deviation from the model results. It is worthwhile mentioning that the temperature deviation in the packed height 0-3.584 m (bottom section) is much larger than that in the height 3.584-7.168 m (top section), and that some temperatures in the bottom stage were surprisingly lower than those in the top stage. Two possible reasons can account for this phenomenon. One is the higher temperature in the bottom stage resulted in higher heat loss. The second is that heat loss took place from the solvent when being transported through the pipelines between the packed sections which are installed outside the stripper column (Figure A-1). This will have resulted in greater heat loss to the environment.

Due to the water vaporization at the high temperatures in the stripper, the CO_2 stream generated in the stripper may require further purification. Condensation is considered to be the effective approach to separating most of the water vapour from the CO_2 stream. In the pilot plant trials, the condenser temperature is controlled in the range of 17 ^oC-30 ^oC. This ensures a high purity of CO_2 product ranging from 97.5 vol% to 99.5 vol%, which meets the requirement for CO_2 compression. The simulation results in Figures A-3(c) and A-3(d) are in excellent agreement with the experimental results in terms of H_2O content and CO_2 concentration in the CO_2 product, which proves that the rate-based stripper model has the capability to predict the condensation process.

The experimental regeneration energy is calculated by summarising three key components: heat for stripping CO_2 from the solvent, sensible heat for heating solvent to the required desorption temperature and the water vapour leaving the stripper in the overhead gas stream. Due to the heat loss along the stripping column, the measured reboiler temperature in pilot trials would be always lower than the actual temperature (Figure A-3(a)), which results in the underestimation of sensible heat and the subsequent regeneration duty. While the model does not take the heat loss into account and uses the high modelling reboiler temperature to calculate the regeneration duty.

As a result, the simulated results of solvent regeneration duty have an average 4.0 % overestimation over the pilot plant results, as shown in Figure A-3 (e).

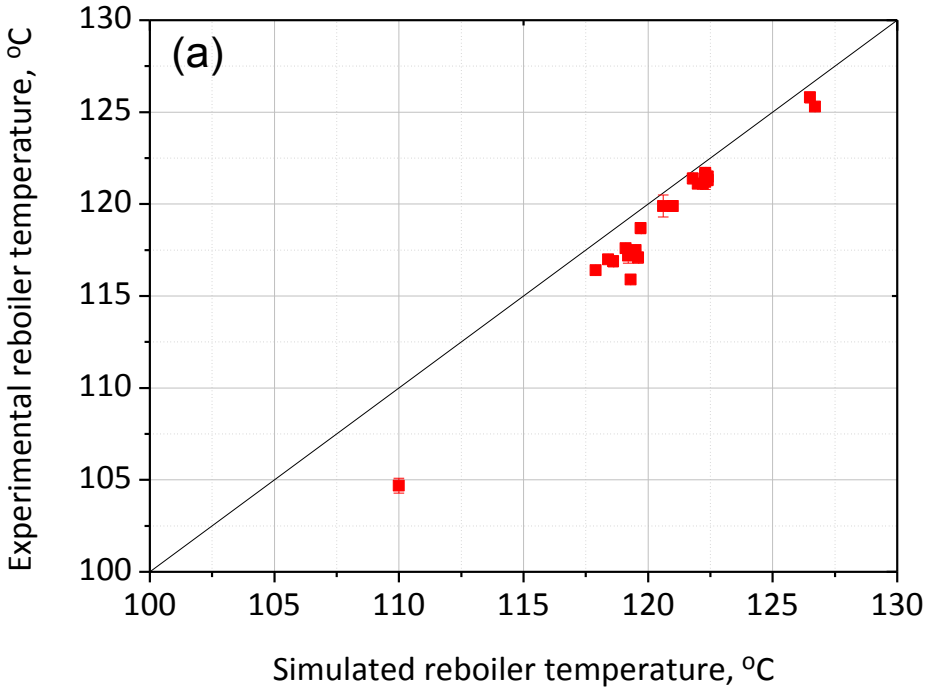

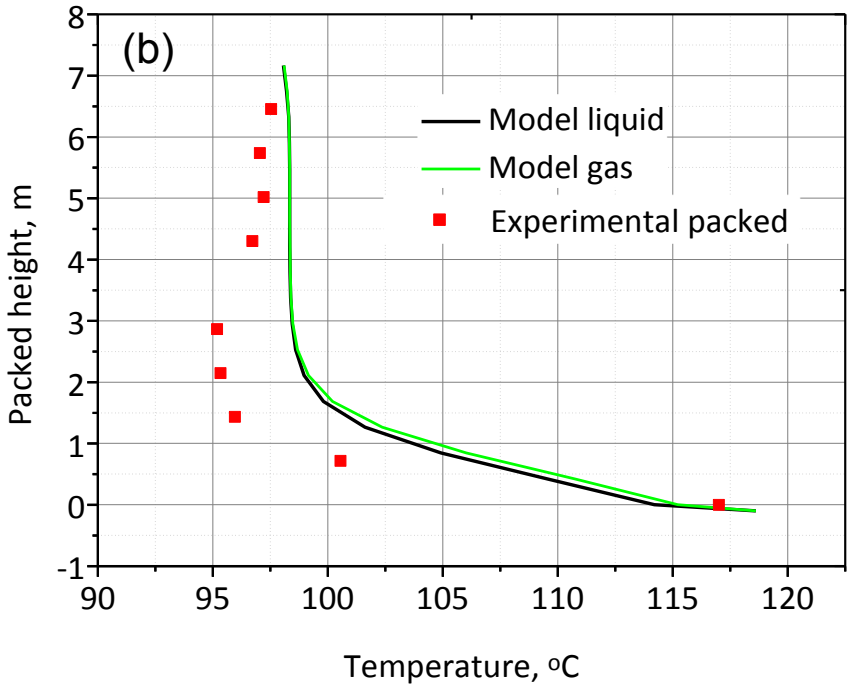

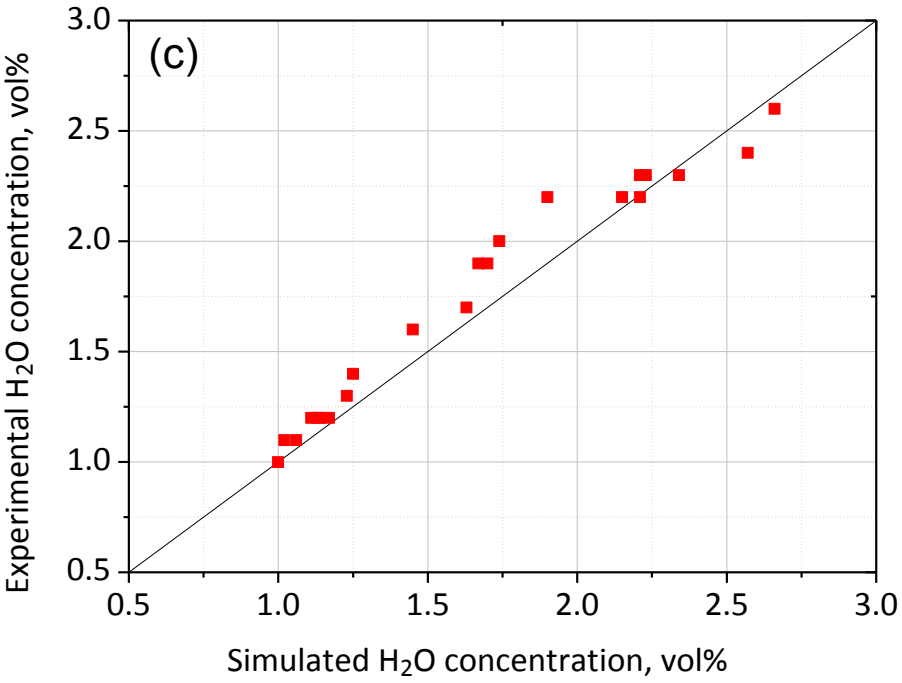
(c)
Experimental H_2O concentration, vol%
Simulated H_2O concentration, vol%
3.0
2.5
2.0
1.5
1.0
0.5
0.5
1.0
1.5
2.0
2.5
3.0

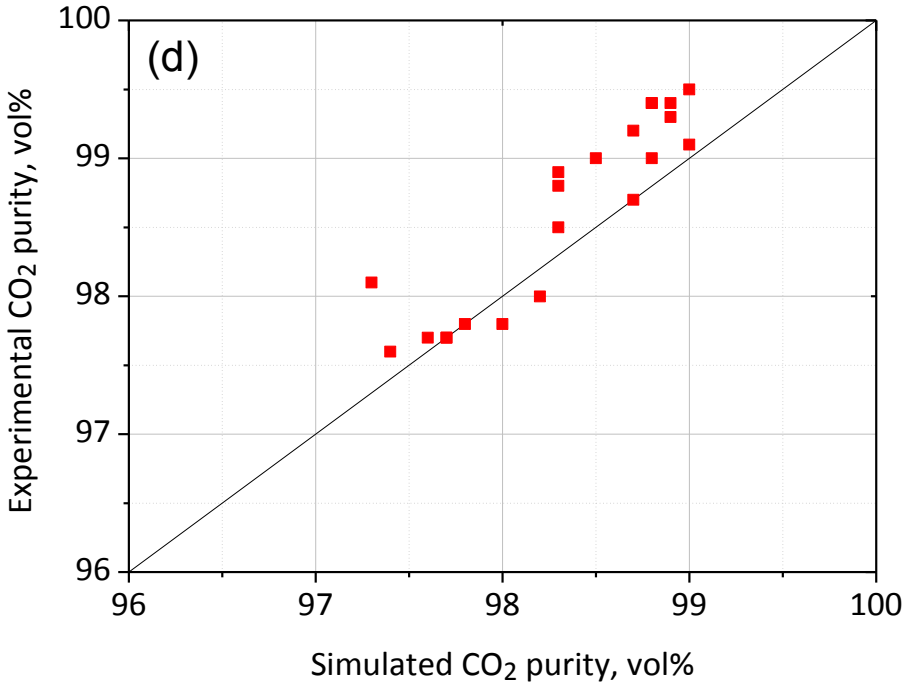
(d)
Experimental CO_2 purity, vol%
Simulated CO_2 purity, vol%
100
99
98
97
96
96
97
98
99
100

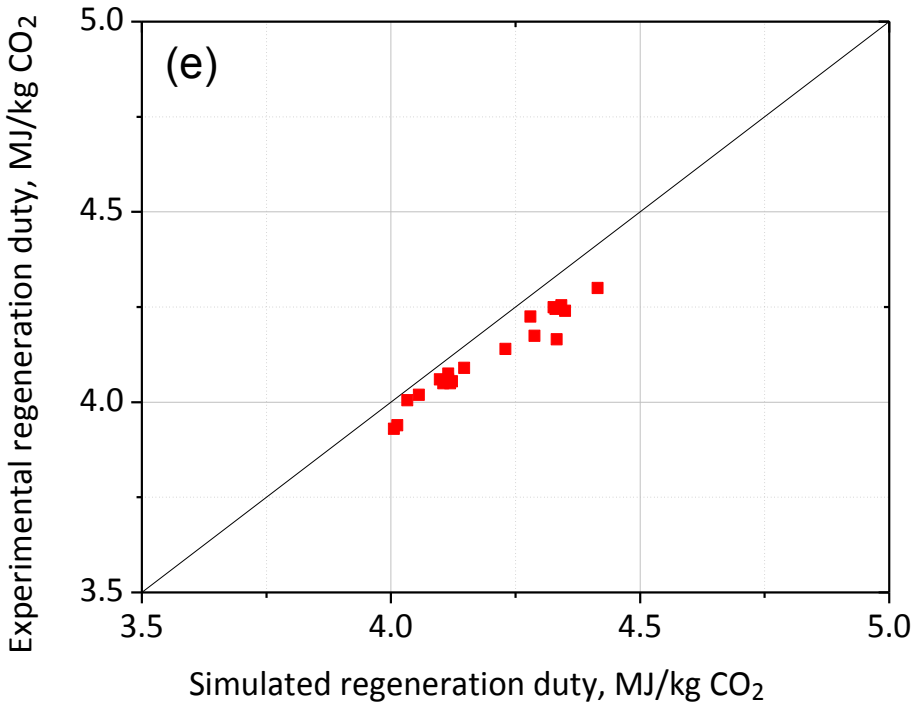

Figure A-3 Results of comparison between simulation and Tarong pilot trials: (a) reboiler temperatures; (b) temperature profiles in packed desorber (Test 01 Feb); (c) CO_2 purity in the CO_2 product; (d) H_2O concentration in the CO_2 product; and (e) solvent regeneration duty

In conclusion, the good agreement between the experimental results and the modelling results for both the CO_2 absorber and CO_2 stripper suggest that the established rate-based model can satisfactorily predict the CO_2 capture process by aqueous MEA.

Appendix B: Techno-economic Performance of MEA-based CO_2 Capture Process

This appendix describes the information regarding the techno-economic performance of the MEA-based CO_2 capture process that is used to support this thesis. More details can be found in:

Kangkang Li, Wardhaugh Leigh, Hai Yu, Paul Feron, Moses Tade. Systematic study of aqueous monoethanolamine (MEA)-based CO_2 capture process: Techno-economic assessment of the MEA process and its improvements. Applied Energy. accepted.

Process description of MEA process

The conventional MEA-based CO_2 capture process consists of a pretreatment unit, a CO_2 capture unit and a CO_2 compression unit, as shown in Figure 1.

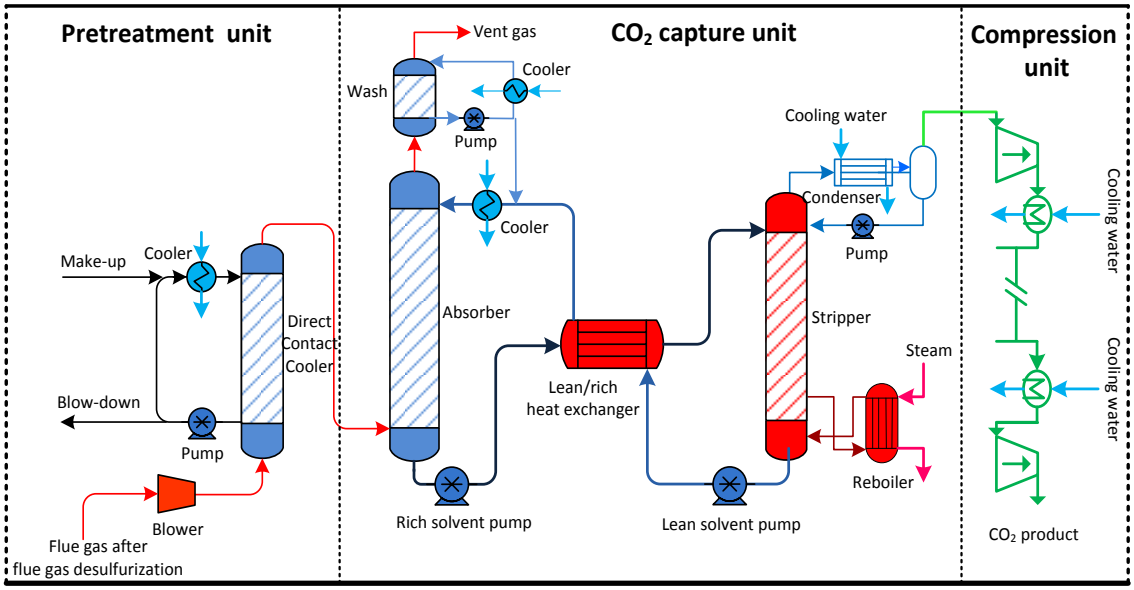

Figure B-1 Flow sheet of the conventional aqueous MEA-based post-combustion capture process

The typical flue gas composition from the power station is taken as being 10.7% CO_2, 6.0% H_2O, 7.8% O_2 and 75.5% N_2. The power station and flue gas composition are the same as the NH_3 process. According to the DOE report (Ramezan *et al.*, 2007), the flue gas temperature after the secondary FGD is at 58 °C, which is still too high for

entering the CO_2 capture unit and, thus, the direct contact cooler is required to cool the flue gas to 40-50°C. The CO_2 capture unit is designed for 85% CO_2 capture efficiency and a high-purity CO_2 product of >99 wt%. The captured CO_2 product is then pressurised to 150 bar for subsequent transportation and geological sequestration. All the technical targets are the same as the NH_3 process. Four process trains in parallel are proposed to deal with the total flue gas from the power station, with each capturing 1 million ton/year CO_2 (140 ton/hour).

Technical performance of the MEA process

Table B-1 shows the energy penalty of a power station integrated with the MEA-based CO_2 capture plant. It is evident that the CO_2 capture is energy intensive, with an energy penalty of 177 MWe electricity. As a result, the power output drops from 650 MWe to 473 MWe and the net efficiency falls from 38.9 to 28.3%, a 27.3% (relative term) and 10.6% (absolute term) decrease.

Capital costs of post-combustion capture plant

Table B-2 shows the capital investment and detailed individual equipment costs of one PCC process train (~1 million ton/year CO_2 capture capacity), including all the necessary equipment involved in the pretreatment unit, CO_2 capture unit and CO_2 compressor. Calculation of all of the equipment costs is based on the assumption that carbon steel materials are used, except for the column cladding and packing material, which are made of SS304 stainless steel to prevent corrosion. The total fixed capital investment of the proposed single PCC plant train, including the indirect cost, contingencies and owner's cost, is estimated at ~$US152.5 million (2013 prices), with an accuracy range of ±30%.

Table B-1 Energy consumption of the power station integrated with the MEA-based post-combustion CO_2 capture plant (four process train)

	Energy type	Power penalty/train, kW	Total power output, kW	Design specification
Power plant				
Power output	Electricity	–	+650,000	–
Net efficiency		–	38.9%	–
Pretreatment unit				
Blower	Electricity	3,586	–14,344	3.5 kPa
Pump	Electricity	19	–76	4×13.3 m^3/min
CO_2 capture unit				
Stripper reboiler	Steam [a]	25,422	–101,688	123.7 °C , 2 bar
Rich solvent pump	Electricity	122	–488	4×27.6 m^3/min
Lean solvent pump	Electricity	61	–244	4 ×27.6 m^3/min
Wash solvent pump	Electricity	0.5	–2.0	4 ×0.1 m^3/min
Condenser pump	Electricity	1.5	–6.0	4 ×5 m^3/min
CO_2 compression unit				
Compressor	Electricity	12,889	–52,556	150 bar
Auxiliary				
Pumps for cooling water	Electricity	390	–1,560	4 ×120 m^3/min
Other[b]	Electricity	1,500	–6,000	–
Total auxiliary power of PCC plant, kW			–176,966	–
Net power output after PCC, kW			+473,034	–
Net plant efficiency after PCC, %			+28.3%	–

[a] The typical regeneration energy of MEA solvent is 4.0 MJ/kg CO_2

[b] Other auxiliary power includes solvent filtration pumps, solvent reclaim pumps, waste treatment pumps, water and solvent make-up pumps

Table B-2 Detailed capital costs of one post-combustion capture (PCC) process train in the MEA-based PCC plant, in 2013 US$

	Material cost[a] 1000 US$	Manpower[b] 1000 US$	Direct cost 1000 US$	Specifications
Pretreatment unit				
Blower	731	81	812	200 m^3/s
Direct contact cooler column	2,082	792	2,875	Ø12 m×H5 m
Packing	1,855	27	1,883	Ø12 m×H3.5 m
Pump	89	19	108	220 L/s
Cooler	165	37	202	275 m^2
Storage tank	74	19	93	90 m^3
CO_2 capture unit				
CO_2 absorber	6,128	2,248	8,376	Ø12 m×H9.5 m
Absorber packing	6,040	77	6,117	Ø12 m×H7 m
Washing column	1,992	850	2,842	Ø12 m×H4 m
Washing column packing	2,036	24	2,060	Ø12 m×H3 m
CO_2 stripper	1,986	286	2,273	Ø7.5 m×H9.5 m
Stripper packing	1,438	25	1,464	Ø7.5 m×H7 m
Reboiler	3,095	97	3,183	4250 m^2
Condenser	260	45	305	800m^2
Main heat exchanger	1,151	351	1,502	9100 m^2
Lean solvent cooler	465	57	522	1200 m^2
Washing solvent cooler	46	22	69	15 m^2
Washing solvent pump	9	8	17	1.3 L/s
Condenser pump	25	10	35	34 L/s
Stripper reflux drum	34	12	46	10 m^3
Lean solvent pump	260	45	159	461 L/s
Solvent storage tank	296	46	342	1800 m^3
Washing solvent tank	34	12	46	10 m^3
CO_2 compression unit				
CO_2 compressor	20,472	3,557	24,028	6 stages, 150 bar
Auxiliary unit				
Solvent stripper reclaimer	144	37	181	–
Solvent reclaimer cooler	135	35	180	–
Solvent filtration	791	75	866	–
Calculated cost [c]				
Total direct cost (TDC)	–	–	60,586	–
Total indirect cost (TIC)	–	–	12,117	0.2 TDC
Bare erected cost (BEC)	–	–	72,703	TDC + TIC
Engineering and contractor	–	–	19,630	0.27 BEC
Engineering procurement and construction (EPC)	–	–	92,333	1.27 BEC
Process contingency	–	–	18,178	0.25 BEC
Project contingency	–	–	22,102	0.2 EPC + 0.05 BEC
Total plant cost (TPC)	–	–	132,611	1.2 EPC + 0.3 BEC
Owner's cost	–	–	19,982	0.15 TPC
Total capital investment (TIC)[c]	–	–	152,502	1.15 TPC

Note; [a] Material cost includes equipment, piping, civil, structural steel, instrumentation, electrical and insulation paint; [b] Manpower cost is the associated labour cost of equipment installation; [c] Percentages used to calculate the TIC are the same as NH_3 process

CO_2 avoided cost

Table B-3 illustrates the cost performance of the APC power station integrated with the PCC plant. The CO_2 capture plant is a capital-intensive process at US$1357/kW, which is 42% of the capital investment of the APC power station. In this study, the O&M cost of the PCC plant is assumed to be higher than that of the power station, due to the immaturity of and limited experience with PCC technology in commercial-scale applications. With the integration of the PCC plant, the LCOE of the power station increases by 81.9% from US$71.9 to US$130.8/MWh. The resulting CO_2 avoided cost of the baseline MEA process is US$86.4/ton CO_2.

Table B-3 Summary of economic performance of power station integrated with MEA-based post-combustion capture process, costs in 2013 US$

Item	Unit	Value
Capital cost and operational and maintenance (O&M) cost		
Capital investment of reference power station	$/kW	3,246
Capital cost of PCC plant including secondary flue gas desulphurisation	$/kW	1,357
Fixed O&M cost of power station	million US$/year	24.6
Variable O&M cost of power station excluding fuel cost	million US$/year	2.16
Coal cost	million US$/year	89.4
Fixed O&M cost of PCC plant	million US$/year	22.6
Variable O&M cost of PCC plant excluding PCC energy penalty	million US$/year	23.2
Economic performance of MEA process		
Levelised cost of electricity (LCOE) of power station	US$/MWh	71.9
LCOE of power station and PCC plant	US$/MWh	130.8
CO_2 avoided cost	US$/ton CO_2	86.4

Appendix C: Theoretical and Experimental Study of NH_3 Suppression by Addition of Me(II) ions (Ni, Cu and Zn) in an Ammonia-based CO_2 Capture Process

This appendix selects the important information of the NH_3 suppression by the metal ions to support this thesis. More detailed descriptions can be found in:

Kangkang Li, Hai Yu, Moses Tade, Paul Feron. Theoretical and experimental study of NH_3 suppression by addition of Me(II) ions in an ammonia-based CO_2 capture process. International Journal of Greenhouse Gas Control, 2014, 24, 54-63. DOI:10.1016/j.ijggc.2014.02.019

Theoretical analysis of NH_3 suppression by metal ions

The interactions of aqueous carbon-containing species and NH_3, complexation reactions between Me(II) (Ni, Cu, Zn) and ligands (NH_3, OH^-), and precipitation of $Me(OH)_2$ and $MeCO_3$ constructs the aqueous system of Me(II)–NH_3–CO_2–H_2O. Table C-1 lists the related reactions and their equilibrium constants or cumulative stability constants.

In the system of Me(II)–NH_3–CO_2–H_2O, the concentrations of various species can be expressed as Equations (1)–(12) shown in Table C-2. $[C]_T$ and $[N]_T$ represent the total concentrations of C-species and N-species in the solution. The total concentrations of Ni(II), Cu(II) and Zn(II) are expressed as $[Ni]_T$, $[Cu]_T$ and $[Zn]_T$, respectively. If the values of pH, $[C]_T$ and $[N]_T$ are known, the parameters such as the concentrations of $[Me^{2+}]$, $[NH_3]$ and $[CO_3^{2-}]$ in the equations can be solved by the iteration method using Matlab programming. The maximum Me(II) solubility under given conditions is then calculated by an Excel program. Similarly, the distribution of Me(II)-containing and N-containing species can be obtained using the Matlab and Excel programmes if pH, $[C]_T$, $[N]_T$ and $[Me]_T$ are known. The thermodynamic calculations are based on the following hypotheses: (1) the solution temperature is 25 ^{0}C; (2) the system is in solid-liquid equilibrium state and no gas is was generated; (3) the concentration is equal to the activity and is not affected by ionic strength or solution system; (4) the thermal effect of the reactions is not considered. Maximum Me(II) solubility, Me(II)-

containing and N-containing species distribution are simulated based on the principle of mass balance and simultaneous equilibrium.

Table C-1 Reactions and corresponding equilibrium constants of Me(II)-NH_3-CO_2-H_2O system (25 ^{0}C)

No.	Reactions	lgK	No.	Reactions	lgK
1	$H_2O \leftrightarrow H^+ + OH^-$	–14.00	20	$Zn(OH)_2 \leftrightarrow Zn^{2+}+2OH^-$	–11.30
2	$NH_4^+ \leftrightarrow NH_3 + H^+$	–9.25	21	$Zn(OH)_3^- \leftrightarrow Zn^{2+}+3OH^-$	–14.14
3	$H_2CO_3 \leftrightarrow HCO_3^- + H^+$	–6.35	22	$Zn(OH)_4^{2-} \leftrightarrow Zn^{2+}+4OH^-$	–17.66
4	$HCO_3^- \leftrightarrow CO_3^{2-} + H^+$	–10.33	23	$Ni(NH_3)^{2+} \leftrightarrow Ni^{2+}+NH_3$	–2.80
5	$NH_3+HCO_3^- \leftrightarrow NH_2COO^- + H_2O$	–0.79	24	$Ni(NH_3)_2^{2+} \leftrightarrow Ni^{2+}+2NH_3$	–5.04
6	$Ni(OH)_{2(s)} \leftrightarrow Ni^{2+} + 2OH^-$	–15.26	25	$Ni(NH_3)_3^{2+} \leftrightarrow Ni^{2+}+3NH_3$	–6.77
7	$Cu(OH)_{2(s)} \leftrightarrow Cu^{2+} + 2OH^-$	–19.66	26	$Ni(NH_3)_4^{2+} \leftrightarrow Ni^{2+}+4NH_3$	–7.96
8	$Zn(OH)_{2(s)} \leftrightarrow Zn^{2+} + 2OH^-$	–16.50	27	$Ni(NH_3)_5^{2+} \leftrightarrow Ni^{2+}+5NH_3$	–8.71
9	$NiCO_3 \leftrightarrow Ni^{2+}+CO_3^{2-}$	–6.85	28	$Ni(NH_3)_6^{2+} \leftrightarrow Ni^{2+}+6NH_3$	–8.74
10	$CuCO_3 \leftrightarrow Cu^{2+}+CO_3^{2-}$	–9.86	29	$Cu(NH_3)^{2+} \leftrightarrow Cu^{2+}+NH_3$	–4.31
11	$ZnCO_3 \leftrightarrow Zn^{2+}+CO_3^{2-}$	–9.94	30	$Cu(NH_3)_2^{2+} \leftrightarrow Cu^{2+}+2NH_3$	–7.98
12	$Ni(OH)^+ \leftrightarrow Ni^{2+}+OH^-$	–4.97	31	$Cu(NH_3)_3^{2+} \leftrightarrow Cu^{2+}+3NH_3$	–11.02
13	$Ni(OH)_2 \leftrightarrow Ni^{2+}+2OH^-$	–8.55	32	$Cu(NH_3)_4^{2+} \leftrightarrow Cu^{2+}+4NH_3$	–13.32
14	$Ni(OH)_3^- \leftrightarrow Ni^{2+}+3OH^-$	–11.33	33	$Cu(NH_3)_5^{2+} \leftrightarrow Cu^{2+}+5NH_3$	–12.86
15	$Cu(OH)^+ \leftrightarrow Cu^{2+}+OH^-$	–7.00	34	$Zn(NH_3)^{2+} \leftrightarrow Zn^{2+}+NH_3$	–2.37
16	$Cu(OH)_2 \leftrightarrow Cu^{2+}+2OH^-$	–13.68	35	$Zn(NH_3)_2^{2+} \leftrightarrow Zn^{2+}+2NH_3$	–4.81
17	$Cu(OH)_3^- \leftrightarrow Cu^{2+}+3OH^-$	–17.00	36	$Zn(NH_3)_3^{2+} \leftrightarrow Zn^{2+}+3NH_3$	–7.31
18	$Cu(OH)_4^{2-} \leftrightarrow Cu^{2+}+4OH^-$	–18.50	37	$Zn(NH_3)_4^{2+} \leftrightarrow Zn^{2+}+4NH_3$	–9.46
19	$Zn(OH)^+ \leftrightarrow Zn^{2+}+OH^-$	–4.40			

Table C-2 The equations used to describe the equilibrium constants and the corresponding reactions

No.	Equations	Reactions
1	$[H^+] = 10^{-pH}$ or$[OH^-] = 10^{pH-14}$	(1)
2	$[NH_4^+] = [NH_3] \times 10^{9.25-pH}$	(2)
3	$[Ni^{2+}] = \min(\frac{10^{-6.85}}{[CO_3^{2-}]}, 10^{12.74-2pH})$	(6), (9)
4	$[Cu^{2+}] = \min(\frac{10^{-9.86}}{[CO_3^{2-}]}, 10^{8.34-2pH})$	(7), (10)
5	$[Zn^{2+}] = \min(\frac{10^{-9.94}}{[CO_3^{2-}]}, 10^{11.5-2pH})$	(8), (11)
6	$[C]_T = [CO_3^{2-}] + [HCO_3^-] + [H_2CO_3] + [NH_2COO^-]$ $=[CO_3^{2-}](1+10^{10.33-pH}+10^{16.68-2pH}+0.79[NH_3]10^{10.33-pH})$	(3)-(5)
7	$[Ni]_T = [Ni^{2+}] + \sum_{i=1}^{3}[Ni(OH)_i^{2-i}] + \sum_{i=1}^{6}[Ni(NH_3)_i^{2+}]$ $= [Ni^{2+}](1+10^{pH-9.03}+10^{2pH-19.45}+10^{3pH-30.67}+10^{2.8}[NH_3] +10^{5.04}[NH_3]^2 +10^{6.77}[NH_3]^3 +10^{7.96}[NH_3]^4 +10^{8.71}[NH_3]^5 +10^{7.74}[NH_3]^6)$	(12)-(14), (23)-(28)
8	$[N]_{T_{(Ni)}} = [NH_3] + [NH_4^+] + [NH_2COO^-] + i \times \sum_{i=1}^{6}[Ni(NH_3)_i^{2+}]$ $=[NH_3]\{1+10^{9.25-pH}+0.79[CO_3^{2-}]10^{10.33-pH}+[Ni^{2+}](10^{2.8}[NH_3] +2[NH_3]^2 10^{5.04} +3[NH_3]^3 10^{6.77}+ 4[NH_3]^4 10^{7.96}+ 5[NH_3]^5 10^{8.71} + 6[NH_3]^6 10^{7.74})\}$	(2),(5), (23)-(28)
9	$[Cu]_T = [Cu^{2+}] + \sum_{i=1}^{4}[Cu(OH)_i^{2-i}] + \sum_{i=1}^{5}[Cu(NH_3)_i^{2+}]$ $= [Cu^{2+}](1+10^{pH-7}+10^{2pH-14.32}+10^{3pH-25}+10^{4pH-37.5}+10^{4.31}[NH_3] +10^{7.98}[NH_3]^2 +10^{11.02}[NH_3]^3 +10^{13.32}[NH_3]^4 +10^{12.86}[NH_3]^5)$	(15)-(18), (29)-(33)
10	$[N]_{T_{(Cu)}} = [NH_3] + [NH_4^+] + [NH_2COO^-] + i \times \sum_{i=1}^{6}[Cu(NH_3)_i^{2+}]$ $=[NH_3]\{1+10^{9.25-pH}+0.79[CO_3^{2-}]10^{10.33-pH}+[Cu^{2+}](10^{4.31}[NH_3] +2[NH_3]^2 10^{7.98} +3[NH_3]^3 10^{11.02}+ 4[NH_3]^4 10^{13.32}+ 5[NH_3]^5 10^{12.86})\}$	(2),(5), (29)-(33)
11	$[Zn]_T = [Zn^{2+}] + \sum_{i=1}^{4}[Zn(OH)_i^{2-i}] + \sum_{i=1}^{4}[Zn(NH_3)_i^{2+}]$ $= [Zn^{2+}](1+10^{pH-9.6}+10^{2pH-16.7}+10^{3pH-27.86}+10^{4pH-38.34}+10^{2.37}[NH_3] +10^{4.81}[NH_3]^2 +10^{7.31}[NH_3]^3 +10^{9.46}[NH_3]^4)$	(19)-(22), (34)-(37)
12	$[N]_{T_{Zn}} = [NH_3] + [NH_4^+] + [NH_2COO^-] + \sum_{i=1}^{6}[Zn(NH_3)_i^{2+}]$ $=[NH_3]\{1+10^{9.25-pH}+0.79[CO_3^{2-}]10^{10.33-pH}+[Zn^{2+}](10^{2.37}[NH_3] +2[NH_3]^2 10^{4.81} +3[NH_3]^3 10^{7.31}+ 4[NH_3]^4 10^{9.46})\}$	(2),(5), (34)-(37)

Figure C-1 shows the distribution of different nitrogen-containing species in the NH_3-based solution with and without metal ions at a pH range of 7–12. It can be seen that the addition of metal ions has a positive effect on reducing free NH_3 concentration (which is directly related to NH_3 loss), especially in the high pH range. This is because a higher pH leads to a higher concentration of free NH_3, which provides sufficient ligands for Me(II) complexation. Of the three metal ions, Ni(II) is the best additive for NH_3 suppression. This is because one Ni(II) ion can complex with as many as six NH_3 ligands, whereas Cu(II) and Zn(II) can complex five and four NH_3 ligands, respectively. The more free NH_3 is coordinated by metal ions, the more efficient NH_3 suppression becomes.

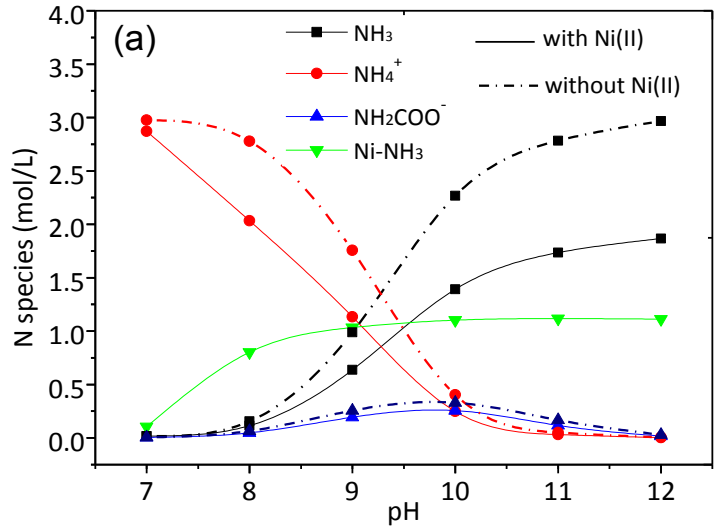

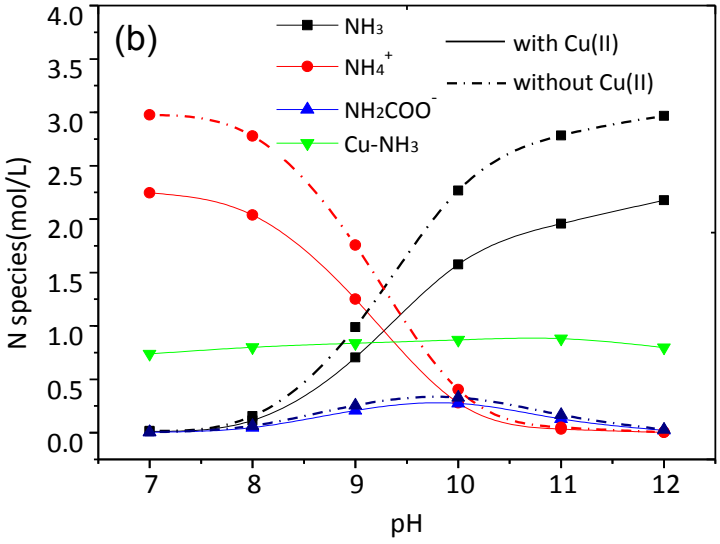

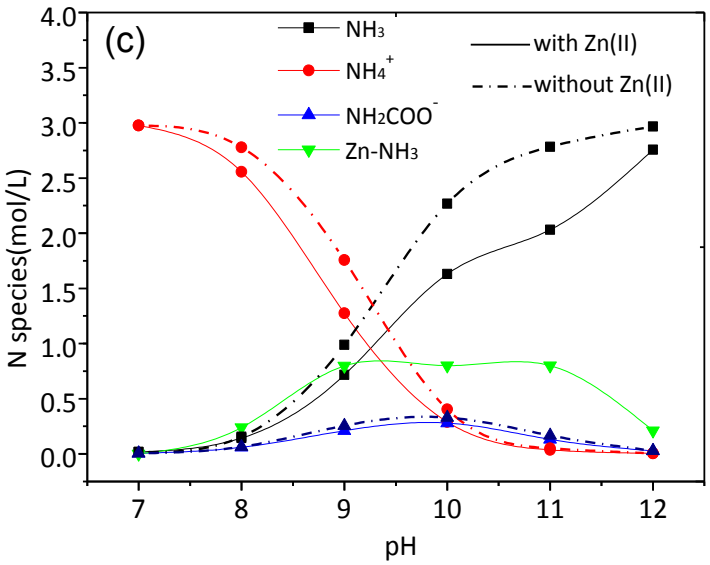

Figure C-1 N-species distribution in ammonia solution with and without Me(II) at [N]T= 3.0 mol/L , [Me] = 0.2 mol/L, C/N ratio 0.2 and 25 ^{0}C. (a) Ni(II), (b) Cu(II), (c) Zn(II)

Theoretically, the maximum NH_3 suppression efficiencies of Ni(II), Cu(II) and Zn(II) at the given conditions are 40.2, 31.6 and 28.8%, respectively. However, it is worthwhile to notice that the concentration of Zn(II)–NH_3 complexes dropped from 0.8 mol/L at pH 11 to 0.2 mol/L at pH 12, and the theoretical NH_3 suppression efficiency subsequently decreased from 27.0 to 7.0%. However, this phenomenon is not found in Ni(II)–NH_3 and Cu(II)–NH_3 species, because of their higher solubility in the pH range of 11-12. These results indicate that the efficiency of NH_3 suppression is mostly determined by Me(II) solubility and the complexation capacity of Me(II) with NH_3. Therefore, Me(II) solubility at different pH levels and C/N ratios must be taken into account to avoid undesired precipitants, and to improve NH_3 suppression efficiency when introducing Me(II) ions into an ammonia solution.

Experimental investigation on NH_3 suppression by metal ions

Measurement of the CO_2 absorption rate by aqueous NH_3 is conducted with an apparatus of wetted wall column (WWC), as shown in Figure C-2. The configuration of WWC allows for the descending liquid film to be contacted with the ascending gas stream in a counter-current method, which simulates the reactions of gas–liquid phase

in real packed columns where a liquid stream is fed into the top and gas stream into the bottom.

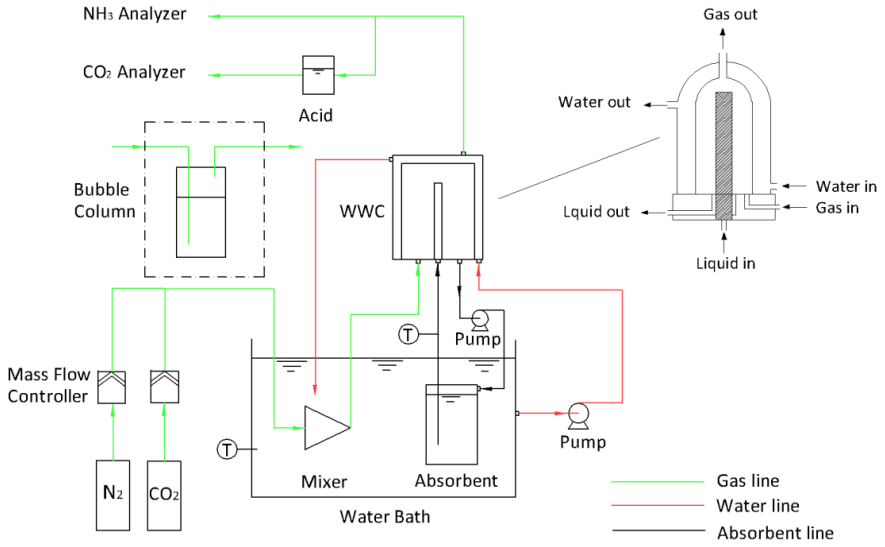

Figure C-2 Schematic diagram of experimental apparatus in this study

In this study, the absorption process is carried out at 25 ^{0}C using the WWC. The N_2 and CO_2 are mixed thoroughly in the mixer which was placed in the water bath. This approach ensures that the CO_2/N_2 gas mixture could be kept at the same temperature as the solvent before going into the WWC. The WWC is used as a counter-current contactor between the gas and liquid phase for measurement of NH_3 loss and CO_2 absorption rate. It consists of a stainless steel tube and a cylindrical glass jacket, through which the water from the bath is circulated to create a temperature-constant reaction atmosphere. The absorbent solution is pumped into the column at a flow rate that generates a homogenous, ripple-free film along the column. The CO_2 and NH_3 concentrations in the gas phase are determined using a CO_2 analyser (Horiba, VA-3000/VS-3000) with a detection range of 0-10 vol % and Fourier Transform Infrared Spectroscopy (FTIR, Gasmet^{TM} Dx-4000) with a detection range of 0-15000 ppmv, respectively. The NH_3 suppression efficiency is defined as follows:

$$\eta\% = \frac{C_{NH_3,Ref} - C_{NH_3,Me(II)}}{C_{NH_3,Ref}} \times 100\% \quad \text{(C-1)}$$

where η is the ammonia suppression efficiency; $C_{NH_3,Ref}$ is the gas ammonia concentration when the reference solution (refer to the sample with no addition of metal ions) is used; and $C_{NH_3,Me(II)}$ is the gas NH_3 concentration when the Me(II)-containing solution is tested.

The relationship between the CO_2 absorption flux and overall mass transfer coefficient K_G is described by the following equation.

$$N_{CO_2} = K_G(P_{CO_2} - P^*_{CO_2}) \quad \text{(C-2)}$$

where N_{CO_2} is the molar absorption flux of CO_2, $mmol \cdot m^{-2}s^{-1}$; K_G is the overall mass transfer coefficient, $mmol \cdot m^{-2} \cdot s^{-1} \cdot kPa^{-1}$; $P^*_{CO_2}$ is the equilibrium partial pressure of CO_2 and determined by temperature and composition; and P_{CO_2} is the bulk partial pressure of CO_2 in gas phase which can be calculated from the log-mean pressure ΔP_m of inlet and outlet CO_2 concentration by the following equation. Thus, the overall mass transfer coefficient (K_G) can be extracted from the slope of the straight line of $N_{CO_2} - P_{CO_2}$ according to the experimental CO_2 absorption flux at different CO_2 partial pressures.

$$\Delta P_m = \frac{P_{CO_2,in} - P_{CO_2,out}}{\ln(P_{CO_2,in}/P_{CO_2,out})} \quad \text{(C-3)}$$

Figure C-3 shows the effect of NH_3 concentration on NH_3 loss and CO_2 absorption rate (K_G) in a Me(II)-containing ammonia solution without CO_2 loading. The addition of metal ions significantly reduces NH_3 loss (FigC-3(a)). Consistent with the theoretical analysis, Ni(II) is the most effective devolatiliser for NH_3, reaching an efficiency of 39.7% (N = 3 mol/L) and 26.0% (N = 6 mol/L) in 0 CO_2 loading NH_3 solutions; this is higher than that of Cu(II) (24.9 and 18.9%) and Zn(II) (28.6 and 23.7%), respectively. This is because the Ni(II) ion can complex with more NH_3 ligands than other two metal species, as discussed before, leading to high NH_3 suppression efficiency.

Fortunately, despite the reduction of free NH_3, the overall mass transfer coefficient (K_G) in Me(II)-containing NH_3 solutions drops only slightly, as shown in Figure C-3(b). The K_G of Ni(II), Cu(II) and Zn(II) in 3 mol/L NH_3 solution are 0.51, 0.52 and 0.57 $mmol/s \cdot m^2$, respectively: slightly lower than the K_G of 0.58 $mmol/s \cdot m^2$ in NH_3 solution without metal ions. Generally, the CO_2 absorption rate using the NH_3 solution is proportional to the square root of NH_3 concentration. According to the coordination chemistry, the electron pair in the coordinated NH_3 is occupied by the metal ions, leaving non-reactive complex NH_3 in the solution. Thus, the introduction of metallic ions consumes part of the free NH_3 and decreases the free NH_3 concentration, which subsequently hinders the CO_2 absorption rate. However, it should be mentioned that

the NH_3 in complex ions is not permanently tied up with Me(II) ions and can thus return NH_3 molecules into the solution when the pH value and NH_3 concentrations fall. In other words, Me(II)–NH_3 complexes can act as an ammonia buffer. The order of CO_2 absorption rate in 3 mol/L ammonia solution is Zn(II)>Cu(II)>Ni(II), which is opposite to the order of NH_3 suppression efficiency: Ni(II)>Cu(II)>Zn(II). This agrees well with the theoretical analysis of Me(II)–NH_3 complexation capability and capacity.

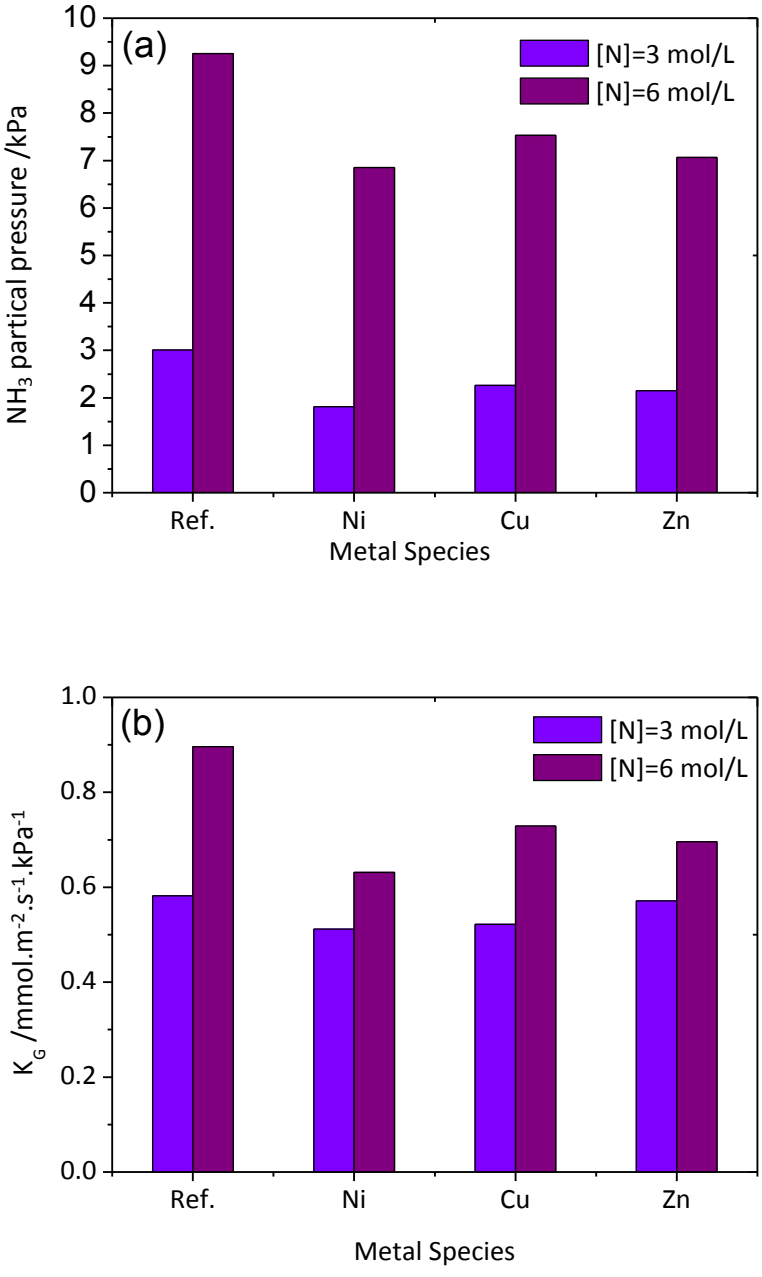

Figure C-3 Effect of ammonia concentration on (a) NH_3 loss and (b) CO_2 absorption rate at Me(II) = 0.2 mol/L, C/N ratio = 0 and 25 ^{0}C

Conclusion

This study theoretically and experimentally investigates the potential of three metal ions – Ni(II), Cu(II) and Zn(II) – as additives to reduce NH_3 volatilisation using the complexation of metal ions with free NH_3. A thermodynamic equilibrium model of the Me(II)–NH_3–CO_2–H_2O system is established to provide theoretical guidance for the study and analysis of experimental results. The experimental results agree with the theoretical simulation. The theoretical and experimental results show that the order of NH_3 suppression efficiency is Ni(II)>Cu(II)>Zn(II). The addition of Me(II) ions (Ni, Cu and Zn) significantly reduces NH_3 loss in the absorption processes, and only slightly decreases the rate of CO_2 absorption, which creates the potential for an industrial application.

Appendix D: Permission of articles reproduction from publishers

1. Permission from American Chemical Society Publication:

Kangkang Li, Hai Yu, Moses Tade, Paul Feron, Jingwen Yu, Shujuan Wang. Process modelling of an advanced NH_3 abatement and recycling system in ammonia based CO_2 capture process. Environment Science & Technology, 2014, 48 (12), 7179–7186. DOI: 10.1021/es501175x

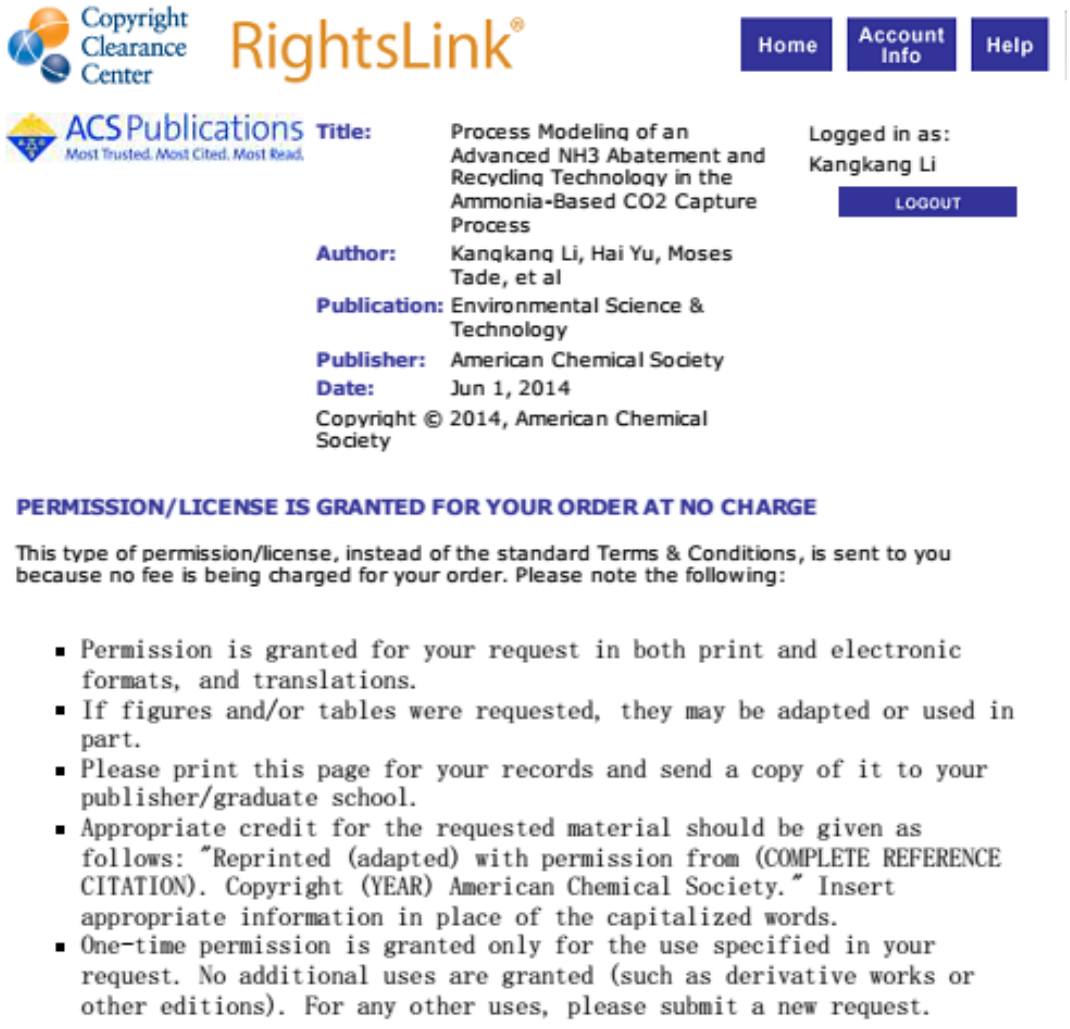

Copyright Clearance Center RightsLink®

Home | Account Info | Help

ACS Publications Most Trusted. Most Cited. Most Read.

Logged in as: Kangkang Li

LOGOUT

Title:	Process Modeling of an Advanced NH3 Abatement and Recycling Technology in the Ammonia-Based CO2 Capture Process
Author:	Kangkang Li, Hai Yu, Moses Tade, et al
Publication:	Environmental Science & Technology
Publisher:	American Chemical Society
Date:	Jun 1, 2014

Copyright © 2014, American Chemical Society

PERMISSION/LICENSE IS GRANTED FOR YOUR ORDER AT NO CHARGE

This type of permission/license, instead of the standard Terms & Conditions, is sent to you because no fee is being charged for your order. Please note the following:

- Permission is granted for your request in both print and electronic formats, and translations.
- If figures and/or tables were requested, they may be adapted or used in part.
- Please print this page for your records and send a copy of it to your publisher/graduate school.
- Appropriate credit for the requested material should be given as follows: "Reprinted (adapted) with permission from (COMPLETE REFERENCE CITATION). Copyright (YEAR) American Chemical Society." Insert appropriate information in place of the capitalized words.
- One-time permission is granted only for the use specified in your request. No additional uses are granted (such as derivative works or other editions). For any other uses, please submit a new request.

Kangkang Li, Hai Yu, Paul Feron, Moses Tade, Leigh Wardhaugh. Technical and energy performance of an advanced, aqueous ammonia-based CO_2 capture technology for a 500-MW coal-fired power station. Environment Science & Technology, 2015, 49, 10243-10252. DOI: 10.1021/acs.est.5b02258

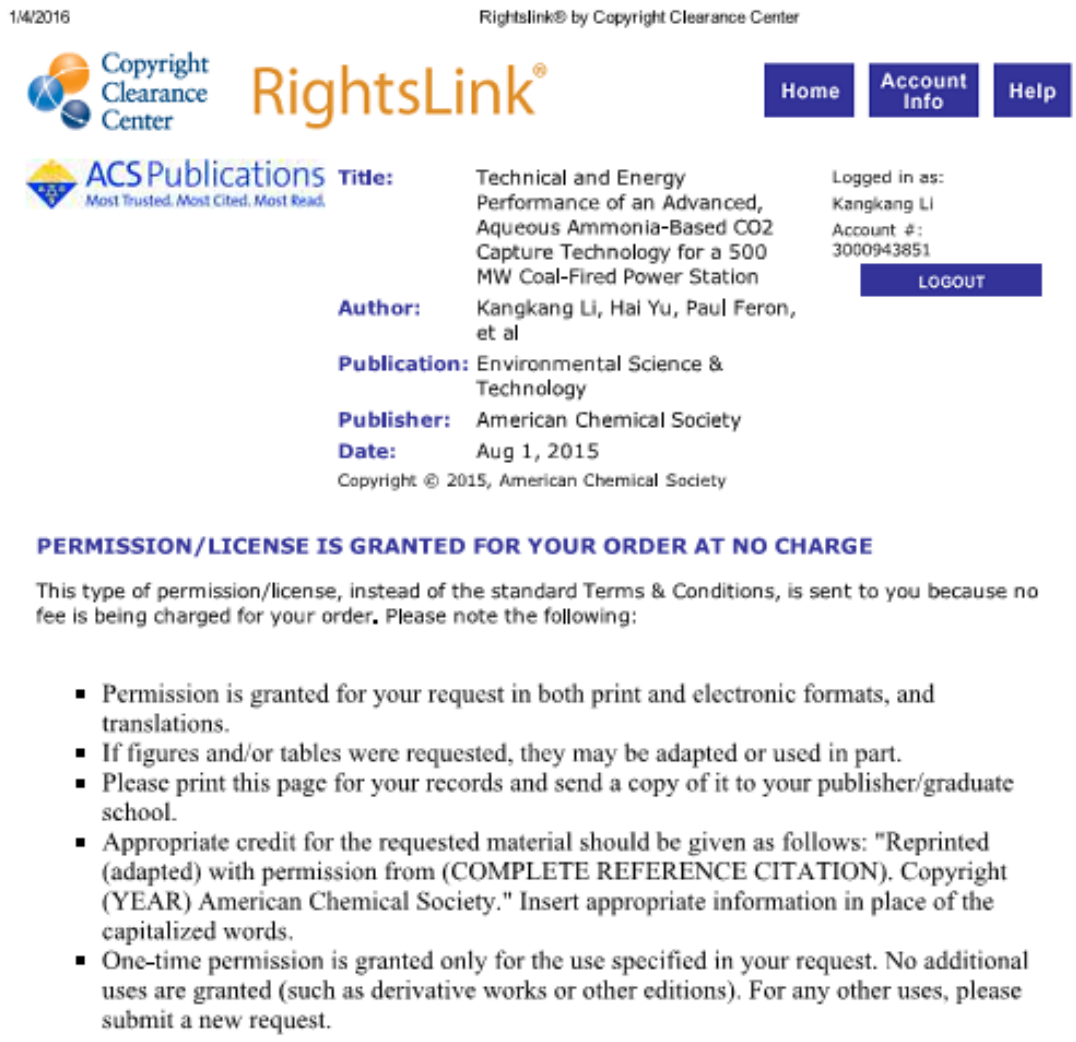

1/4/2016 Rightslink® by Copyright Clearance Center

Copyright Clearance Center RightsLink®

Home | Account Info | Help

ACS Publications Most Trusted. Most Cited. Most Read.

Title: Technical and Energy Performance of an Advanced, Aqueous Ammonia-Based CO2 Capture Technology for a 500 MW Coal-Fired Power Station

Author: Kangkang Li, Hai Yu, Paul Feron, et al

Publication: Environmental Science & Technology

Publisher: American Chemical Society

Date: Aug 1, 2015

Copyright © 2015, American Chemical Society

Logged in as: Kangkang Li
Account #: 3000943851
LOGOUT

PERMISSION/LICENSE IS GRANTED FOR YOUR ORDER AT NO CHARGE

This type of permission/license, instead of the standard Terms & Conditions, is sent to you because no fee is being charged for your order. Please note the following:

- Permission is granted for your request in both print and electronic formats, and translations.
- If figures and/or tables were requested, they may be adapted or used in part.
- Please print this page for your records and send a copy of it to your publisher/graduate school.
- Appropriate credit for the requested material should be given as follows: "Reprinted (adapted) with permission from (COMPLETE REFERENCE CITATION). Copyright (YEAR) American Chemical Society." Insert appropriate information in place of the capitalized words.
- One-time permission is granted only for the use specified in your request. No additional uses are granted (such as derivative works or other editions). For any other uses, please submit a new request.

2. Permissions from Elsevier Publication:

Kangkang Li, Wardhaugh Leigh, Paul Feron, Hai Yu, Moses Tade. Systematic study of aqueous monoethanolamine-based CO_2 capture process: Techno-economic assessment of the MEA process and its improvement. Applied Energy, 2015, accepted

Kangkang Li, Hai Yu, Paul Feron, Moses Tade, Jingwen Yu, Shujuan Wang. Rate-based modelling of combined SO_2 removal and NH_3 recycling integrated with an aqueous NH_3-based CO_2 capture process. Applied Energy, 2015, 148, 66-77. DOI:10.1016/j.apenergy.2015.03.060

Kangkang Li, Hai Yu, Moses Tade, Paul Feron. Theoretical and experimental study of NH_3 suppression by addition of Me(II) ions in an ammonia-based CO_2 capture process. International Journal of Greenhouse Gas Control, 2014, 24, 54-63. DOI:10.1016/j.ijggc.2014.02.019

Elsevier retains the author's right for article reuse for Ph.D. thesis, as stated:

https://www.elsevier.com/about/company-information/policies/copyright/personal-use

Authors can use their articles, in full or in part, for a wide range of scholarly, non-commercial purposes as outlined below:

- Use by an author in the author's classroom teaching (including distribution of copies, paper or electronic)
- Distribution of copies (including through e-mail) to known research colleagues for their personal use (but not for Commercial Use)
- Inclusion in a thesis or dissertation (provided that this is not to be published commercially)
- Use in a subsequent compilation of the author's works
- Extending the Article to book-length form
- Preparation of other derivative works (but not for Commercial Use)
- Otherwise using or re-using portions or excerpts in other works

These rights apply for all Elsevier authors who publish their article as either a subscription article or an open access article. In all cases we require that all Elsevier

authors always include a full acknowledgement and, if appropriate, a link to the final published version hosted on Science Direct.

A confirmation email from Elsevier Permission Helpdesk

Li, Kangkang (Energy, Newcastle)

From: Permissions Helpdesk <permissionshelpdesk@elsevier.com>
Sent: Wednesday, 6 January 2016 3:34 AM
To: Li, Kangkang (Energy, Newcastle)
Subject: RE: permission of reuse of published articles in Ph.D. thesis

Dear Kangkang,

As an Elsevier journal author, you retain various rights including Inclusion of the article in a thesis or dissertation whether in part or *in toto*; see http://www.elsevier.com/about/company-information/policies/copyright#Author%20rights for more information. As this is a retained right, no written permission is necessary provided that proper acknowledgement is given.

This extends to the online version of your thesis and would include any version of the article including the final published version provided that it is not available as an individual download but only embedded within the thesis itself.

If the article would be available as an individual download, only the preprint or (subject to the journal-specific embargo date) Accepted Author Manuscript version, but not the final published version, may be made available; see http://www.elsevier.com/journal-authors/sharing-your-article for more information. For more information regarding embargo dates, please see: http://www.elsevier.com/__data/assets/pdf_file/0018/121293/external-embargo-list.pdf.

If I may be of further assistance, please let me know.

Best of luck with your PhD thesis and best regards,

Laura

Laura Stingelin
Permissions Helpdesk Associate
Elsevier
1600 John F. Kennedy Boulevard
Suite 1800
Philadelphia, PA 19103-2899
T: (215) 239-3867
F: (215) 239-3805
E: l.stingelin@elsevier.com
Questions about obtaining permission: whom to contact? What rights to request? When is permission required? Contact the Permissions Helpdesk at:
+1-800-523-4069 x 3808 *permissionshelpdesk@elsevier.com*

References

AACE, 2011. Cost estimate classification system – as applied in engineering, procurement, and construction for the process industries. AACE International Recommended Practice No. 18R-97.

Aaron, D., Tsouris, C., 2005. Separation of CO_2 from flue gas: a review. Separation Science and Technology 40, 321-348.

Abu-Zahra, M.R., Schneiders, L.H., Niederer, J.P., Feron, P.H., Versteeg, G.F., 2007. CO_2 capture from power plants: Part I. A parametric study of the technical performance based on monoethanolamine. International Journal of Greenhouse Gas Control 1, 37-46.

Alopaeus, V., Aittamaa, J., Nordén, H.V., 1999. Approximate high flux corrections for multicomponent mass transfer models and some explicit methods. Chemical Engineering Science 54, 4267-4271.

Aspen, 2010a. Aspen physical property system: Physical property models. Burlington, MA, U.S.A..

Aspen, 2010b. Rate-based model of the CO_2 capture process by NH_3 using Aspen Plus. Burlington, MA, U.S.A..

Aspen, 2014. Aspen Capital Cost Estimator V8.6. Burlington, U.S.A.: Aspen Technology, Inc.

Bailey, D., Feron, P., 2005. Post-combustion decarbonisation processes. Oil & Gas Science and Technology 60, 461-474.

Bishnoi, S., Rochelle, G.T., 2002. Absorption of carbon dioxide in aqueous piperazine/methyldiethanolamine. AIChE Journal 48.

Black, J., 2010. Cost and performance baseline for fossil energy plants volume 1: Bituminous coal and natural gas to electricity. Final report (2nd edition), National Energy Technology Laboratory (2010 Nov) Report no.: DOE20101397.

Boot-Handford, M.E., Abanades, J.C., Anthony, E.J., Blunt, M.J., Brandani, S., Mac Dowell, N., Fernández, J.R., Ferrari, M.-C., Gross, R., Hallett, J.P., 2014. Carbon capture and storage update. Energy & Environmental Science 7, 130-189.

Bougie, F., Lauzon-Gauthier, J., Iliuta, M.C., 2009. Acceleration of the reaction of carbon dioxide into aqueous 2-amino-2-hydroxymethyl-1,3-propanediol solutions by piperazine addition. Chemical Engineering Science 64.

Busca, G., Pistarino, C., 2003. Abatement of ammonia and amines from waste gases: a summary. Journal of Loss Prevention in the Process Industries 16, 157-163.

Caplow, M., 1968. Kinetics of carbamate formation and breakdown. Journal of the American Chemical Society 90, 6795-6803.

CEPCI, 2014. Chemical Engineering Plant Cost Index. http://www.chemengonline.com/

Chapel, D.G., Mariz, C.L., Ernest, J., 1999. Recovery of CO_2 from flue gases: commercial trends, Canadian Society of Chemical Engineers Annual Meeting, pp. 4-6.

Chilton, T.H., Colburn, A.P., 1934. Mass transfer (absorption) coefficients prediction from data on heat transfer and fluid friction. Industrial & Engineering Chemistry 26, 1183-1187.

Chowdhury, F.A., Yamada, H., Higashii, T., Goto, K., Onoda, M., 2013. CO_2 capture by tertiary amine absorbents: A performance comparison study. Industrial & Engineering Chemistry Research 52.

Cichanowicz, J.E., 2010. Current capital cost and cost-effectiveness of power plant emissions control technologies. January.

Ciferno, J.P., DiPietro, P., Tarka, T., 2005. An economic scoping study for CO_2 capture using aqueous ammonia. Final Report, National Energy Technology Laboratory, US Department of Energy, Pittsburgh, PA.

Cousins, A., Cottrell, A., Lawson, A., Huang, S., Feron, P.H., 2012. Model verification and evaluation of the rich-split process modification at an Australian-based post combustion CO_2 capture pilot plant. Greenhouse Gases: Science and Technology 2, 329-345.

Cousins, A., Wardhaugh, L., Feron, P., 2011a. A survey of process flow sheet modifications for energy efficient CO_2 capture from flue gases using chemical absorption. International Journal of Greenhouse Gas Control 5, 605-619.

Cousins, A., Wardhaugh, L.T., Feron, P.H., 2011b. Preliminary analysis of process flow sheet modifications for energy efficient CO_2 capture from flue gases using chemical absorption. Chemical Engineering Research and Design 89, 1237-1251.

Darde, V., Maribo-Mogensen, B., van Well, W.J., Stenby, E.H., Thomsen, K., 2012. Process simulation of CO_2 capture with aqueous ammonia using the Extended UNIQUAC model. International Journal of Greenhouse Gas Control 10, 74-87.

Darde, V., Thomsen, K., Van Well, W.J., Stenby, E.H., 2010a. Chilled ammonia process for CO_2 capture. International Journal of Greenhouse Gas Control 4, 131-136.

Darde, V., Van Well, W.J., Fosboel, P.L., Stenby, E.H., Thomsen, K., 2011a. Experimental measurement and modeling of the rate of absorption of carbon dioxide by aqueous ammonia. International Journal of Greenhouse Gas Control 5, 1149-1162.

Darde, V., van Well, W.J., Stenby, E.H., Thomsen, K., 2010b. Modeling of carbon dioxide absorption by aqueous ammonia solutions using the Extended UNIQUAC model. Industrial & Engineering Chemistry Research 49, 12663-12674.

Darde, V., van Well, W.J., Stenby, E.H., Thomsen, K., 2011b. CO_2 capture using aqueous ammonia: kinetic study and process simulation. Energy Procedia 4, 1443-1450.

Dave, N., Do, T., Palfreyman, D., 2008. Assessing post-combustion capture for coal fired power stations in APP countries. CSIRO Internal Report ET/IR–1083.

Dave, N., Do, T., Puxty, G., Rowland, R., Feron, P., Attalla, M., 2009. CO_2 capture by aqueous amines and aqueous ammonia–a comparison. Energy Procedia 1, 949-954.

Derks, P., Versteeg, G., 2009. Kinetics of absorption of carbon dioxide in aqueous ammonia solutions. Energy Procedia 1, 1139-1146.

Dey, A., Aroonwilas, A., 2009. CO_2 absorption into MEA-AMP blend: mass transfer and absorber height index. Energy Procedia 1.

Dinca, C., Badea, A., 2013. The parameters optimization for a CFBC pilot plant experimental study of post-combustion CO_2 capture by reactive absorption with MEA. International Journal of Greenhouse Gas Control 12, 269-279.

DOE, 2010. Cost and performance baseline for fossil energy plants. U.S. Department of Energy, National Energy Technology Laboratory.

DOE, 2011. Quality guidelines for energy systems studies: cost estimation methodology for NETL assessments of power plant performance. U.S. Department of Energy, National Energy Technology Centre, Pittsburgh, PA.

Drbal, L., Boston, P., Westra, K., 1995. Power plant engineering. Springer, M. S.

Dugas, R., Rochelle, G., 2009. Absorption and desorption rates of carbon dioxide with monothanolamine and poperazine. Energy Procedia 1.

Dugas, R.E., 2009. Carbon dioxide absorption, desorption and diffusion in aqueous piperazine and monoethanolamine. Ph.D. dissertation, University of Texas, Austin.

Duncan, J., McLarnon, C., Alix, F., 2010. Removal of carbon dioxide from flue gas streams using mixed ammonium/alkali solutions. Google Patents.

EIA, 2013. Updated capital cost estimates for utility scale electricity generating plants. Energy Information Administration, United States of America.

Ermatchkov, V., Kamps, A.P.S., Maurer, G., 2005. The chemical reaction equilibrium constant and standard molar enthalpy change for the reaction {$2HSO_3^-(aq) \rightleftharpoons S_2O_5^{2-}(aq)+H_2O(l)$}: a spectroscopic and calorimetric investigation. Journal of Chemistry Thermodynamic 37, 187-199.

Fang, M., Xiang, Q., Zhou, X., Ma, Q., Luo, Z., 2014. Experimental study on CO_2 absorption into aqueous ammonia-based blended absorbents. Energy Procedia 61, 2284-2288.

Frailie, P.T., 2014. Modeling of carbon dioxide absorption/stripping by aqueous methyldiethanolamine/Piperazine. Ph.D. dissertation, University of Texas, Austin.

Frailie, P.T., Madan, T., Sherman, B.J., Rochelle, G.T., 2013. Energy performance of advanced stripper configurations. Energy Procedia 37, 1696-1705.

Freeman, S.A., Dugas, R.E., Wagener, D.H., Nguyen, T., Rochelle, G.T., 2010. Carbon dioxide capture with concentrated, aqueous piperazine. International Journal of Greenhouse Gas Control 4, 119–124.

Gal, E., 2006. Ultra cleaning combustion gas including the removal of CO_2. World Intellectual Property, Patent WO 2006022885.

GCCSI, 2012. CO_2 capture technologies: Post combustion capture. Report.

Goff, G.S., Rochelle, G.T., 2006. Oxidation inhibitors for copper and iron catalyzed degradation of Monoethanolamine in CO_2 capture processes. Industrial & Engineering Chemistry Research 45, 2513–2521.

Göppert, U., Maurer, G., 1988. Vapor–liquid equilibria in aqueous solutions of ammonia and carbon dioxide at temperatures between 333 and 393 K and pressures up to 7 MPa. Fluid Phase Equilibria 41, 153-185.

Goto, K., Yogo, K., Higashii, T., 2013. A review of efficiency penalty in a coal-fired power plant with post-combustion CO 2 capture. Applied Energy 111, 710-720.

Han, K., Ahn, C.K., Lee, M.S., Rhee, C.H., Kim, J.Y., Chun, H.D., 2013. Current status and challenges of the ammonia-based CO_2 capture technologies toward commercialization. International Journal of Greenhouse Gas Control 14, 270-281.

Hanak, D.P., Biliyok, C., Manovic, V., 2015. Rate-based model development, validation and analysis of chilled ammonia process as an alternative CO_2 capture technology for coal-fired power plants. International Journal of Greenhouse Gas Control 34, 52-62.

Haszeldine, R.S., 2009. Carbon capture and storage: how green can black be? Science 325, 1647-1652.

Hegg, D.A., Hobbs, P.V., 1978. Oxidation of sulfur dioxide in aqueous systems with particular reference to the atmosphere. Atmospheric Environment 12, 241-253.

Herzog, H., Meldon, J., Hatton, A., 2009. Advanced post-combustion CO_2 capture. Clean Air Task Force, 1-39.

Hikita, H., Asai, S., Katsu, Y., Ikuno, S., 1979. Absorption of carbon dioxide into aqueous monoethanolamine solutions. AIChE Journal 25, 793-800.

IEA, 2009. Criteria for technical and economic assessment of plant with low CO_2 emission. International Energy Agency Report.

IEA, 2014a. CO_2 emissions from fuel combustion-highlights. International Energy Agency, http://www.pbl.nl/en/publications/co2-emissions-from-fuel-combustion-2014-edition, accessed in January 2015.

IEA, 2014b. World Energy Outlook 2014. http://www.worldenergyoutlook.org/weo2014/, accessed in May 2015.

Jilvero, H., Eldrup, N.-H., Normann, F., Andersson, K., Johnsson, F., Skagestad, R., 2014a. Techno-economic evaluation of an ammonia-based post-combustion process integrated with a state-of-the-art coal-fired power plant. International Journal of Greenhouse Gas Control 31, 87-95.

Jilvero, H., Normann, F., Andersson, K., Johnsson, F., 2012. Heat requirement for regeneration of aqueous ammonia in post-combustion carbon dioxide capture. International Journal of Greenhouse Gas Control 11, 181-187.

Jilvero, H., Normann, F., Andersson, K., Johnsson, F., 2014b. The rate of CO_2 absorption in ammonia–Implications on absorber design. Industrial & Engineering Chemistry Research 53, 6750-6758.

Karimi, M., Hillestad, M., Svendsen, H.F., 2012. Positive and negative effects on energy consumption by inter–heating of stripper in CO_2 capture plant. Energy Procedia 23, 15-22.

Kozak, F., Petig, A., Morris, E., Rhudy, R., Thimsen, D., 2009. Chilled ammonia process for CO_2 capture. Energy Procedia 1, 1419-1426.

Kuramochi, T., Faaij, A., Ramírez, A., Turkenburg, W., 2010. Prospects for cost-effective post-combustion CO_2 capture from industrial CHPs. International Journal of Greenhouse Gas Control 4, 511-524.

Kurz, F., Rumpf, B., Maurer, G., 1995. Vapor-liquid-solid equilibria in the system NH_3-CO_2-H_2O from around 310 to 470 K: New experimental data and modeling. Fluid Phase Equilibria 104, 261-275.

Leung, D.Y.C., Caramanna, G., Maroto-Valer, M.M., 2014. An overview of current status of carbon dioxide capture and storage technologies. Renewable and Sustainable Energy Reviews 39, 426-443.

Li, L., Zhao, N., Wei, W., Sun, Y., 2013. A review of research progress on CO_2 capture, storage, and utilization in Chinese Academy of Sciences. Fuel 108, 112-130.

Lichtfers, U., 2000. Spektroskopische Untersuchungen zur Ermittlung von Speziesverteilungen im System Ammoniak-Kohlendioxid-Wasser. Ph.D. thesis

Linnenberg, S., Darde, V., Oexmann, J., Kather, A., van Well, W.J., Thomsen, K., 2012. Evaluating the impact of an ammonia-based post-combustion CO_2 capture process on a steam power plant with different cooling water temperatures. International Journal of Greenhouse Gas Control 10, 1-14.

Lombardo, G., Agarwal, R., Askander, J., 2014. Chilled ammonia process at technology center Mongstad – first results. Energy Procedia 51, 31-39.

Manzolini, G., Fernandez, E.S., Rezvani, S., Macchi, E., Goetheer, E., Vlugt, T., 2015. Economic assessment of novel amine based CO_2 capture technologies integrated in power plants based on European Benchmarking Task Force methodology. Applied Energy 138, 546-558.

Markewitz, P., Kuckshinrichs, W., Leitner, W., Linssen, J., Zapp, P., Bongartz, R., Schreiber, A., Müller, T.E., 2012. Worldwide innovations in the development of carbon capture technologies and the utilization of CO_2. Energy & Environmental Science 5, 7281-7305.

Mathias, P.M., Reddy, S., O'Connell, J.P., 2010. Quantitative evaluation of the chilled-ammonia process for CO_2 capture using thermodynamic analysis and process simulation. International Journal of Greenhouse Gas Control 4, 174-179.

McCann, N., Maeder, M., Attalla, M., 2008. Simulation of enthalpy and capacity of CO_2 absorption by aqueous amine systems. Industrial & Engineering Chemistry Research 47, 2002-2009.

McKay, H., 1971. The atmospheric oxidation of sulphur dioxide in water droplets in presence of ammonia. Atmospheric Environment 5, 7-14.

McLarnon, C.R., Duncan, J.L., 2009. Testing of ammonia based CO_2 capture with multi-pollutant control technology. Energy Procedia 1, 1027-1034.

Miller, J., Pena, R.G., 1972. Contribution of scavenged sulfur dioxide to the sulfate content of rain water. Journal of Geophysical Research 77, 5905-5916.

MIT, 2015a. Carbon Capture and Sequestration Technologies. https://sequestration.mit.edu/tools/projects/boundary_dam.html, Accessed in May 2015.

MIT, 2015b. Technology Review. http://www.technologyreview.com/demo/533351/a-coal-plant-that-buries-its-greenhouse-gases, Accessed in May 2015.

Mondal, M.K., Balsora, H.K., Varshney, P., 2012. Progress and trends in CO_2 capture/separation technologies: A review. Energy 46, 431-441.

Moullec, Y., Neveux, T., Al Azki, A., Chikukwa, A., Hoff, K.A., 2014. Process modifications for solvent-based post-combustion CO_2 capture. International Journal of Greenhouse Gas Control 31, 96-112.

Niu, Z., Guo, Y., Zeng, Q., Lin, W., 2012. Experimental studies and rate-based process simulations of CO_2 absorption with aqueous ammonia solutions. Industrial & Engineering Chemistry Research 51, 5309-5319.

Niu, Z., Guo, Y., Zeng, Q., Lin, W., 2013. A novel process for capturing carbon dioxide using aqueous ammonia. Fuel Processing Technology 108, 154-162.

Notz, R., Mangalapally, H.P., Hasse, H., 2012. Post combustion CO_2 capture by reactive absorption: pilot plant description and results of systematic studies with MEA. International Journal of Greenhouse Gas Control 6, 84-112.

Oexmann, J., Hensel, C., Kather, A., 2008. Post-combustion CO_2-capture from coal-fired power plants: Preliminary evaluation of an integrated chemical absorption process with piperazine-promoted potassium carbonate. International journal of greenhouse gas control 2, 539-552.

Oexmann, J., Kather, A., 2009. Post-combustion CO_2 capture in coal-fired power plants: comparison of integrated chemical absorption processes with piperazine promoted potassium carbonate and MEA. Energy Procedia 1, 799-806.

Onda, K., Takeuchi, H., Okumoto, Y., 1968. Mass transfer coefficients between gas and liquid phases in packed columns. Journal of Chemical Engineering of Japan 1, 56-62.

Pachauri, R.K., Allen, M., Barros, V., Broome, J., Cramer, W., Christ, R., Church, J., Clarke, L., Dahe, Q., Dasgupta, P., 2014. Climate Change 2014: Synthesis Report.

Contribution of Working Groups I, II and III to the Fifth Assessment Report of the Intergovernmental Panel on Climate Change.

Pinsent, B., Pearson, L., Roughton, F., 1956. The kinetics of combination of carbon dioxide with hydroxide ions. Transactions of the Faraday Society 52, 1512-1520.

Powerspan, 2010. Powerspan announces results of independent assessment of its CO_2 capture technology. Press Release, http://www.powerspan.com, Accessed in April 2015.

Qi, G., Wang, S., Lu, W., Yu, J., Chen, C., 2015. Vapor–liquid equilibrium of CO_2 in NH_3–CO_2–SO_2–H_2O system. Fluid Phase Equilibria 386, 47-55.

Qi, G., Wang, S., Yu, H., Wardhaugh, L., Feron, P., Chen, C., 2013. Development of a rate-based model for CO_2 absorption using aqueous NH_3 in a packed column. International Journal of Greenhouse Gas Control 17, 450-461.

Qin, F., Wang, S., Hartono, A., Svendsen, H.F., Chen, C., 2010a. Kinetics of CO_2 absorption in aqueous ammonia solution. International Journal of Greenhouse Gas Control 4, 729-738.

Qin, F., Wang, S., Hartono, A., Svendsen, H.F., Chen, C., 2010b. Kinetics of CO_2 absorption in aqueous ammonia solution. International Journal of Greenhouse Gas Control 4, 729-738.

Que, H., Chen, C.-C., 2011. Thermodynamic modeling of the NH_3–CO_2–H_2O system with electrolyte NRTL model. Industrial & Engineering Chemistry Research 50, 11406-11421.

Raksajati, A., Ho, M.T., Wiley, D.E., 2013. Reducing the cost of CO_2 capture from flue gases using aqueous chemical absorption. Industrial & Engineering Chemistry Research 52, 16887-16901.

Ramezan, M., Skone, T.J., Nsakala, y., Liljedahl, G., Gearhart, L., Hestermann, R., Rederstorff, B., 2007. Carbon dioxide capture from existing coal-fired power plants. National Energy Technology Laboratory, DOE/NETL Report.

Rao, A.B., Rubin, E.S., 2002. A technical, economic, and environmental assessment of amine-based CO_2 capture technology for power plant greenhouse gas control. Environmental Science & Technology 36, 4467-4475.

Rochelle, G.T., 2009. Amine scrubbing for CO_2 capture. Science 325, 1652-1654.

Rubin, E.S., 2012. Understanding the pitfalls of CCS cost estimates. International Journal of Greenhouse Gas Control 10, 181-190.

Rumpf, B., Weyrich, F., Maurer, G., 1993. Simultaneous solubility of ammonia and sulfur dioxide in water at temperatures from 313.15 K to 373.15 K and pressures up to 2.2 MPa. Fluid phase equilibria 83, 253-260.

Sada, E., Kumazawa, H., Butt, M., 1976. Gas absorption with consecutive chemical reaction: absorption of carbon dioxide into aqueous amine solutions. The Canadian Journal of Chemical Engineering 54, 421-424.

Sakwattanapong, R., Aroonwilas, A., Veawab, A., 2009. Reaction rate of CO_2 in aqueous MEA-AMP solution: experiment and modeling. Energy Procedia 1.

Salkuyeh, Y.K., Mofarahi, M., 2013. Reduction of CO_2 capture plant energy requirement by selecting a suitable solvent and analyzing the operating parameters. International Journal of Energy Research 37, 973-981.

Sarkisian, P., Kirol, L.D., 2003. Improved aqua-ammonia absorption system generator utilizing structured packing. Google Patents.

Scott, W., McCarthy, J., 1967. The system sulfur dioxide-ammonia-water at 25° C. Industrial & Engineering Chemistry Fundamentals 6, 40-48.

Shakerian, F., Kim, K.-H., Szulejko, J.E., Park, J.-W., 2015. A comparative review between amines and ammonia as sorptive media for post-combustion CO_2 capture. Applied Energy 148, 10-22.

Singh, D., Croiset, E., Douglas, P.L., Douglas, M.A., 2003. Techno-economic study of CO_2 capture from an existing coal-fired power plant: MEA scrubbing vs. O_2/CO_2 recycle combustion. Energy Conversion and Management 44, 3073-3091.

Stéphenne, K., 2013. Start-up of world's first commercial post-combustion coal fired CCS project: Contribution of Shell Cansolv to SaskPower Boundary Dam ICCS project.

Stichlmair, J., Bravo, J., Fair, J., 1989. General model for prediction of pressure drop and capacity of countercurrent gas/liquid packed columns. Gas Separation & Purification 3, 19-28.

Strube, R., Manfrida, G., 2011. CO_2 capture in coal-fired power plants–Impact on plant performance. International Journal of Greenhouse Gas Control 5, 710-726.

Telikapalli, V., Kozak, F., Francois, J., Sherrick, B., Black, J., Muraskin, D., Cage, M., Hammond, M., Spitznogle, G., 2011. CCS with the Alstom chilled ammonia process development program–Field pilot results. Energy Procedia 4, 273-281.

Tobiesen, F.A., Svendsen, H.F., Juliussen, O., 2007. Experimental validation of a rigorous absorber model for CO_2 postcombustion capture. AIChE journal 53, 846-865.

Valenti, G., Bonalumi, D., Macchi, E., 2012. A parametric investigation of the chilled ammonia process from energy and economic perspectives. Fuel 101, 74-83.

Versteeg, P., Rubin, E.S., 2011. A technical and economic assessment of ammonia-based post-combustion CO_2 capture at coal-fired power plants. International Journal of Greenhouse Gas Control 5, 1596-1605.

Whitman, W.G., 1923. Preliminary experimental confirmation of the two-film theory of gas absorption. Chemical & Metallurgical Engineering 29, 146-148.

XE, 2015. XE Currency exchange. http://www.xe.com/.

Yang, N., Yu, H., Xu, D., Conway, W., Maeder, M., Feron, P., 2014. Amino acids/NH_3 Mixtures for CO_2 capture: Effect of neutralization methods on CO_2 mass transfer and NH_3 vapour loss. Energy Procedia 63, 773-780.

Yeh, A.C., Bai, H., 1999. Comparison of ammonia and monoethanolamine solvents to reduce CO_2 greenhouse gas emissions. Science of the Total Environment 228, 121-133.

You, J.-K., Park, H.-S., Hong, W.-H., Park, J.-K., Kim, J.-N., 2007. Effect of precipitation on operation range of the CO_2 capture process using ammonia water absorbent. Korean Chemical Engineering Research 45, 258-263.

Yu, C.H., Huang, C.H., Tan, C.S., 2012. A review of CO_2 capture by absorption and adsorption. Aerosol and Air Quality Research 12, 745.

Yu, H., Morgan, S., Allport, A., Cottrell, A., Do, T., McGregor, J., Wardhaugh, L., Feron, P., 2011. Results from trialling aqueous NH_3 based post-combustion capture in a pilot plant at Munmorah power station: Absorption. Chemical Engineering Research and Design 89, 1204-1215.

Yu, H., Qi, G., Wang, S., Morgan, S., Allport, A., Cottrell, A., Do, T., McGregor, J., Wardhaugh, L., Feron, P., 2012. Results from trialling aqueous ammonia-based post-combustion capture in a pilot plant at Munmorah Power Station: Gas purity and solid precipitation in the stripper. International Journal of Greenhouse Gas Control 10, 15-25.

Yu, J., Wang, S., Yu, H., 2013. Experimental studies on suppression of ammonia vaporization by additives. Greenhouse Gases: Science and Technology 3, 415-422.

Yu, J., Wang, S., Yu, H., 2014a. Modelling analysis of solid precipitation in an ammonia-based CO2 capture process. International Journal of Greenhouse Gas Control 30, 133-139.

Yu, J., Wang, S., Yu, H., Wardhaugh, L., Feron, P., 2014b. Rate-based modelling of CO_2 regeneration in ammonia based CO_2 capture process. International Journal of Greenhouse Gas Control 28, 203-215.

Zhang, M., Guo, Y., 2013a. Process simulations of large-scale CO_2 capture in coal-fired power plants using aqueous ammonia solution. International Journal of Greenhouse Gas Control 16, 61-71.

Zhang, M., Guo, Y., 2013b. Process simulations of NH_3 abatement system for large-scale CO_2 capture using aqueous ammonia solution. International Journal of Greenhouse Gas Control 18, 114-127.

Zhang, M., Guo, Y., 2014. A comprehensive model for regeneration process of CO_2 capture using aqueous ammonia solution. International Journal of Greenhouse Gas Control 29, 22-34.

Zhao, B., Su, Y., Tao, W., Li, L., Peng, Y., 2012. Post-combustion CO_2 capture by aqueous ammonia: a state-of-the-art review. International Journal of Greenhouse Gas Control 9, 355-371.

Zhou, W., Zhu, B., Fuss, S., Szolgayová, J., Obersteiner, M., Fei, W., 2010. Uncertainty modeling of CCS investment strategy in China's power sector. Applied Energy 87, 2392-2400.